

**The interactions of surface-active engine oil additives in low
viscosity engine oils and their effect on tribological
performance**

Aaron Thornley

Submitted in accordance with the requirements for the degree of
Doctor of Philosophy

The University of Leeds
School of Mechanical Engineering
Leeds, UK

March 2023

The candidate confirms that the work submitted is his/her own, except where work which has formed part of jointly-authored publications has been included. The contribution of the candidate and the other authors to this work has been explicitly indicated below. The candidate confirms that appropriate credit has been given within the thesis where reference has been made to the work of others.

- Thornley A, Wang Y, Wang C, Chen J, Huang H, Liu H, Neville A, Morina A. Optimizing the Mo concentration in low viscosity fully formulated oils. *Tribology International*. 2022 Apr 1;168:107437.

This copy has been supplied on the understanding that it is copyright material and that no quotation from the thesis may be published without proper acknowledgement.

The right of Aaron Thornley to be identified as author of this work has been asserted by him in accordance with the Copyright, Designs and Patents Act 1988.

Acknowledgements

I would like to express my deep appreciation and gratitude to everyone who supported me throughout my studies and research. First and foremost, I would like to thank my supervisor team, Anne Neville, Ardian Morina, Chun Wang and Yuechang Wang, for their invaluable guidance, support, and encouragement throughout this journey. Their expertise, insight, and constructive criticism have been instrumental in shaping my research and academic growth.

I would also like to extend my sincere gratitude to the Sinopec Lubrication Company for providing financial support for my research project. Their generosity and belief in my work have been crucial in helping me achieve my academic goals.

In addition, I am deeply grateful to my family members and partner for their unwavering support, encouragement, and patience throughout my studies. Their love and support have been my constant source of inspiration, motivation, and strength.

Finally, I would like to express my appreciation to all the individuals from the University of Leeds who participated in my research study. Without their cooperation, dedication, and willingness to share their time and insights, this research would not have been possible.

To all those who have contributed in their own unique ways, I extend my heartfelt thanks and appreciation. Your support has been invaluable and has played a significant role in my academic success. Thank you.

Abstract

One of the main ways of increasing the fuel economy of the internal combustion engine (ICE) is by using lower-viscosity oils, which directly reduces CO₂ emissions. The challenges of lower viscosity oils include decreased lambda ratios in tribo-contacts. To address this, the engine oil additive package plays a crucial role in maintaining low friction and ensuring engine durability. High concentrations of molybdenum dithiocarbamate (MoDTC) are added to counteract oil viscosity reduction and oxidation effects. An investigation into the optimization of the MoDTC concentration in low viscosity engine oil is undertaken in this study by conducting friction and wear tests on SAE 0W-8 oil with different MoDTC concentrations using a Mini Traction Machine (MTM) and NPFlex. Tribofilm growth is studied through spacing layering imaging (SLIM) imaging, and chemical composition is analyzed using X-ray Photoelectron Spectroscopy (XPS) and Raman Spectroscopy. The optimum Mo concentration falls between 180 and 350 ppm, significantly influencing friction induction time, MoS₂ and ZDDP film thicknesses.

Understanding the interactions of boundary active additives becomes critical in low-viscosity engine oil. Detergents, which have received less attention than MoDTC and zinc dithiophosphate (ZDDP), form tribofilms with good wear properties. Investigating different detergents' influence and interactions with ZDDP and MoDTC in ultra-low viscosity oil, three detergent formulations within a 0W-8 oil grade engine oil are examined. Detergents impact friction, wear, and tribofilm composition, showing synergistic effects with ZDDP and MoDTC. The same techniques used in the first study are applied.

It has been proven that extending the oil drain interval (ODI) is as essential as reducing the viscosity to reduce CO₂ emissions. However, ageing occurs within the oils during operation and is a detrimental process for low viscosity engine oil additives. Little research has been conducted comparing artificial and engine ageing processes. Thus, the same tribological testing equipment is utilised to investigate a comparison study between the two ageing processes as in the previous studies. The artificial aging process cannot fully replicate engine aging effects on oils. Regardless of the engine ageing process, the impact on oils remains relatively constant, while artificial ageing produces inconsistent results.

Table of Contents

Acknowledgements	iii
Abstract	iv
Table of Contents	vi
List of Tables	xi
List of Figures	xii
Abbreviations	xviii
Chapter 1 Introduction	1
1.1 The impact of Green House Gases from engine emissions	1
1.2 Increasing fuel economy	2
1.2.1 The impact of reducing oil viscosity.....	3
1.3 Aims and objectives	5
1.4 Thesis outline	7
Chapter 2 Fundamentals of Tribology	8
2.1 Tribology overview	8
2.2 Contact mechanics.....	10
2.3 Fundamentals of Friction.....	11
2.3.1 Adhesion	12
2.3.2 Ploughing	13
2.3.3 Stick-slip.....	14
2.3.4 Frictional Heating	15
2.4 Fundamentals of Wear	16
2.4.1 Adhesion	17
2.4.2 Abrasion	19
2.4.3 Fatigue	20
2.4.4 Erosion	21
2.5 Lubricants and Lubrication	22
2.5.1 Viscosity	22
2.5.2 Base oils & Additives	25
2.5.3 Lubrication Regimes.....	28
2.6 Summary.....	32
Chapter 3 Literature Review	33
3.1 Introduction to Internal Combustion Engines.....	33
3.1.1 Tribological Problems	33
3.1.2 Preventing Tribological Problems.....	34

3.2	Increasing Fuel Economy.....	36
3.2.1	Low-viscosity Engine Oil	37
3.3	ZDDP Additive.....	40
3.3.1	Tribofilm formation	41
3.3.2	Tribofilm properties and chemistry	43
3.3.3	ZDDP tribofilm characterization via XPS	47
3.4	Friction Modifiers.....	49
3.4.1	MoDTC Additive	49
3.4.2	MoDTC tribofilm characterization via Raman Spectroscopy	57
3.5	Detergent Additive.....	59
3.5.1	Tribological Properties & synergisms with other additives.....	60
3.6	Additive Depletion	62
3.6.1	Oxidation	63
3.7	Summary.....	69
Chapter 4	Experimental Procedures	72
4.1	Introduction	72
4.2	Oil Rheology.....	72
4.3	Oil Ageing.....	74
4.3.1	Artificial Ageing Process.....	74
4.3.2	Field Engine Ageing Processes.....	75
4.4	Oil Analysis	77
4.4.1	Inductively Coupled Plasma Atomic Emission Spectroscopy (ICP-AES).....	77
4.4.2	Fourier Transform Infrared Spectroscopy (FTIR)	78
4.5	Friction	80
4.5.1	Lambda Ratio Calculations	80
4.5.2	Test Rig.....	81
4.5.3	Operating Conditions.....	83
4.6	ZDDP Film Thickness	86
4.7	Tribochemical Surface Analysis	87
4.7.1	X-ray Photoelectron Spectroscopy (XPS)	87
4.7.2	Raman Spectroscopy	88
4.8	Wear Analysis	90
4.8.1	Tribofilm Removal	92

4.9 Summary.....	93
Chapter 5 The critical role of MoDTC to counteract low viscosity in ultra-low viscosity engine oils.....	94
5.1 Introduction	94
5.2 Test oils.....	95
5.3 Oil Viscosity Reduction	96
5.4 The Critical Role of Friction Modifiers in Low Viscosity Oil.....	98
5.4.1 MoDTC Influence on Friction.....	98
5.4.2 Tribofilm Chemistry	101
5.4.3 MoDTC Influence on Wear	105
5.5 Summary.....	107
Chapter 6 Optimizing of Mo Concentration in Ultra-low Viscosity Engine Oil.....	108
6.1 Introduction	108
6.2 Test Oils	109
6.3 Friction Analysis	111
6.3.1 Constant Lambda Ratio.....	111
6.4 Varying Lambda Ratio.....	115
6.4.1 Induction Time.....	119
6.5 Tribofilm Thickness	123
6.5.1 Tribofilm Growth Rate and Steady-state Film Thickness..	123
6.6 Tribofilm Chemical Composition.....	129
6.6.1 MoS ₂ and Mo oxides	129
6.6.2 Tribofilm Chemical Composition	139
6.7 Mo Concentrations Influence on the MoS ₂ Growth	142
6.8 Wear Analysis	146
6.8.1 Wear Coefficient.....	147
6.9 Summary.....	149
Chapter 7 Detergents Influence on the Tribological Properties of Ultra-low Viscosity Oil	151
7.1 Introduction	151
7.2 Test Oils.....	152
7.3 Detergents Chemical Structures	153
7.4 Friction Performance.....	154
7.5 Tribofilm Growth Rate and Thickness	160
7.6 Tribochemical changes within the Tribofilms.....	162

7.6.1 Raman Analysis	162
7.6.2 XPS Analysis.....	165
7.7 Wear Performance	169
7.8 Summary.....	171
Chapter 8 The effect on Tribological Properties: a comparison between lab-based simulated oil ageing process and oil ageing in engine conditions.....	173
8.1 Introduction	173
8.2 Test Oils	174
8.3 Oil Analysis	176
8.3.1 Viscosity	176
8.3.2 Additive Depletion and By-products	178
8.4 Friction Analysis	183
8.4.1 Oil A.....	183
8.4.2 Oil B.....	187
8.5 Tribofilm Thickness	192
8.5.1 Oil A.....	192
8.5.2 Oil B.....	193
8.6 MoS ₂ Raman Analysis.....	195
8.6.1 Oil A.....	195
8.6.2 Oil B.....	198
8.7 XPS Tribofilm Analysis	201
8.7.1 Oil A	201
8.7.2 Oil B	210
8.8 Wear Analysis	219
8.8.1 Oil A	219
8.8.2 Oil B.....	221
8.9 Summary.....	224
Chapter 9 Discussion.....	225
9.1 Optimum Mo Concentration	225
9.1.1 Criteria.....	225
9.1.2 Friction and Wear	226
9.2 Mo Concentration effect on the initial MoS ₂ Formation	229
9.2.1 Induction Time.....	231
9.2.2 Early-stage MoS ₂ Formation	232

9.2.3 Mo concentration and friction reduction time mechanism.....	234
9.3 Mo Concentrations effect on the ZDDP Thickness.....	236
9.3.1 Tribofilm chemistry	238
9.3.2 Mechanism of MoDTC and ZDDP tribofilm formation.....	240
9.4 Detergents' effect on Tribofilms Tribological Properties	241
9.4.1 Friction and Wear	242
9.4.2 Tribofilm Chemistry	243
9.4.3 Mechanism for the interaction of detergent and ZDDP/MoDTC	248
9.5 Artificial Oil Ageing vs Engine oil Ageing.....	249
9.5.1 Differences in Oil Ageing Processes	249
9.5.2 Effect of Ageing Oil on Wear	251
9.5.3 Effect of Ageing on Oil Chemistry.....	254
Chapter 10 Conclusions and Future Work	260
10.1 Conclusions.....	260
10.1.1 Optimization of Mo concentration.....	260
10.1.2 Mo concentrations effect on tribological performance	260
10.1.3 Mo concentrations influence on MoS ₂ formation	261
10.1.4 Mo concentrations influence on ZDDP formation	261
10.1.5 Detergent formulations effect on tribological performance	262
10.1.6 Detergents influence on tribofilm chemistry	262
10.1.7 Artificial vs field engine ageing processes.....	263
10.2 Future Work	265
List of References	267

List of Tables

Table 2-1 Units of measurements for viscosity.....	23
Table 2-2 API base oil categories.....	26
Table 2-3 Classification of the most common oil additives [29].	27
Table 2-4 Most common chemical additives found in engine oils [28].....	28
Table 4-1 Field Ageing Oil Processes.....	76
Table 4-2 Wavelength ranges used in this study.	80
Table 4-3 Chapter 5 MTM operating conditions.....	84
Table 4-4 Chapters 6 to 8 MTM operating conditions.	85
Table 5-1 Test oils used in the oil viscosity reduction study.	95
Table 5-2 Test oils used in the friction modifier study.....	96
Table 6-1 Test oils for the optimization of Mo concentration study. ..	110
Table 6-2 Binding energy values from previous literature for the Mo 3d peak fitting.....	129
Table 6-3 Mo (IV): Mo (VI) ratios for Mo concentrations \geq 180 ppm. ...	132
Table 6-4 Ca 2p, S 2p, and Zn 2p peak binding energies and associated bonding for all Mo concentrations.	139
Table 6-5 BO/NBO ratios and the peak difference between Zn3s and P2p.	140
Table 6-6 Average wear scar width for 0, 350, and 1000 ppm of Mo...	148
Table 7-1 Test oils used in detergent study.....	152
Table 8-1 Test oils used to compare artificial and engine ageing processes.	175
Table 8-2 Oil A's dynamic viscosities.....	176
Table 8-3 Oil B's dynamic viscosities.....	177
Table 8-4 BO/NBO ratio and Δ binding energy between Zn 3s and P 2p for oil A.....	210
Table 8-5 BO/NBO ratio and Δ binding energy between Zn 3s and P 2p for oil B.....	218
Table 9-1 Phosphate chain length as Mo concentration changes.	239
Table 9-2 Detergent formulations	244
Table 9-3 Engine oil artificial vs engine ageing impact on tribological properties compared to their fresh oils.	250
Table 9-4 Mo compounds detected within fresh, artificial and engine aged tribofilms.....	257
Table 9-5 Mo (V) binding energy for fresh and aged oils.....	257

List of Figures

Figure 1-1 Fuel economy benefits from decreasing oil viscosity [7].....	3
Figure 1-2 ICE components lambda ratios with changing viscosity.....	4
Figure 2-1 Main tribological factors which influence Tribology.....	9
Figure 2-2 (a) Hertzian contact and pressure distribution between two elastic solids, (b) Hertzian contact and pressure distribution between elastic solid and rigid plane, (c) Hertzian contact and pressure distribution between two cylinders [15].....	11
Figure 2-3 Adhesive asperity contact.....	13
Figure 2-4 Ploughing of a groove in a soft counterface by a hard asperity.	14
Figure 2-5 Rabinowicz stick-slip model [19].	15
Figure 2-6 Wear mechanism processes.	17
Figure 2-7 Adhesion wear theory for a single asperity contact [11].	18
Figure 2-8 Erosion rate for brittle and ductile materials [26].....	21
Figure 2-9 Lubricant influencing factors.....	22
Figure 2-10 Graph of the relationship between viscosity and shear.	25
Figure 2-11 Schematic of the boundary lubrication regime [31].....	30
Figure 2-12 Schematic of the mixed lubrication regime [31].....	31
Figure 2-13 Schematic of the hydrodynamic regime [31].	32
Figure 3-1 Passenger car energy consumptions breakdown [34].	33
Figure 3-2 Oil flow cycle through an engine [36].....	36
Figure 3-3 Percent decrease in fuel consumption as a function of percent fuel economy increase [37].	37
Figure 3-4 The effect of lowering viscosity on the tribo-contact of two surfaces.	38
Figure 3-5 Chemical structure of ZDDP [12].	40
Figure 3-6 ZDDP tribofilm layers [43].	42
Figure 3-7 Comparison of wear track width for a base oil and a ZDDP containing oil [50].....	44
Figure 3-8 Comparison of Stribeck curves from a base oil and a ZDDP containing oil [52].....	45
Figure 3-9 Mechanical properties of a ZDDP tribofilm [56].....	46
Figure 3-10 Characterization of zinc polyphosphate chains [59].....	48
Figure 3-11 Example of BO/NBO ratio obtained from O 1s high resolution signal [61].	48

Figure 3-12 Chemical structure of MoDTC.....	49
Figure 3-13 Mechanism for the decomposition of MoDTC [65].....	51
Figure 3-14 Comparison of friction as a function of time for dry friction, base oil and MoDTC containing oil [65].	53
Figure 3-15 Comparison of friction as a function of time for a base oil, base oil + ZDDP and a base oil + ZDDP + MoDTC [75].	56
Figure 3-16 Wear coefficients for different formulations of ZDDP and MoDTC oils [71].....	57
Figure 3-17 Raman spectra of a MoDTC tribofilm [68].	58
Figure 3-18 Surfactant and base oil synergies of detergents [79].	59
Figure 3-19 Comparison of specific wear rates for different oil formulations containing ZDDP and OBCS [82].....	61
Figure 3-20 Oil degradation and additive depletion over time.	63
Figure 3-21 Oil oxidation stages [86].....	64
Figure 3-22 Oxidation stability of base oils using ASTM standard engine test [89].....	66
Figure 3-23 Schematic for CEC L-48-00.	69
Figure 4-1 Kinexus rheometer.....	73
Figure 4-2 Artificial ageing process schematic.	74
Figure 4-3 Typical ICP-AES setup [100].	77
Figure 4-4 FTIR example spectrum.....	79
Figure 4-5 MTM-SLIM schematic.....	82
Figure 4-6 Chapter 5 MTM test procedure.....	83
Figure 4-7 Chapters 6 to 8 MTM test procedure.	84
Figure 4-8 SLIM mechanism [106].....	86
Figure 4-9 Raman example spectra of MoS ₂ peaks.....	90
Figure 4-10 Examples of (a) NPFlex scanned image and (b) Y-profile of a wear scar.	91
Figure 4-11 Selected areas for wear analysis.	92
Figure 5-1 Reduction of oil viscosity influence on boundary and mixed lubrication regimes.....	97
Figure 5-2 (a) Friction values at 0 and 120 minutes under a constant lambda ratio, (b) Stribeck curves taken at 0 and 120 minutes under a varying lambda ratio.	99
Figure 5-3 XPS High-resolution scans for 0W-20 without MoDTC sample, (a) - Mo 3d, (b) - S 2p, (c) - P 2p, (d) - Zn 2p, and (e) - Ca 2p.	102

Figure 5-4 XPS High-resolution scans for 0W-20 with MoDTC sample, (a) - Mo 3d, (b) - S 2p, (c) - P 2p, (d) - Zn 2p, and (e) - Ca 2p.	103
Figure 5-5 Wear volume loss taken from a specific area for sample with and without MoDTC.	106
Figure 6-1 First 3000 seconds in the traction phase at a constant speed for all Mo concentrations.	112
Figure 6-2 Final 3000 seconds of the 24 hours of traction for all Mo concentrations.	112
Figure 6-3 Steady-state friction values under a constant lambda ratio.	114
Figure 6-4 Final Stribeck curves for all Mo concentrations.....	116
Figure 6-5 Stribeck curves for (a) 180 ppm of Mo and (b) 1000 ppm of Mo.	118
Figure 6-6 Induction time to reach ≈ 0.04 friction for Mo concentration ≥ 180 ppm.	119
Figure 6-7 Induction period after Stribeck curves for (a) 180 ppm, (b) 350 ppm and (c) 1000 ppm.....	122
Figure 6-8 SLIM images captured at specific intervals for 0, 350 and 1000ppm Mo concentrations.	124
Figure 6-9 Tribofilm growth rate and steady-state thickness values for 0, 350 and 1000ppm Mo concentrations.....	124
Figure 6-10 Tribofilm thickness with friction values over time for (a) 0 ppm, (b) 350 ppm and (c) 1000 ppm.....	127
Figure 6-11 Mo 3d deconvolute signals for 0s and 120s etch times, (a) 0 ppm, (b) 85 ppm, (c) 180 ppm, (d) 350 ppm, (e) 500 ppm, (f) 750 ppm and (g) 1000 ppm.....	131
Figure 6-12 Raman spectroscopy; 180ppm – (a) intensity mapping, (b) intensity frequency distribution, 350ppm – (c) intensity mapping, (d) intensity frequency distribution, 500ppm – (e) intensity mapping, (f) intensity frequency distribution, 750ppm – (g) intensity mapping, (h) intensity frequency distribution, and 1000ppm – (i) intensity mapping, (j) intensity frequency.....	135
Figure 6-13 Total intensity counts of MoS ₂ vs friction for all friction-reducing Mo concentrations.....	137
Figure 6-14 Mean Raman spectra for Mo concentrations greater than 180 ppm.....	141
Figure 6-15 Total intensity counts of MoS ₂ within the tribofilm matrix at intervals during the friction tests for 350 and 1000 ppm oils.	143
Figure 6-16 Film thickness and total intensity counts of MoS ₂ within the tribofilm at intervals during testing for 350 ppm.	144

Figure 6-17 Film thickness and total intensity counts of MoS ₂ within the tribofilm at intervals during testing for 1000 ppm.	145
Figure 6-18 Friction values for all intervals total intensity counts of MoS ₂ for both 350 and 1000 ppm.	146
Figure 6-19 Wear coefficients for 0, 350, and 1000 ppm of Mo.	147
Figure 7-1 Detergent chemical structure for (a) Salicylates and (b) Sulfonates.....	153
Figure 7-2 (a) Start and steady-state friction values and (b) first 600s of traction.....	155
Figure 7-3 Stribeck curves for (a) initial and final for all three oils (b) Detergent A, (c) Detergent B , and (d) Detergent C.	159
Figure 7-4 Film thickness growth rate vs time for all three detergent formulations.	161
Figure 7-5 Raman spectra example from all three tribofilms.	163
Figure 7-6 Total intensity counts of MoS ₂ within each tribofilm.	165
Figure 7-7 Mo 3d signal peaks for all HR scans (a) Detergent A, (b) Detergent B and (c) Detergent C.....	166
Figure 7-8 Average weight % of elements associated with ZDDP and detergent decomposition products within 120 seconds etching time.....	168
Figure 7-9 Average wear loss for a 0.4x0.35 μm area.	170
Figure 8-1 Oil A's ZDDP (P-O-C and P=S) bonding peak.	179
Figure 8-2 Oil A's sulphation (S=O and S-O) bonding peaks.	179
Figure 8-3 Oil A's Carbon oxidation (C=O) bonding peak.	180
Figure 8-4 Oil B's ZDDP (P-O-C and P=S) bonding peak.	181
Figure 8-5 Oil B's sulphation S-O bonding peaks.	182
Figure 8-6 Oil B's Carbon oxidation (C=O) bonding peak.	182
Figure 8-7 (a) initial and (b) final Stribeck curves for oil A before and after ageing.	184
Figure 8-8 All Stribeck curves for the fresh engine oil.	186
Figure 8-9 All Stribeck curves for the artificially aged engine oil.	186
Figure 8-10 All Stribeck curves for the engine aged oil.....	187
Figure 8-11 (a) initial and (b) final Stribeck curves for oil B before and after ageing.	188
Figure 8-12 All Stribeck curves for the fresh engine oil.	190
Figure 8-13 All Stribeck curves for the artificially aged engine oil.	191
Figure 8-14 All Stribeck curves for the engine aged engine oil.	191
Figure 8-15 Oil A's ZDDP tribofilm thickness.	193
Figure 8-16 Oil B's ZDDP tribofilm thickness.	194

Figure 8-17 Raman spectra comparison for oil A.....	195
Figure 8-18 Total intensity counts and steady-state friction for oil A	196
Figure 8-19 Artificially aged oil A's film thickness with MoS ₂ intensity counts at set intervals during testing.....	198
Figure 8-20 Raman spectra comparison for oil B.....	199
Figure 8-21 Total intensity counts and steady-state friction for oil B.	200
Figure 8-22 XPS element weight %s after each etching time for oil A (a) fresh, (b) artificially aged and (c) engine aged tribofilms...	204
Figure 8-23 Mo 3d signals for oil A's (a) fresh, (b) artificially aged and (c) engine aged tribofilms.	207
Figure 8-24 P 2p signals for oil A's tribofilms.....	208
Figure 8-25 Zn 2p signals for oil A's tribofilms.....	209
Figure 8-26 XPS element weight %s after each etching time for oil B (a) fresh, (b) artificially aged and (c) engine aged tribofilms...	213
Figure 8-27 Mo 3d signals for oil B's tribofilms.....	214
Figure 8-28 P 2p signals for oil B's tribofilms.....	216
Figure 8-29 Zn 2p signals for oil B's tribofilms.....	217
Figure 8-30 Example NPflex image of EDTA solution removal.	219
Figure 8-31 Wear loss of 0.4x0.4 µm area with wear scar widths for oil A.	221
Figure 8-32 Wear loss of 0.4x0.4 µm area with wear scar widths for oil B.	223
Figure 9-1 Schematic of the key points within the discussion.	225
Figure 9-2 Average friction values for a constant and varying lambda ratio at different Mo concentrations.....	228
Figure 9-3 Steady-state friction and wear coefficients for selected Mo concentrations.	229
Figure 9-4 Oil viscosity influence on Mo concentration's ability to reduce friction within the tribofilm.	230
Figure 9-5 Dependence of low friction induction time as a function of MoDTC concentration in the oil.....	231
Figure 9-6 Total intensity counts of MoS ₂ at set intervals for 350 and 1000 ppm of Mo oils.	233
Figure 9-7 Mechanism for increasing Mo concentration which leads to a decrease in friction reduction induction time, (a) low MoDTC concentration and (b) high MoDTC concentration. .	236
Figure 9-8 ZDDP film thickness vs time for multiple different Mo concentrations using SLIM.	237

Figure 9-9 ZDDP XPS element weight percentages at different Mo concentrations (a) Fe, (b) P and (c) Zn.....	239
Figure 9-10 Tribofilm formations of a fully formulated oil containing ZDDP and detergent and the additional MoDTC in a friction-reducing concentration.	240
Figure 9-11 Friction and wear values for each detergent formulation	243
Figure 9-12 Detergents friction and MoS₂ total intensity counts within the tribofilm.	245
Figure 9-13 Average weight % for anti-wear and detergent species with wear volume loss for all three formulations.	247
Figure 9-14 Wear loss for both oil A and B.	252
Figure 9-15 Average element weight percentage of Zn and P for (a) oil A and (b) oil B.....	259

Abbreviations

<u>Abbreviation</u>	<u>Definition</u>
API	American petroleum Institute
ASTM	American society for testing materials
CCL	Coordinating European council
CPS	Counts per second
EDS	Energy dispersive spectrometry
EHL	Elastohydrodynamic
FTIR	Fourier transform infrared spectroscopy
GED	Global engine durability
GHG	Greenhouse gas
HD	Hydrodynamic
HR	High resolution
HSAB	Hard and soft acid bases
HTHS	High-temperature high shear
ICE	Internal combustion engine
ICP	Inductively coupled plasma
MoDTC	Molybdenum dithiocarbamate
MTM	Mini traction machine
OBCS	Over-based calcium sulphonate
ODI	Oil drain interval
OEMs	Original equipment manufacturers
PAO	Polyalphaolefin
SAE	Society of automotive engineers
SLIM	Spacing layering imaging
SRR	Slide to roll
XPS	X-ray photoelectron spectroscopy
ZDDP	Zinc dithiophosphates

Chapter 1 Introduction

1.1 The impact of Green House Gases from engine emissions

Over 60% of the one billion vehicles globally use ICE as their power source [1]. The average efficiency of spark-ignition ICEs is around 30-36%, showing how inefficient they are at converting fuel to usable energy [2]. As a result of engineering and re-development over the years since the first ICE was manufactured, larger efficiencies have been reached by using higher compression ratios and engine management systems [3]. The process within an ICE to convert the energy stored within the fuel to mechanical energy, which drives the wheels, produces the main greenhouse gas (GHG) CO₂, which is proportional to the amount of fuel used.

Over recent years, there has been much more significant interest in the impacts these CO₂ emissions produced by engines have on our environment. The GHGs can directly cause water shortages, sea levels rise, and forest damage. Although there are different contributors to GHG emissions, such as industry and electricity, transportation generates the most significant GHGs. The projected CO₂ emissions produced, and energy use from transportation is expected to grow to about 80% higher than in 2030 if no significant action is taken to reduce the produced emissions [4].

The future projections and concerns for our environment from countries and regions such as China and Europe are forcing them to change laws for the future, implanting strict CO₂ regulations. Original equipment manufacturers (OEMs) have to implement different solutions into the engine to meet these requirements set by international governments. From extensive research, the

two main ways to decrease CO₂ emissions are increasing fuel economy and using renewable fuels.

1.2 Increasing fuel economy

The cheapest and most efficient way to increase the fuel economy of an ICE is by decreasing the viscosity of the engine oil. Previous research on the potential savings achieved using a lower viscosity engine oil directly increasing fuel economy has shown large values. An example of estimation would be a \$370 million per year saving if all USA car owners used cars with a 0.5% fuel economy improvement [5]. More recent studies show that a 2.75% fuel efficiency increase can be achieved using an SAE 5W-20 oil compared to an SAE 10W-30 [6]. Lowering the viscosity even further still produces positive results, a 1.5% increase can be observed using a 0W-20 following international lubricants standardization and approval committee (ILSAC) GF-2 standards compared to 5W-30 engine oil [7].

The general trend for fuel economy % increase when lowering the viscosity of the engine oil is shown in Figure 1-1 [8]. As the kinematic viscosity at 100°C is decreased, there is a linear increase in fuel economy % based on the reports of multiple authors. It must be noted that the graph is of base oils. Currently, Japanese OEMs are leading the market for ultra-low viscosity engine oil, with large amounts of research being put into developing an industry-available 0W-8 engine oil. However, it is relatively unknown how far the engine oil's viscosity can be lowered before fuel economy % increases are not positive or beneficial.

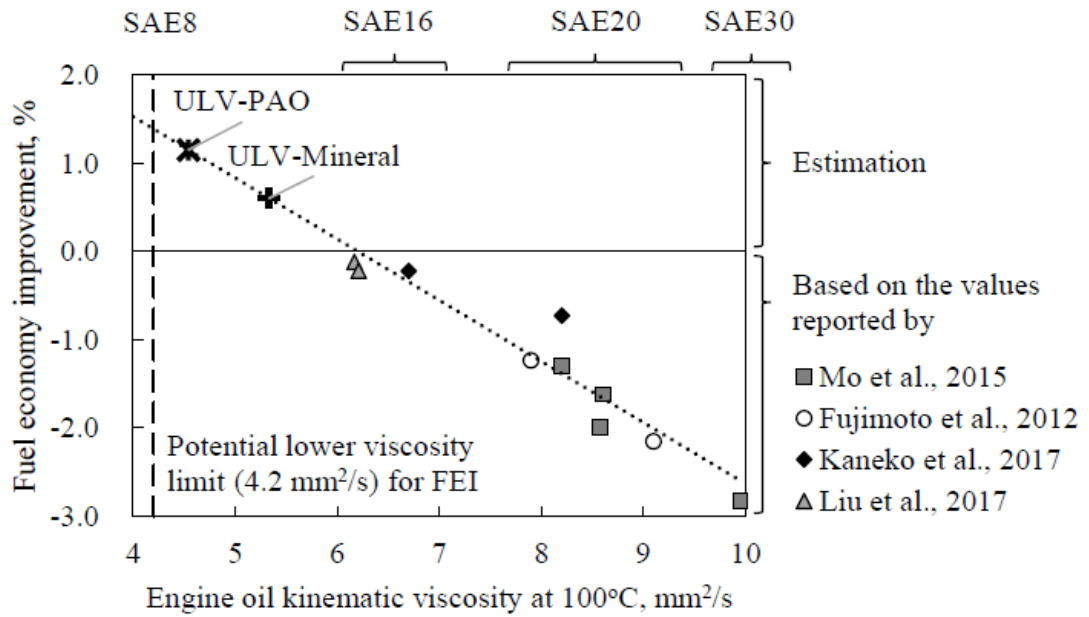


Figure 1-1 Fuel economy benefits from decreasing oil viscosity [7].

1.2.1 The impact of reducing oil viscosity

Decreasing the viscosity of the oil improves the pumping ability during cold starts. It enables the oil to be thin enough to lubricate the components upon engine start-up, ensuring the least amount of time it takes to complete an entire cycle of lubrication within the ICE. In terms of friction, lowering the oil's viscosity decreases the hydrodynamic friction in the bearings and piston/cylinder area, where a large proportion of the fuel economy increase is generated [9]. However, lowering the viscosity of the lubricating oil also has its disadvantages. It shifts all the components' lubrication regimes towards the boundary regime and decreases the tribo-contacts lambda ratios. Lambda ratio is a parameter used to quantify the lubrication regime. More "metal-to-metal" contact occurs between the components, especially at high temperatures where the oil is at its thinnest. Thus, components in which tribo-

contacts operated in low lambda ratios are expected to have increased friction and wear, as shown in Figure 1-2.

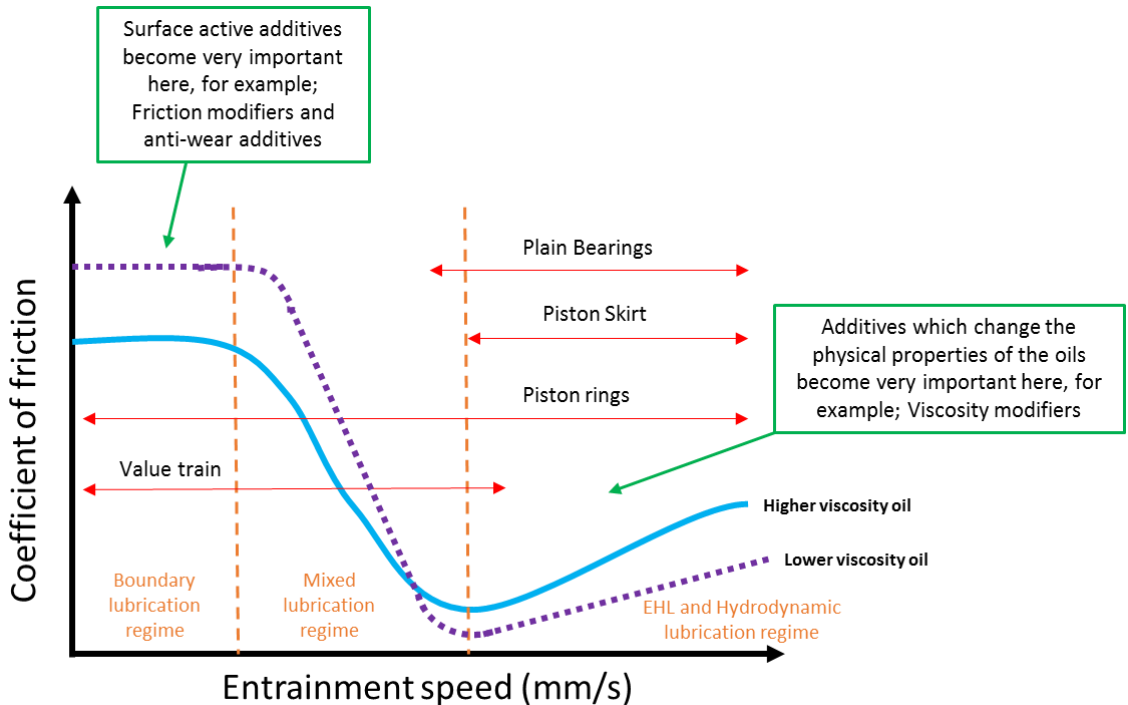


Figure 1-2 ICE components lambda ratios with changing viscosity.

Additives become more and more critical to understand as the oil's viscosity is lowered to ensure necessary low friction and wear in components with lowered lambda ratios towards the boundary and mixed lubrication regimes. Hence, specific attention must be given to the boundary additives that form the tribofilm matrix with friction and wear-reducing properties. These main additives are known as friction modifiers and anti-wear additives.

Countries are increasing the friction modifier concentration to very high amounts of 1000+ppm of Mo to counteract the impact of lowering the oil's viscosity on its tribological properties. However, the increase in friction modifier concentration has its disadvantages and problems. The

concentration of boundary additives has to be increased due to decreased lambda ratios at the tribo-contacts, additive depletion due to oxidation and the need for an increased ODI. An increase in sulfur content and its relatively high cost are both factors that create a need for the friction modifier concentration to decrease [10].

The two essential additives, MoDTC and ZDDP, that form tribofilms directly reduce friction, and wear must not be negatively impacted by other boundary-active additives. Previous research has shown detergents to form tribofilms [11]. However, the detergent formulation to improve its function must not hinder the friction and wear additives with the harsher conditions produced by reducing the oil viscosity.

Another driving force in increasing fuel economy is obtaining longer ODI. Therefore, it is crucial to test and analyze the performance of the ultra-low viscosity engine oils in a new state and while aged, giving specific attention to the oxidation of additives.

1.3 Aims and objectives

This study aims to advance our understandings of the interactions of surface-active engine oil additives in low viscosity engine oils and their effect on tribological performance. The research was carried out through three main studies.

Optimization of Mo concentration in ultra-low viscosity engine oil. This study investigated the effect of Mo concentration on various tribological aspects, including friction and wear performance, ZDDP film thickness, tribofilm chemistry, and MoDTC decomposition products. The objective was to

determine the critical concentration range for Mo in low viscosity and develop mechanisms to explain how changes in Mo concentration effect friction and wear performances.

Detergents influence on the tribological properties of ultra-low viscosity engine oil. In this study, the focus was on examining the influence of detergent formulations on tribological properties. The investigation includes friction performance, wear performance, ZDDP film thickness, tribofilm chemistry, and MoDTC decomposition products. The objective is to gain insights into the effects of different detergent compositions on the tribological behaviour of ultra-low viscosity engine oils.

The effect of oil ageing on tribological properties: a comparison between lab-based simulated oil ageing process and oil ageing in engine conditions. This study aims to compare the effects of artificial lab-based simulated oil ageing processes and real-world engine conditions on tribological properties. It involves analyzing the impact of ageing on bulk properties of the oil, friction performance, wear performance, ZDDP film thickness, decomposition products of ZDDP and MoDTC. The objective is to understand the differences between simulated and actual oil ageing and their implications for tribological performance.

1.4 Thesis outline

- **Chapter 2 – Introduction to the fundamental tribology relevant to the study.**
- **Chapter 3 – Literature review of the relevant topics on low-viscosity oil and additives used to counteract it. It also details oil ageing effects on engine oils.**
- **Chapter 4 – Detailed overview of the experimental procedures used to complete the study.**
- **Chapter 5 – The critical role of MoDTC to counteract low viscosity in ultra-low viscosity engine oils.**
- **Chapter 6 – Optimizing the Mo concentration in low viscosity fully formulated oils.**
- **Chapter 7 – Detergents influence on the tribological properties of low viscosity fully formulated oils.**
- **Chapter 8 – The effect of oil ageing on tribological properties: a comparison between lab-based simulated oil ageing process and oil ageing in engine conditions.**
- **Chapter 9 – Detailed discussion on the results obtained from Chapters 5 to 8.**
- **Chapter 10 – Main conclusions of the study and future research work plans.**

Chapter 2 Fundamentals of Tribology

This chapter provides a basic understanding of the science of tribology. It is split into five main sections. The first introduces a brief history of the word's origins with the impact and factors influencing tribology. The second section explains the Hertzian contact mechanics between two surfaces. The third and fourth sections explain the fundamentals of friction and wear. Finally, the last section gives an overview of the functions and factors which influence lubricants used in the current market and the different lubrication regimes in which a lubricant will be during its operation.

2.1 Tribology overview

The word tribology comes from the Greek word tribos, meaning "rubbing", and the suffix – ology meaning "the study of" [12]. It was defined in the United Kingdom in 1966. However, it can be dated back to Egyptian times, from 3500 to 30 B.C. The first known pictorial records show how the Egyptians used lubricant to prevent friction when transporting a statue. The Egyptians' technique enabled them to transport large objects over large distances more efficiently than before.

Tribology is the science of technology of interacting surfaces in relative motion and of related subjects and particles [13]. This definition implies that at least two bodies must be involved with relative motion in different forms, such as sliding, rolling, spinning, and bouncing, which can be individual or combinations of these motions. The more wider scope of tribology brings together three main subjects: friction, wear and lubrication. These three subjects are critical for efficiency in many diverse modern applications that

use different motions, such as sliding and rolling in machinery. Typical examples include rolling element bearings, gears, engines, polishing and shaving. The sheer impact of tribology on everyone's day-to-day lives can take many forms, including energy loss, noise, control, environment, safety, quality of life and economics.

Figure 2-1 shows a schematic breakdown of the tribological factors that are very influential in tribology. Materials are chosen to perform under the worst-case scenario conditions, the direct surface-to-surface contact. Therefore, sub-factors such as basic mechanical properties, friction, wear resistance and compatibility all influence the selected material for operation.

Lubricants are the most common way of reducing tribological problems such as friction and wear. Therefore, factors including viscosity and chemical additives become crucial. Finally, the system's operating conditions can be influenced by any change in the mechanical design, potentially leading to severe friction and wear problems.

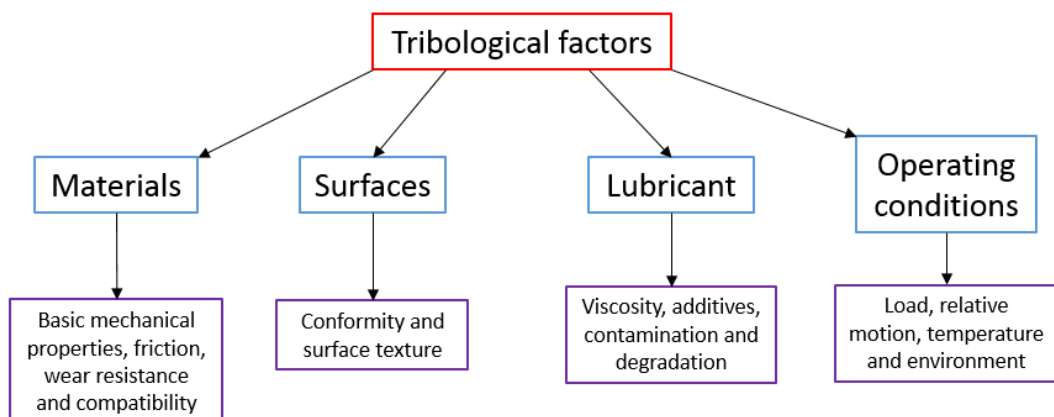


Figure 2-1 Main tribological factors which influence Tribology.

2.2 Contact mechanics

Inevitably in most situations, surfaces come into contact during operation, which makes the subject of contact mechanics between surfaces become an essential factor in tribology. As surfaces come into contact with one another, they suffer elastic or plastic deformation. Elastic deformation occurs when there is a simple linear relationship between stress and strain, which is reversible. In comparison, plastic deformation occurs when there is complex stress and strain relationship with stresses high enough to cause permanent surface deformation [14]. The factor which determines whether the contact behaves elastically or plastically is stress, which is influenced by the load applied, surface texture, conformity (high conformity = two parallel plates loaded against one another, low conformity = sphere loaded upon a plate) and mechanical properties of the materials (elastic modulus and Poisson's ratio). Hertzian was the first to investigate stresses in two elastic solid contacts in 1882 [14]. The Hertz theory is widely used for solutions in tribological problems, for example, a real contact area of rough surfaces, rolling and sliding contact, contact stiffness etc. However, it must be noted that Hertz's theory has assumptions based on the ideal properties of contact surfaces and conditions. These include contacting bodies being elastic and homogeneous, surfaces being smooth and non-conforming, surface shape not changing, and finally, a frictionless contact between the two surfaces, neglecting Van der Waals forces and adhesive interactions. Figure 2-2 depicts the schematic diagrams with pressure distribution for the basic Hertz contact models [15]. The assumptions made for the Hertz theory are often ill-advised in some tribological problems, as the ideal properties of contact surfaces and conditions do not occur in the real world.

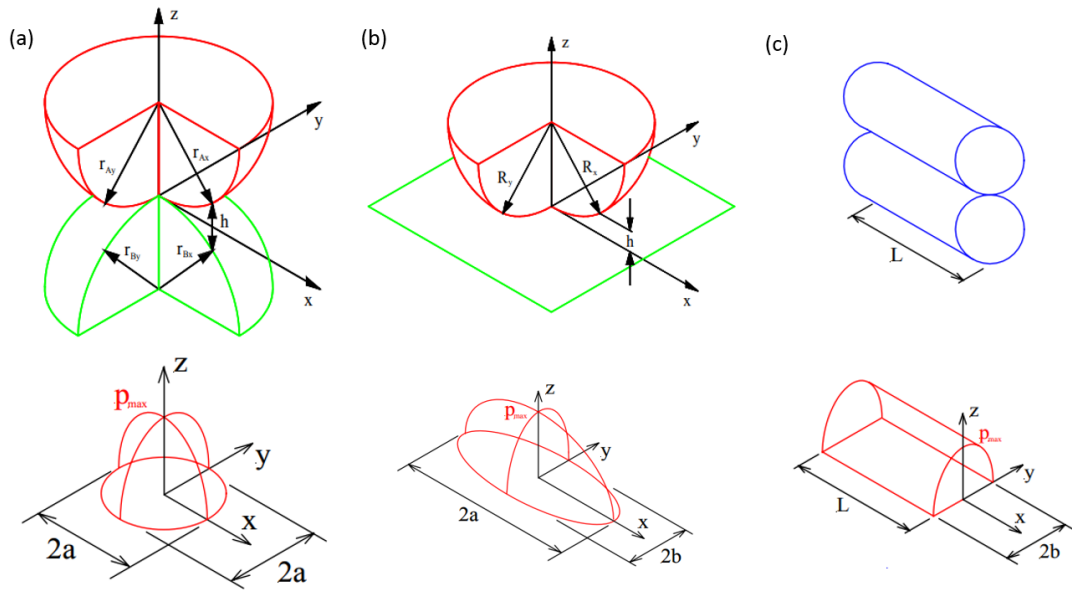


Figure 2-2 (a) Hertzian contact and pressure distribution between two elastic solids, (b) Hertzian contact and pressure distribution between elastic solid and rigid plane, (c) Hertzian contact and pressure distribution between two cylinders [15].

2.3 Fundamentals of Friction

Friction is the resistance one body encounters in moving over another [16]. Two classes of relative motion are involved in this definition of friction: sliding and rolling. In an ideal scenario of sliding and rolling, a force (tangential) is needed to move the main body (ball or cube) over a stationary counterface (plate). Therefore, the ratio between the normal load (W) and frictional force (F) is known as the coefficient of friction (μ), shown in equation 1, which is derived from the first law of dry friction.

$$\mu = \frac{F}{W} \tag{1}$$

There are three laws of dry friction, of which the first two can be dated back to Leonardo da Vinci and Amontons. All laws apply to most interacting surfaces

under dry friction, meaning no lubricant is present. The three laws of dry friction are [16];

1. Frictional force (F) is proportional to the normal load (W).
2. Frictional force (F) is independent of the apparent contact area (A).
3. Frictional force (F) is independent of the sliding velocity (V).

There have been many theories on mechanisms for how dry friction occurs between two surfaces when rubbing. The most commonly used theories are adhesion and ploughing, which consider rough surfaces and asperity influence. Both mechanisms can also combine as well as act individually, creating friction.

2.3.1 Adhesion

Adhesion was a theory created by Bowden and Tabor, assuming that when the two rough surfaces are loaded and rubbed, only the asperities tips come into contact with one another, as shown in Figure 2-3. Thus, the contact area is very small, and the pressure is high enough to plastically deform the asperity tips. From the assumptions made, Bowden and Tabor also proposed that if strong adhesion occurs at the asperity tips, their contacting material cold welds, meaning they fuse without needing heat. Another factor which impacts the dry friction in this theory is the shear to overcome the adhesion occurring, also known as junction growth [16]. This junction growth accounts for the increases in friction coefficient seen in experimentation compared to the simple theoretical value calculated. However, this theory is useful to a certain degree, as surfaces can become contaminated in practical situations by oxides or other contaminants. Any contaminated surface would change the

coefficient of friction in dry friction situation, so therefore this theory only explains adhesion on a perfectly clean surface.

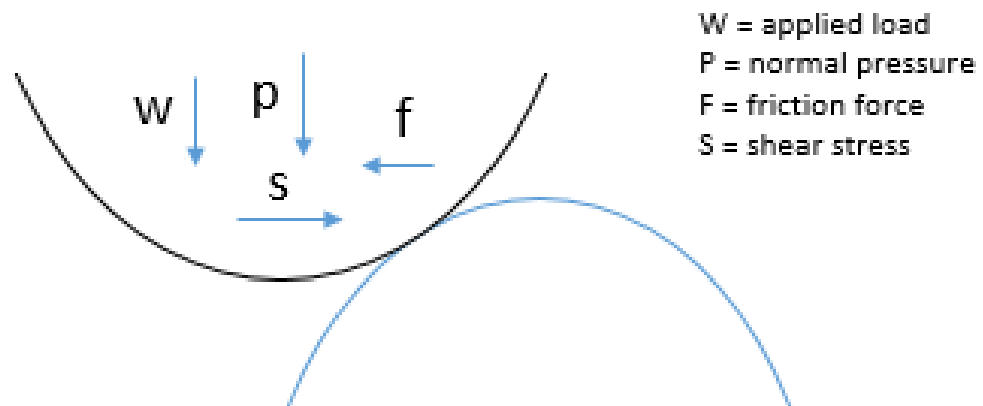


Figure 2-3 Adhesive asperity contact.

2.3.2 Ploughing

The second dry friction theory, ploughing, shown in Figure 2-4, suggests that friction occurs due to the ploughing out of a groove by a hard asperity by penetrating a softer surface material. Plastic deformation occurs as the hard asperity ploughs out the groove, and friction occurs due to resisting the deformation. Factors including geometry and hardness of the two surfaces significantly impact the coefficient of friction value during ploughing. However, to create a realistic analysis of ploughing dry friction, lots of detail regarding asperity geometry is required while also lacking the ability to reflect experimental observation [17].

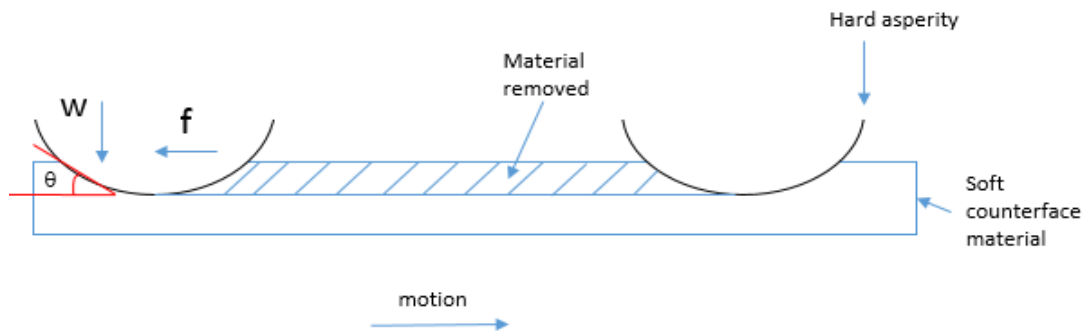


Figure 2-4 Ploughing of a groove in a soft counterface by a hard asperity.

2.3.3 Stick-slip

Another very important characteristic to consider in dry friction contact is static and kinematic coefficients of friction. The static coefficient of friction is defined as the friction to initiate motion; hence, the kinematic coefficient of friction is defined as the friction to maintain motion [18]. The terminology used in applications when static and kinematic friction occurs is stick-slip. The Stick phase occurs when the shear and coefficient of friction increase to overcome the static coefficient of friction, often denoted as μ_s . Once the static coefficient of friction is reached, the surfaces start to slide. In the slip phase, the surfaces start to slip at a low coefficient of friction, causing the stick phase to occur again, eventually leading to no relative motion, causing the stick phase to occur again. The kinematic coefficient of friction, often denoted as μ_k , is the average value of the slip phase. As depicted in Figure 2-5, the slip phase depends upon asperity height and slopes, sliding speed and elastic compliance of the surfaces [19].

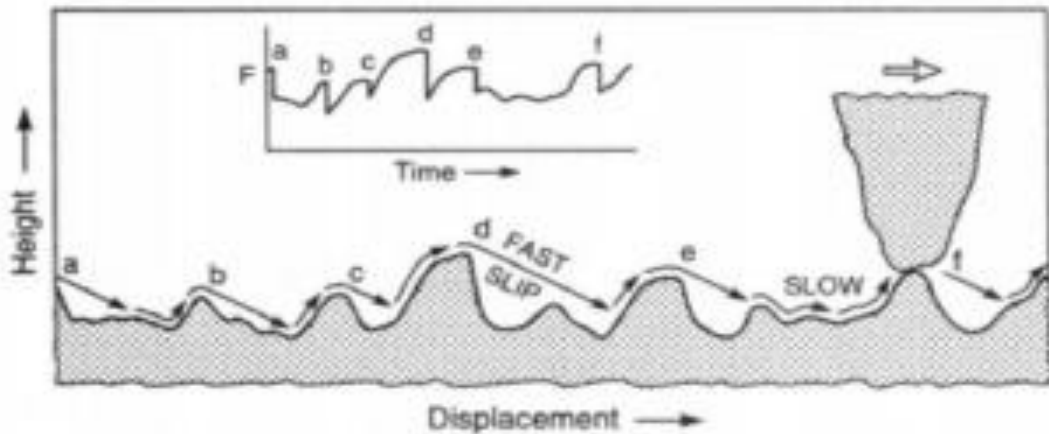


Figure 2-5 Rabinowicz stick-slip model [19].

The stick-slip mechanism can be very damaging to machine systems. High friction, noise, wear, and a loss of accuracy are some problems that can occur due to stick-slip. Surface interaction with high conformity over a large area is more susceptible to stick-slip. However, steps can be taken to reduce the chance of stick-slip, which include reducing the conformity interaction of the surfaces, choosing two materials with similar static and kinematic friction coefficients, and using a lubricant and a surface coating.

2.3.4 Frictional Heating

The final factor to consider in friction is heat. Whenever friction occurs, some of the mechanical energy is transformed into heat. Heat release will occur with a rise in temperature due to work done against friction, often known as frictional heating. The temperature at the asperity contacts is significantly higher than the average surface temperature due to friction occurring at asperity tips. Therefore, there is often a rise in temperature at the asperity tips during friction, referred to as flash temperature. It should be noted, however,

that frictional heating is not applicable under the third friction law. Thus the third law is less applicable in tribology than the first two [20].

2.4 Fundamentals of Wear

Wear can be defined as the progressive loss of material from the operating surface of a body occurring as a result of relative motion at its surface [21]. However, this is a very old definition. More new definitions do not limit it to just material loss but define it as a progressive change to a part that adversely affects damage [22]. Wear is very important to understand in tribology as it has major impacts on reliability, useful life, cost etc., in any manufactured component. The same for friction; in total, wear has three main laws, which include [15];

1. Wear increases with sliding distance (x).
2. Wear increases with the normal load (W).
3. Wear decreases as the hardness of the interacting surfaces increases (H).

Unlike the first two laws of friction, all the wear laws are not generally applicable to most situations. However, from the three laws of wear, an equation, shown in equation 2 for the volume loss of material (V) removed during wear can be deduced. P_0 is the yield pressure, W is normal load and x as sliding distance.

$$V \propto \frac{Wx}{P_0} \quad (2)$$

Like friction, there are many theories about the origin of wear and its mechanisms. The two most important mechanisms for wear are adhesion and abrasion. Figure 2-6 shows a schematic of the other different wear

mechanisms, including adhesion and abrasion, along with their effects on surface damage and wear debris generation. The effects of surface damage, such as fretting, which has more than one mechanism, are known as synergism. For example, abrasion, adhesion, and corrosion synergise together to create fretting.

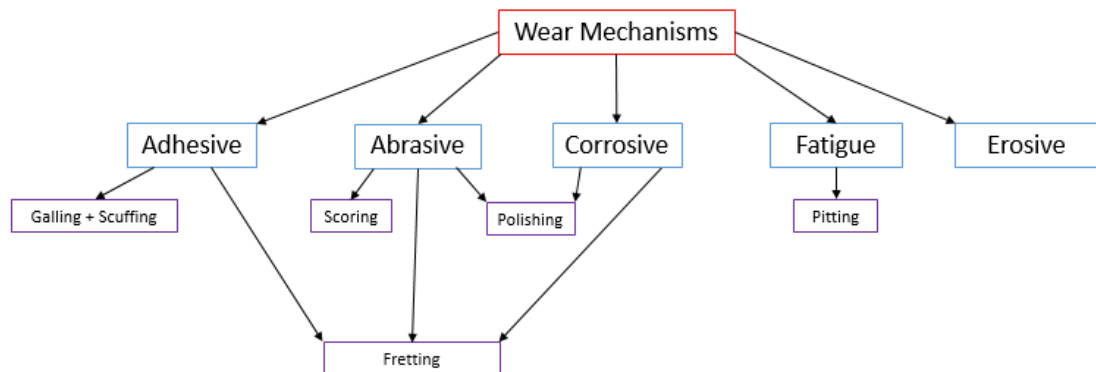


Figure 2-6 Wear mechanism processes.

As an overall subject, out of the three that create the science of tribology, it is generally accepted that wear has the most need for control but is also the least understood. It must be noted that corrosion and fatigue are not considered forms of wear but elements of wear. Corrosion is not caused by relative motion, while fatigue is more of a body phenomenon where contact nor relative motion are not required for the mechanism [11].

2.4.1 Adhesion

Adhesion is the most common form of wear but also the least preventable. The wear theory of adhesion was first proposed by Archard in 1951 and helped develop the three laws of wear [12]. It was shown that when the two interacting surfaces are rubbed against one another, only the tips of the asperities come into contact. The contact area is very small. Therefore, the

pressure is high enough to cause plastic deformation of the asperities, and cold welding, as shown in Figure 2-7 [11]. As the two surfaces in contact are forced to move, some of the original material will deform so that fragments of the softer material are welded and plucked out by the harder material [13].



Figure 2-7 Adhesion wear theory for a single asperity contact [11].

As stated before, the Archard adhesion theory helped develop the laws of wear. Assuming that failure occurs within the material with the wear particle being hemispherical, the wear particle (V) volume can be calculated, equation 3. This equation is known as the Archard wear law, where k is the dimensionless wear coefficient. Surface material properties, structure and adhesion strength of the contacting asperities are all factors that will influence the wear coefficient in a given situation.

$$V = k \frac{Wx}{3p_0} \quad (3)$$

Typically, the wear mechanism adhesion is known to produce galling, scuffing, and the synergism of fretting effects upon surfaces. Both galling and scuffing are forms of severe adhesive wear. Large material particles are removed or plastically deformed on the surfaces, causing failure. Frictional heating often occurs due to galling or scuffing, which increases the temperature. Scuffing is used when a lubricant is present; therefore, galling is used in dry contact.

2.4.2 Abrasion

The abrasion wear theory is adapted from the dry friction abrasion theory with many similarities. Wear is generated by a hard particle ploughing out a groove into a soft counterface. Adapting the Archard wear law, the total wear volume (V) for the whole surface can be calculated using equation 4, assuming that the ploughing results in wear rather than plastic deformation [23]. θ is the asperity slope as shown in Figure 2-4.

$$V = k_{abrasive} \frac{W_x}{3p_0}, \text{ where } k = \frac{6 \tan \theta}{\pi} \quad (4)$$

Generally, this equation applies to two types of abrasive wear, two-body and three-body. Two-body abrasion is the more straightforward mechanism of the two. It occurs when one hard particle ploughs out a groove into a softer counterface. For two-body abrasion between two surfaces, two requirements must be met. The asperities in contact must have a high value of θ , and one surface must be harder than the other. Abrasive wear can also occur due to a hard particle being trapped and entrained between two surfaces, known as third body abrasion. This abrasion can occur due to trapped wear debris, dirt contamination, corrosion products, etc. Typical values of two-body compared to third-body abrasion found in experiments are higher, suggesting that two-body is much more damaging than third-body abrasion. Solutions to prevent two-body abrasion have already been put into place regarding machinery, paying particular attention to surface finish and material selection. While third-body abrasion is preventable by filtration, effectively removing the particles from the surface [24].

Scoring, fretting and polishing are the surface effects that the wear mechanism abrasion is known to cause [24]. Scoring is seen as a pattern of scratches on the surface as a direct result of severe abrasion, which can lead to failure. Polishing is different from the usual surface effects caused by the wear mechanisms, as it can be used to benefit an application. A smooth surface finish can be achieved via polishing using mild two-body abrasion. However, if the polish surface effect occurs in the wrong application, it can lead to failure. For example, polished smooth surfaces are very poor at retaining lubricants.

2.4.3 Fatigue

Fatigue wear is a unique mechanism compared to adhesion and abrasion since wear can occur without direct contact between the two surfaces. There are two mechanisms of fatigue wear: high and low cycle fatigue [25]. A component with high-cycle fatigue has a high number of cycles before fatigue failure occurs, meaning that it has a long-life span. Alternatively, a component with low-cycle fatigue has a low number of cycles before fatigue failure occurs, meaning the life span is short. In a rolling contact, fatigue wear occurs from the cyclic variation of the shear stress at subsurface locations, which results in fragments detaching from the surface. Fatigue wear in sliding contacts is due to contact between the asperities but without physical contact between them. The presence of a lubricant can repeatedly hit the asperities during operation, eventually leading to asperity failure due to fatigue. Pitting is the most common surface effect that the wear mechanism fatigue causes.

2.4.4 Erosion

Erosive wear is the mechanism of material removal by hard solid particles in a fluid that bombard the surface at high velocity. Parameters affecting erosion wear are impact velocity, angle and hardness of the particles. The wear rate is directly proportional to the kinetic energy of the particles. Figure 2-8 shows the erosion rate for brittle and ductile materials. Brittle materials exhibit good resistance at low angles, such as glancing blows and impacts at shallow angles, but have more severe damage under normal impacts. These impacts cause surface cracks in brittle materials, which conjoin, forming wear particles. Ductile materials resist normal impacts but have a maximum erosion rate at an impact angle of 20°. Repeated impacts upon ductile materials usually lead to fatigue wear [26].

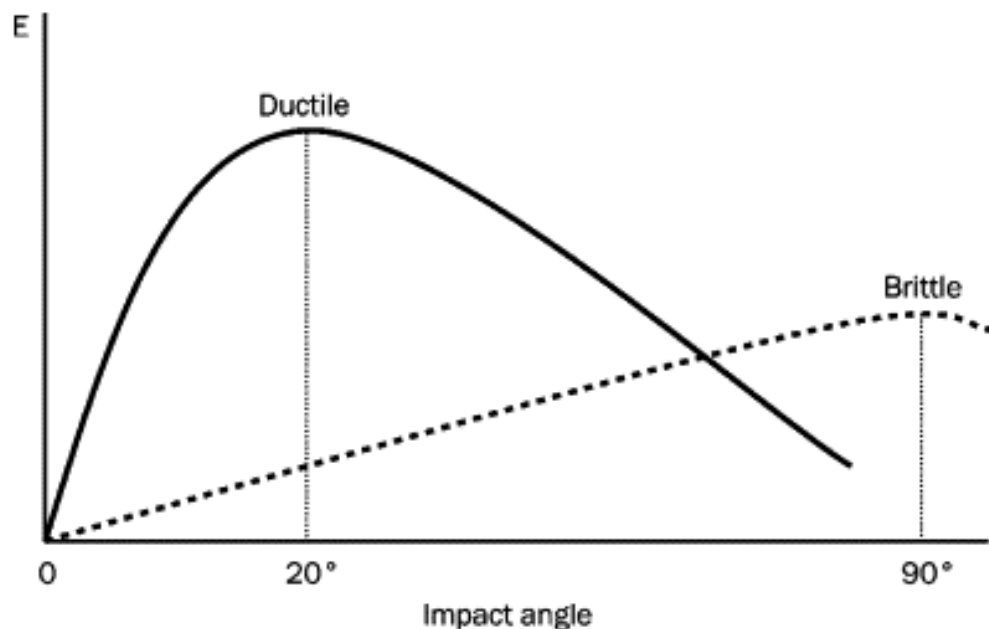


Figure 2-8 Erosion rate for brittle and ductile materials [26].

2.5 Lubricants and Lubrication

Lubrication is the effective interposition of a substance between two bodies to reduce friction and or wear during operation. Any liquid, gas or solid substance effectively interposes between two surfaces is called a lubricant. The critical functions of a lubricant are to lubricate, cool, transmit power, clean, seal and protect. Understanding the interactions between the surfaces and lubricant is vital to ensure the components have a satisfactory life span. All moving parts with lubricated contacts travel through different lubrication regimes during operation. In total, there are four known regimes: boundary, mixed, Elastohydrodynamic (EHL) and hydrodynamic (HD) [17]. The main factors that influence the lubricant are shown in Figure 2-9.

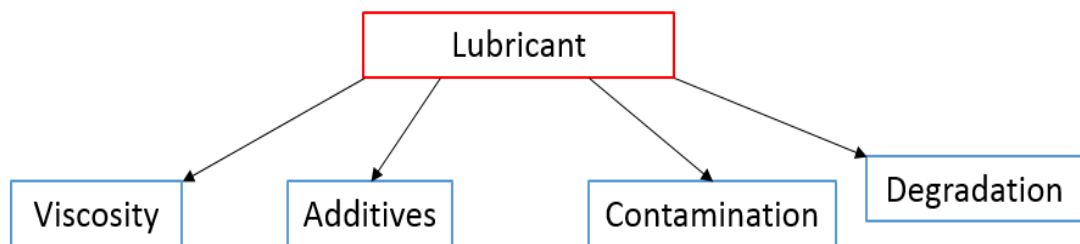


Figure 2-9 Lubricant influencing factors.

2.5.1 Viscosity

The main physical property of oil is viscosity, a fluid's resistance to shear. If the temperature of the fluid is low, it naturally becomes very thick (higher viscosity), and with high temperatures, the fluid naturally becomes very thin (low viscosity). In every application that uses oils as lubrication, It is a critical property as it influences factors such as oil film thickness, which is critical for preventing friction and wear at high and low temperatures.

2.5.1.1 Measuring Viscosity

Two methods are used to measure the fluid's viscosity, dynamic and kinematic. Dynamic, also known as absolute viscosity, is the fluid's resistance to shear when subjected to a force. Kinematic viscosity is the fluid's resistance to flow under forces of gravity and is often defined as the ratio of absolute viscosity to density. The units of these different viscosities can be found in Table 2-1. To measure dynamic viscosity, ball bearings' magnetic properties are utilised using a viscometer to measure the speed at which it travels through the fluid. Alternatively, using time sensors to measure kinematic viscosity, the gravitational force is utilised to measure the rate at which the fluid travels from one point to another. The dynamic viscosity technique is usually used as an on-site test/screening as it has problems with consistency within its results. While the kinematic viscosity technique is commonly used to analyse used lubricants, it has become more dominant due to its ease of use, with most laboratories containing an auto viscometer used to measure kinematic viscosity. Along with the viscosity measurement, the temperature, usually 40°C and 100°C, at which the viscosity is measured is vital to record, as the temperature significantly impacts the fluid's viscosity.

Table 2-1 Units of measurements for viscosity.

Viscosity	Cgs Units	Common Unit	Derivation
Dynamic (Absolute)	Poise	Centipoise (1P = 100cP)	$1 P = 1 g \cdot cm^{-1} \cdot s^{-1}$
Kinematic	Stoke	Centistokes (1St = 100cSt)	$1 St = 1 cm^{-1} \cdot s^{-1}$

2.5.1.2 Effect of Shear

Along with temperature, shear is another factor which affects a fluid's viscosity and must be considered when measuring or testing a fluid. If the fluid's viscosity is independent of the shear force applied, it is called a Newtonian fluid. However, if the fluid's viscosity profile changes regarding the shear force applied, it is called a non-Newtonian fluid. A visual representation of the changes in viscosity with shear force can be found in Figure 2-10. When measuring the viscosity of a near-Newtonian fluid, most lubricating oils, it does not matter which technique, kinematic or dynamic, is used as there is little difference between them. However, with non-Newtonian fluid, the fluid shows a high viscosity when the shear force is low using the kinematic technique. Alternatively, when the fluid's shear force is high, using the dynamic technique, the viscosity of the fluid decreases.

Special care must be taken when measuring the viscosity of a non-Newtonian fluid. Typical lubricating oils which display non-Newtonian properties are degraded oils, oil emulsions and oils with viscosity modifiers [27,28].

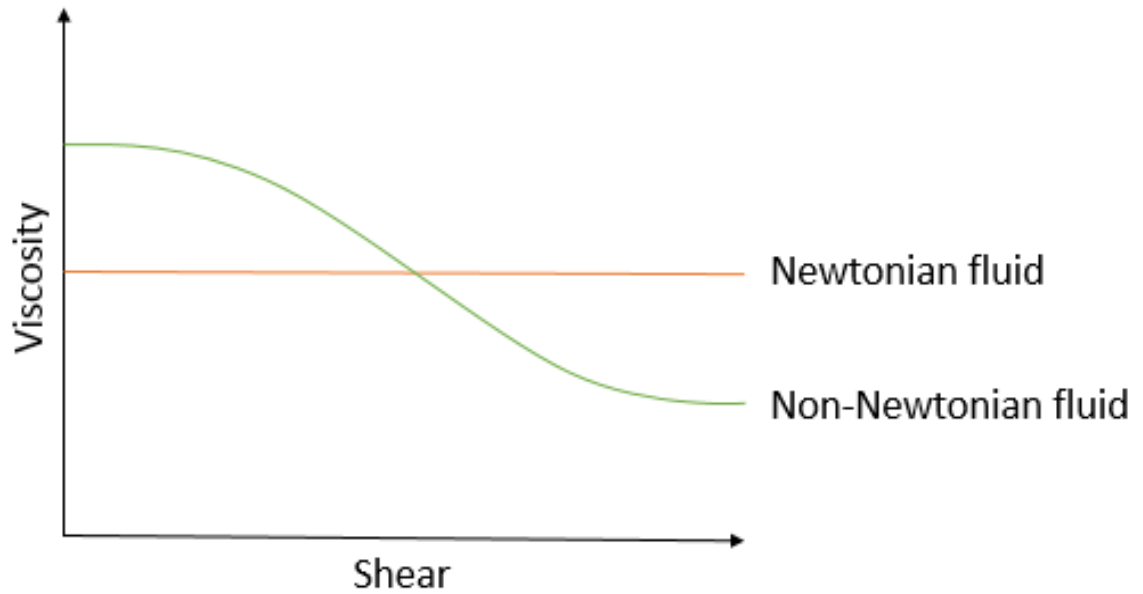


Figure 2-10 Graph of the relationship between viscosity and shear.

2.5.2 Base oils & Additives

According to the American petroleum institute (API), base oils are categorised into five groups. Groups 1 to 3 are mineral oils with different sulfur, saturates and viscosity indexes. While group 4 is polyalphaolefin (PAO) synthetic lubricants, and group 5 is any base oil that is not classified through groups 1 to 4. Table 2-2 shows the different base oil groups according to API.

Table 2-2 API base oil categories.

Category	Classification	Contents			Viscosity index
		Saturates, Mass %	Aromatics, Mass %	Sulfur, ppm	
Group 1	Solvent-refined mineral oil	65-85	15-35	300-3000	80-119
Group 2	Hydro-processed mineral oil	≥ 93	< 7	5-300	80-119
Group 3	Hydro-cracken mineral oil	≥ 95	< 5	0-30	≥120
Group 4	Oligomers of 1-alkene	-	-	-	-
Group 5	All fluids not included in groups 1 to 4	-	-	-	-

Additives are chemicals added to the base oil to increase the performance of the oil, which would not be achievable with the base oil alone. Factors which additives can reduce, maintain, and minimise greatly are Friction, wear, viscosity, fluid properties, contaminants and cleanliness. The working mechanisms of the additives can be split into two categories: chemical and physical, Table 2-3. Chemical additives can be described as additives which require a chemical reaction to perform their function and are usually irreversible reactions. Thus, physical additives can be described as additives which do not require a chemical reaction to perform their function, with the physical changes needing less activation energy and can be reversible. Typical chemical additives in engine oils are anti-wear agents and friction modifiers, with viscosity modifiers being the most common physical additive. The most common additives found in engine oils, with a basic description and example of each, are shown in Table 2-4. Being able to fully understand how

these additives work alone and interact with each other is extremely important [29].

Table 2-3 Classification of the most common oil additives [29].



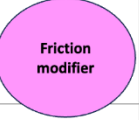
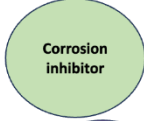

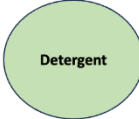



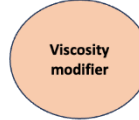
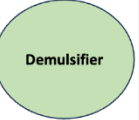
Working Mechanism	Working Site			
	Interface			Bulk
Chemically				
Physically				
				
	Working Function	Tribo-improvers	Maintainers	Rheo-improvers

Table 2-4 Most common chemical additives found in engine oils [28].

Type of Chemical Additive	Basic description of the function	Most common examples
Antioxidants	Reduces the rate of oxidation occurring in the lubricant by disrupting the three-step oxidation process by decomposing peroxide radicals or reacting with free radicals.	Zinc Dialkyl dithiophosphates (ZDDP).
Friction modifiers	Reduces the friction that occurs when surfaces come into contact by surface film formation.	Molybdenum dithiocarbamate (MoDTC), Organic friction modifiers.
Anti-wear additives	Reduces the wear between rubbing surfaces under a load.	ZDDPs.
Detergents	Reduces insoluble deposits formed on the surfaces at high temperatures.	Calcium or magnesium compounds.
Dispersants	Keep insoluble material suspended within the oil.	Ashless (non-metal) compounds.
Viscosity modifiers	Reduces the decrease in viscosity due to the increase in temperature.	Polymethacrylate polymers (PMAs)
Pour point depressants	Reduces the pour point of oils by keeping the lubricant flowing at low temperatures.	Paraffinic compounds.

2.5.3 Lubrication Regimes

The example used to explain the lubrication regimes in a real application relevant to this thesis is engine oils and the different lubrication regimes that occur during the engine's operation. As the engine is started and oil is pumped through the system, all the moving parts' lubricant contacts travel through different lubrication regimes. The Lubrication regimes found in ICEs can be categorised into four main regimes: boundary, mixed, EHL and HD. Boundary and hydrodynamic regimes are known as the two extremes of the forms of

lubrication. The Stribeck curve, a fundamental tool in tribology, enables engineers to visualise the overall view of friction variation in the different lubrication regimes.

Lambda ratio (λ), equation 5 is a widely used term in tribology to define the relationship between the lubricant's minimum film thickness and the contact material's surface roughness. Each lubrication regime is associated with a different range of lambda ratio values, enabling the engineer to determine where a component's lubricant regime will be during operation.

$$\lambda = \frac{h_{min}}{\Sigma R_a} \quad (5)$$

A boundary lubrication regime is where the lubricant in operation does not separate the two surfaces, developing similar features to dry contact. Figure 2-11 shows a schematic of the boundary contact between two surfaces. Friction and wear are characterised by the surface materials and boundary films formed on the surfaces. Bulk fluid properties such as viscosity become less important as boundary films reduce friction and wear. Boundary lubricants, such as ZDDP, form films on the surfaces during rubbing. The strength of these films can be split into three categories, increasing order of film strength; physically absorbed layers, chemically absorbed layers and chemical reaction. The ZDDP tribofilm is chemically reacted onto the surface for the greatest strength, which enables it to be used for lubricating in harsh operating conditions. Usually, boundary lubrication occurs at low speeds, high loads, and low-viscosity environments. $\lambda < 1$

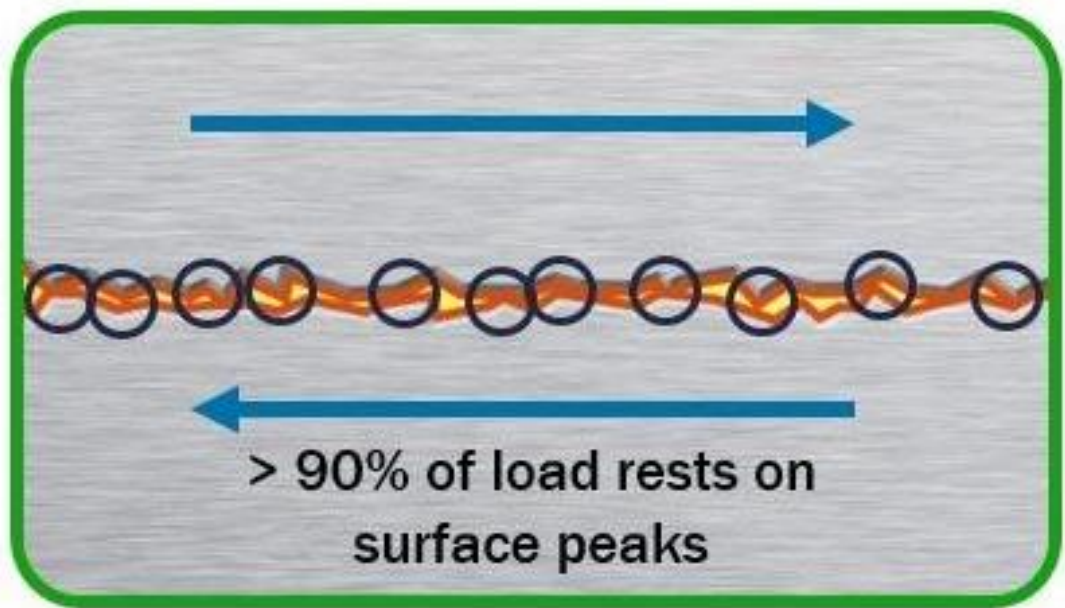


Figure 2-11 Schematic of the boundary lubrication regime [31].

The mixed Lubrication regime is a mixture of the boundary and HD regimes shown in Figure 2-12. Regions can be seen where there is separation due to lubrication and regions where asperities are in contact between the two surfaces. The physical properties of the bulk lubricant and the boundary film lubricant's chemical properties are equally important. $1 < \lambda < 4$

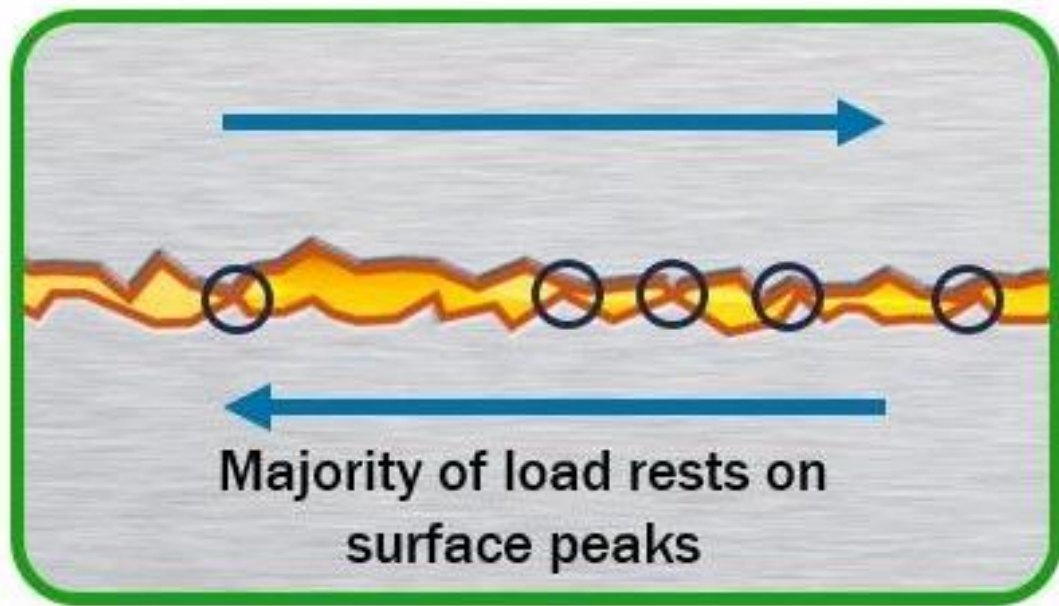


Figure 2-12 Schematic of the mixed lubrication regime [31].

The EHL lubrication regime is very similar to the HD regime in that the lubricant fully separates both surfaces. However, the difference is that local elastic deformation occurs at the surfaces with an increase in viscosity due to high contact pressures. The EHL regime usually occurs in low conformity and highly loaded components, such as gears. $4 < \lambda < 10$

The HD lubrication regime occurs when the lubricant with no elastic deformation fully separates the two surfaces. The schematic of this regime is shown in Figure 2-13. This regime is the ideal form of lubrication, where low frictional force and minimal wear occur. The lubricant's bulk property governs the contact's characteristics rather than the chemistry of the boundary lubricant. Any friction which occurs is solely down to the shearing of the lubricant. Usually, the HD regime occurs in high speeds, low loads, and high-viscosity environments [30–33]. $10 < \lambda$

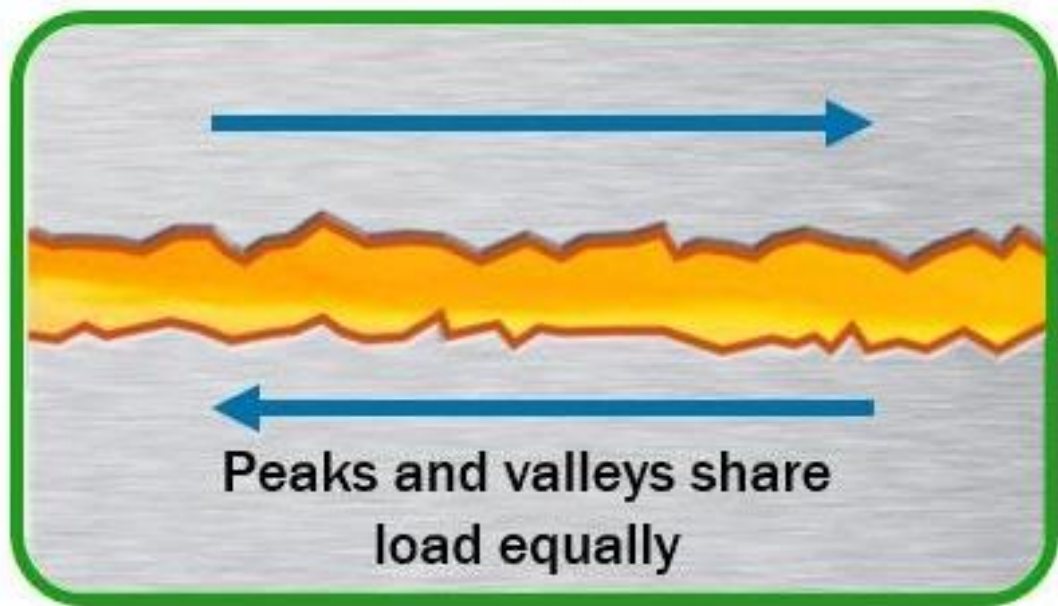


Figure 2-13 Schematic of the hydrodynamic regime [31].

2.6 Summary

This chapter has introduced the fundamental principles which drive the field of tribology. The three main aspects of tribology, friction, wear and lubrication, were explained in detail. All the aspects of tribology discussed in this chapter are the fundamental principles behind the science within this thesis.

Chapter 3 Literature Review

This section of the thesis will introduce the tribological issues within ICEs, the measures to increase fuel economy and review the research conducted on the role tribofilms perform when trying to prevent these issues.

3.1 Introduction to Internal Combustion Engines

3.1.1 Tribological Problems

Tribological issues can be found in any component with moving parts, of which an ICE is a prime example since it has multiple components with reciprocating parts. However, friction also occurs within the ICE via tire-road contact, transmission systems, and brake contact. Figure 3-1 shows the breakdown of a passenger car's significant contributors to friction losses [34]. The total friction loss of the mechanical power is 33%.

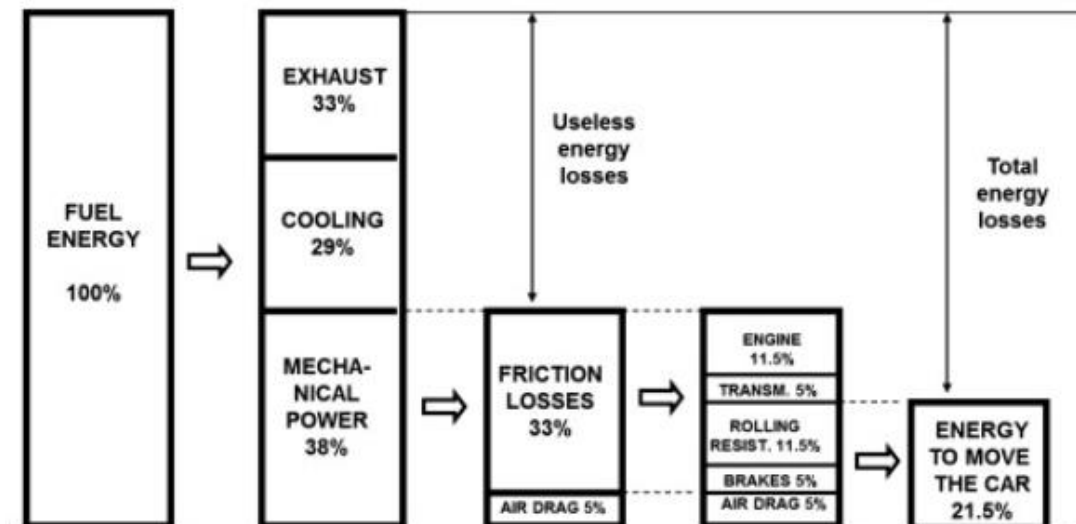


Figure 3-1 Passenger car energy consumptions breakdown [34].

For a passenger car, the ICE is the most crucial part since it is the system that converts fuel to usable energy. Previous research has shown tribologists how much energy is needed to overcome friction within the main components of an ICE. The ICE components can be split into three main categories: piston assembly, valve train, bearings, and seals. The breakdown is as follows; 38-68% is depleted via the piston assembly, 20-44% via bearings and seals, 3-34% via the valve train, and 10% via pumping and hydraulic viscous losses [34]. All the components mentioned so far exhibit different lubrication regimes when in operation. Some components have multiple regimes, while others usually have one regime that dominates after a specific time during the running. The HD regime dominates engine bearings and seals, while the mixed regime dominates the valve train. However, the piston assembly is much more complex than the other components mentioned since the different parts, for example, the piston rings, can undergo all the different regimes, from boundary to HD and experience significant variations in speed, load, and temperature. Previous research shows that the piston assembly tribocontacts undergo 40% HD lubrication, 40% EHD sliding lubrication, 10% mixed and 10% boundary lubrication [35].

3.1.2 Preventing Tribological Problems

The main contributor to the tribological issues found within an ICE is friction. The phenomenon of wear occurs as a direct result of friction between two moving surfaces in contact with one another. Friction can be split into two categories; contact friction and viscosity friction. Contact friction is the friction resulting from metal-on-metal contact occurring, and viscosity friction is the friction that occurs between the oil and the surfaces when in operation, which is mainly influenced by the film thickness of the oil.

Multiple methods are currently in place to reduce friction and wear on the ICE components. The two main areas focused on primarily in recent research are; lubricants, surface treatments, and coatings. This thesis will focus entirely on lubrication.

3.1.2.1 Lubrication

Lubrication is the most common way of reducing friction and wear between two moving surfaces. For an ICE, the lubricant used is oil. The critical functions of engine oil are to reduce friction, protect components against wear, and excellent frictional parts, remove impurities and hold gas and oil leakage. Upon engine start-up, the engine oil is pulled through a strainer from the oil pan via the oil pump to remove large contaminants in the oil. Then it passes through a filter and is sent through channels to numerous components like the pistons and bearings. Finally, the engine oil goes down to the oil pan using gravity, which repeats the cycle [36]. A visualisation of the flow of engine oil through the engine to the various components is shown in Figure 3-2.

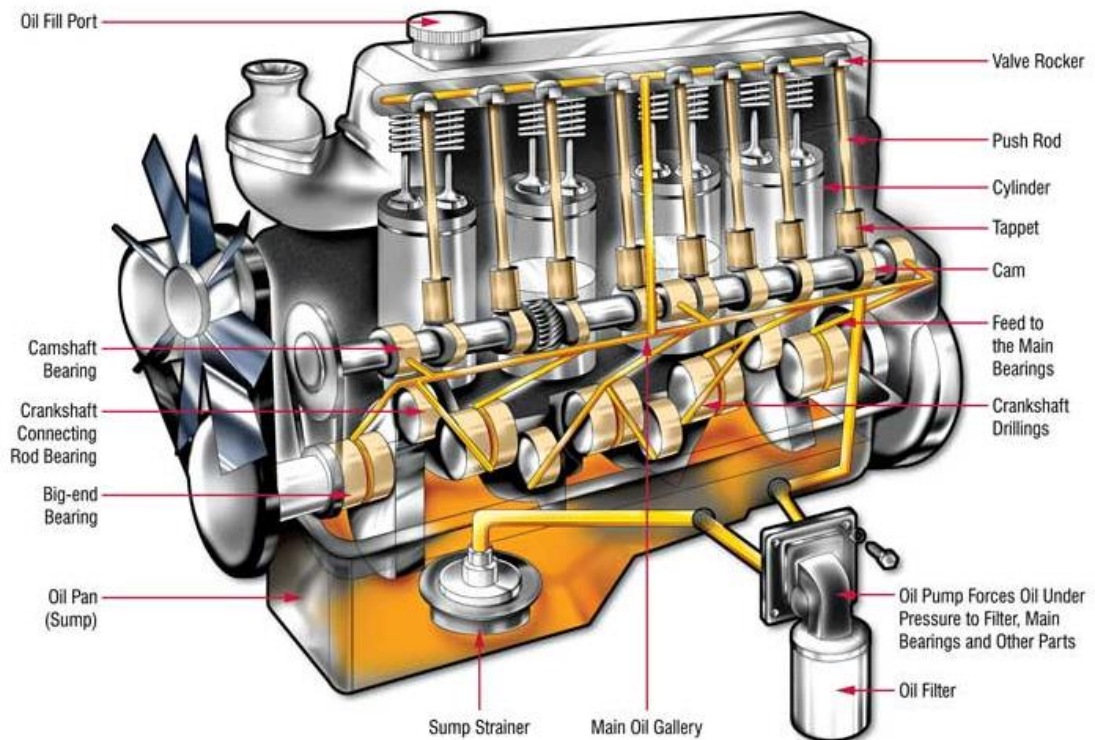


Figure 3-2 Oil flow cycle through an engine [36].

3.2 Increasing Fuel Economy

As explained in the introduction, the main drive for OEMs, besides reducing CO₂ emissions, is to increase a car's fuel economy or decrease fuel consumption. These two terms are widely used in the industry, but there can often be confusion between the two. Fuel economy is the distance a vehicle can travel with a gallon of fuel, with units of miles per gallon. This term is mainly used in the United States to communicate with the public. Fuel consumption, however, is widely used as an engineering measure. The fuel consumed per 100 kilometres can measure volumetric fuel savings [37]. Figure 3-3 displays the relationship between fuel economy and consumption.

It must be noted that there is not a proportionate relationship between improving fuel economy and decreasing fuel consumption.

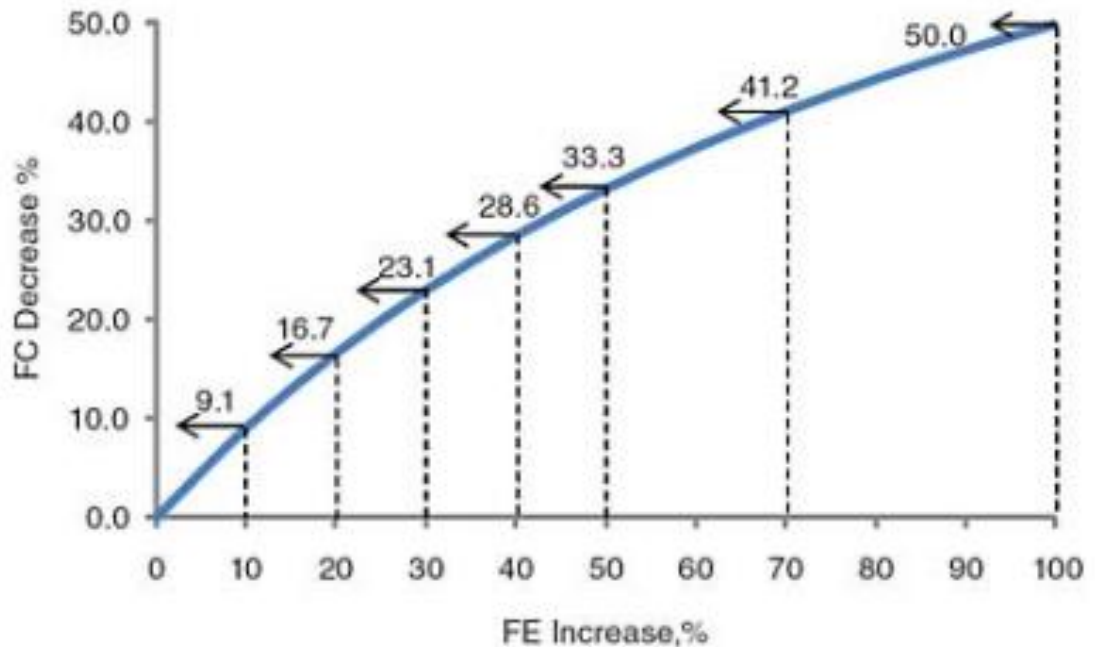


Figure 3-3 Percent decrease in fuel consumption as a function of percent fuel economy increase [37].

3.2.1 Low-viscosity Engine Oil

The primary approach to increase fuel economy is to reduce the friction losses in the tribo-contacts of the engine. It will improve the engine's efficiency, directly reducing the CO₂ emissions produced. As stated in a previous section, a lubricant is used to reduce friction within an ICE. However, to increase fuel economy further, the friction has to be reduced even more. The most proven way is to lower engine oil viscosity [38].

Understanding how lowering the viscosity can increase fuel economy, engine friction and lubrication is critical. A lower viscosity oil will increase the oil's pumping ability to the engine start-up components. It reduces the time that metal-on-metal contact occurs, thus reducing friction and wear. Thinner films

are also formed in HD and EHD lubrication regimes, reducing the oil's viscous drag and decreasing friction. As shown in Figure 1-2, all the major components of the ICE undergo different lubrication regimes. Most of the components already mentioned, such as piston assembly and bearings, mainly sit within the HD lubrication regime. The valve train is mostly within the mixed lubrication regime during operation. Therefore, reducing the oil's viscosity will reduce the friction between components where HD, EHD, and mixed regimes occur to a certain extent [39]. The impact of oil viscosity reduction in the mixed regime is shown in Figure 3-4. Decreasing oil viscosity decreases the oil film thickness and lambda ratio, directly leading to increased friction.

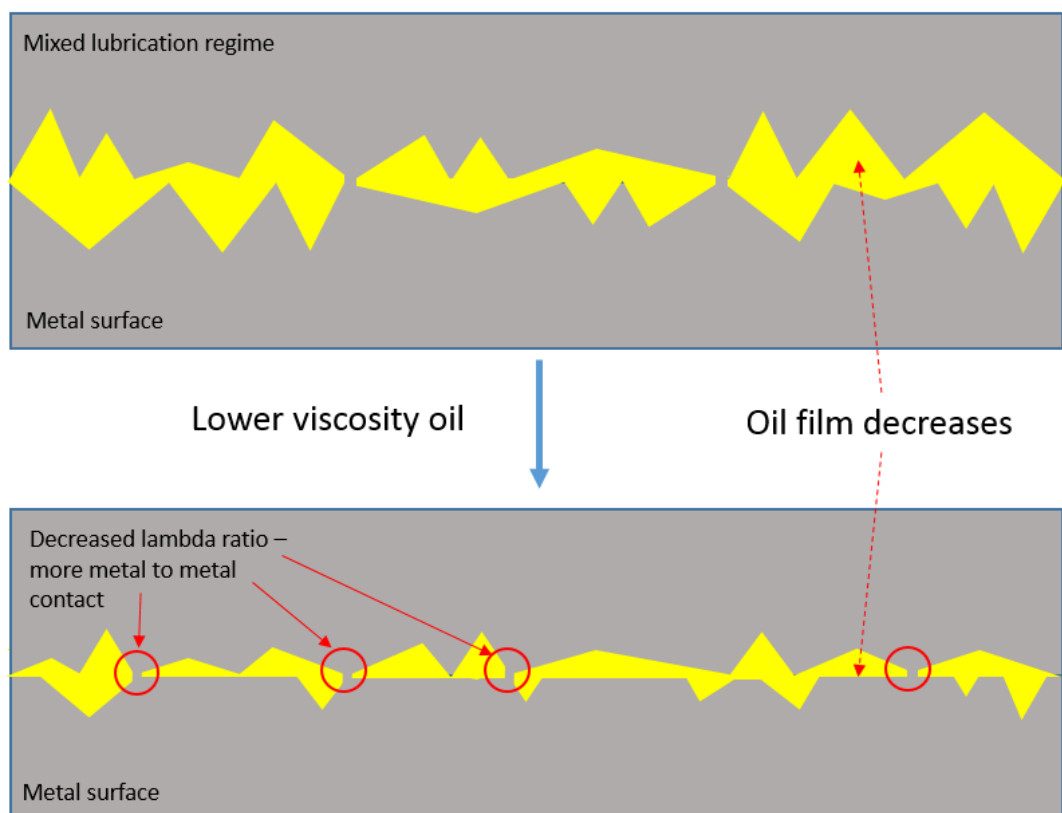


Figure 3-4 The effect of lowering viscosity on the tribo-contact of two surfaces.

There has been extensive research into the fuel economy improvements that lower-viscosity engine oil can incur. A review of the trends in engine lubricants over the past 10-15 years concluded that today's lubricants perform far better than their counterparts over the previous decade [40]. Particular attention still has to be paid to older technology engines on the road and newer technology engines. The newer formulated oil specifications need to be compatible with older engines and meet the newer specifications. However, this can be challenging due to the new chemical limits of sulfur and phosphorus. Previous research has shown that a 2.75% fuel efficiency increase can be achieved using an SAE 5W-20 oil compared to an SAE 10W-30 [6]. Lowering the viscosity even further still produces positive results, a 1.5% increase using a 0W-20 in accordance with ILSAC GF-2 standards compared to a 5W-30 [7]. Other research has also investigated how low viscosity engine oil can affect fuel economy [41,42]. Both produced similar results and concluded that lowering the viscosity produces excellent fuel-saving performance and fuel economy improvements.

However, lowering the oil's viscosity shifts the components on the Stribeck curve to the left. There will be a reduced minimum film thickness value for components contacts. For example, the valve train and piston ring, which operate in boundary and mixed regimes, will have more tribo-contacts in the boundary regime. Lowering the oil's viscosity also increases the entrainment speed required to enter higher lambda ratio lubrication regimes.

When the viscosity of the engine oil is lowered to counteract the lambda ratio reduction, chemical additives are incorporated into a base oil, as explained in a previous section. In the boundary lubrication regime, surface-active

additives such as ZDDP, MoDTC and detergents become very important. The synergism between these additives must reduce friction and wear in the boundary and mixed lubrication regimes to the same standard or improvement compared to the higher viscosity engine oils to enable the overall friction reduction, which will come from components operating in the EHD and HD lubrication regimes.

3.3 ZDDP Additive

ZDDP in engine oils is a multi-functional additive. They can act as antioxidants, corrosion inhibitors, and anti-wear additives, their primary function. A tribofilm is formed on the two surfaces during rubbing from its molecular structural formula shown in Figure 3-5 [12]. It performs its primary function in the boundary lubrication regime where the surface-to-surface contact occurs.

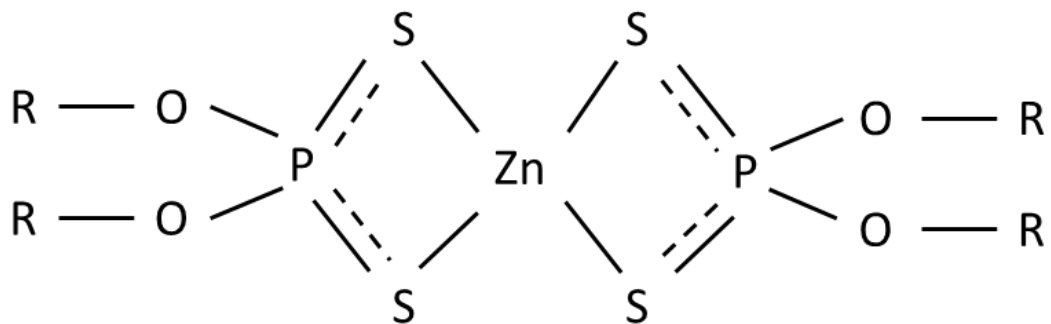


Figure 3-5 Chemical structure of ZDDP [12].

The literature has well-documented how ZDDP functions as an anti-wear additive. There are three main ways; forming a mechanical protective film, removing corrosive peroxides, and digesting hard abrasive iron oxide particles [43]. The first mechanism is a film formed on the surfaces when rubbing

occurs. It prevents the surfaces from directly coming into contact, reducing adhesion and stresses at the asperity tips. Another mechanism concludes that the ZDDP tribofilm reacts with any peroxides in the lubricant to prevent them from wearing the surfaces in a corrosive manner. The final mechanism suggests that iron oxide particles are digested into the tribofilm, thus reducing the chance of any 3rd body abrasion. However, it is known that this is the most controversial technique, as there has been little evidence to suggest it is happening.

Extensive research into ZDDPs' mechanisms, functions and interactions with other additives has been conducted for more than 60 years, but not everything is known about ZDDP as an additive. Due to new environmental legislation, the need to reduce metallic compounds within engine oil additives and the phosphorus and sulfur pollutants is becoming more apparent. The ZDDP breakdown products also shorten the catalytic converters' lifetime [44]. Thus, new research is being conducted to find alternative solutions to anti-wear additives to comply with the new legislation. However, the new anti-wear additive has to perform just as well as the current solution. Therefore, there is still a significant need to understand the defining mechanisms of how ZDDP performs its function as an anti-wear additive and its interactions with other additives.

3.3.1 Tribofilm formation

The formation of the tribofilm from ZDDP on the surface during rubbing is shown in Figure 3-6 [43]. It consists of three layers: chemically reacted film, the chemical adsorbed layer and the physically adsorbed layer. Various

research using different techniques, such as the SLIM unit, has shown the film thickness of the ZDDP tribofilm to be in the range of 100-150nm [45,46].

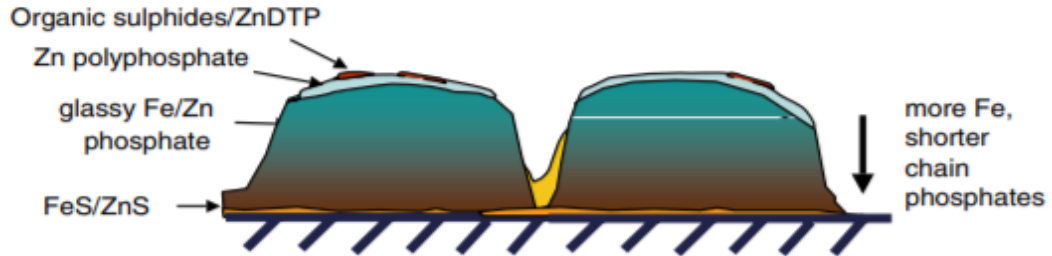


Figure 3-6 ZDDP tribofilm layers [43].

There has been extensive research into the mechanism behind ZDDP forming a tribofilm onto a surface to reduce wear. Previous literature has suggested how the ZDDP forms upon the rubbing surfaces; pressure, flash temperature, triboemission and shear stress.

The theory that very high pressure can affect the formation of the ZDDP tribofilm has been proposed in applications such as rolling bearings and gears [47]. Nanometre resolution on a ZDDP tribofilm shows that the films on top of the asperities where pressures are high are harder than films formed between the asperities. Flash temperature is the heat generated when two surfaces rub against one another, which has been proposed to affect tribofilm formation. Typically, high flash temperatures occur at high rolling speeds rather than lower speeds. However, research has shown that ZDDP tribofilms can form at very low speeds where flash temperatures are small, roughly around 100 mm/s [48]. It shows that flash temperature is not a leading contributor to the formation of ZDDP tribofilms. The triboemission effect has also been used to describe the formation of ZDDP. However, it has been documented that ZDDP

films can form when rubbing surfaces are not in contact due to lubrication [49]. This finding does not agree with the theory that triboemission is a driving force for ZDDP formation since rubbing is required for the triboemission effect. Research has shown that ZDDP tribofilms form in high EHD-friction fluids suggesting that shear stress is the mechanism behind its formation [49]. The mechanism also explains why ZDDP tribofilms can form upon different surfaces. Formation promotion occurs from stress generated between two rubbing surfaces rather than a chemical reaction between the surface and ZDDP.

3.3.2 Tribofilm properties and chemistry

The mechanisms for forming the ZDDP film's tribofilm, properties and chemistry are also fundamental to understand. Tribological and mechanical properties of the ZDDP tribofilm have been a crucial part of its research to understand better its ability to function [44].

3.3.2.1 Tribological properties

ZDDPs' primary function as an additive is to reduce wear, as shown in Figure 3-7. The graph shows the variation of the wear track width with rubbing time. Test conditions were set at 40 °C with an SRR of 50 % and maximum Hertzian contact pressure equal to 0.95 GPa. A base oil with ZDDP compared to just a base oil reduces wear track width considerably as the rubbing time increases [50].

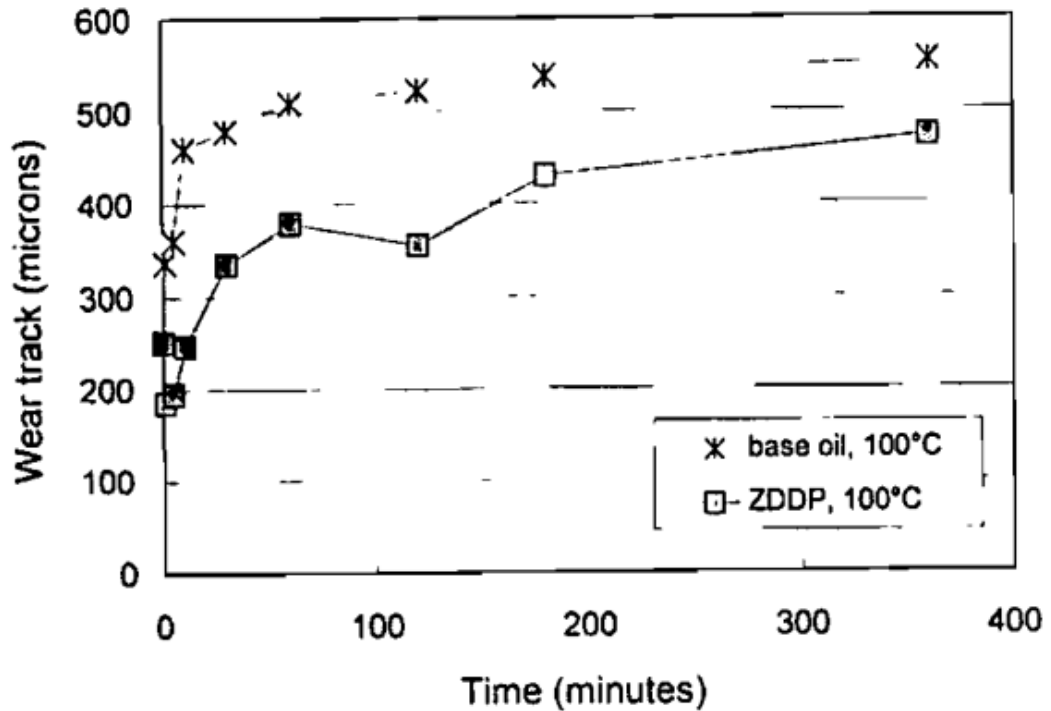


Figure 3-7 Comparison of wear track width for a base oil and a ZDDP containing oil [50].

ZDDP tribofilms not only affect the wear of the tribo-contact but also have been recorded through previous literature that the formation of the tribofilm and its final steady-state thickness affects the coefficient of friction [51]. Figure 3-8 taken from [52] shows the Stribeck-style plot of a base oil solution and a ZDDP solution. Operating conditions used in the tests were set at 100 °C, 50 % SRR, with the traction phase constant at 100mm/s and entrainment speeds ranging from 10 to 3000 mm/s. The coefficient of friction for the final Stribeck curve at very low entrainment speeds is similar in value for both the base oil and ZDDP solutions. It suggests that the roughness of the ZDDP tribofilm does not have much of an effect at very low lambda ratios on the coefficient of friction compared to the just the base oil. Both however, do increase in friction from the initial Stribeck curve, suggesting that the ZDDP roughness is

higher than the substrates surface at the start of the test, which would inhibit the entrainment of the lubricant. For the base oil, wear has occurred on the surface of the substrate, which increases the friction over time. The formation of the ZDDP also extends the boundary lubrication regime to higher entrainment speeds. The coefficient of friction from the ZDDP oil increases much more than just a base oil at higher entrainment speeds. It was previously thought that this was due to the roughness of the ZDDP tribofilm; however, the increase still occurred with smooth tribofilms. Previous research showed that it was not the case. It was suggested that the ZDDP film inhibited the lubricant entrainment into the contact, which reduces the EHD film thickness compared to a base oil test [53].

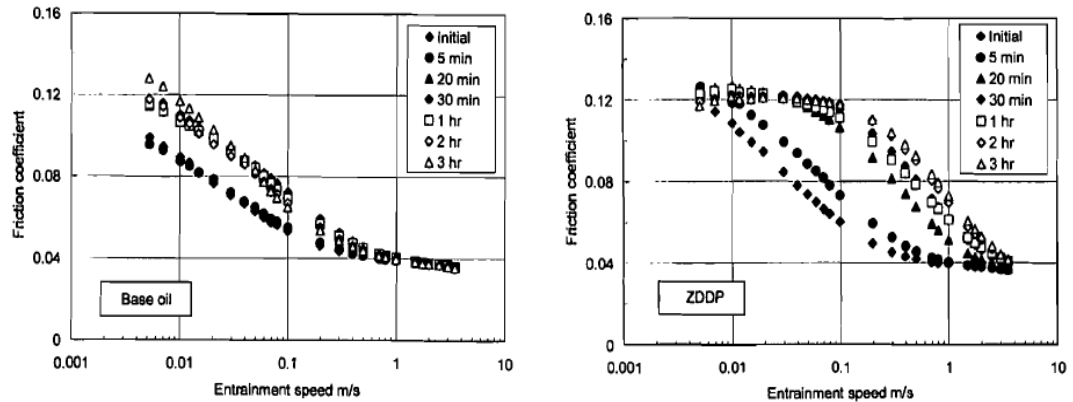


Figure 3-8 Comparison of Stribeck curves from a base oil and a ZDDP containing oil [52].

3.3.2.2 Mechanical Properties

Extensive research has also been conducted into the mechanical properties of the ZDDPs tribofilm [54,55]. Figure 3-9 depicts the structure and mechanical properties of a tribofilm formed from a ZDDP solution [56]. The author states that the polyphosphate layer is heterogeneous in thickness

which impacts the elastic properties. It is also important to note that the polyphosphate layers do not always cover the sulphide/oxide layers, usually the valleys. The polyphosphate layers could flow into the valleys when subjected to an Amsler friction test. However, they would then form a weak adhesion that can be easily removed with solvents. The polyphosphate film's properties, like hardness, depend on applied pressure in the tribo-contact.

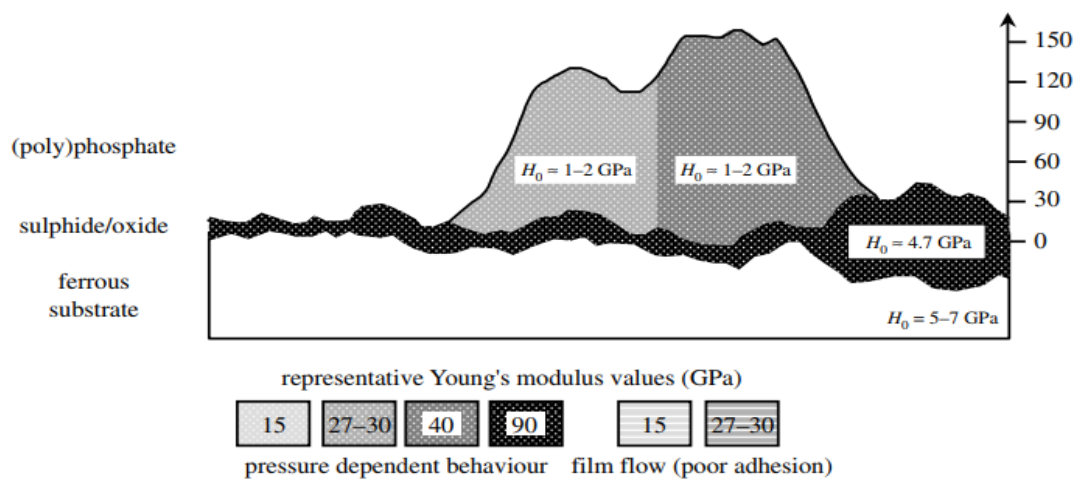


Figure 3-9 Mechanical properties of a ZDDP tribofilm [56].

3.3.2.3 Chemistry

The chemistry of the ZDDP tribofilm has been analysed using various techniques such as XPS, EDX, and XANES. Research has reported that a ZDDP tribofilm consists of a physically adsorbed layer on the outer edge, easily removable by solvents and then, closer to the surface, a chemically reacted layer consisting of polyphosphates with different chain lengths. Shorter chain phosphate layers are found closer to the substrate, increasing longer chain phosphates towards the top surface of the tribofilm with no carbon within the bulk. AES profiling has been able to give strong evidence to show this [57]. ToF-SIMS has also been applied to analyse the ZDDP tribofilm,

which agrees with XPS profiling, confirming that there is very little iron oxide within the tribofilm and that the phosphate glass is present throughout all the thicknesses of the film [58].

3.3.3 ZDDP tribofilm characterization via XPS

XPS is the most used technique for identifying critical chemical components of the ZDDP tribofilm. As explained in this chapter section, the ZDDP tribofilm is mainly comprised of polyphosphate chains.

Using XPS, a technique has been developed to characterise the surface chemistry of the polyphosphate chains. It combines the ratio of the bridging oxygen and non-bridging oxygen (P-O-P / P=O and P-O-M) and the difference in Zn 3s – P 2p_{3/2} binding energy to identify the chain lengths. Figure 3-10 shows the bridging oxygen (BO) to non-bridging oxygen (NBO) ratios for chain length identification from previous literature [59,60].

An example of the high-resolution scan deconvolution of the O 1s signal to obtain BO/NBO ratios is shown in Figure 3-11 [61].

	Phosphate Glass	BO/NBO
Longer chain	Metaphosphate	0.48 ± 0.02
	Polyphosphate	0.37 ± 0.05
	Pyrophosphate	0.20 ± 0.05
Shorter chain	Orthophosphate	----

Figure 3-10 Characterization of zinc polyphosphate chains [59].

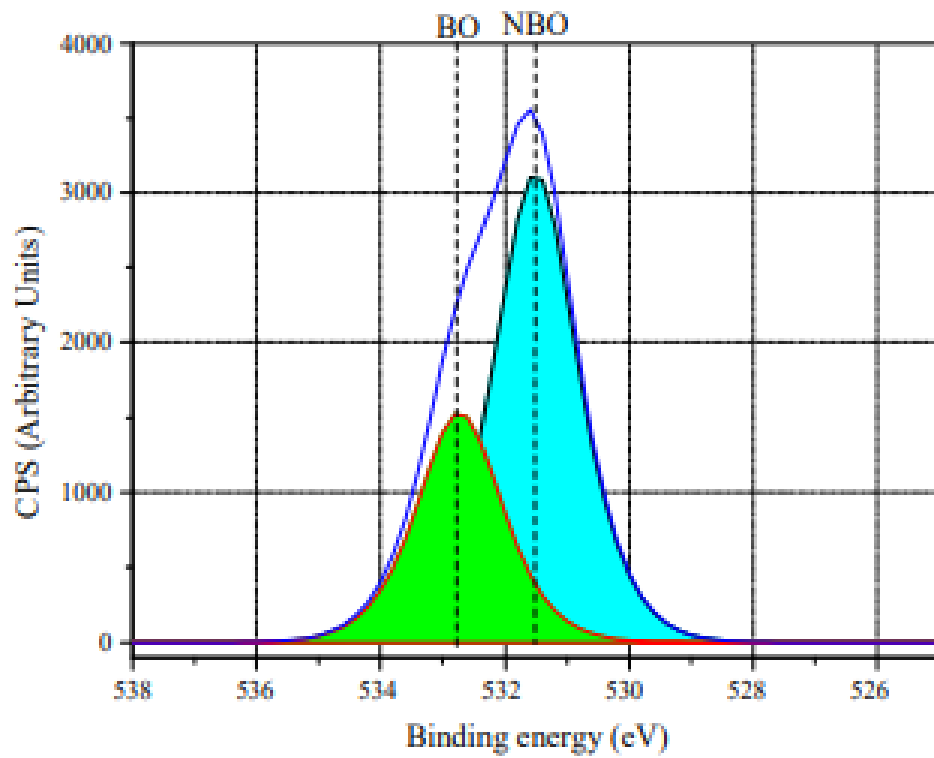


Figure 3-11 Example of BO/NBO ratio obtained from O 1s high resolution signal [61].

3.4 Friction Modifiers

As stated in the previous sections, understanding boundary additives in low viscosity engine oils are critical. When the oil's viscosity is reduced, the friction in the boundary lubrication regime increases. Friction modifiers are used to counteract the friction increases. Friction modifiers currently used in engine oils can be split into two main sections: inorganic and organic. The research undertaken in this study will concentrate solely on an inorganic friction modifier.

3.4.1 MoDTC Additive

MoDTC, an inorganic compound, is the most widely used friction modifier, reducing friction in the boundary lubrication regime. It has been used to formulate engine oils over many decades, essential for friction reduction at the tribo-contacts within engine components and, thus, fuel economy performance. The chemical structure of MoDTC is shown in Figure 3-12.

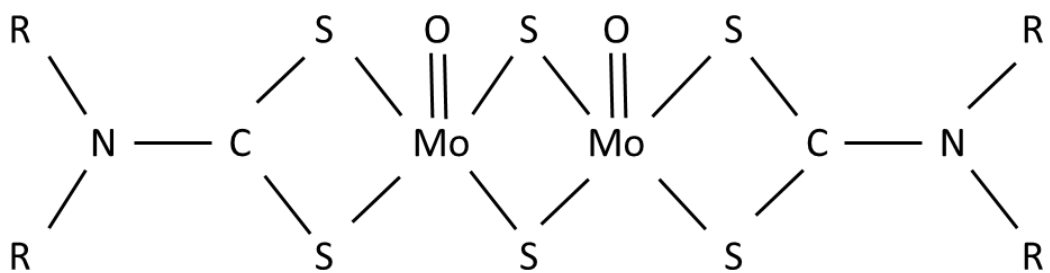


Figure 3-12 Chemical structure of MoDTC.

3.4.1.1 Tribofilm formation and decomposition

There has been extensive research into the mechanism of how MoDTC tribofilms form to reduce friction over the past few decades [62–64]. During tribological testing with oil containing MoDTC, operating conditions with high temperatures must decompose the molecule to form MoS₂. It was first reported that the breakdown of MoDTC to form MoS₂ was attributed to electron transferring occurring in the Mo-S bonding. It results in the two radicals combining to form thiuram disulphide and the other core molecule of MoDTC to decompose to form MoS₂ and Mo oxides. However, recent research has shown that this is not the case. A new decomposition pathway has been determined since the old mechanism could not explain the decomposition products obtained at 20 °C. The author could not detect any Mo oxides within the wear scar using Raman spectroscopy [65]. The proposed mechanism for the decomposition of MoDTC is shown in Figure 3-13.

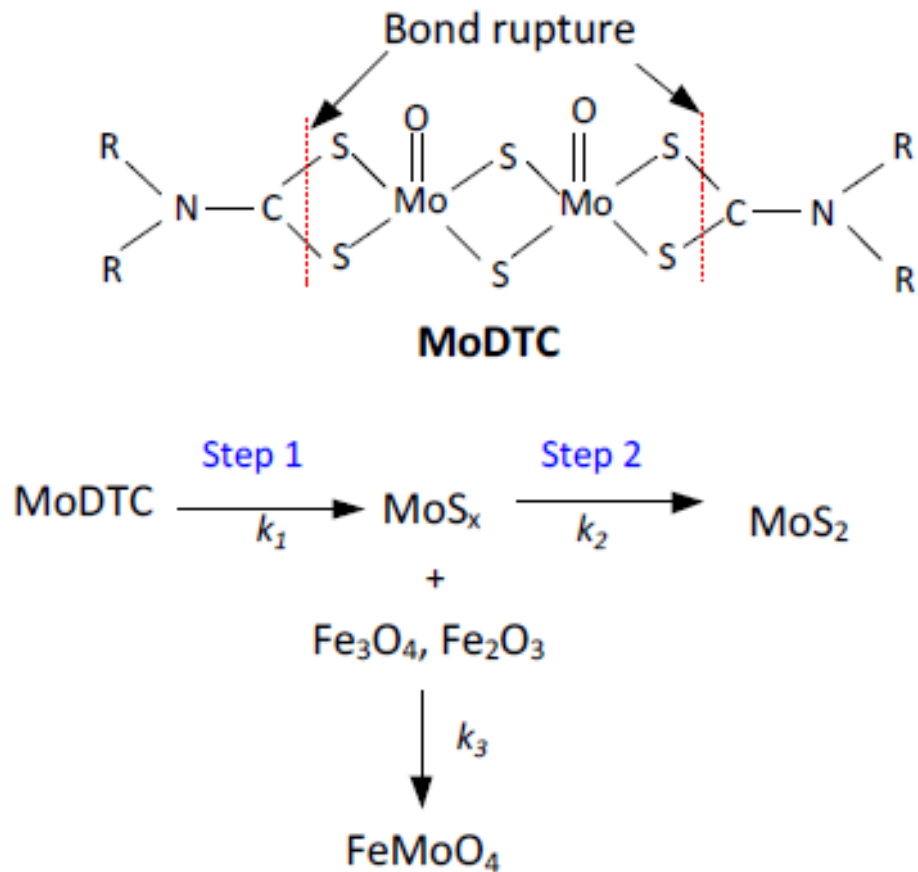


Figure 3-13 Mechanism for the decomposition of MoDTC [65].

The hypothesis behind this mechanism is that MoDTC decomposes via shear stress through rupturing bonds during rubbing. The C-S bond has the lowest dissociation energy through literature, meaning it is the most effortless bond to break. The author used a 4 step process to describe the decomposition of MoDTC.

- Step 1 MoDTC adsorbs onto the tribo-contact surfaces.
- Step 2 Decomposition occurs via shear stress applied to MoDTC from the tribo-contact. C-S bond rupturing occurs, which results in the formation of amorphous MoS_x.
- Step 3 MoS_x is converted to MoS₂ due to increased energy at the tribo-contact from increasing temperatures or shear stresses.

Step 4 Reactions of iron oxides upon the steel surfaces with MoS_x result in the formation of FeMoO_4 .

3.4.1.2 Tribological Properties

The MoS_2 tribofilm formed from the inorganic friction modifier MoDTC is known for its significant friction-reducing properties. MoS_2 individual sheets (<10nm in length) are embedded into the MoDTC tribofilm with several tens of nanometres of film thickness. The sheets have a crystal-like structure similar to graphite. Van der Waals forces between the MoS_2 sheets enable it to be easily sheared to produce a low friction regime. Previous research has shown MoS_2 to produce a coefficient of friction value in the range of 0.04-0.06 in the boundary and mixed lubrication regimes [65,66]. Figure 3-14 shows the results from a tribometer test using 0.5 wt% MoDTC lubricant at 100 °C. The base oil and dry friction are included on the graph as references. There is high friction for the MoDTC lubricant oil at the beginning of the test. However, after a few minutes of rubbing, the friction rapidly drops and slowly increases to a steady-state of roughly 0.04-0.06, a significant characteristic of a MoS_2 tribofilm.

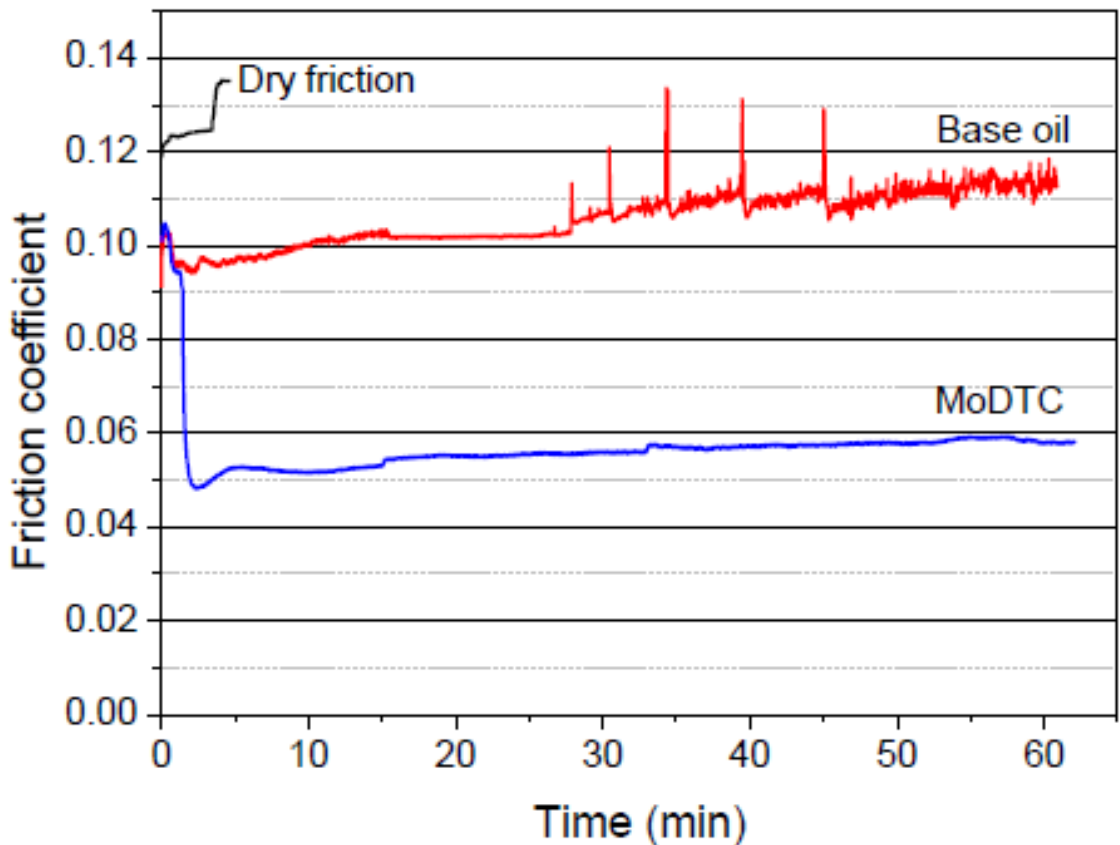


Figure 3-14 Comparison of friction as a function of time for dry friction, base oil and MoDTC containing oil [65].

The main factors which influence the friction-reducing property of MoDTC are [65–69];

- 1) Concentration – MoDTC is more effective with a higher additive concentration coupled with a high temperature.
- 2) Surface roughness – MoDTC has been found to produce MoS₂ on rougher surfaces compared to smoother surfaces.
- 3) Operating conditions
 - a. Temperature – An increase in temperature leads to an increase in the performance of MoDTC.
 - b. Load – An increase in load leads to an increase in the performance of MoDTC.

- c. Slide-to-roll ratio – For MoS₂ to form solid on solid, contact must occur. Therefore, obtaining friction reduction in sliding rolling contacts becomes more challenging than pure sliding. Increasing the sliding rolling ratio leads to an increase in MoDTC performance.
- d. Contact orientation – MoDTC is more effective in high stroke length reciprocating conditions since it only requires MoS₂ formation within the tribo-contact for friction reduction.

The primary function of MoDTC is to reduce friction. However, research has also shown that it can only reduce wear compared to base oil [70]. During rubbing, FeS₂ forms within the wear scar from the sulfur in the MoDTC molecule. The FeS₂ is a protective layer against wear, enabling MoS₂ to form. However, the mechanism that reduces the wear from MoDTC is not the level ZDDP can reduce wear.

3.4.1.3 Synergism with ZDDP

It is well known that MoDTC is incorporated into fully formulated engine oils. It must perform its function alongside multiple additives incorporated into the oil. The most common interaction between boundary additives is MoDTC and ZDDP. Since one reduces friction and the other wear, it is essential to understand how they work together in a tribo-contact. The effect that ZDDP has on the friction-reducing properties of MoDTC has been investigated in previous research [71–74]. All work agrees that the friction and wear of the tribo-contact improve when using both MoDTC and ZDDP. Figure 3-15 shows the coefficient of friction that can be achieved when using both additives together [75]. In terms of friction, the ZDDP does not have a negative effect on MoDTCs ability to function as a friction modifier. It has been noted that the lowest coefficient of friction can be achieved when small dosages of ZDDP

are added to high concentrations of MoDTC. The main reason for adding ZDDP to MoDTC is to reduce the wear, as shown in Figure 3-16. Oil 004A with ZDDP and MoDTC produces less wear than 001A, base oil only, and 003A with MoDTC only. It shows that ZDDP can still reduce wear when added to oil with MoDTC. However, 004A does not reduce the wear levels to that of 003A with ZDDP only. It must also be noted that when MoDTC is added to a fully formulated oil, the wear increases compared to a fully formulated oil without MoDTC which is the opposite to when it is only ZDDP and MoDTC within the oil [76]. When both additives are within the same oil, using different chemical analysis techniques such as XPS, EDX, XANES, it has been found that phosphate layers formed from ZDDP with FeS_2 and N organic layers with MoS_2 formed from the decomposition of MoDTC. Longer phosphate chains are found within the tribofilm formed from ZDDP and MoDTC when compared to ZDDP only, which explains the higher wear found. This shows that both additives associated tribofilms were able to form to generate a multi additive tribofilm with the main functions of anti-wear and friction reducing being present.

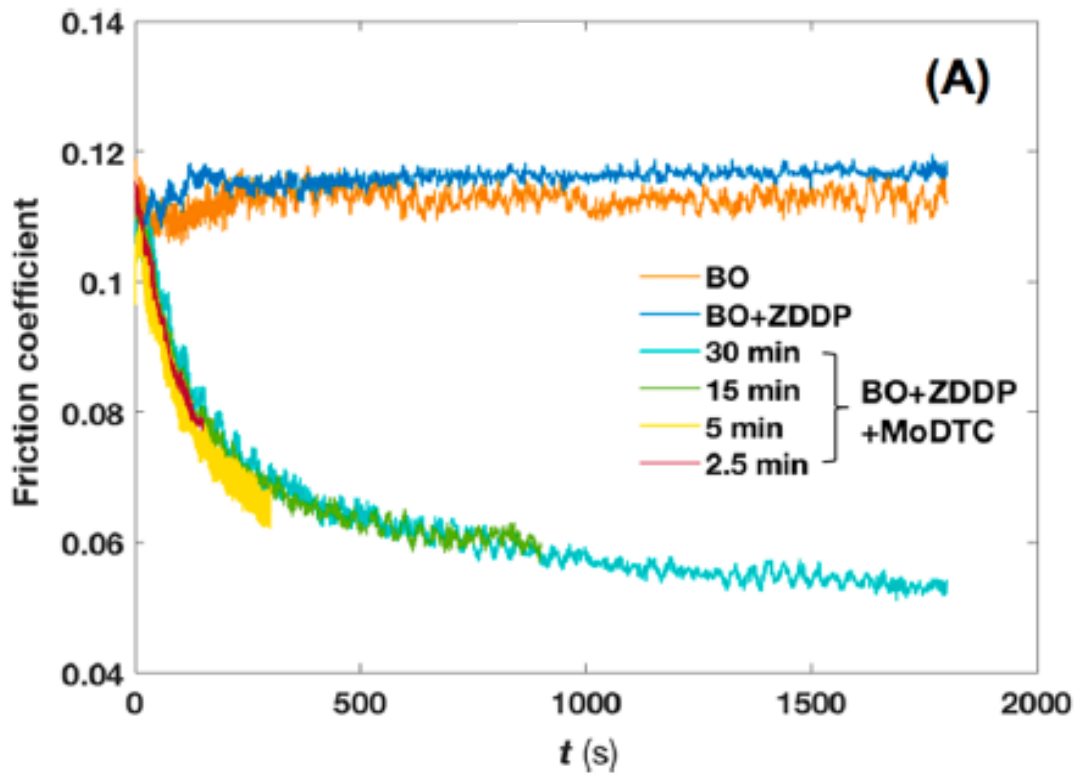


Figure 3-15 Comparison of friction as a function of time for a base oil, base oil + ZDDP and a base oil + ZDDP + MoDTC [75].

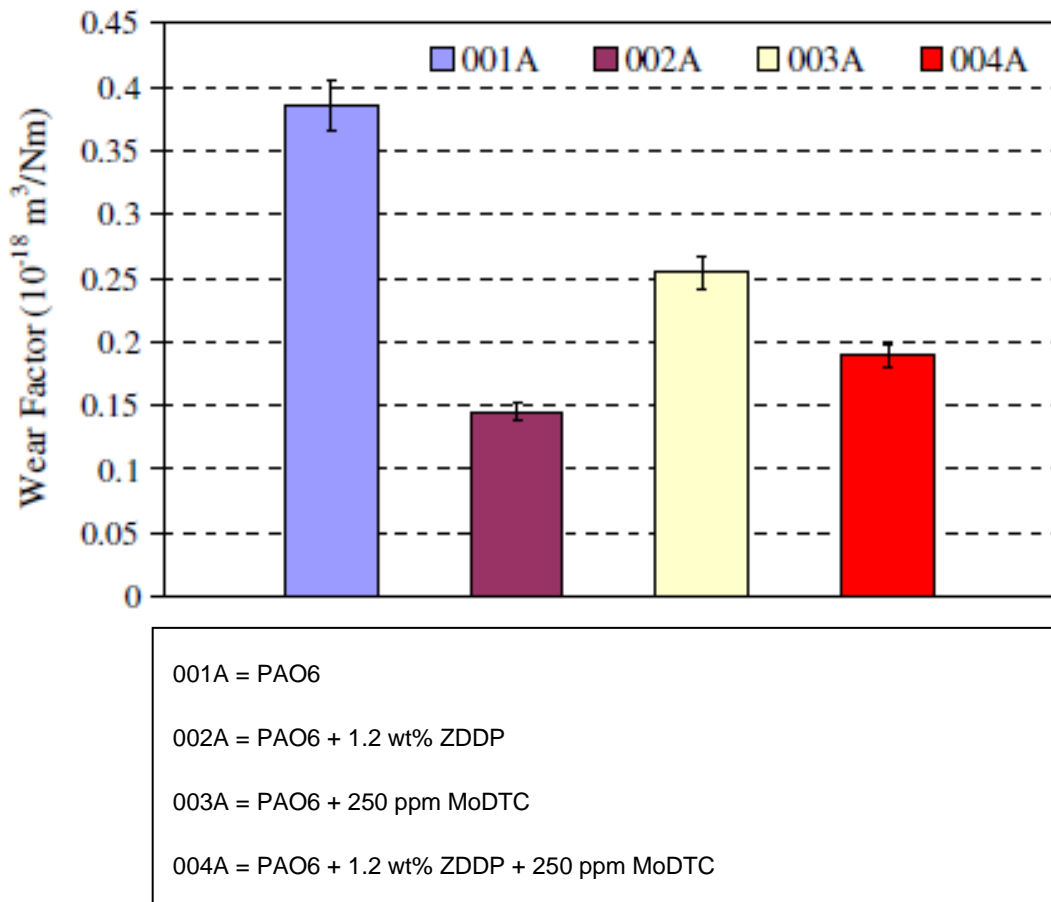


Figure 3-16 Wear coefficients for different formulations of ZDDP and MoDTC oils [71].

3.4.2 MoDTC tribofilm characterization via Raman Spectroscopy

The most common technique used in research to detect MoS₂ is Raman spectroscopy. It has been extensively used in research [65,68,75,77,78]. Figure 3-17 displays a Raman spectra example from a tribofilm generated from MoDTC [68]. The test was carried out using a 0.5-weight percentage MoDTC oil. The set-up for the friction test was a ball on disc at 200 rpm, 1.7 GPa and 80 °C.

MoS₂ is detected within the tribofilm at the peaks 379 and 411 cm⁻¹. Peaks at 1302 and 1444 are from mineral oil. Additionally, other decomposition products of MoDTC can also be detected. S-S bridging sulfur is detected at

512 and 556. The structural feature is typically found in the amorphous molybdenum sulfides [47].

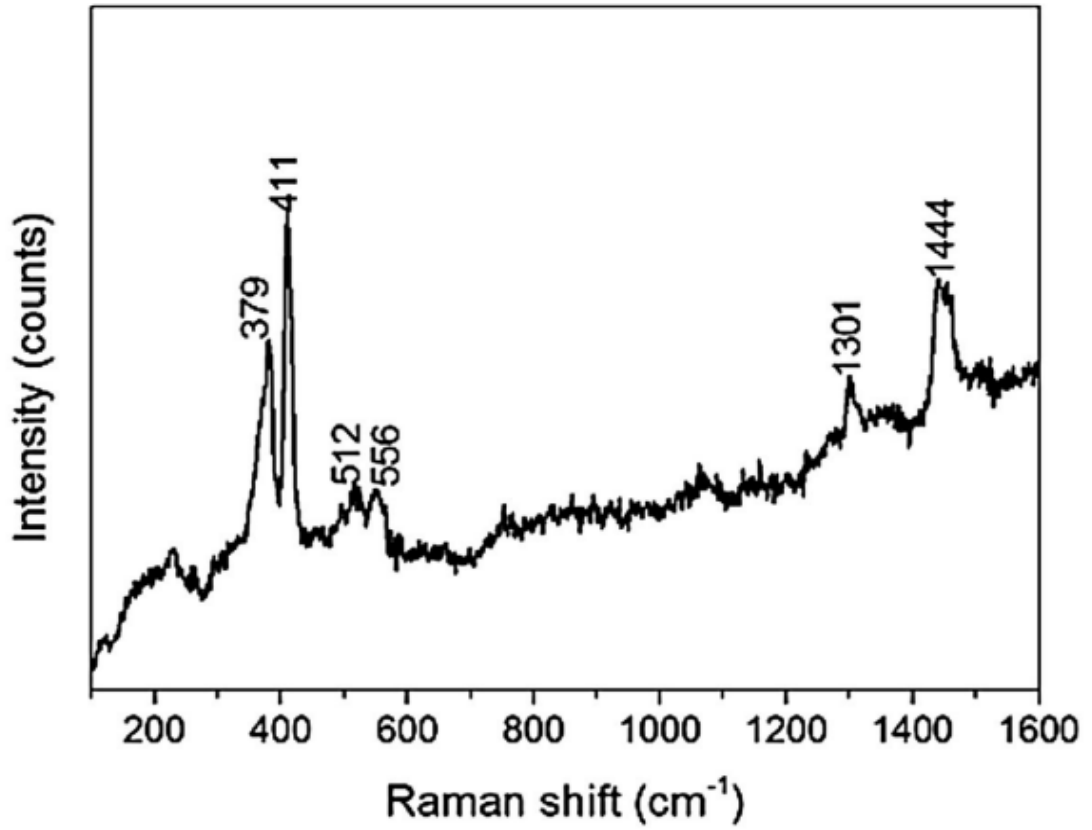


Figure 3-17 Raman spectra of a MoDTC tribofilm [68].

3.5 Detergent Additive

Around 10 to 15% of an engine oil additive package comprises detergents. The structural features of the molecules are shown in Figure 3-18. They contain a polar head, hydrocarbon tail and one or multiple metal ions. The polar head is usually an acidic group that reacts with hydroxides or metal oxides. Hydrocarbon tail ensures the detergent is soluble within the oil, and the metal ions commonly used are calcium, sodium, and magnesium. Calcium is by far the most common. Their primary function is to protect metallic components within ICE. They perform this function by neutralising inorganic acids from combustion products and organic acids from oil degradation. The left of Figure 3-18 shows an inorganic core, calcium carbonate, combined with a surfactant molecule. The detergent suspends soot, sludge, insoluble combustion, and oxidation products. It enables the detergent to neutralise acids and solubilise any polar material within the oil. To the figure's left, the detergent can also form a protective layer on the surfaces, preventing high-temperature deposits from occurring [79].

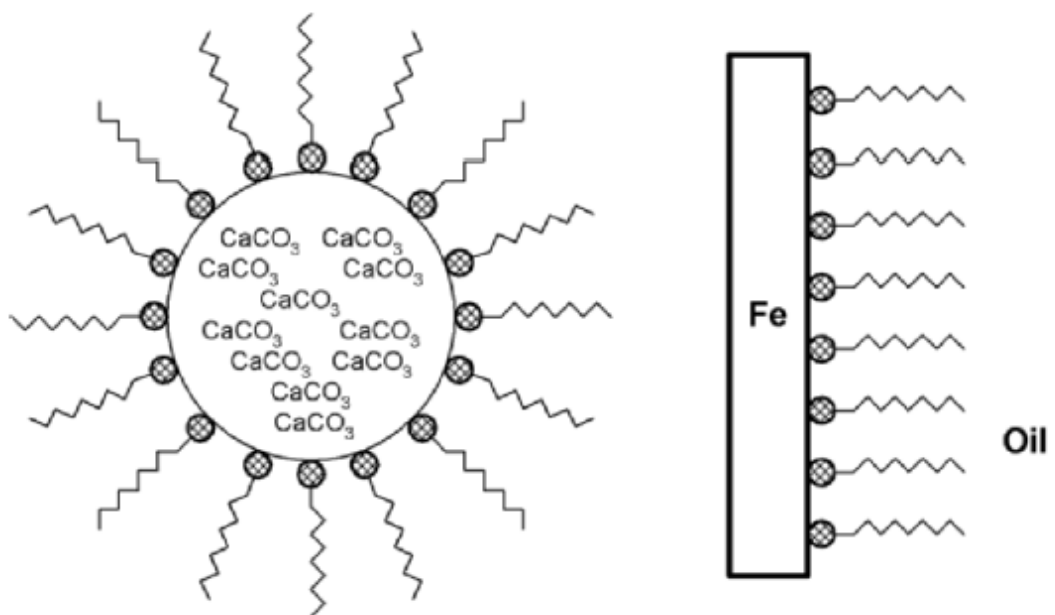
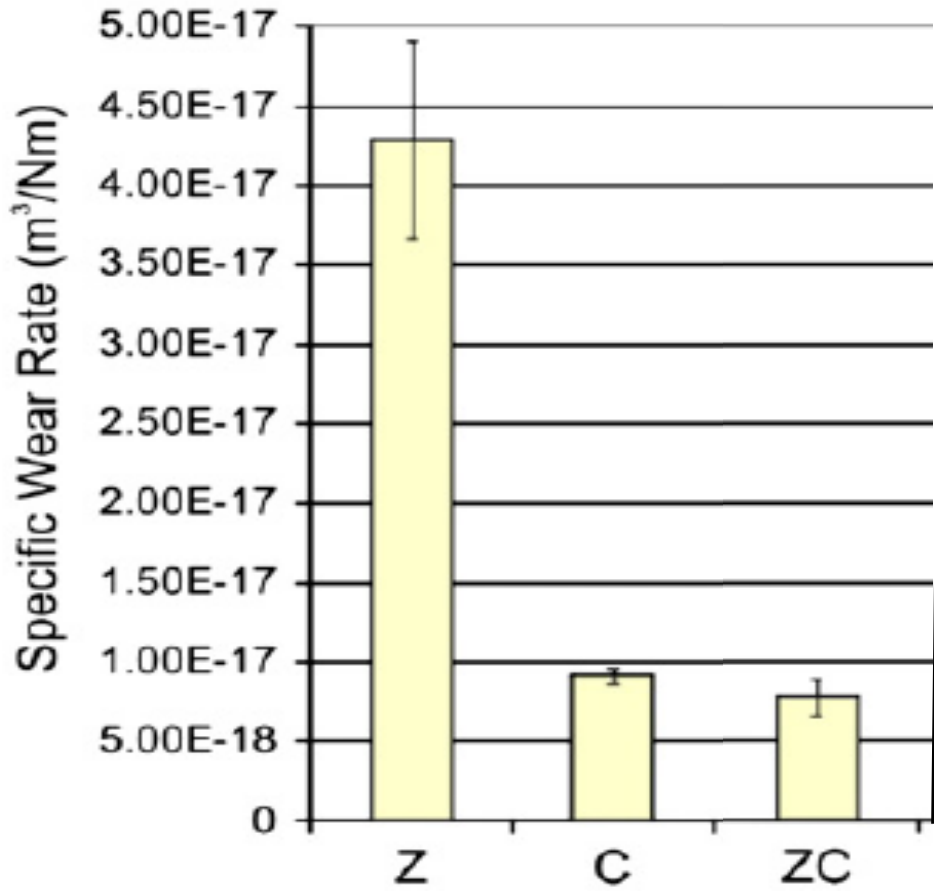


Figure 3-18 Surfactant and base oil synergies of detergents [79].

3.5.1 Tribological Properties & synergisms with other additives

As a detergent makes up a relatively large proportion of additives within a fully formulated engine oil, the interactions that could occur with other additives again becomes essential to understand whether it hinders or enhances other additives. The most common interaction detergents have with the ZDDP tribofilm is documented in previous research [80,81]. In fact, on its own, the most common detergent used in engine oils, known as over-based calcium sulphonate (OBCS), can form a tribofilm with wear-reducing properties. It has been documented that the molecule breaks down to the calcium carbonate core by breaking the bonding between sulfur and calcium to form a film on the rubbing surfaces. As high temperatures and rubbing occur upon the film's core, it can result in thick CaCO_3 films also forming on the surfaces. An OBCS tribofilms effect on the wear is shown in Figure 3-19. Specific wear rates of the pin material for a 3.5-hour TE77 test are used in the graph, with oil formulations shown below the figure. The author stated that the high wear rate from the 0.5 wt % ZDDP oil is due to the low concentration of ZDDP used. Usually, a 1.0 wt % ZDDP oil would reduce the wear rate of the 0.5 wt % ZDDP oil by a further 50%. Sample C produces a lower wear rate from the graph than sample Z, showing the wear-reducing properties of an OBCS tribofilm. When OBCS is blended with ZDDP, sample ZC further reduces the wear rate of sample C. It shows that there is a synergism between the two additives [82]. Other research has shown similar results with OBCS, ZDDP, and other detergents [83,84].



Z = PAO6 (99.5 wt %) + ZDDP (0.5 wt %)
C = PAO6 (99.06 wt %) + OBSCS (0.94 wt %)
ZC = PAO6 (98.56 wt %) + ZDDP (0.5 wt %) + OBSCS (0.94 wt %)

Figure 3-19 Comparison of specific wear rates for different oil formulations containing ZDDP and OBSCS [82].

3.6 Additive Depletion

Oil ageing has been a problem in ICEs due to its effect on performance, fuel economy and CO₂ emissions. A direct result of oil ageing is additive depletion, an extensive OEM research area over the years.

Additives are depleted in ICE oils in two main ways. The first is via mass transfer. It occurs when the additives concentrations are reduced when performing their function. For example, friction modifiers are depleted by forming a tribofilm with friction-reducing properties. The second way is by decomposition, where oil oxidation is an example.

Multiple factors influence the oils' ageing, including temperature, metal and contamination content, additive package and base oil, and airflow rate. Additive depletion, primarily through decomposition, is a destructive process that can increase friction and wear of the tribo-contact [50]. As shown in Figure 3-20, in the initial stages of service, the protective functions of the additives slow down the rate of oil degradation. However, as the additives are depleted, the oil degradation increases significantly [85].

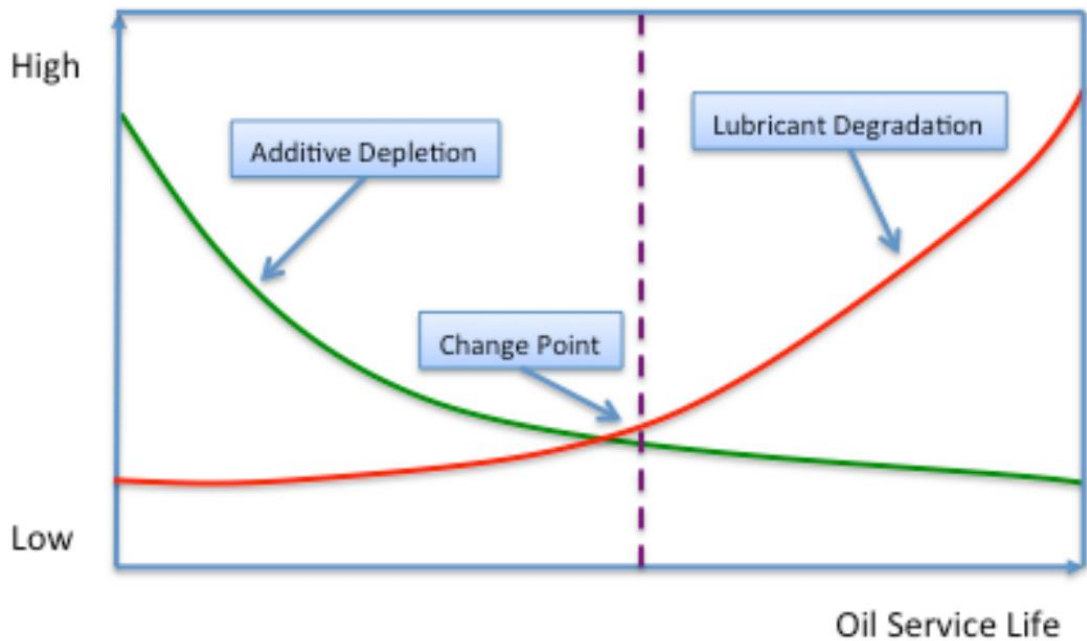


Figure 3-20 Oil degradation and additive depletion over time.

3.6.1 Oxidation

Oxidation is the most significant contribution to oil degradation and dramatically impacts the additives' lifetime. It can be a highly complex process that forms unwanted products and changes the physical and chemical properties of the engine oil. The destructive process occurs when molecules within the oil react with oxygen molecules. This process can be accelerated by increased temperatures, acids, water and metal catalysts [86]. The process also increases the oil's viscosity, leading to decreased fuel economy. By-products directly resulting from oxidation are sludge, varnish and deposits. Oil oxidation stages that occur during oxidation degradation are shown in Figure 3-21.

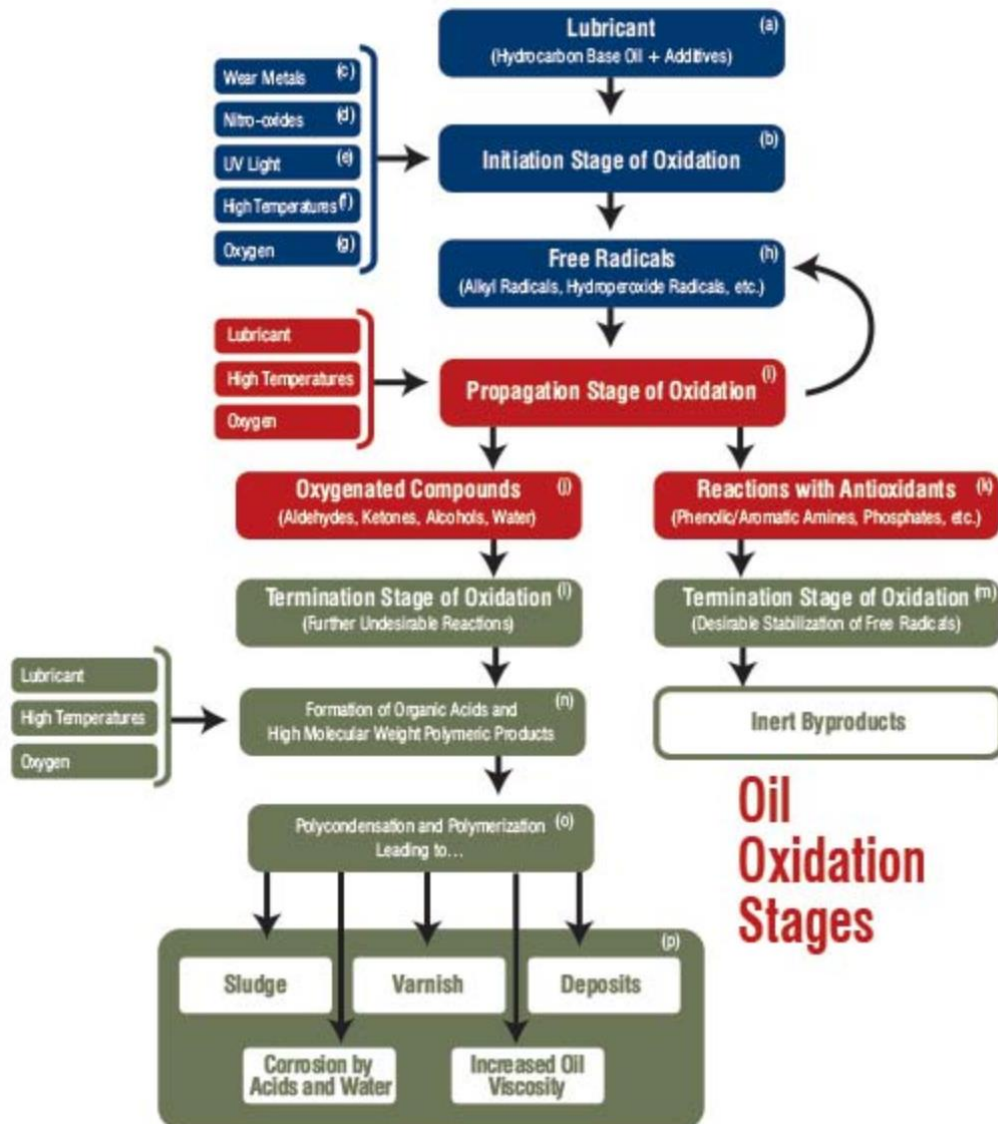


Figure 3-21 Oil oxidation stages [86].

3.6.1.1 Base Oils

Base oils refined from crude oil are mineral oils, and others created via chemical synthesis are commonly known as synthetic base oils. Typically, a base oil consists of hydrocarbons with multiple carbon atoms and low amounts of nitrogen, sulfur and organic compounds containing oxygen. They are split into different categories according to API, as in Table 2-2. Sulfur content

saturates %, and viscosity index are some categories defining the base oils. Usually, synthetic-based oils are better overall performers than mineral-based oils, as a recent study has shown [8]. Some advantages they have over mineral oils are higher temperature stability, low-temperature pump ability, deposit protection, and higher VI and oxidation stability. However, there are some disadvantages that synthetic oils have over minerals base oils which are, higher costs and insufficient additive solvency.

Base oils, due to their molecular structure, are subject to oxidation. The theory of autoxidation of hydrocarbons includes chain initiation, propagation and termination by free radicals [87]. Previous research has shown that oxidation stability is crucial in base oils, enabling longer drain intervals [88]. It has been determined that regardless of the content of antioxidants present and temperature, the quantity of oxygen consumed, and the viscosity increase have a precise correlation in base oil oxidation. Figure 3-22 shows the oxidation stability of three different base oils for an ASTM sequence IIIE engine test [89]. The graph shows that synthetic PAO base oil has the highest oxidation stability since it has the lowest viscosity increase % with test duration.

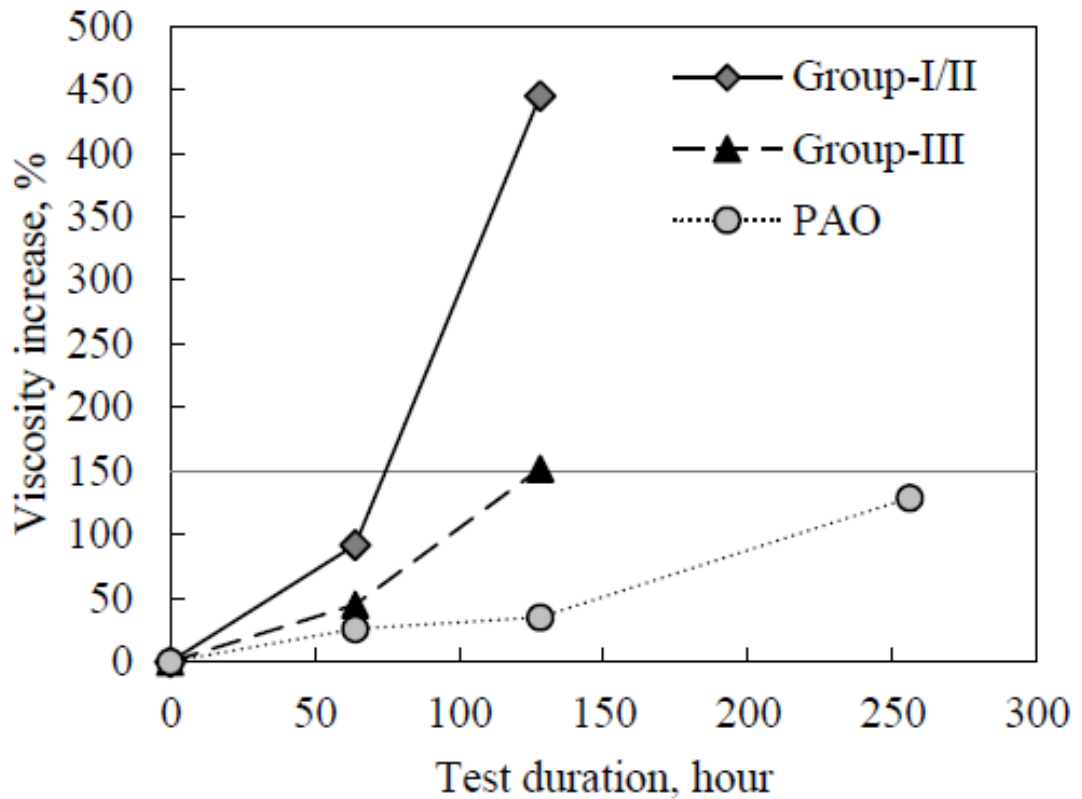


Figure 3-22 Oxidation stability of base oils using ASTM standard engine test [89].

3.6.1.2 Additives

As stated previously, oil oxidation is one of the main factors that negatively impact additives' ability to function. Engine oils are usually used in passenger cars for roughly 15,000 km or a year, with the engine metallic components acting as a catalyst for oxidation. Therefore, it is essential to understand how oxidation depletes additives, the impact on the tribo-contact and ways to slow down the oxidation process. Specific attention needs to be given to boundary additives in ultra-low viscosity engine oil since a lower viscosity oil decreases the lambda ratio of the tribo-contact, increasing the importance of friction and wear and reducing protective tribofilm.

Extensive research of ZDDPs degradation mechanism to which it forms an anti-wear protective tribofilm has been performed in the past, with less attention to its deterioration during oxidation and ageing. However, engine oil degradation, specifically the influence of ZDDP deterioration on the tribochemistry and behaviour, has been investigated in a recent study [90]. Fresh engine oil showed improved overall tribological performance than aged engine oil, expressed through low friction and wear. It was found that aged oils at intervals of 4 and 8 hours into the ageing process showed degradation of dihexyl dithiophosphate with organic ZDDP degradation products created from the substitution of sulfur atom(s) for oxygen atom(s). Interestingly, these aged oils at intervals of 4 and 8 hours provided better wear protection than fresh oil. It must be noted that even though improvements in wear were seen for aged oils compared to fresh oils, the low friction observed in fresh engine oil was not achievable for aged oils. An explanation for the better wear protection after ageing is due to effects of oxidation on other boundary active additives, such as MoDTC, which reduces competitive surface adsorption and enables ZDDP to form its tribofilm.

The oxidation degradation of additives, including ZDDP, MoDTC and detergents, all incorporated into oils, have been investigated by researchers to understand better the mechanism that causes their loss of function [91,92]. A simplified oil containing ZDDP, MoDTC and a calcium borate overbased detergent was aged for 16 hours with oil collected at intervals every 4 hours. The results showed that the oil's friction-reducing properties were lost after 8 hours of ageing. XPS analysis confirmed a reduction of MoS₂ found within the tribofilm as ageing time increases. The authors suggested a mechanism by which MoDTC loses its friction-reducing properties. As MoDTC and ZDDP are

consumed via oxidation, a ligand exchange occurs between ZDDP and MoDTC to form ZnDTC and Modtp with insoluble species. It would prevent the formation of MoS₂ with a possible correlation between the size of MoS₂ nanocrystals and MoDTC concentration within the aged oil [93].

3.6.1.3 Artificial ageing process

Artificial or laboratory ageing processes were invented to accelerate oil degradation faster than engine ageing processes. Harsh conditions, such as high temperatures and large airflows, are applied to the engine oil to mimic the conditions typically found within the engine.

The Coordinating European Council (CEC) L-48-00 is oxidation stability artificially ageing process of lubrication oils [94]. Its method uses oxygen from the air to oxidize the lubricant oil at temperatures >100 °C. Previous research has used this standard to investigate the artificial ageing processes' impact on engine oil performance [92–95]. The main disadvantage of this process is the relatively long ageing duration across multiple days. However, the use of a metal catalyst can reduce it. A schematic for the artificial ageing process standard is shown in Figure 3-23.

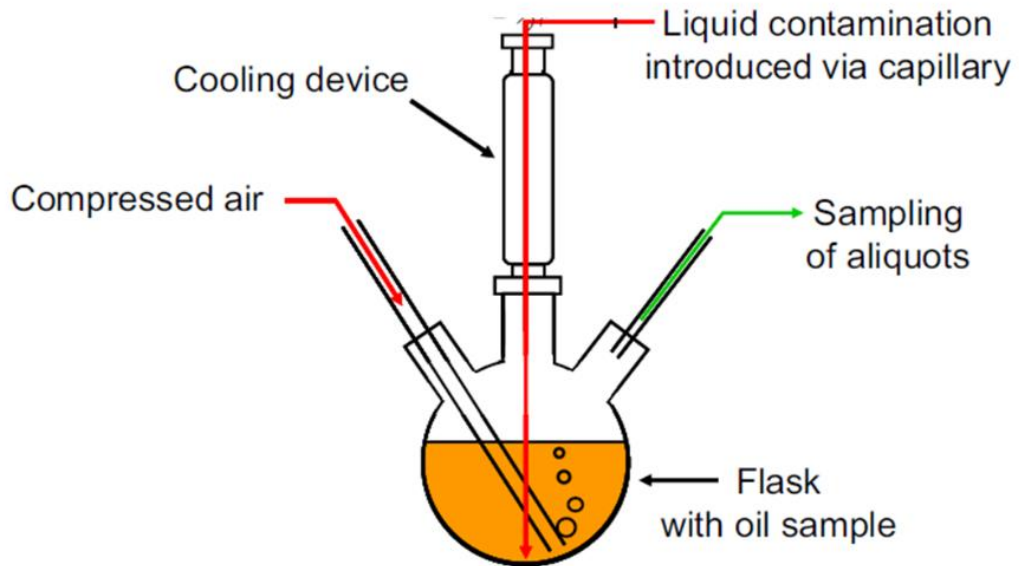


Figure 3-23 Schematic for CEC L-48-00.

3.7 Summary

This chapter has discussed and reviewed the tribological issues in internal combustion engines with lubrication. Particular attention has been given to how these tribological issues are prevented using engine oils with the most critical additives incorporated into them to produce the performances achieved using standard engine oils. As explained in more detail in this chapter, the oil's viscosity decreases to increase fuel economy. As the viscosity of the oil decreases, the tribo-contacts within the internal combustion engine change. For example, a minimum film thickness decrease results in a lower lambda ratio. This consequence means that boundary additives become more and more critical to understand. The research in this thesis concentrates on

knowledge gaps in developing the new ultra-low viscosity engine oil in conjunction with the Sinopec lubrication company.

To date, there has been extensive research on friction modifiers, specifically MoDTC, with different conditions such as concentration, operating conditions, and synergism with ZDDP, as explained in this chapter. However, little research has been conducted on fully formulated low viscosity 0W-8 engine oil, as this grade of oil is relatively new. When additives are incorporated into these 0W-8 engine oils, specifically boundary additives, their concentrations must be increased. Especially in the Japanese market, the new low viscosity engine oils contain vast amounts of friction modifiers concentration, 1000ppm+. Due to the harmful products that sulfur, and phosphorus-containing additives can produce, and its relatively high cost, there is a need to reduce the amount of MoDTC within the oils. Thus, for these new 0W-8 engine oils, there must be an optimum concentration of MoDTC, which produces a low coefficient of friction and does not affect the tribofilm contents or wear negatively compared to lower or higher concentrations.

In new ultra-low viscosity engine oil, it is paramount that both MoDTC and ZDDP, friction and anti-wear additives, can perform their function without being influenced negatively by other surface-active additives. OEMs use different detergent formulations to enhance their function as the oil viscosity is lowered for higher fuel economy. This chapter explains that detergents can decompose to form a tribofilm layer. Therefore, it becomes critical to ensure the new detergent formulation designs for better function performance do not negatively impact the functions of the friction and anti-wear additives.

Ageing oil in a real-world engine or engine simulation is a long process, not adequate for initial and quicker testing. Artificial ageing processes were conducted in a laboratory to enable a faster ageing method for test oils for efficient analysis. However, little research has been conducted to compare and understand the differences between the standard artificial ageing and engine ageing processes. The artificial ageing process needs to simulate the effects on the oil within a field engine to understand the tribological effects better.

Chapter 4 Experimental Procedures

4.1 Introduction

The experimental procedures chapter introduces the overview of each technique used in this study.

Viscosity measurements and oil analysis included using a rheometer, ICP, and FTIR, well-known techniques for oil analysis. Artificial oil ageing was conducted using the CCL-48-00 standard, and all field engine ageing was performed by the Sinopec lubrication company in Beijing, China.

All tribological tests in this study were conducted using an MTM for friction analysis. A SLIM unit attached to the MTM enabled ZDDP tribofilm film thickness measurements to be obtained at set intervals during a test. Raman spectroscopy and XPS techniques performed tribochemical analysis on tribofilms formed from selected engine oils. Finally, wear produced during tribological testing was analyzed using an NPFlex non-contact technique.

All test oils formulations for the individual results chapters can be found within their respective section. MTM operating conditions for all the studies are outlined with the MTM methodology. The same setting for all other techniques are kept constant throughout the studies.

4.2 Oil Rheology

As shown in Figure 4-1, all sample oils' dynamic viscosities used in this research were obtained using a Kinexus Rheometer. Two temperatures were measured at 40 °C and 100 °C for each oil, and the shear rate was kept constant with three repeats taken for validity.



Figure 4-1 Kinexus rheometer.

The dynamic viscosities measured by the rheometer were converted to kinematic viscosities using equation 6, where V is kinematic viscosity, ρ is the fluid density, and η is dynamic viscosity. Fluid density for each oil was calculated by measuring the mass of a given volume by dividing the mass by its volume for a specific temperature.

$$V = \frac{\eta}{\rho} \quad (6)$$

4.3 Oil Ageing

4.3.1 Artificial Ageing Process

The fresh engine oils in the final results chapter were artificially aged according to the standard from the coordinating European council (CCL) L-48-00. Researchers have used this to artificially age engine oils [96–99]. However, little comparison of this method has been made with engine ageing. A schematic of the artificially ageing process used in this study is shown in Figure 4-2. All sample oils, 200 mL, were aged for 96 hours, equivalent to 10,000 km. The temperature was kept constant throughout the ageing process at 160 °C to emulate the high temperatures of the oil around the combustion chamber. Compressed air was pumped into the oil to provide a source of oxygen with an airflow of roughly 10 L/h. A condenser was used to avoid evaporation.

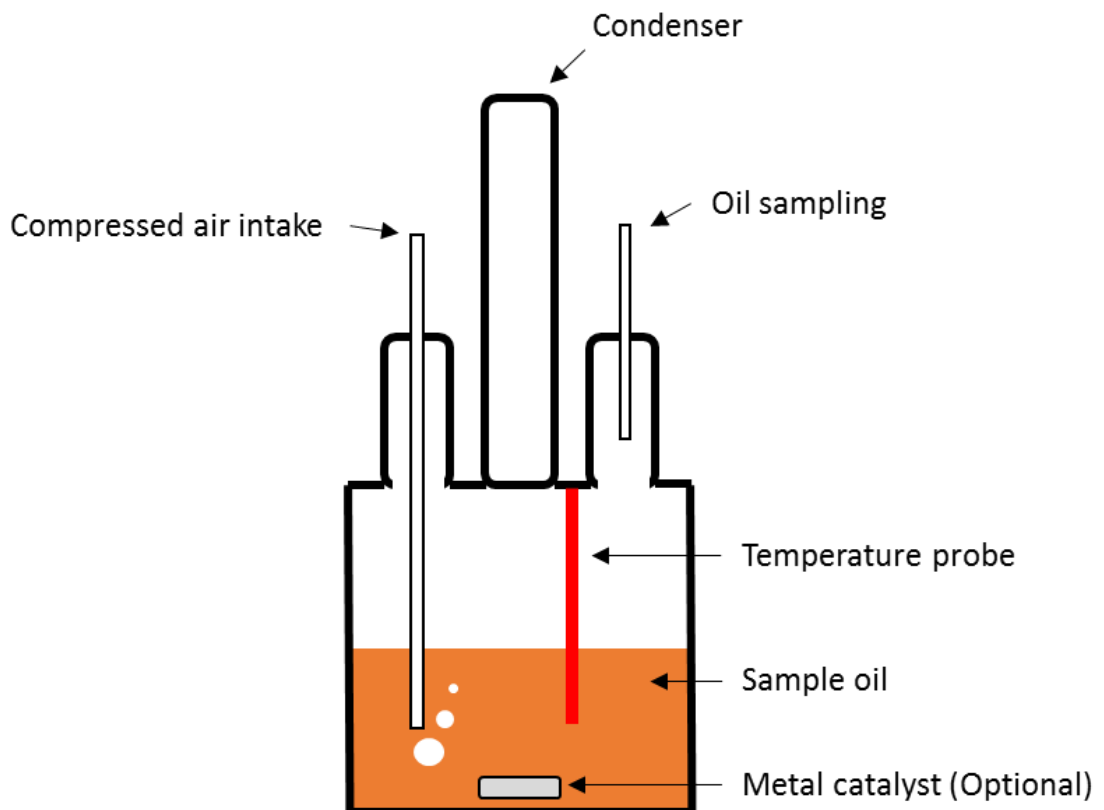


Figure 4-2 Artificial ageing process schematic.

4.3.2 Field Engine Ageing Processes

All engine oil ageing was conducted by the Sinopec lubrication company in Beijing, China. The engine oil ageing processes for each oil pair are shown in Table 4-1.

Oil A's engine oil ageing process was conducted using a Global Engine Durability (GED) engine test. The engine used was an inline-four. Oil was taken from the engine after 100 hrs, equivalent to 10,000 km according to the OEM, enabling a comparison with the artificial ageing process.

Oil B's engine oil ageing process was conducted using a naturally aspirated engine. A continuous high-speed durability ageing process involved a high engine speed of 6600~6800 rpm. The test duration lasted 180 hrs, equivalent to 10,000 km, to enable comparisons with the artificial ageing process.

Table 4-1 Field Ageing Oil Processes.

Sample labels engine ageing process	Oil A		Oil B
Test name	GED engine test		Continuous high-speed durability
Engine type	4-cylinder inline		Naturally aspirated
Test duration (hrs)	100		180
Rated speed (rpm)	5400	Maximum engine speed (rpm)	6600~6800
Idle speed (rpm)	750±50		
Maximum power (KW/rpm)	95/5400		
Maximum torque (Nm/rpm)	220/(2200-4000)		
Oil temperature (°C)	90-129	Maximum oil temperature (°C)	120
Intake air temperature (°C)	16-38	Backpressure (kPa)	44±5
Inlet air pressure (kPa)	95-105	Maximum system pressure (kPa)	85
		Cooling water flow rate (L/min)	70±5

4.4 Oil Analysis

4.4.1 Inductively Coupled Plasma Atomic Emission Spectroscopy (ICP-AES)

ICP-AES enables the mass percentage quantification of elements within a liquid. However, the technique is unsuitable for elements such as C, H, N, and O. The most significant disadvantages are physical and spectral interferences and the lack of some elemental sensitivity. A schematic representation of a typical ICP-AES setup is shown in Figure 4-3, taken from [100].

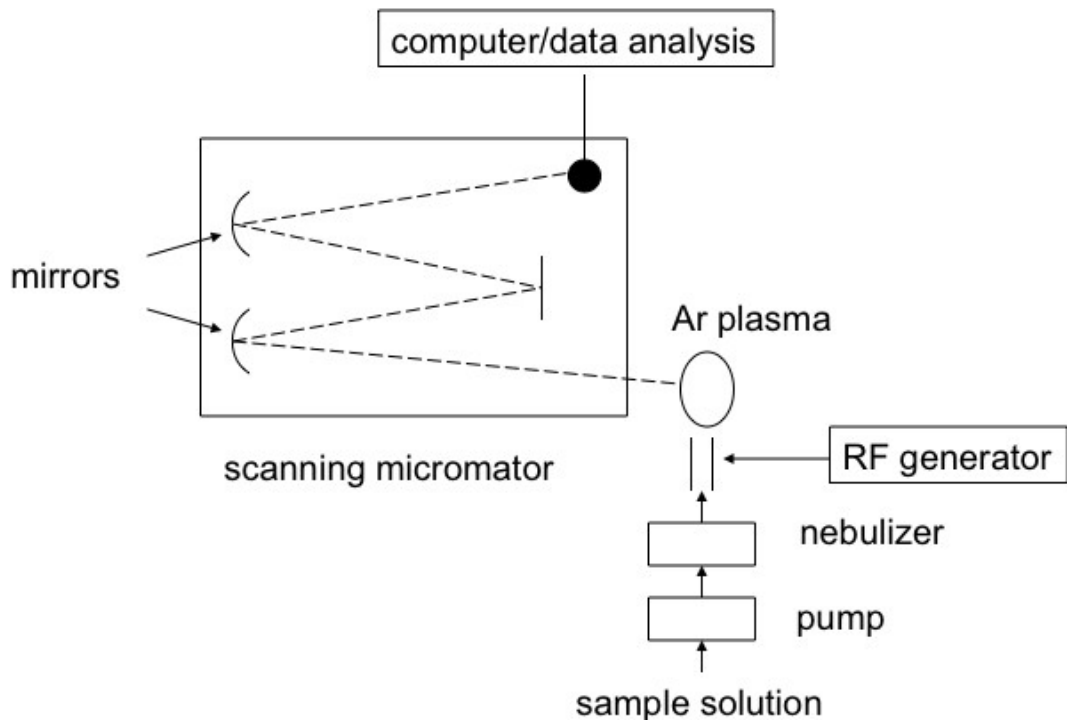


Figure 4-3 Typical ICP-AES setup [100].

The principle of the technique is based on the emission of photons from atoms by exposure to high-energy plasma. The act of exciting electrons produces light wavelengths dependent on the difference between the energy levels of the electrons. This principle enables different elements and their mass percentage to be determined.

The primary use of ICP in this study was to measure the concentration of the chemical elements within the fully formulated engine oils. These oils are created using many additives with various elements, some of which solely belong to one additive and others found in multiple additives within the oil. The concentration of elements, not the concentration of compounds, can be determined using the ICP technique. ICP analysis can also determine additive depletion due to oxidation by comparing the before and after engine oil spectrum [101].

4.4.2 Fourier Transform Infrared Spectroscopy (FTIR)

FTIR is a well-known analysis technique that compares used and fresh engine oils [101]. The principle of the technique utilizes the interactions molecules have when exposed to infrared radiation. Each molecule adsorbs radiation from infrared at specific wavelengths. The specific adsorbed wavelength enables the technique to distinguish different substances as no two molecules produce the same signal. Therefore, each spectrum produced from the FTIR scans contains semi-quantitative data if two substances are compared.

FTIR enables the identification of oil degradation, some additives, by-products, contaminants, and wear debris. The majority of the time, it is used as a screening tool.

The FTIR used in this thesis was a Perkin Elmer FTIR spectrometer with a spectra resolution of 4 cm^{-1} within the range of $650\text{-}4500\text{ cm}^{-1}$.

As shown in Figure 4-4, an example FTIR spectrum of a fully formulated engine oil contains three major peaks associated with the base oil hydrocarbons.

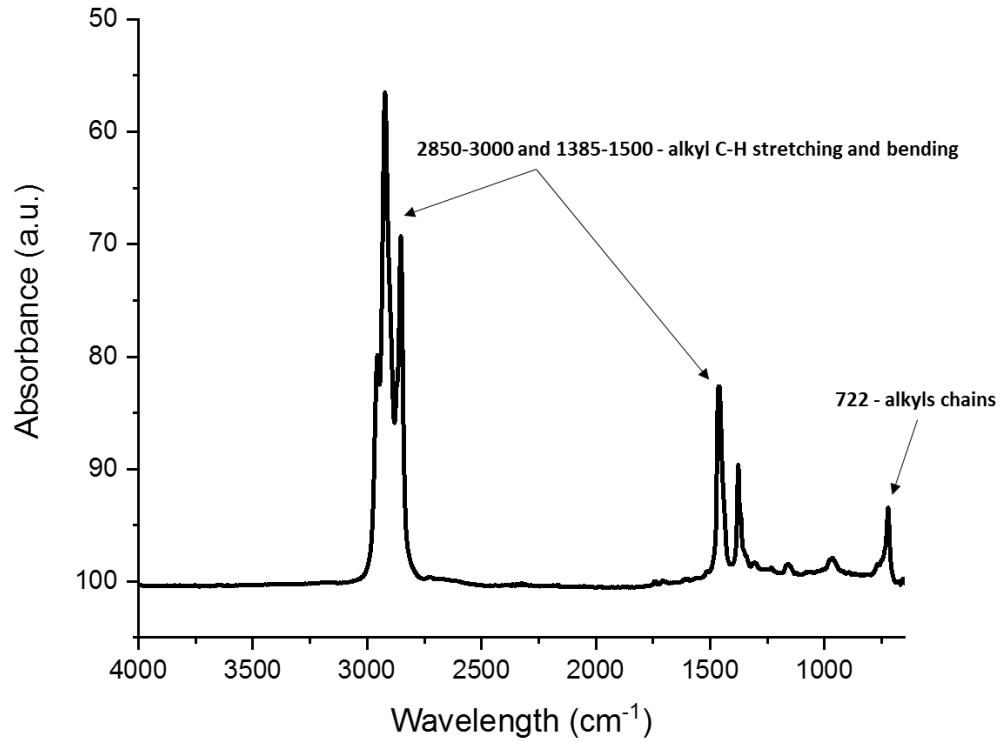


Figure 4-4 FTIR example spectrum.

The region is known as the fingerprint region between 400 and 2000 cm⁻¹ and has become the area of interest in identifying oil degradation. The specific areas used when analyzing oil degradation in passenger car oils are shown in Table 4-2. These values are typically found in previous research [101,102].

Table 4-2 Wavelength ranges used in this study.

Approx wavelength number (cm ⁻¹)	Component	Molecule
3400	Water	-
1700-1800	Oxidation	Carbonyl-containing degradation products – e.g. carboxylic acid
1100-1200	Sulphation	Sulfur oxides and acids
900-1000	ZDDP (Anti-wear additive)	P-O-C and P=S bond
750	Gasoline	-

4.5 Friction

4.5.1 Lambda Ratio Calculations

Theoretical lambda ratios are calculated for each sample oil to determine the lubrication regime the tribocontacts operates. This enables the user to tailor operating conditions such as load and entrainment speed to obtain the desired lubrication regime. The traction phases with a constant speed operate under the boundary lubrication regime where a low entrainment speed is required for this research. The lambda ratios for a point contact are calculated using equations 7 and 8, the Dowson & Higginson: Minimum thickness for a point contact equation [103].

$$\lambda = \frac{h_{min}}{\left[(R_{q1})^2 + (R_{q2})^2 \right]^{\frac{1}{2}}} \quad (7)$$

$$\frac{h_{min}}{R^*} = 3.63 \left(\frac{U\eta_0}{E^*R^*} \right)^{0.68} (\alpha E)^{0.49} \left(\frac{W}{E^*R^*} \right)^{-0.073} (1 - e^{-0.68k}) \quad (8)$$

4.5.2 Test Rig

Ball and disc specimens are cleaned in methanol using an ultra-sonicating bath for 5-10 minutes before running the friction tests. This is to prevent any contamination affecting the performance of the oils and results obtained.

The test rig to test the friction performance and generate tribofilms from the sample oils for each research area was an MTM. The schematic setup is shown in Figure 4-5. The contact orientation is a ball on a disc, driven independently to create the required sliding to rolling conditions. Slide to roll ratio (SRR) is defined as $(U_B - U_D)/U$ where the sliding speed is $U_B - U_D$ and entrainment speed or mean rolling speed is $U = (U_B + U_D)/2$. A steel alloy ball with a diameter of 19.05 mm is loaded against a flat steel alloy disc with a diameter of 46 mm, submerged in ≈ 35 ml of the sample oil. Sensors with a friction transducer monitoring the frictional force between both surfaces control operating conditions such as load and lubricant temperature.

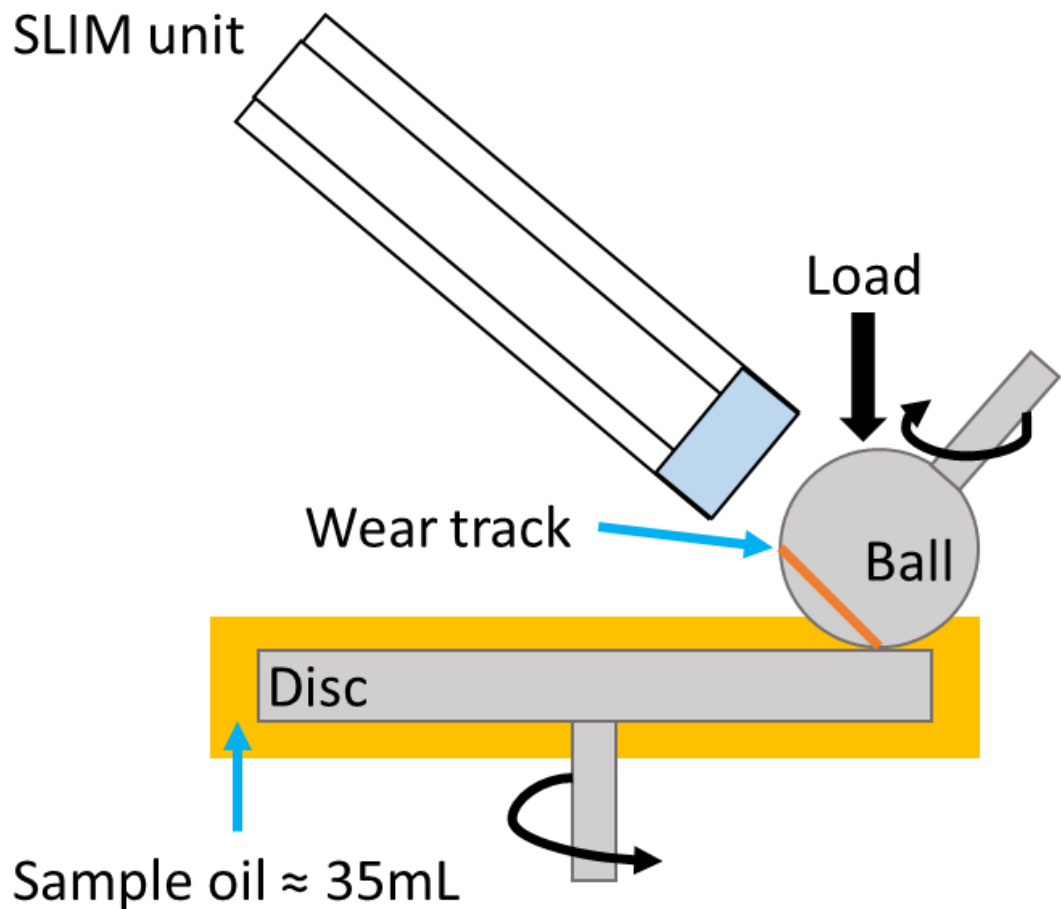


Figure 4-5 MTM-SLIM schematic.

Two phases can be used to create the tests. The first phase is called a Stribeck curve phase. Operating conditions such as load and temperature, except entrainment speed, are kept constant. Entrainment speeds descend from the highest value to the lowest to protect any tribofilm formed on the specimen from the previous phase. The second is called the traction phase. This phase is when all operating conditions, such as load, temperature, and speed, are constant. The operating conditions are designed to keep the traction phase in the boundary lubrication regime where $\lambda < 1$.

4.5.3 Operating Conditions

4.5.3.1 Chapter 5

The MTM test procedure used in Chapter 5 consisted of traction and Stribeck curve phases, as shown in Figure 4-6. Stribeck curves were taken at intervals of 0, 1, 5, 15, 30, 60, and 120 minutes, with the test procedure starting with a Stribeck curve and ending with a traction phase. The total traction time equals 210 minutes or 3.5 hours.

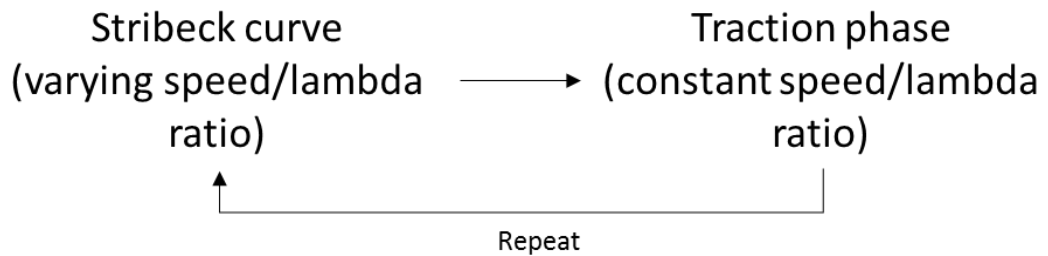


Figure 4-6 Chapter 5 MTM test procedure.

The operating conditions used on the MTM for Chapter 5 are shown in Table 4-3. The operating conditions selected are typical of those found in an ICE [104]. Both phases had a constant SRR of 50 %, 40 N load force corresponding to 1 GPa of pressure, and lubrication temperature of 100 °C. The Stribeck curve phase had a varying entrainment speed, starting from 2000 and decreasing to 10 mm/s. The highest speed within the Stribeck curve does not exceed past the mixed lubrication regime. A constant speed of 100 mm/s was set for the traction phase to emulate the boundary lubrication regime. The ball and disc material were made from AISI 52100 steel with surface roughness's of < 0.02 μm .

Table 4-3 Chapter 5 MTM operating conditions.

Parameters	Stribeck curve phase	Traction phase
Materials	AISI 52100 Steel ball and disc	AISI 52100 Steel ball and disc
Sliding rolling ratio % (SRR)	50	50
Load (N)	40	40
Hertzian/contact pressure (GPa)	1.0	1.0
Speed (mm/s)	2000 ~ 10	100
Temperature (°C)	100	100

4.5.3.2 Chapters 6 to 8

A schematic of the MTM test procedure used in Chapters 6 to 8 is shown in Figure 4-7. The test starts and ends with a mapper step with SLIM measurements and Stribeck curves obtained at intervals of 0, 5, 15, 30, 60, 120, 180, and 240 minutes. The mapping step was included to understand the ZDDP/phosphate glass tribofilm film formation during the test.

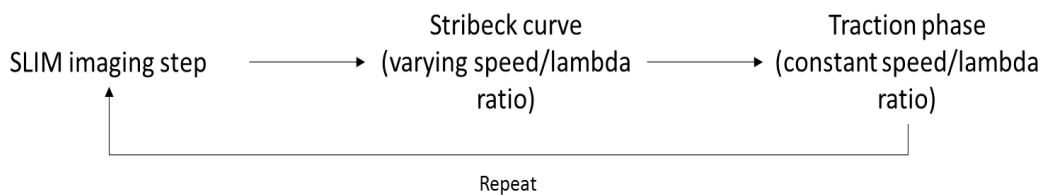


Figure 4-7 Chapters 6 to 8 MTM test procedure.

The MTM operating conditions used in Chapters 6 to 8 are shown in Table 4-4. Both phases had a constant SRR of 100 %, 40 N load force corresponding to 1 GPa of pressure, and a lubrication temperature of 120 °C. Temperature and SRR were increased to favour MoS₂ formation and emulate different ICE conditions. Entrainment speed was fixed at 100 mm/s, corresponding to a typical lambda ratio value of 0.2 found in the ICE [103].

Table 4-4 Chapters 6 to 8 MTM operating conditions.

Parameters	Stribeck curve phase	Traction phase
Materials	AISI 52100 Steel ball and disc	AISI 52100 Steel ball and disc
Sliding rolling ratio % (SRR)	100	100
Load (N)	40	40
Hertzian/contact pressure (GPa)	1.0	1.0
Speed (mm/s)	2000 ~ 10	100
Temperature (°C)	120	120

4.6 ZDDP Film Thickness

To measure the optical film thickness of the tribofilms over time a SLIM unit attached to the MTM was used. The schematic of the SLIM unit with the MTM is shown in Figure 4-5. Previous research showed that the SLIM technique could measure the optical film thickness of boundary active additives such as detergents, MoDTC, and ZDDP when formulated together [105,106].

The ball is unloaded from the disc and loaded against a thin Cr layer coated glass disc during the test to obtain the SLIM images, as shown in Figure 4-8. White light is then illuminated down a microscope, and a picture of the tribofilm is taken. The ball is reloaded onto the disc, and the next step begins. This process is repeated at set intervals stated in the test process.

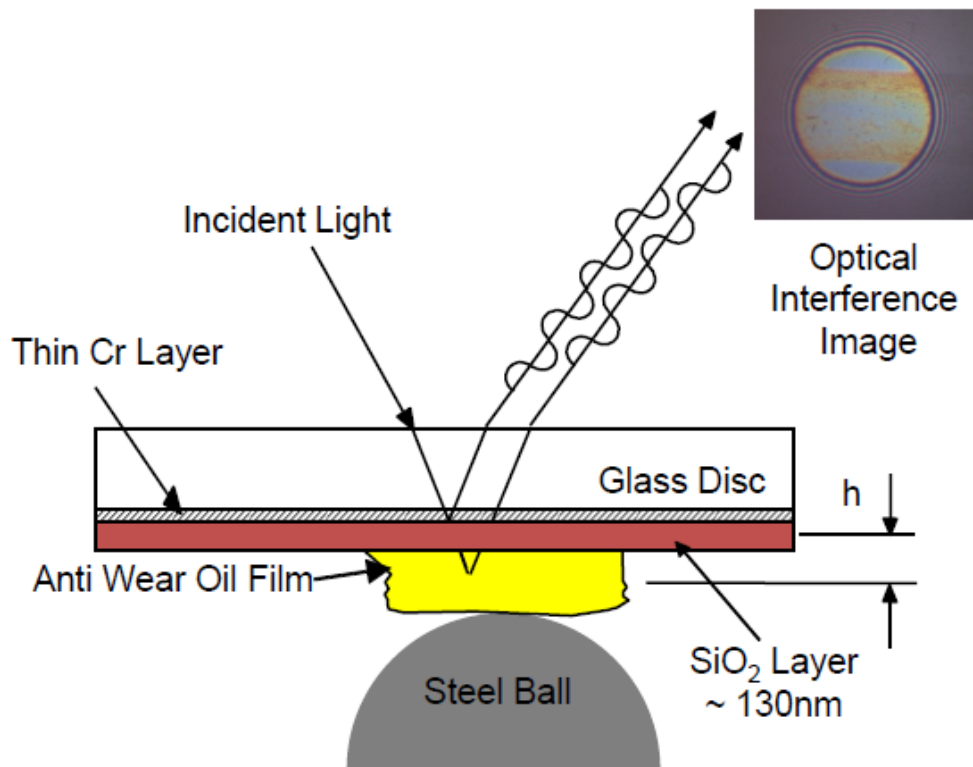


Figure 4-8 SLIM mechanism [106].

4.7 Tribochemical Surface Analysis

After friction testing, the ball and disc specimens were cleaned with heptane before any surface analysis was conducted to remove excess oil remaining on the samples.

4.7.1 X-ray Photoelectron Spectroscopy (XPS)

XPS is a powerful chemical surface analysis technique used to analyze the chemistry of tribofilms formed by rubbing two surfaces. The principle of the method is called the photoemission process, where x-rays are fired onto the surface, which causes electrons to be emitted and detected from interactions between the x-rays and surface atoms. These detected electrons emitted from the surface contain valuable information such as kinetic energy. Using the kinetic energy of the emitted electrons and the photon energy of the X-rays, the binding energy, BE, can be calculated using equation 9, where KE is the kinetic energy of the emitted electron, $h\nu$ is the photon energy, and ϕ_2 is the spectrometer work function. The x-ray photons have a penetrating depth of up to ≈ 10 nm [107].

$$KE = h\nu - BE - \phi_2 \quad (9)$$

Part of the chemical analysis for the tribofilms in this research was conducted using XPS. A high-power monochromatic Al K α X-ray source (1486.6 eV), with an energy resolution of ≈ 0.5 eV, was used to obtain two types of scans within a pre-defined area of interest; survey and high resolution (HR). Survey scans were used to identify the elements and their weight % within the area of interest. HR scans were performed to obtain the chemical composition of the tribofilm, specifically identifying chemical bonding associated with selected

elements' chemical states such as Mo 3d and Zn 2p. The spin orbitals of the 2p and 3d split the signals into $2p_{3/2}$, $2p_{1/2}$, and $3d_{5/2}$, $3d_{3/2}$.

Before any analysis of the signals is undertaken, the C1s signal peak is used for calibration due to potential charging during acquisition and is set to 285 eV [108]. Shirley's line type was used as a standard baseline, and different line shapes were used for the peaks to distinguish the various components within the signals. General and specific conditions and constraints must be applied when deconvoluting signals. They are as follows.

- The area of $2p_{1/2}$ is always 0.5 times smaller than the area of $2p_{3/2}$.
- The area of $3d_{3/2}$ is always 0.67 times smaller than the area of $3d_{5/2}$.
- Spin orbitals with a larger denominator always have higher binding energy, for example, $2p_{3/2} < 2p_{1/2}$ binding energy.
- The binding energy difference between $3d_{5/2}$ and $3d_{3/2}$ in the deconvolution of the Mo3d signals is constrained to 3.13 eV [109].

To understand the chemical composition of the different layers in the tribofilms, etching was performed using an Ar⁺ ion beam at 2 keV with a sputtering current of 1 uA. Previous literature determined that using these settings produces an etch rate on steel of 4.5 nm per minute by Wyko [110].

4.7.2 Raman Spectroscopy

The vibrational characteristics of a molecule can be studied using Raman spectroscopy. A monochromatic light laser power source produces molecular vibrations when incident light energy is transferred to the molecules. These vibrations of the molecules are characterized by a wavelength number with different molecule vibrations producing different wavelength numbers. The

scattered light composition highly depends on the molecule it has vibrated, enabling the technique to create a fingerprint of the specimen [111].

Wire 3.4 software is used in conjunction with the Reinshaw Raman spectrometer system. This enables the user to adjust numerous parameters, including laser power, exposure time, and the number of scans. Spectral resolution of the Reinshaw Raman spectrometer is $\approx 1 \text{ cm}^{-1}$. Spectra for all tribofilms generated on the balls were obtained from the Raman using a 488 nm wavelength laser with a 10 % power filter, 10 s exposure time, and two accumulations per acquisition. The 488 nm wavelength laser was selected as previous research has shown it is critical for MoS₂ tribofilm detection [68]. Power filter at 10 %, low exposure time of 10 s, and two accumulations were selected to prevent the laser from damaging the tribofilm. The peaks and associated vibration modes from a typical MoS₂ spectrum are shown in Figure 4-9. The vibration modes E_{2g} wavelength number is $\approx 381 \text{ cm}^{-1}$, and A_{1g} is $\approx 408 \text{ cm}^{-1}$. The Raman maps and data generated in this research were created using the A_{1g} peak intensities [75].

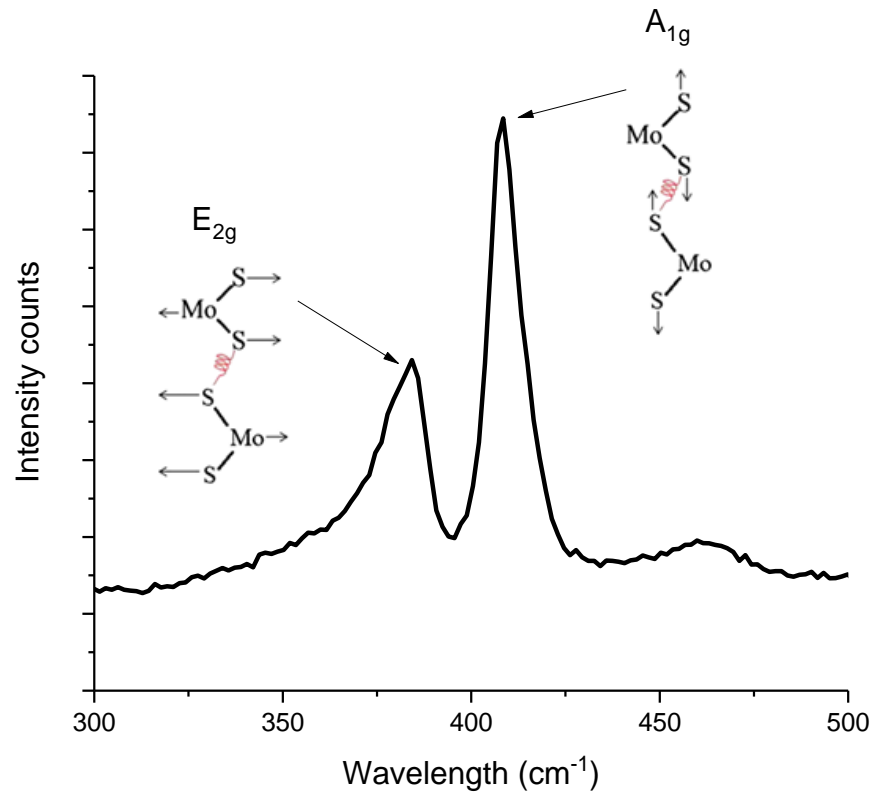


Figure 4-9 Raman example spectra of MoS₂ peaks.

4.8 Wear Analysis

Wear analysis was conducted using an NPFlex. It is a non-contact technique that prevents any damage from occurring on the surface during scanning and uses white light interferometry to generate an image used for analysis. The method works by light interference, which occurs when the light path's distance is different from the light path from the surface. Bruker Vision 64 is the software used to analyze the wear scar image taken from the NPFlex, and an example image of the surface of an MTM disk captured by the software along with a cross-section profile is shown in Figure 4-10.

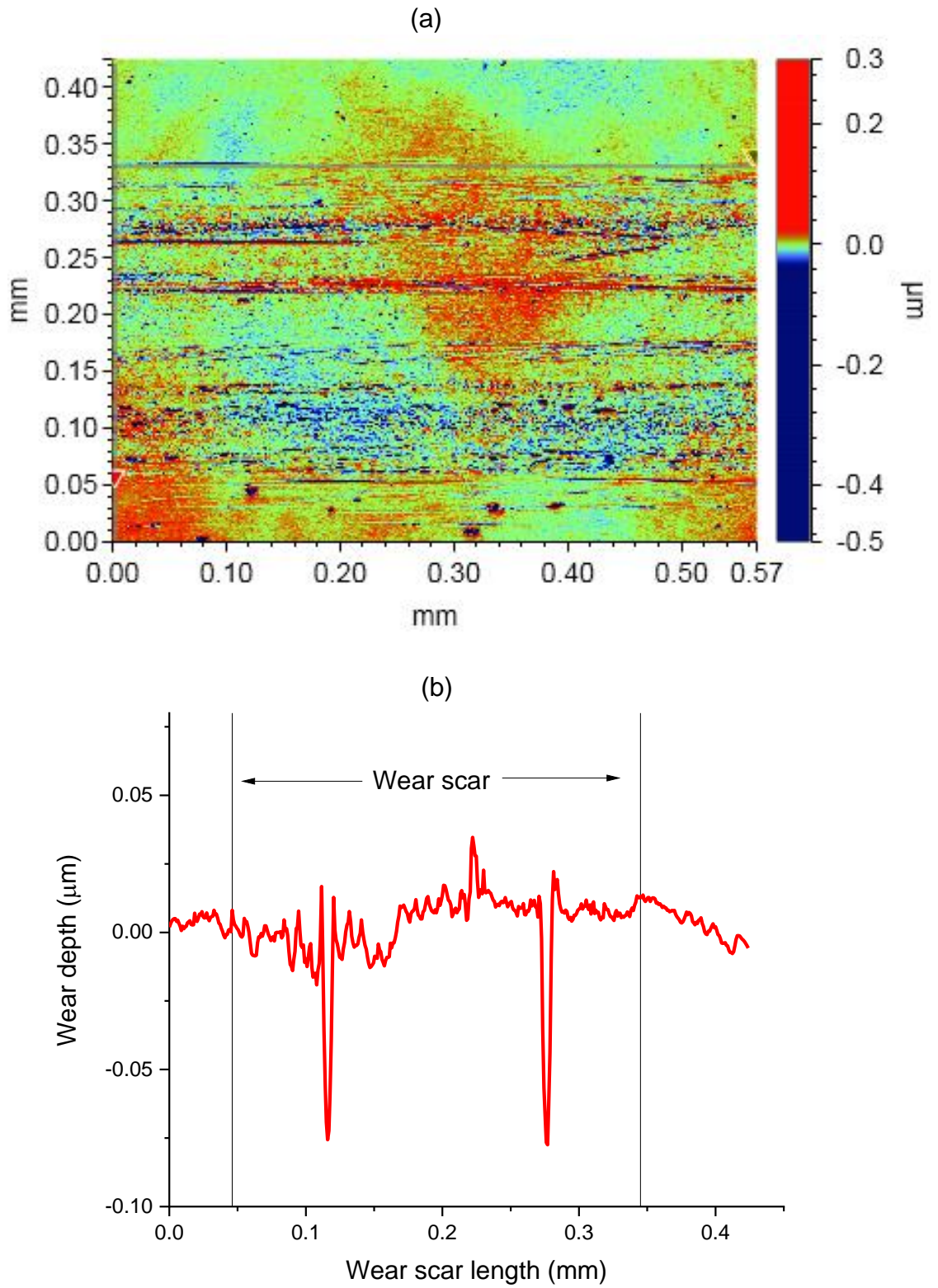


Figure 4-10 Examples of (a) NPFlex scanned image and (b) Y-profile of a wear scar.

4.8.1 Tribofilm Removal

Since white light interferometry is used to obtain topography images of the wear scars, the tribofilm must be removed. To remove the tribofilms, an EDTA (ethylene-diamine-tetraacetic acid) solution was used [112,113]. The solution was applied to the tribofilm for roughly 2 minutes and then removed by rubbing the wear scar gently with tissue paper. This procedure is repeated to ensure that all the tribofilm has been removed.

Wear analysis on all the selected samples in this research was conducted via the same methodology. Excess oil was removed using heptane, and tribofilm was removed using EDTA acid solution [112]. Due to the contact being unidirectional with the wear scar not concentrated in a straight line, three areas of interest on the discs were chosen for analysis using the NPFlex, as shown in Figure 4-11. An average of the three regions was calculated and presented as wear volume loss. The wear measurements were repeated once for validity.

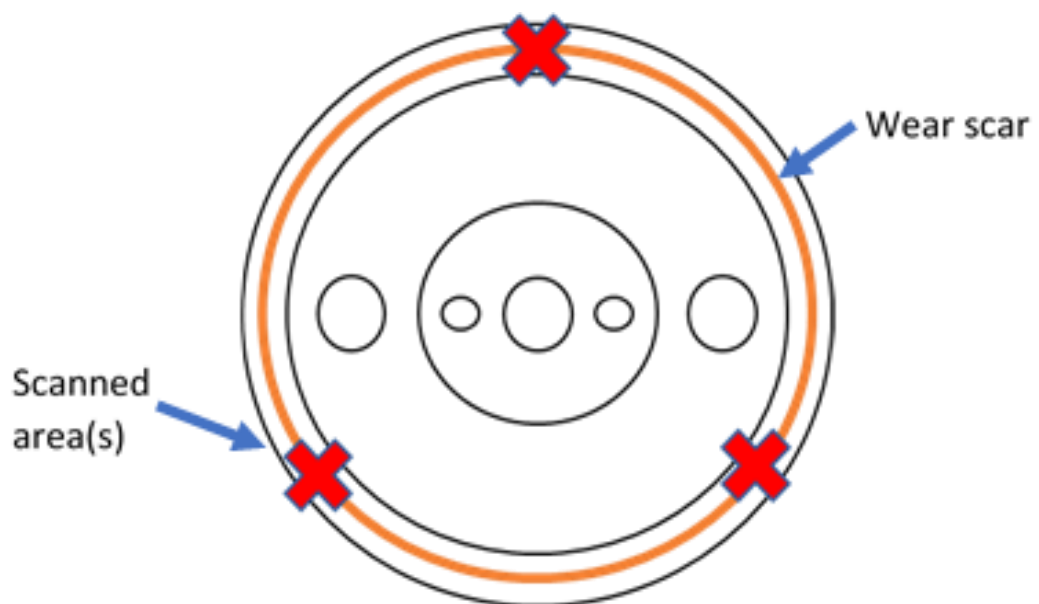


Figure 4-11 Selected areas for wear analysis.

4.9 Summary

This chapter has outlined the experimental procedures used in this study. A section on the fundamentals of each technique was introduced. The operating conditions for each technique kept constant throughout the studies were detailed. The operating conditions on the MTM for each results chapter was also outlined.

The following chapters present the experimental results and key findings, and discussions.

Chapter 5 The critical role of MoDTC to counteract low viscosity in ultra-low viscosity engine oils

5.1 Introduction

As explained in the introduction and literature review, reducing the viscosity of engine oil is the most cost-effective way to increase the engine's fuel economy to achieve the overall aim of reducing CO₂ emissions [8,114]. However, reducing the viscosity negatively impacts the friction and wear of the tribo-contact in boundary and mixed lubrication regimes. Therefore, to increase fuel economy when reducing the oil viscosity, the friction in boundary and mixed lubrication regimes must be equal to or smaller than its higher viscosity counterparts [115]. Therefore, understanding the impact that lowering the oil viscosity has on the lower lambda ratio regimes and the additives used to counteract the effect is very important.

This chapter shows the impact of reducing oil viscosity on the boundary and mixed lubrication regimes and how this phenomenon is counteracted with MoDTC. Friction tests were conducted using the MTM to simulate rolling/sliding conditions and varying lambda ratios within the boundary and mixed lubrication regimes. Wear was measured using NPFlex non-contact technique after tribofilm removal. Finally, tribochemical analysis of the tribofilm was performed using XPS.

5.2 Test oils

The test oils used to show the impact oil viscosity reduction has on the boundary, and mixed lubrication regimes are shown in Table 5-1. The Sinopec Lubrication Company supplied all oils. Four oils with different viscosities were chosen to highlight the impact of lowering the oil's viscosity on the tribo-contact. According to the American Society for Testing and Materials (ASTM), each oil's kinematic viscosities are within their respective oil grade brackets.

Table 5-1 Test oils used in the oil viscosity reduction study.

	5W-30	0W-20	0W-16	0W-8
KV 100/ D445	12.22	8.38	6.18	5.34
KV 40/ D445	72.35	35.96	27.99	25.46
HTHS 150/D4683	2.91	2.66	2.3	1.92

Test oils used to highlight the importance of using a friction modifier and its influence on the overall performance of the oil are shown in Table 5-2. Both 0W-20 fully formulated engine oils are identical, except one has no MoDTC, and the other contains 200 ppm of Mo.

Table 5-2 Test oils used in the friction modifier study.

	5W-30	0W-20 no MoDTC	0W-20 With MoDTC
Base oil	-	3+	3+
KV 100/ D445	12.22	8.2	8.2
Mo (ppm)	-	0	200

MTM operating conditions used in these studies are shown in Table 4-3.

5.3 Oil Viscosity Reduction

The effect of reducing the oil viscosity on the boundary and mixed lubrication regimes is shown in Figure 5-1. The Figure displays the initial Stribeck curve of 4 different SAE viscosity grade oils ranging from 5W-30 to 0W-8 taken at 0 minutes into the test. Since the oils additive packages differ, only the first Stribeck curve can show oil viscosity reduction in boundary and mixed lubrication regimes.

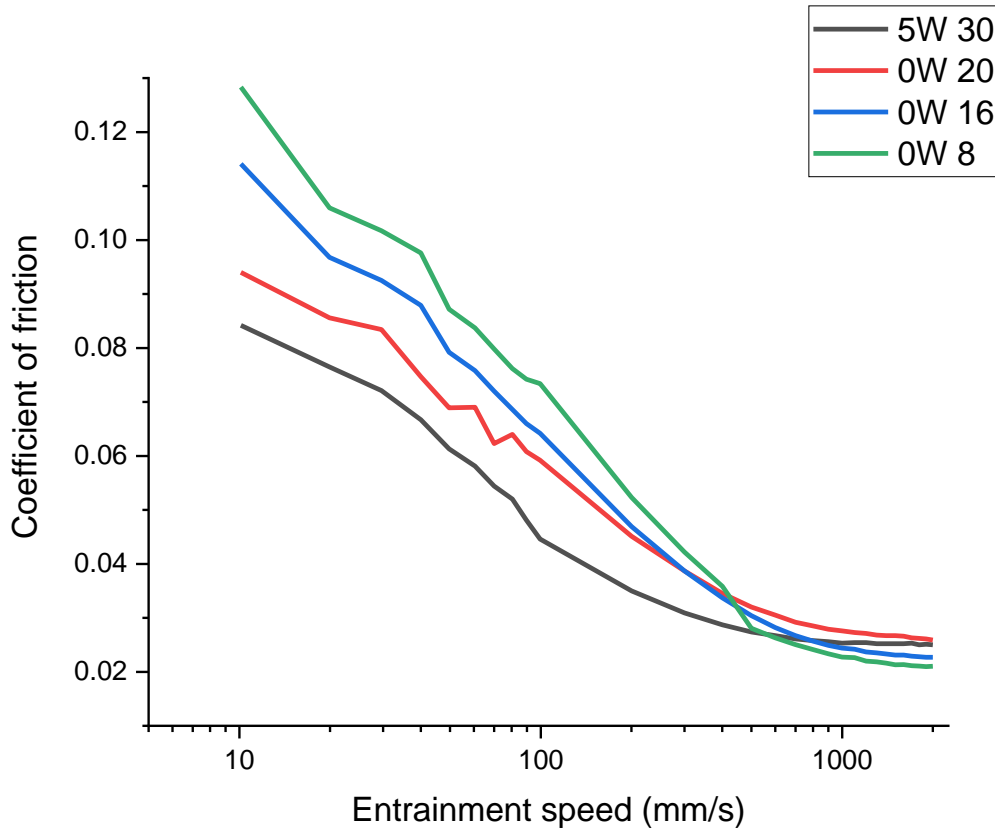


Figure 5-1 Reduction of oil viscosity influence on boundary and mixed lubrication regimes.

The results highlight the negative impact of lowering the oil's viscosity on the tribo-contact and the need to counteract it. It is clear from the results that the general trend of lowering the oil's viscosity increases the friction at lower entrainment speeds and decreases the friction at higher entrainment speeds which are also documented in previous research [115–117]. Higher friction is observed at lower entrainment speeds or in the boundary lubrication regime because the oil film thickness reduces with viscosity, leading to more metal-on-metal contact. Viscosity reduction has the opposite effect as the entrainment speed is increased. The reduced oil film thickness reduces viscosity friction or oil shear strength, leading to reduced friction in mixed and

hydrodynamic lubrication regimes for lower viscosity engine oils. It must also be noted that a higher entrainment speed is required for a lower viscosity engine oil to move to higher lambda ratios.

5.4 The Critical Role of Friction Modifiers in Low Viscosity Oil

5.4.1 MoDTC Influence on Friction

Friction modifiers such as MoDTC reduce the friction to ≈ 0.04 to counteract the increased friction caused by lowering oil viscosity in boundary and mixed regimes [71,72,118]. Figure 5-2 shows the MTM analyzed friction data of three oils, using the same operating conditions in Table 4-3. The three oils used were a 5W-30 reference oil, a 0W-20 fully formulated oil with no friction modifier, and the same oil with a friction modifier to highlight the friction modifier's importance. The friction modifier used is MoDTC, with a Mo concentration of $\approx 200\text{ppm}$.

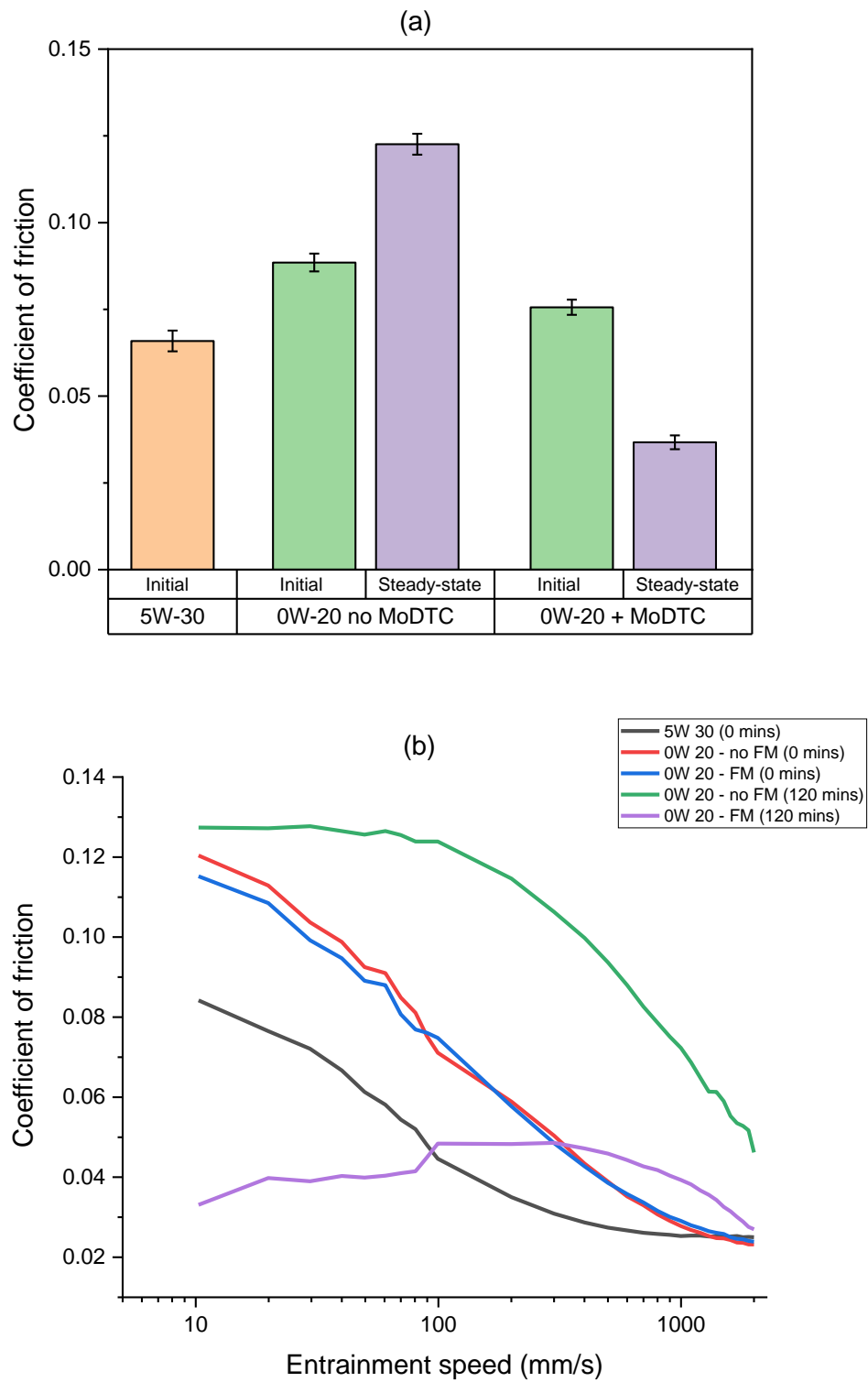


Figure 5-2 (a) Friction values at 0 and 120 minutes under a constant lambda ratio, (b) Stribeck curves taken at 0 and 120 minutes under a varying lambda ratio.

Part (a) of the Figure displays the coefficient of friction values at 0 minutes into the test with the final steady-state friction from the traction phase at a constant lambda ratio and speed of 100mm/s in the boundary lubrication regime. At the beginning of the test, at 0 minutes, the impact of decreasing the oil's viscosity is transparent, with an increased friction value for both 0W-20 oils compared to the 5W-30. The steady-state friction towards the end of the test increases by $\approx 38\%$ to 0.1226 for the sample oil with no MoDTC, a typical value for a tribofilm comprised mainly of the anti-wear and detergent additives [71,82]. For the 0W-20 engine oil with MoDTC, the steady-state friction decreases by $\approx 51.45\%$ to ≈ 0.04 . This friction reduction is due to the formation of MoS_2 in the tribofilm matrix, which is the most crucial molecule created from the decomposition of MoDTC [65]. The tribochemical analysis in the next section will confirm the presence of MoS_2 .

To further understand the influence MoDTC has in low viscosity engine oils, the friction under a varying lambda ratio must be analyzed along with a constant ratio. Part (b) of the Figure shows the Stribeck curves of the three oils taken at 0 and 120 minutes into the test. As expected, at 0 minutes into the test, both 0W-20 oils have similar Stribeck curves due to the only difference being the addition of MoDTC. However, there is a clear distinction between the Stribeck curves taken at 120 minutes of the two 0W-20 oils. Again, as expected, the 0W-20 oil with no MoDTC produces a Stribeck curve similar to tribofilms, comprised mainly of anti-wear and detergent additives, as shown in previous research [50,52]. An increase of friction over the varying lambda ratios and speeds is observed for the oil due to the tribofilm mainly comprising ZDDP. At higher entrainment speeds towards 2000mm/s, in the

mixed lubrication regime, the act of the ZDDP tribofilm growing increases the friction where metal-to-metal contact occurs. Additionally, the tribofilm thickening causes the lambda ratio to decrease, requiring higher speeds to transition from a boundary to a mixed lubrication regime. In the hydrodynamic regime, the impact of the tribofilm on friction would be negligible. The 0W-20 oil with MoDTC decreases friction at lower entrainment speeds. However, at speeds ≥ 300 mm/s, the friction increases compared to the Stribeck curve at 0 minutes but still has reduced friction compared to the oil with no MoDTC at 120 minutes into the test. The results in Figure 5-2 show the critical role MoDTC has on friction when lowering the oil's viscosity.

5.4.2 Tribofilm Chemistry

The contents and chemistry of tribofilms are essential aspects when investigating new engine oil grades and additive packages. As previous research has shown, it helps to understand the friction and wear results and create mechanisms for new phenomena [49,77].

Figure 5-3, and **Error! Reference source not found.** display the high-resolution XPS scans of Mo, S, P, Zn, and Ca taken from the top layer of both tribofilms generated via friction tests using the 0W-20 fully formulated oil without and with MoDTC.

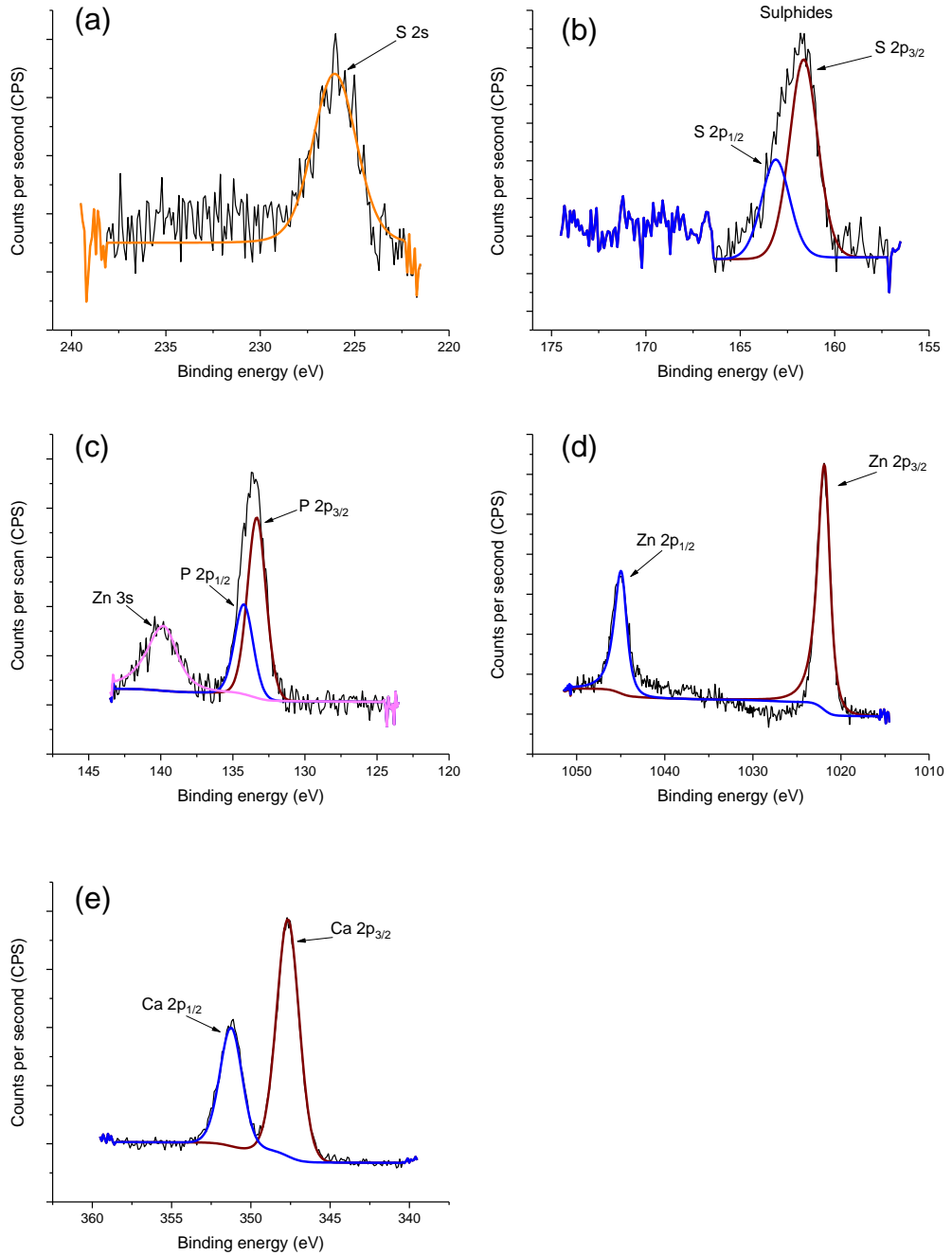


Figure 5-3 XPS High-resolution scans for 0W-20 without MoDTC sample, (a) - Mo 3d, (b) - S 2p, (c) - P 2p, (d) - Zn 2p, and (e) - Ca 2p.

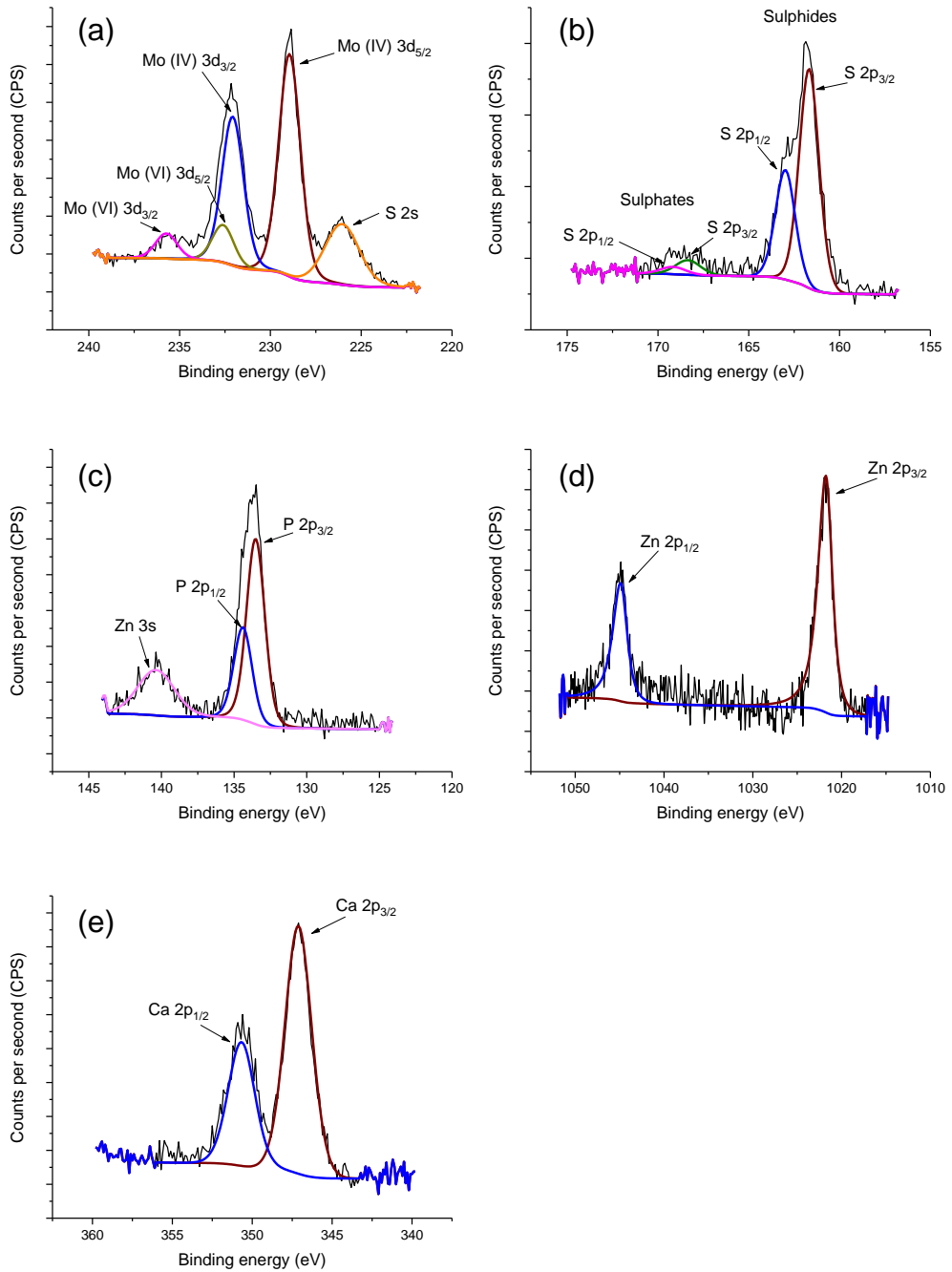


Figure 5-4 XPS High-resolution scans for 0W-20 with MoDTC sample, (a) - Mo 3d, (b) - S 2p, (c) - P 2p, (d) - Zn 2p, and (e) - Ca 2p.

Part (a) of Figure 5-3, without MoDTC, has only one peak detected by the XPS analysis for Mo3d. This peak is associated with a metal sulfide with a binding energy of ≈ 226 eV [119,120]. Since no MoDTC within the oil formulation, the metal sulfide must be linked to Zn or Fe. Moreover, the Mo 3d signal for the sample with MoDTC has multiple more peaks, as shown in part (a) of Figure 5-4. These peaks are typically detected in the presence of MoDTC with a friction-reducing tribofilm [65,71,119,120]. The two chemical states detected in the top layer of the tribofilm for the sample oil with MoDTC are Mo (IV) and (VI). Mo (IV) is associated with bonding with sulfide, indicating that the compound MoS_2 is formed, the most crucial decomposition product of MoDTC [77].

Part (b) from Figure 5-3 and Figure 5-4 displays the high-resolution scan deconvolution of the S2p scan. Only one peak is detected for the sample without MoDTC, in part (b) of Figure 5-3, split into the spin orbitals $2p_{3/2}$ and $2p_{1/2}$ with binding energies of ≈ 162 eV and ≈ 164 eV. This peak is typically associated with sulfides within the tribofilm from previous work [121]. Since no MoDTC within the oil, the sulfide peak must be linked to a compound formed from ZDDP, for example, ZnS or FeS from the metal surface. The peak associated with sulfides is also detected in the tribofilm of the oil-containing MoDTC, as shown in part (b) of Figure 5-4. Due to the addition of MoDTC, this peak could also be linked to MoS_2 , as previous research has shown [122].

The other three high-resolution scans, P, Zn, and Ca are associated with the composition products of ZDDP and detergent, which form within the tribofilm matrix. Regardless of the addition of MoDTC within the oil formulation, the same decomposition products from ZDDP and detergents are formed, as

shown by the same peaks detected in Figure 5-3 and Figure 5-4. The P 2p and Zn 2p peaks detected in the high-resolution scans in both tribofilms are typical of a ZDDP-only tribofilm [121]. Ca 2p peaks are associated with CaCO_3 , the decomposition product of the detergent which forms within the tribofilm matrix [123].

Overall, for the tribochemistry, MoDTC decomposes into MoS_2 and Mo oxides within the tribofilm matrix. The MoS_2 lattice layers enable low friction to be achieved, which are embedded within the ZDDP dominant tribofilm. ZDDP decomposition products can still form regardless of adding MoDTC; however, the amounts are reduced due to competitive absorption. A later chapter will discuss the tribochemistry matrix in more detail.

5.4.3 MoDTC Influence on Wear

The impact of MoDTC on the wear in low viscosity fully formulated oil is shown in Figure 5-5. An increase in wear volume is observed for the 0W-20 engine oil with MoDTC. An explanation of an increase in wear can be attributed to a reduction in ZDDP species.

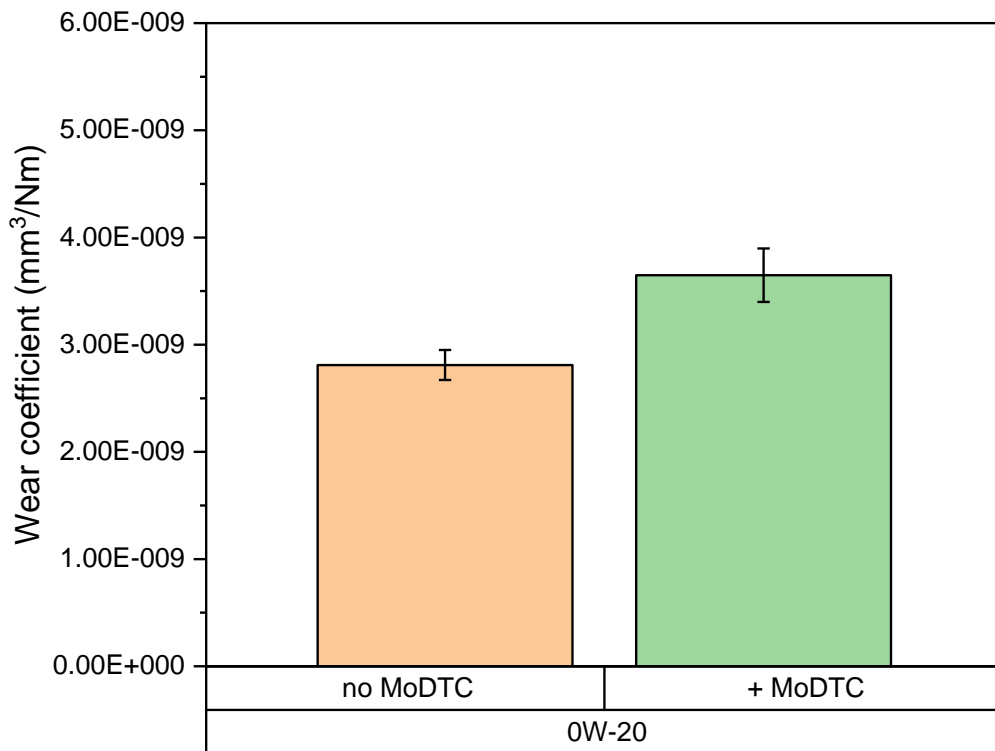


Figure 5-5 Wear volume loss taken from a specific area for sample with and without MoDTC.

The results are similar to recent research investigating organic and inorganic friction modifiers [124]. A 0W-20 fully formulated engine oil with 250 ppm of Mo in the form of MoDTC produced a 48% increase in wear compared to the same oil without MoDTC. However, it must be noted that the wear obtained for a specific area shown in Figure 5-5 is very small. Therefore, in the real-world application of the engine, the wear increase due to MoDTC is negligible [125]. The next chapter will produce more results regarding Mo concentration influence on the tribofilm chemistry and wear mechanisms.

5.5 Summary

This chapter has highlighted the negative implications of reducing the oil's viscosity on the boundary and mixed lubrication regimes. Increased friction is observed in these regimes due to reducing film thicknesses. The friction in the boundary and mixed regimes must be reduced to ≈ 0.04 to enable the oil viscosity reduction to improve fuel efficiency. To achieve this, MoDTC must be used as a friction modifier. The results also highlighted the importance of counteracting the increased friction at low entrainment speeds. MoDTC decomposes to form MoS₂ and Mo oxides within the ZDDP dominant tribofilm matrix, with MoS₂ enabling a reduction in friction.

The next chapter will present results from optimising Mo concentration in new ultra-low viscosity engine oil. This chapter will discuss friction, tribochemistry, and wear in more detail regarding the impact of Mo concentrations in fully formulated engine oil.

Chapter 6 Optimizing of Mo Concentration in Ultra-low Viscosity Engine Oil

6.1 Introduction

The increased fuel economy demands are causing countries like Japan to increase the concentration of MoDTC to very high amounts of 1000+ ppm as the oil grade is lowered. Increasing the Mo concentration to very high amounts compared to higher viscosity engine oil is thought to enable prolonged fuel economy boosts, longer ODI, and increased life span performance.

The main disadvantages of increasing the Mo concentration are the higher sulfur levels and its relatively high cost. Sulfur produces harmful by-products, impacting catalyst effectiveness and interfering with filters, directly degrading the exhaust [126,127]. Previous research has shown that using boundary-active additives with a low amount of sulfur can produce worse performance regarding friction and wear [10,128]. Therefore, it is crucial to keep the strong performance of higher sulfur concentration additives when researching reducing the overall sulfur with lower viscosity engine oils. Reducing the concentration of the additive also cuts costs in the oil formulation on a larger scale.

This chapter aims to investigate the optimization of the Mo concentration in new ultra-low viscosity oil developed for fuel economy increases. MoDTC needs to perform in low viscosity conditions, but the optimum concentration of MoDTC for producing friction of around 0.04 in these oils is still not clear. The optimum additive concentration must achieve low friction of ≈ 0.04 under constant and varying lambda ratio conditions and have minimal wear. All friction tests were conducted using an MTM. A SLIM unit attached to the MTM enabled tribofilm thickness measurements to be obtained at set intervals

during the test. XPS and Raman techniques were used to understand Mo concentration's influence on tribochemistry. Finally, wear generated during the tribometer testing was analyzed using an NPFlex. All oil formulations and operating conditions for the selected tribometer and surface analysis techniques are located in the experimental procedures chapter.

6.2 Test Oils

The Sinopec lubrication company provided a fully formulated 0W-8 engine oil with no MoDTC. Using equation 10, six different Mo concentrations were formulated for testing.

$$\text{ppm concentration} = \frac{\text{mass solute (mg)}}{\text{volume solution (L)}} \quad (10)$$

The test oils used to investigate the optimization of Mo concentrations in new low viscosity engine oils are shown in Table 6-1. The only difference between the oils is the concentration of MoDTC. All the sample oils' kinematic viscosities are within the 0W-8 engine oil grade bracket according to ASTM D445. In addition, the Sinopec lubrication company performed high-temperature high shear viscosities (HTHS) according to ASTM D4683 standards.

ICP-AES was used to measure the concentration of Mo within the sample oils and the elements associated with other additives within the fully formulated oils to ensure the correct Mo ppm concentration was achieved. The ppm concentrations of the main elements associated with boundary active additives are also shown in Table 6-1.

Table 6-1 Test oils for the optimization of Mo concentration study.

Sample number	1	2	3	4	5	6	7
Base oil	Group 3+						
HTHS 150/D4683	1.92-1.94						
Mo (ppm)	0	85	180	350	500	750	1000
S (ppm)	2976	3200	3309	3614	4349	4544	5059
Zn (ppm)	854-919						
P (ppm)	721-808						
Ca (ppm)	1344-1521						

The MTM operating conditions used in this study is shown in Table 4-4. Methodologies for tribochemical and wear analysis are also shown in Chapter 4.

6.3 Friction Analysis

Friction is one of the most critical factors when investigating the critical and optimum Mo concentration within a selection of engine oils. Two aspects of friction, steady-state and Stribeck curve, from the MTM results, can be used to help understand how Mo concentration changes influence the coefficient of friction values during operation. Steady-state friction is the friction value under a constant speed and lambda ratio. In contrast, Stribeck curve friction is when the contact is under a varying entrainment speed and lambda ratio.

This chapter will concentrate on the influence of Mo concentration on friction and its implications for determining the critical and optimum concentration.

6.3.1 Constant Lambda Ratio

Figure 6-1 displays the coefficient of friction vs time graph for all the sample oils for the first 3000 seconds during the traction phase at a constant speed highlighting the induction friction. Figure 6-2 shows the final 3600 seconds of traction to end the 24-hr test highlighting the steady-state friction for all the Mo concentrations.

The main friction phases are shown in the friction data. The induction time and friction reduction during the test are shown in Figure 6-1. The induction time is the time taken for the friction to reduce to ≈ 0.04 . In comparison, friction reduction is simply the curve drop observed when the friction values decrease due to MoS₂ formation. Steady-state friction is shown in Figure 6-2. When the friction becomes constant and does not fluctuate by a significant amount, then the friction is considered steady-state.

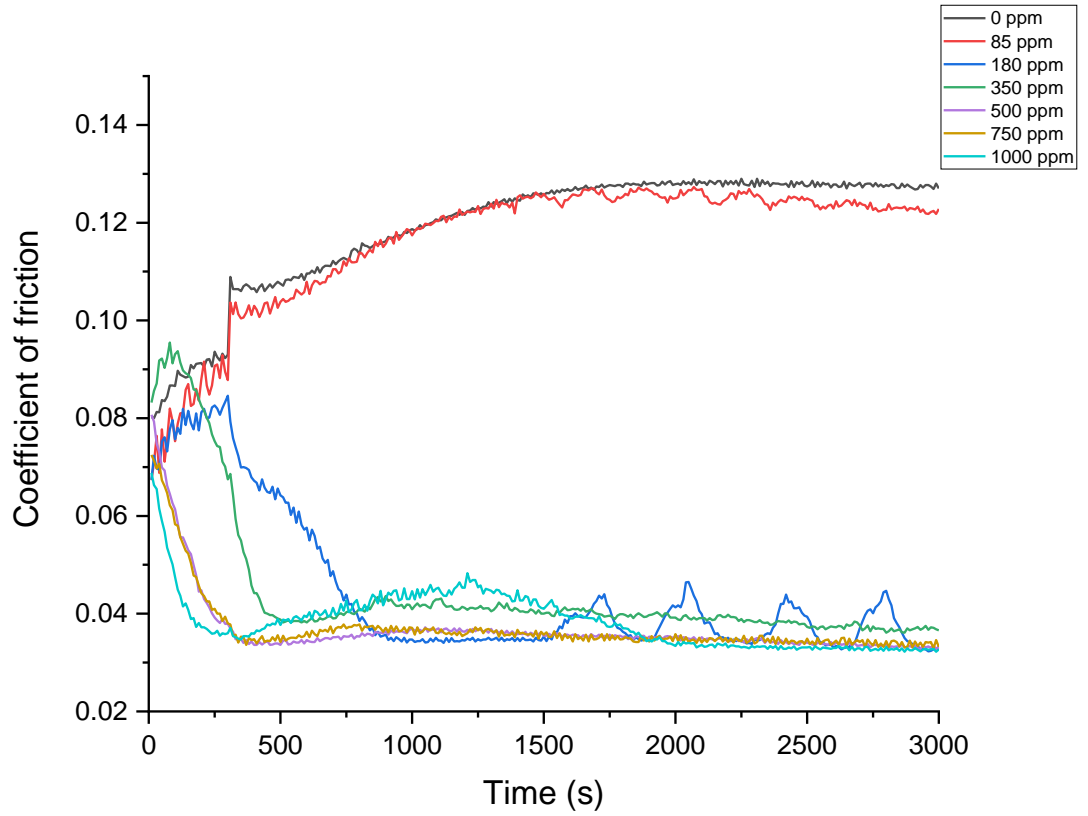


Figure 6-1 First 3000 seconds in the traction phase at a constant speed for all Mo concentrations.

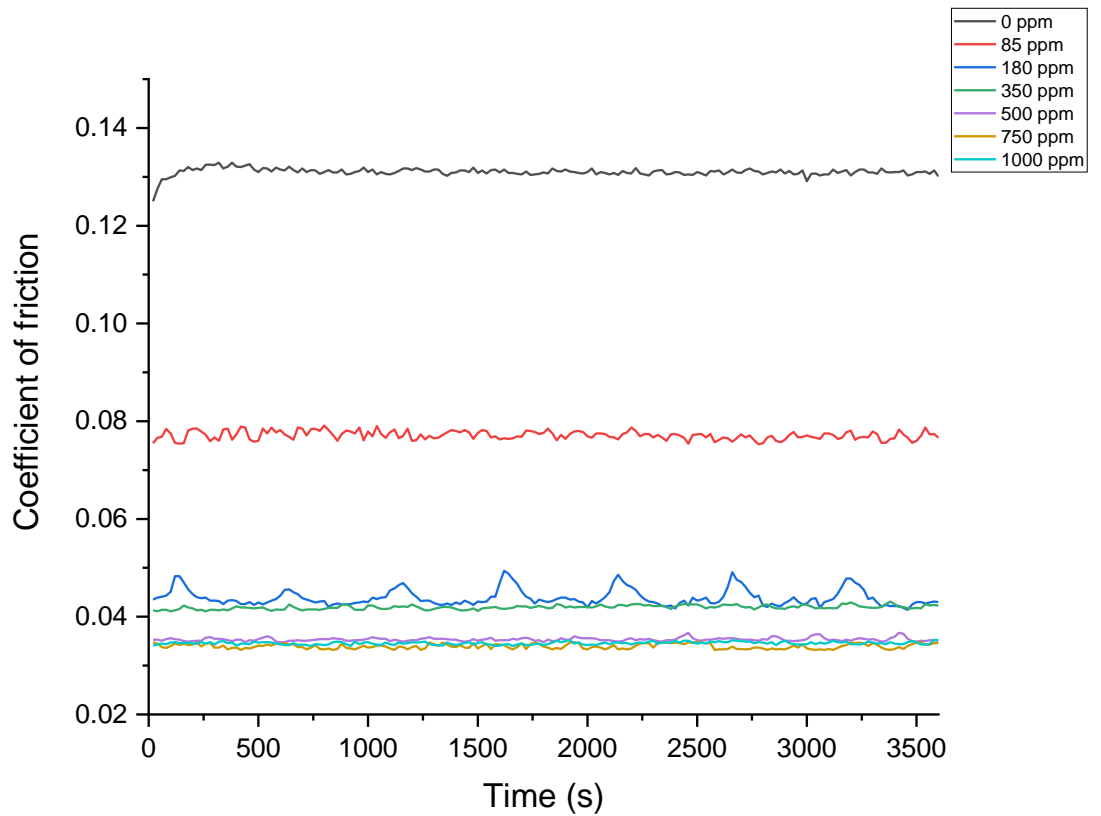


Figure 6-2 Final 3000 seconds of the 24 hours of traction for all Mo concentrations.

It is clear from Figure 6-1 that all concentrations ≥ 180 ppm reduce the friction coefficient to ≈ 0.04 in the traction phase. A general trend of increasing Mo concentration to reduce the friction induction time is also observed, and the theory behind this is discussed in Chapter 9. The friction induction periods are typical of MoDTC in fully formulated or formulated with base oils from previous research, where a sharp drop is observed due to MoS₂ formation within the tribofilm matrix [129–131]. Towards the end of the 24 hrs of traction, all Mo concentrations are at their steady-state friction values, as shown in Figure 6-2. However, 180 ppm of Mo's friction fluctuates more than the other concentrations. The possible reasons behind this performance are discussed in the later sections.

The steady-state coefficient of friction values from the traction phase for the range of Mo concentrations tested on the MTM is shown in Figure 6-3. These values are calculated by averaging the friction for each concentration towards the end of the traction phase in Figure 6-2. Three Mo concentrations were chosen for repeatability tests. The error bars are depicted in the figure.

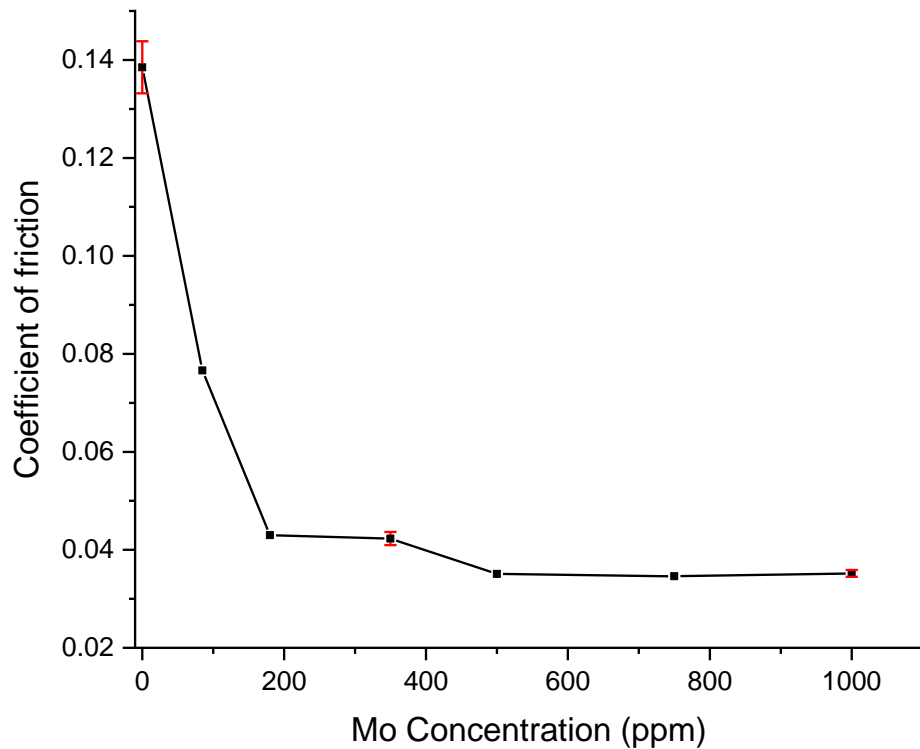


Figure 6-3 Steady-state friction values under a constant lambda ratio.

As expected, the sample oil with no Mo concentration produces a high coefficient of friction value. This value is typical of oils that do not contain a friction modifier, with the tribofilm containing anti-wear and detergent additives [82]. As the Mo concentration increases to 85 ppm, steady-state friction drops from ≈ 0.14 to ≈ 0.08 . However, the friction reduction is only ≈ 0.08 , not the typical value of ≈ 0.04 expected from a MoS_2 -rich tribofilm [66]. Thus, 85ppm of Mo provides a sufficient concentration to reduce friction but not enough to generate the ≈ 0.04 friction value. To fully understand the mechanism for 85 ppm of Mo reducing friction, an in-depth tribochemical analysis is required. It will be discussed in a later section of this chapter.

The study's minimum Mo concentration, which produces a steady-state friction value of ≈ 0.04 in the traction phase at a constant lambda ratio, is 180

ppm. The concentration chosen is only based on friction under a constant lambda ratio. However, the friction reduction must be kept under varying lambda ratios in the boundary and mixed regimes. It must be noted that no concentration between 85 and 180 ppm of Mo was tested, and the minimum concentration could be within the upper limit of the range between them. All concentrations greater than 180 ppm produced steady-state friction values \approx 0.04. Research has shown that the critical concentration within a binary system of base oil and MoDTC with a kinematic viscosity of 5.28 cSt at 100 °C is \approx 180 ppm, dependent on temperature [66], which agrees with the findings in this study for fully formulated oil. In theory, the reduction in viscosity causes the contacts lambda ratio to reduce, potentially influencing the tribofilm formation. Previous research has shown that increasing oil viscosity with low Mo concentration impacts friction at lambda ratios ranging from 0.1 to 0.3 [132]. However, regardless of oil viscosity, higher Mo concentrations are impacted less. To optimize the Mo concentration further in ultra-low viscosity with application to the ICE, the optimum concentration must keep low friction over varying lambda ratios as its higher concentration counterparts and a similar steady-state friction value.

6.4 Varying Lambda Ratio

Figure 6-4 displays the final Stribeck curves obtained when the steady-state friction value has been well achieved in the traction phase. The figure also shows the entrainment speed transition from boundary to mixed lubrication regimes marked at 1320 mm/s.

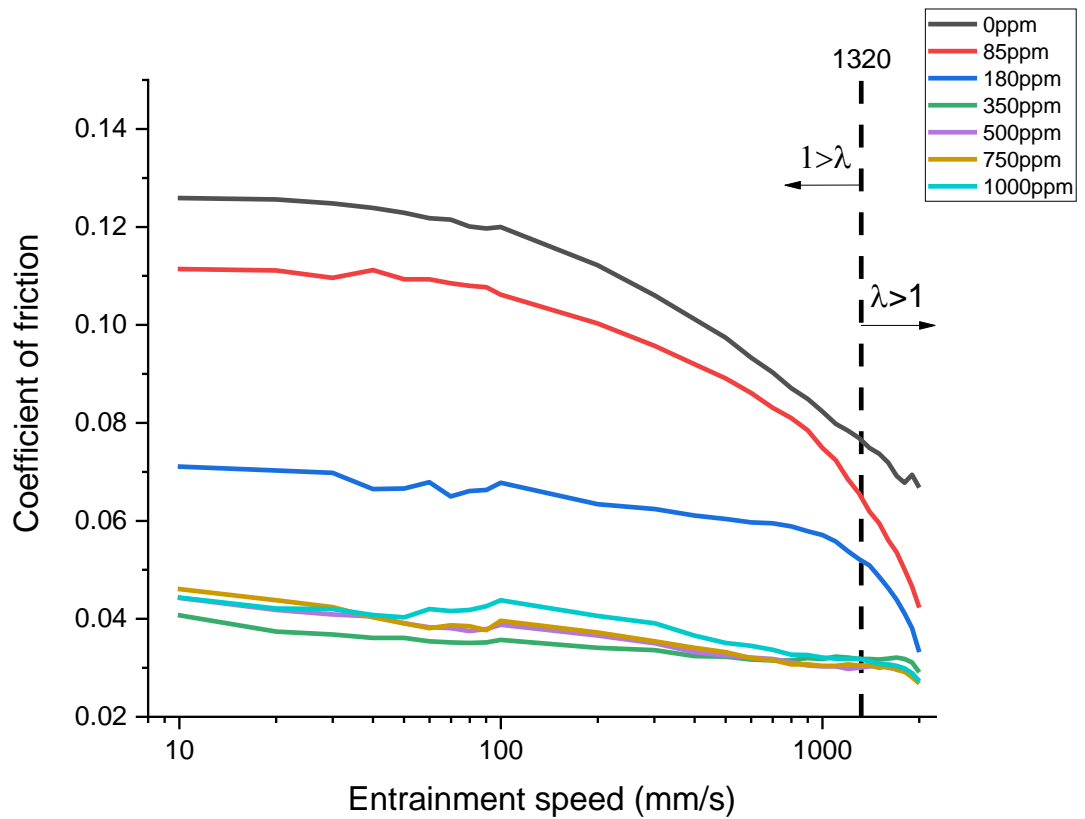


Figure 6-4 Final Stribeck curves for all Mo concentrations.

The sample with 0 ppm of Mo clearly shows the highest friction values over the entire range of entrainment speeds. This Stribeck curve resembles recent research that tested fully formulated higher viscosity oils, 0W 20, with no friction modifier [124]. Regardless of oil viscosity, as long as anti-wear and detergent additives are present within the fully formulated oil, an increase of steady-state friction to ≈ 0.12 - 0.13 will be observed in the boundary lubrication regime due to the tribofilm comprising ZDDP and detergent decomposition products [82].

It is very clear from the final Stribeck curves that Mo concentrations ≥ 350 ppm all exhibit similar friction behaviour. The Stribeck curves for these concentrations, where the friction ≈ 0.04 does not significantly differ with

lambda ratio changes in the boundary and mixed regimes, are typical for fully formulated oils with high Mo concentrations [104,133].

The graph's attention on analysis must be given to the 180 ppm of Mo sample oil. In the previous section, 180 ppm produced a steady-state friction value at a constant lambda ratio of ≈ 0.04 . However, under varying lambda ratios, it is clear that the low friction value of ≈ 0.04 is unattainable. This could be related to the amount of MoS₂, 180 ppm of Mo produced, and its formation and removal rate. Concentrations greater than 180 ppm can keep a low friction value of ≈ 0.04 under the varying lambda ratios. The Stribeck curves taken at every interval for the 180 ppm concentration are shown in part (a) of Figure 6-5, and for comparison, the 1000 ppm concentration is also included in part (b) of Figure 6-5. Higher friction values are obtained across the whole range of entertainment speeds than higher Mo concentrations. It shows the importance of testing fresh oils under varying and constant lambda ratios.

Further tribochemical analysis is required to explain the concentration at 180 ppm producing increased friction under a varying lambda ratio. The initial hypothesis is linked to the formation rate and removal of MoS₂ and its layer thickness within the tribofilm in the initial rubbing stages.

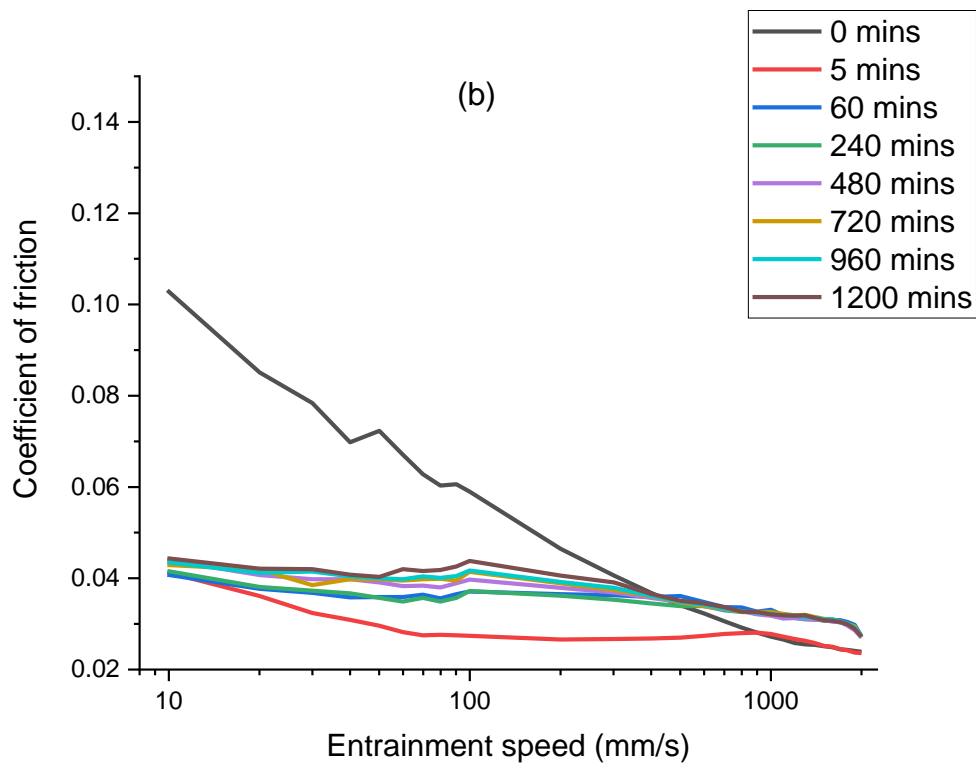
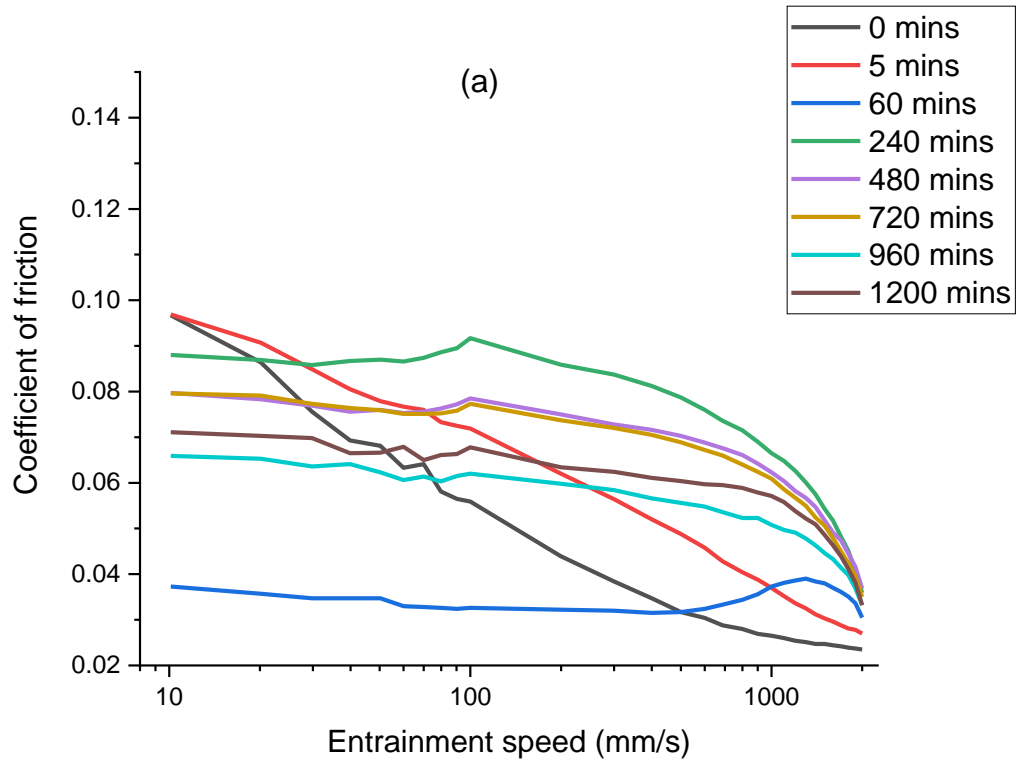


Figure 6-5 Stribeck curves for (a) 180 ppm of Mo and (b) 1000 ppm of Mo.

6.4.1 Induction Time

Another factor to consider when investigating the optimum Mo concentration for ultra-low viscosity engine oils is the time for the friction to reduce to its steady-state value. Previous research has shown that induction time is linked to Mo concentration in friction reduction [65,66]. However, little attention has been given to the hypothesis behind it. The induction time to reach each Mo concentration steady-state value is shown in Figure 6-6. Only the Mo concentrations, which reduced the friction to ≈ 0.04 , are included. Standard deviations for the repeated tests are also included.

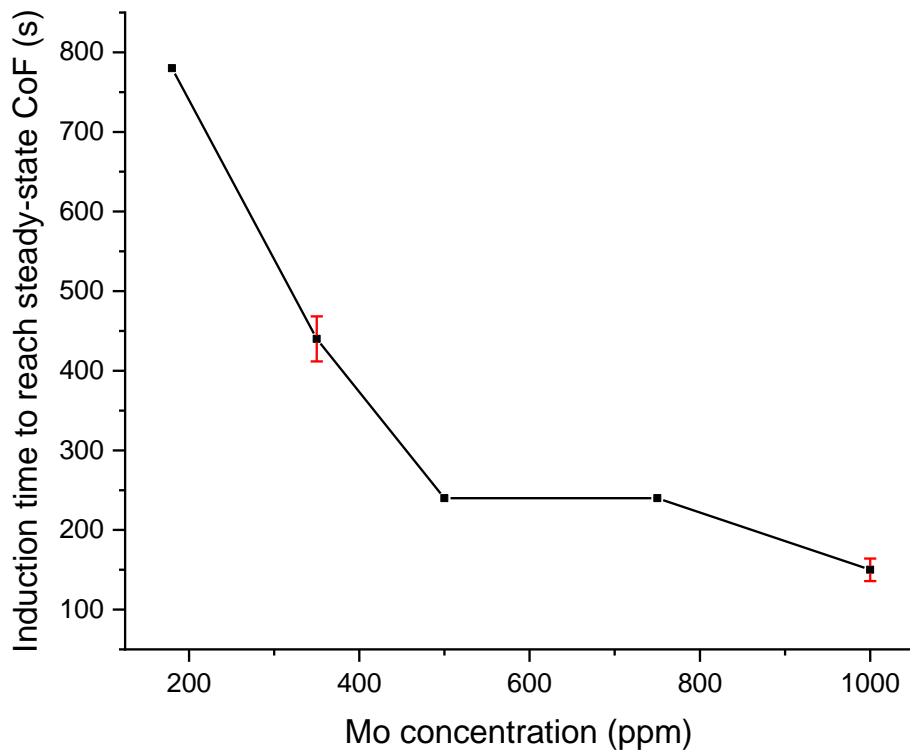
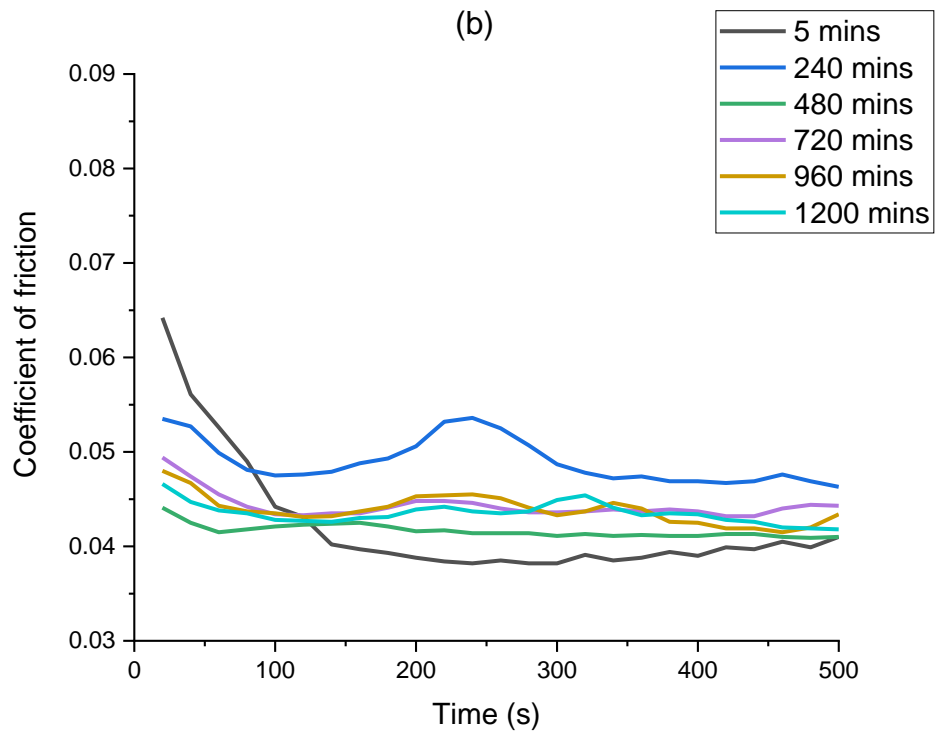
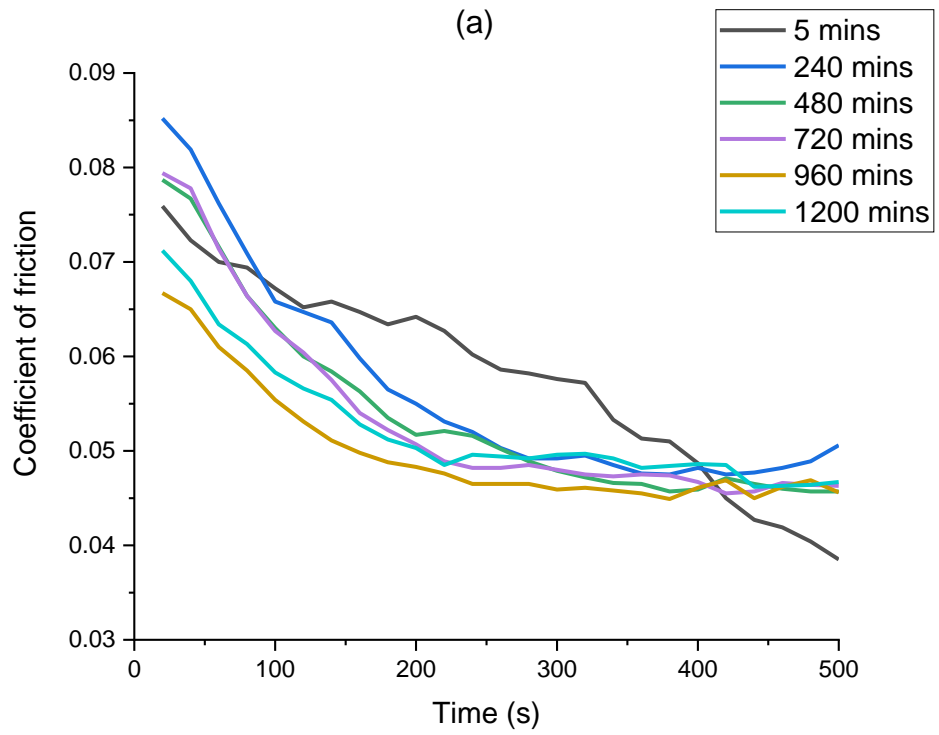


Figure 6-6 Induction time to reach ≈ 0.04 friction for Mo concentration ≥ 180 ppm.

A clear trend is observed; increasing the Mo concentration decreases the induction time to reach its steady-state friction value. The induction time reduction with higher concentration can be explained by the formation and removal of MoS₂ in the tribofilm matrix. Previous research determined that in the initial stages of the rubbing period, the tribofilm matrix is very thin, with amorphous MoS₂ structures dispersed. As the surfaces continue to rub, the tribofilm matrix becomes thicker with a layer-lattice structure of MoS₂, which leads to friction reduction and an induction time. At that point in the tribofilm formation, the formation rate of MoS₂ is greater than the removal rate [75]. Mo concentration must significantly contribute to the formation rate of MoS₂, which increases the formation vs. removal rate as Mo concentration increases. When the formation rate of MoS₂ becomes more significant at the initial tribofilm formation, the induction time decreases. In theory, more and thicker MoS₂ layers are formed within the MoDTC/ZDDP tribofilm matrix in the initial stages of the tribofilm formation. Steady-state friction is achieved once the formation rate equals the removal rate. Increasing the Mo concentration greater than 1000 ppm will decrease the induction time. However, there should be a maximum Mo concentration to which further increases do not reduce the induction time. This concentration would be a lot greater than 1000 ppm.

After each Stribeck phase has occurred, there is also an induction period for the coefficient of friction to reach its steady-state value. To highlight the influence Mo concentration has on this induction period, 180, 350, and 1000 ppm sample oils during the first 500 seconds of traction after Stribeck curves are shown in Figure 6-7.



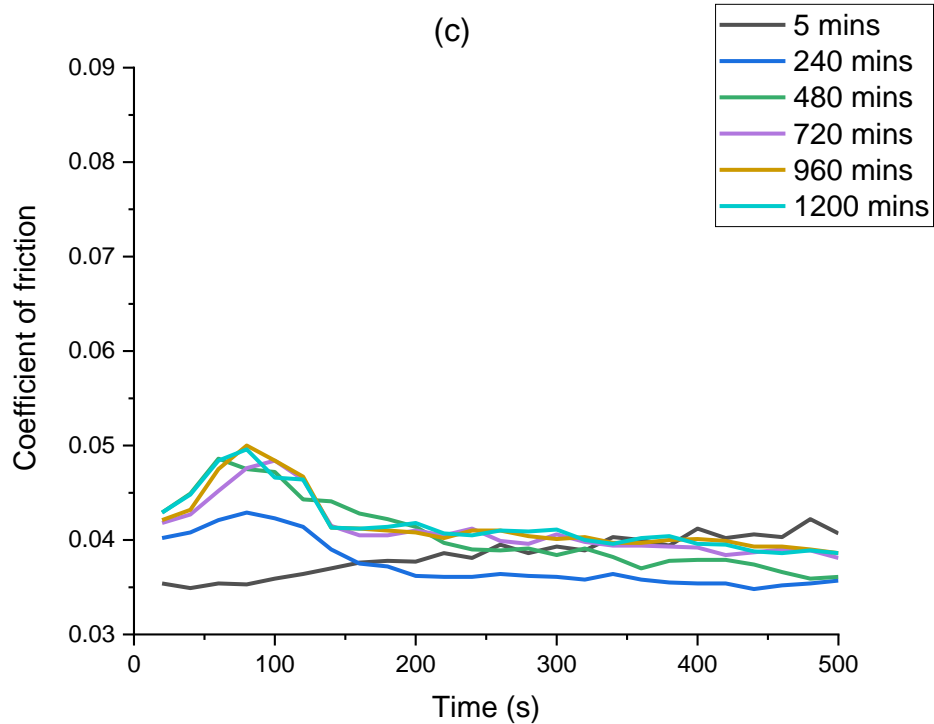


Figure 6-7 Induction period after Stribeck curves for (a) 180 ppm, (b) 350 ppm and (c) 1000 ppm.

The Stribeck curves varying lambda ratio and entrainment speed create instability in the tribofilm matrix mainly due to the very low lambda ratios used in the Stribeck curve, much lower than in the traction phase. This can increase the friction once the traction phase initiates after the Stribeck curve phase. To return to steady-state friction, the MoS₂ must replenish.

Part (a) of Figure 6-7, for 180 ppm, clearly shows that the friction value in the traction phase has to decrease after the Stribeck curve phases have been completed. Regardless of test time, there is still an induction period for friction to reach its steady-state value.

Once the Mo concentration is increased to 350 ppm, part (b) of Figure 6-7, the friction after the Stribeck curve phase at the start of the traction is lower, and the induction time decreases, suggesting a more stable tribofilm matrix with the ability to keep low friction. Again, when increasing the Mo concentration

to 1000 ppm, the same effect is observed in part (c) of Figure 6-7. Therefore, Mo concentration significantly influences the friction function of the tribofilm matrix well after steady-state friction and full tribofilm formation have occurred.

6.5 Tribofilm Thickness

Optical film thickness measurements using the SLIM technique are critical to understanding the influence Mo concentration has on the growth of the ZDDP/phosphate glass tribofilm and steady-state film thickness values. Three of the Mo concentration were selected for friction test repeats with the SLIM. 0 ppm, 350 ppm, and 1000 ppm. The selections were based on the friction analysis from the initial tests, choosing a concentration with no MoDTC, the lowest, which produces ≈ 0.04 friction under a constant and varying lambda ratio, and the highest Mo concentration available.

The SLIM technique is optimized to measure phosphate film thickness by using the refractive index of phosphate glass. Literature has also shown that determining MoS₂ thickness using the SLIM technique cannot be done [65,112]. Therefore, the tribofilm thickness measured by the SLIM technique with a complex tribofilm matrix formed from multiple additives is mainly phosphate glass from ZDDP.

6.5.1 Tribofilm Growth Rate and Steady-state Film Thickness

Figure 6-8 displays the optical film thickness growth during the test duration for the selected Mo concentrations. The SLIM images at intervals of 5, 15, 30, and 60 minutes are shown in Figure 6-8 to highlight the difference in tribofilm image colours between the three concentrations. The SLIM images for the

final measurement towards the end of the test are also shown on the graph's right-hand side in Figure 6-9.

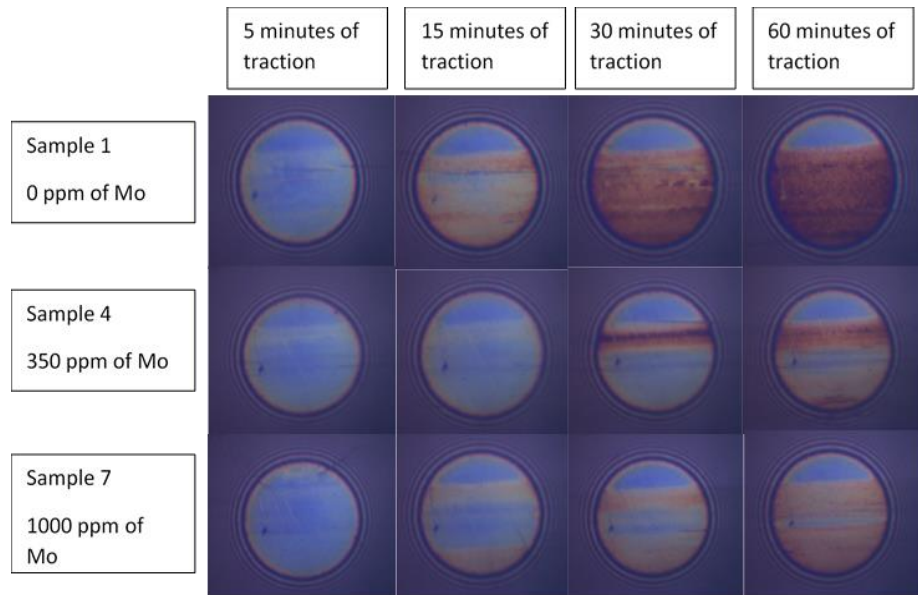


Figure 6-8 SLIM images captured at specific intervals for 0, 350 and 1000ppm Mo concentrations.

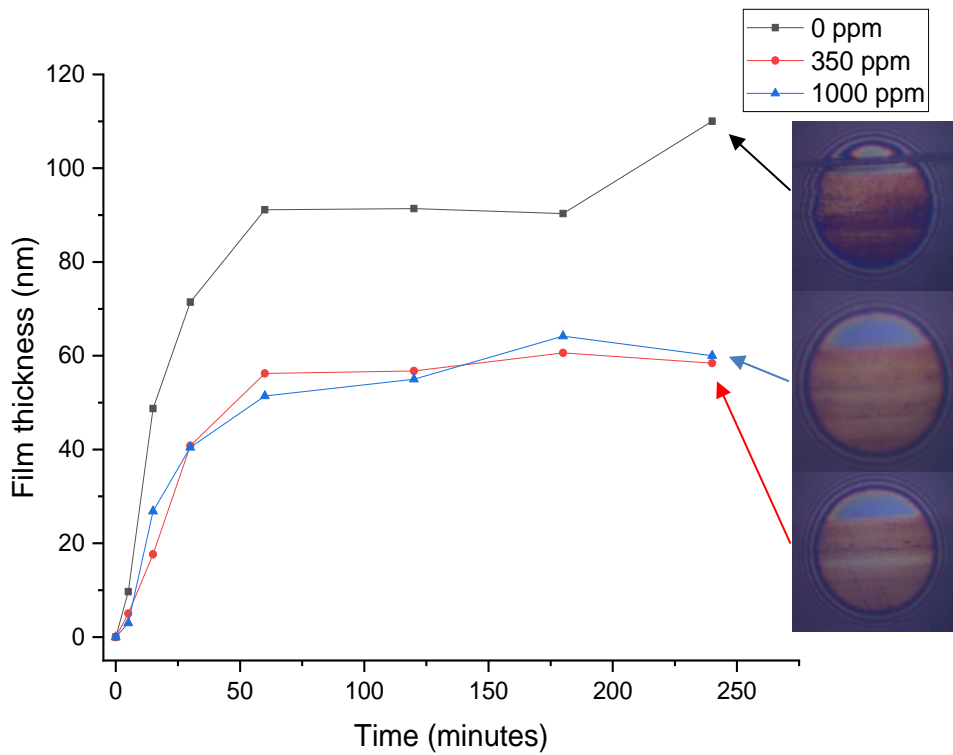
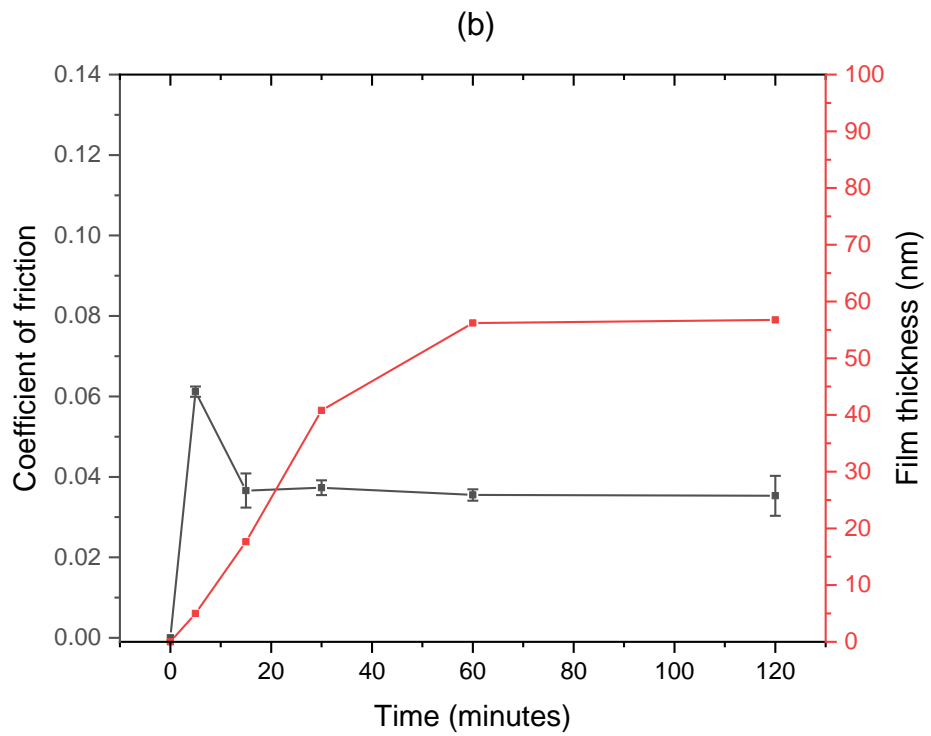
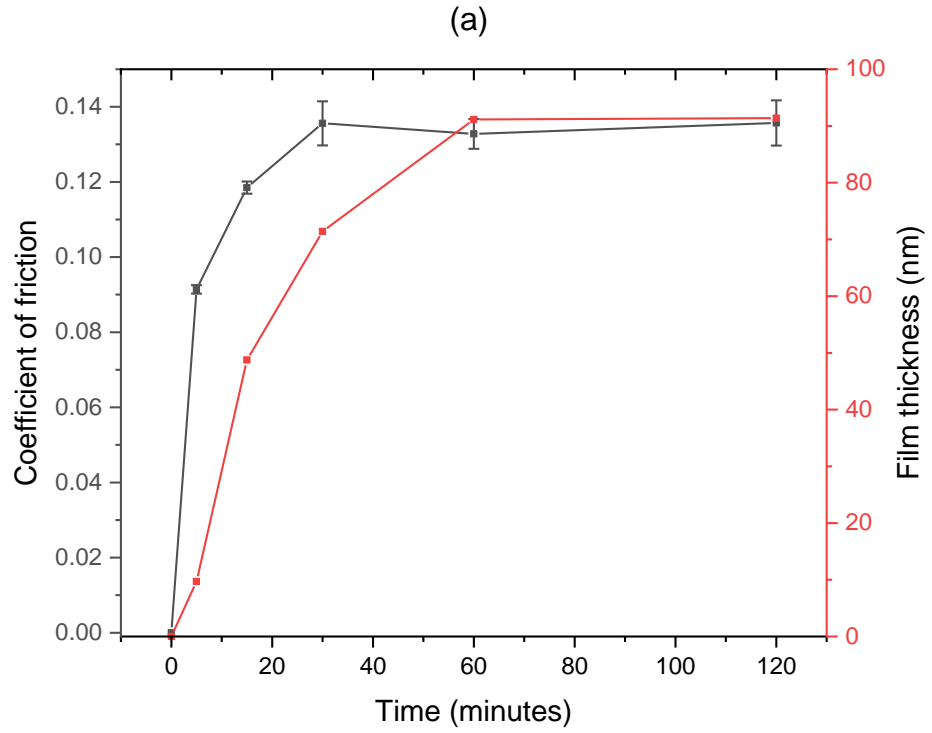


Figure 6-9 Tribofilm growth rate and steady-state thickness values for 0, 350 and 1000ppm Mo concentrations.

The 0 ppm of Mo test shows a steady-state optical film thickness of ≈ 110 nm, typical of tribofilms consisting of ZDDP products such as zinc sulfide, glassy phosphates, and zinc polyphosphate chains formed during rubbing [112]. The addition of MoDTC into the oil, which is sufficient to reduce the friction to ≈ 0.04 , clearly shows a decrease in steady-state optical film thickness. The decrease observed when adding MoDTC can be explained by the competitive adsorption between the boundary-active additives [123]. The theory suggests that MoDTC prevents the complete formation of a ZDDP tribofilm. The decomposition product MoS_2 formed from MoDTC form in nanosheets within the tribofilm matrix, reducing friction and thus inhibiting ZDDP full formation [106].

The differences in film thickness and the SLIM images become apparent once the test duration increases to 15 minutes. 0 ppm and 350 ppm have optical film thickness values of roughly half of their steady-state values, and from the SLIM images, light brown colours within the tribofilm start to form. 350 ppm tribofilm at this stage in the test has roughly a third of its steady-state thickness value. As the test duration increases to 30 minutes, all the samples have roughly three-quarters of their steady-state values. At this point in the test, all three concentrations have the same tribofilm growth rate in relation to their steady-state film thickness values. The Slim images, however, are very different. 0ppm has a large area of the tribofilm, a dark brown colour, indicating a thick ZDDP tribofilm has formed. From previous research, a darker-coloured tribofilm SLIM image is a thick ZDDP tribofilm [48,112,134]. A dark brown strip with light brown suggests that thick and thin ZDDP areas have formed in 350 ppm tribofilm. Finally, 1000 ppm displays only a light brown colour, suggesting a thinner ZDDP tribofilm has been formed than 350 ppm.

Figure 6-10 shows the friction and tribofilm thickness against time for the three Mo concentrations to understand how the ZDDP film thickness changes with friction.



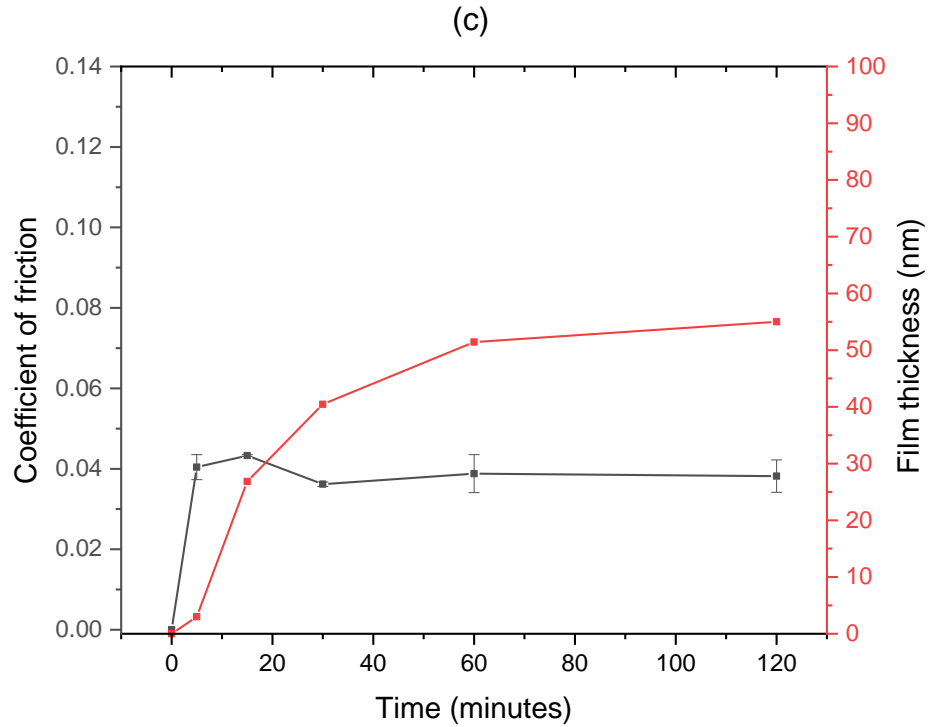


Figure 6-10 Tribofilm thickness with friction values over time for (a) 0 ppm, (b) 350 ppm and (c) 1000 ppm.

For 0 ppm of Mo, the ZDDP tribofilm thickness increases as the friction increases. The steady-state friction is achieved shortly after the steady-state ZDDP tribofilm thickness is reached. The friction does not significantly differ once the film thickness becomes steady-state after 60 minutes of traction. This is the typical trend for tribofilms that do not contain friction modifiers [105,112,134].

The 350 ppm of Mo tribofilm reduces the friction to ≈ 0.04 between 5 and 15 minutes of traction. After 5 minutes of traction, the film thickness is roughly half that of the 0 ppm tribofilm at the same test stage. A slight decrease in friction is observed at 5 minutes, indicating that the MoS₂ layers are starting to form. Previous research using an in-situ tribometer with Raman spectroscopy determined that in the initial rubbing period with the friction value at ≈ 0.07 - 0.08 , MoS₂ nanocrystal flakes covered tiny areas within the

MoDTC/ZDDP tribofilm matrix. As the rubbing time increased, more and more areas in the wear scar were covered in MoS₂, creating thicker lattice layers within the MoDTC/ZDDP tribofilm matrix [75]. After 15 minutes of traction, the friction is reduced to ≈ 0.04 , and thick MoS₂ layers are formed. The ZDDP film thickness is significantly reduced compared to 0 ppm at 15 minutes. The 1000 ppm tribofilm reduces the friction within the first 5 minutes to ≈ 0.04 , and the ZDDP tribofilm thickness is lower than both 0 and 350 ppm tribofilms at the same stage in the test. After 15 minutes, the ZDDP tribofilm for 1000 ppm increases compared to 350 ppm, suggesting that once the MoS₂ thickness is fully formed, the ZDDP tribofilm growth rate increases. After 30 minutes, for 350 ppm, the ZDDP tribofilm thickness increases significantly after the steady-state friction is achieved. Both 350 and 1000 ppm's ZDDP tribofilms after MoS₂ layer thickness create a ≈ 0.04 friction value increase significantly in thickness and becomes steady-state after 60 minutes.

Overall, the results show that the ZDDP thickness decreases with the addition of MoDTC, as indicated by the light brown colours and values. Increasing the Mo concentration from 350 to 1000 ppm does not significantly change the steady-state film thickness values. The difference between the Mo concentrations is the tribofilm growth rate. After 5 minutes of traction, 350 ppm of Mo has a slightly thicker tribofilm than 1000 ppm, suggesting a thicker ZDDP part of the tribofilm with MoS₂ formed within. The increased Mo concentration creates thicker MoS₂ layers in the initial stages of the traction, suppressing the ZDDP tribofilm growth. MoDTC surface supply is the reason behind the hypothesis, which increases with concentration. Once ≈ 0.04 steady-state friction is achieved, the ZDDP tribofilm significantly increases in

growth rate and becomes steady-state after 60 minutes due to the MoS₂ layer thickness fully forming.

6.6 Tribofilm Chemical Composition

Tribochemical analysis is fundamental to understanding the mechanisms that create various friction and wear results. Analysis of the tribofilms was performed using Raman and XPS techniques. All analysis was performed on the ball after removing excess oil with heptane.

6.6.1 MoS₂ and Mo oxides

To investigate Mo concentration's impact on the MoDTC decomposition products, MoS₂ and Mo oxides within the tribofilm matrix, both XPS and Raman are used.

6.6.1.1 XPS analysis

From XPS analysis, Table 6-2 shows the typical binding energies and peaks found in the literature for the deconvolution of the Mo 3d signals.

Table 6-2 Binding energy values from previous literature for the Mo 3d peak fitting.

Peak	Oxidation state	Binding energy (eV)	Standard deviation (eV)	Bonding	References
S 2s	-	227	0.2	Metal sulphide	[65,71,119,120]
Mo 3d	Mo (IV)	229	0.4	MoS ₂	
	Mo (V)	229.7	0.5	MoO _x S _y	
	Mo (VI)	232	0.2	MoO ₃	

Using data from Table 6-2, conditions and constraints listed for the HR scan in the experimental procedure section, the deconvolution of the Mo3d signals at 0 and 120s etch time was conducted and are shown in Figure 6-11. The Mo (IV): Mo (VI) ratios for both 0s and 120s etch times are shown in Table 6-3. Previous research has shown that Mo (IV): Mo (VI) ratios can be used to analyze the MoS₂ to Mo oxides ratio to understand the Mo species formed from MoDTC in terms of quantity [109,130].

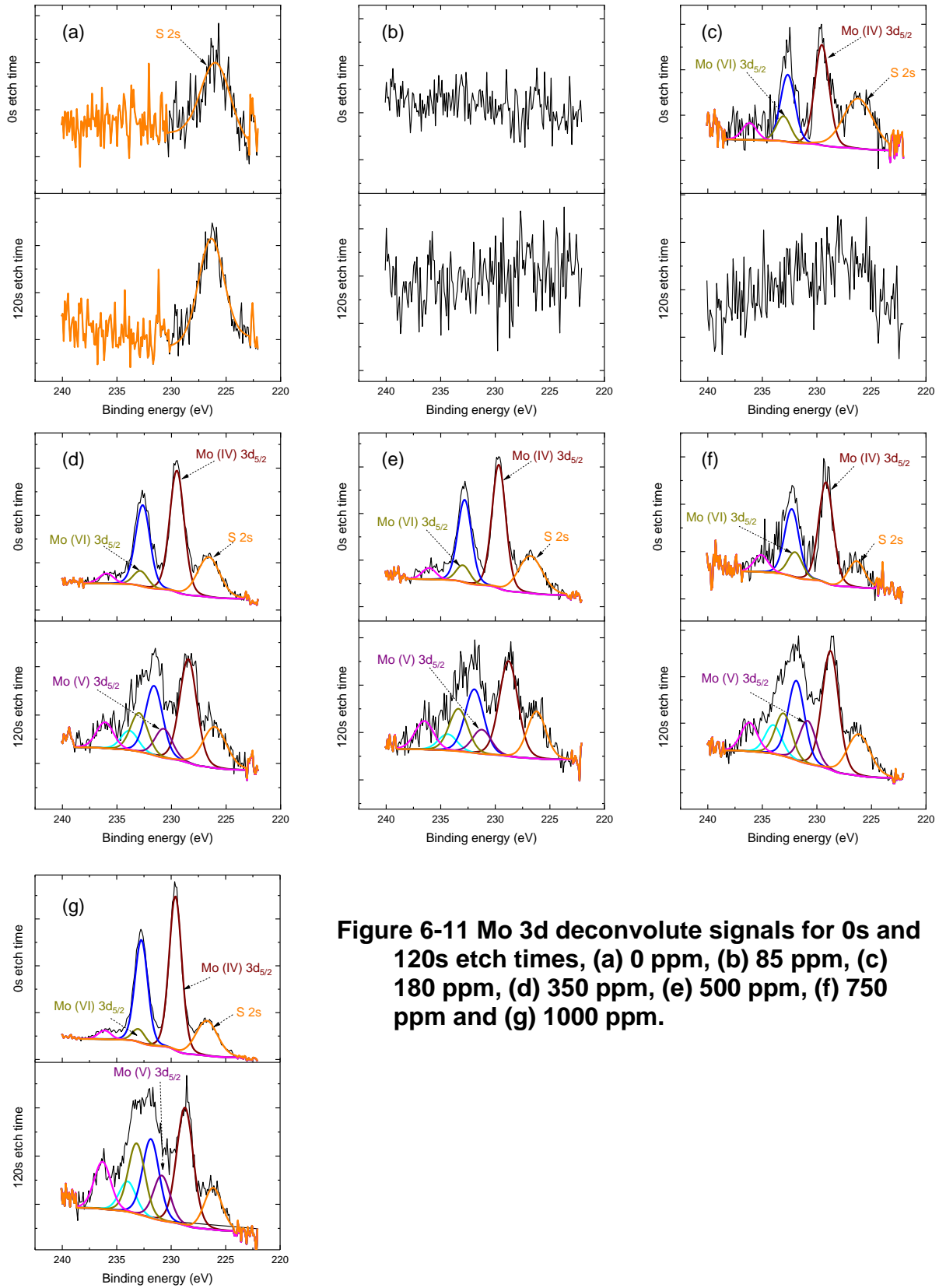


Figure 6-11 Mo 3d deconvolute signals for 0s and 120s etch times, (a) 0 ppm, (b) 85 ppm, (c) 180 ppm, (d) 350 ppm, (e) 500 ppm, (f) 750 ppm and (g) 1000 ppm.

Table 6-3 Mo (IV): Mo (VI) ratios for Mo concentrations \geq 180 ppm.

Mo concentration (ppm)	Steady-state coefficient of friction	Mo (IV): Mo (VI)	
		0s etch time	120s etch time
180	0.0430	51.42: 13.36	-
350	0.0423	70.02: 8.71	50: 19.29
500	0.0351	68.87: 9.41	49.99:22.26
750	0.0346	69.77: 17.54	49.59: 17.87
1000	0.0352	75.88: 6.41	50.5: 18.84

As expected, the 0 ppm of Mo concentration produces no Mo3d signal with just one peak visible, as shown in Figure 6-11 (a). This peak is associated with a metal sulfide with a binding energy of \approx 226.4 eV. Since no MoDTC within this oil, the metal sulfide must be linked with Zn or Fe. No MoS₂ detected within the tribofilm via XPS explains no friction reduction observed during the MTM test.

Three Mo concentrations around the critical concentration, 85, 180, and 350 ppm, show many differences between 0 and 120s etch time signals. 85 ppm of Mo, which reduces the steady-state friction from \approx 0.13 to \approx 0.08, produces a weak XPS signal which cannot be analyzed. However, other peaks for 85 ppm concentration tribofilm, for example, Zn2p, were significant and could be analyzed. The lack of Mo XPS peak suggests no Mo species are formed within the top layers of the tribofilm. Raman analysis in the next section can verify if this is the case for the overall tribofilm.

The 180 ppm and 350 ppm Mo3d signals produced the same peaks at 0 s etch time. Peaks at S2s and two chemical states of Mo at (IV) and (IV) were

detected, suggesting that at the top layer of both tribofilms, metal sulfide, MoS_2 , and Mo oxides are present. Peaks detected at 0 s are typical of tribofilms with Mo species decomposed from MoDTC in fully formulated oils [109,119,122,123]. The difference between the two HR scans at 0 s etch time is the Mo (IV): Mo (VI) ratios, as shown in Table 6-3. 350 ppm has a higher ratio of MoS_2 to Mo oxides than 180 ppm. However, the steady-state friction value is very similar. Therefore, the smallest Mo (IV): Mo (VI) ratio, which produces low friction, must be close to that value. As the concentration is increased further past 350 ppm, the ratios at 0 and 120 s etch times do not significantly differ. Therefore, increasing the Mo concentration increases the Mo (IV): Mo (VI) ratio to a maximum value. Any further Mo concentration increases will not increase the ratio.

Moreover, all concentrations past 350 ppm have low friction under a constant and varying lambda ratio. Therefore, Mo (IV): Mo (VI) ratio value required to produce these results must be close to the values observed for the Mo concentrations past 350 ppm. After 120 s of etching, 180 ppm produces a weak signal, similar to 85 ppm, which cannot be analyzed, suggesting no Mo species are detected. 350 ppm, however, does produce a signal with multiple peaks associated with S_2s and three chemical states of Mo being (IV), (V), and (VI). The additional Mo (V) chemical state peak is associated with Mo oxysulphide [119].

For all Mo concentrations ≥ 180 ppm, the Mo (IV): Mo (VI) ratios decrease as the etching time increases from 0 to 120 s. It implies that the amount of MoS_2 decreases as the tribofilm layers are etched. The ratios in Table 6-3 show no correlation with Mo concentration with the etch times used. However, as Mo concentration increases, Mo (IV) ratio (VI) could be larger closer to the

substrate if more etching and HR scans were conducted. Increasing Mo concentration reduces the induction time, producing more MoS₂ and Mo species within the first layers of the tribofilm.

Increasing the Mo concentration past ≈ 350 ppm does not negatively or positively affect the Mo species found within the tribofilms top layers. However, decreasing the concentration reduces the Mo species found within the top layers of the tribofilm, which has a negative effect, as seen in the friction analysis for 85 ppm and 180 ppm.

6.6.1.2 Raman Analysis

Raman mapping and intensity frequency distribution graphs of the A_{1g} peak for Mo concentrations of ≥ 180 ppm are shown in Figure 6-12. The scale bars are the same for each Raman map to enable comparisons, and only maps with MoS₂ detected are included. The methodology behind creating the Raman maps can be found in Chapter 4.

The friction and tribofilm analysis results clearly show that 85 ppm does not have enough concentration of MoDTC to create a friction-reducing tribofilm. The 85 ppm of Mo's Raman mapping did not detect any MoS₂ present. It agrees with the XPS results, where no peaks were detected for the Mo3d signal. However, compared to 0 ppm, a friction drop to ≈ 0.08 was observed for 85 ppm of Mo. It suggests that some friction reduction mechanism has taken place within the tribofilm. Previous research has shown that a tribofilm with a steady-state friction value of ≈ 0.08 has tiny amounts of MoS₂ intensity counts and little coverage within the tribofilm [16].

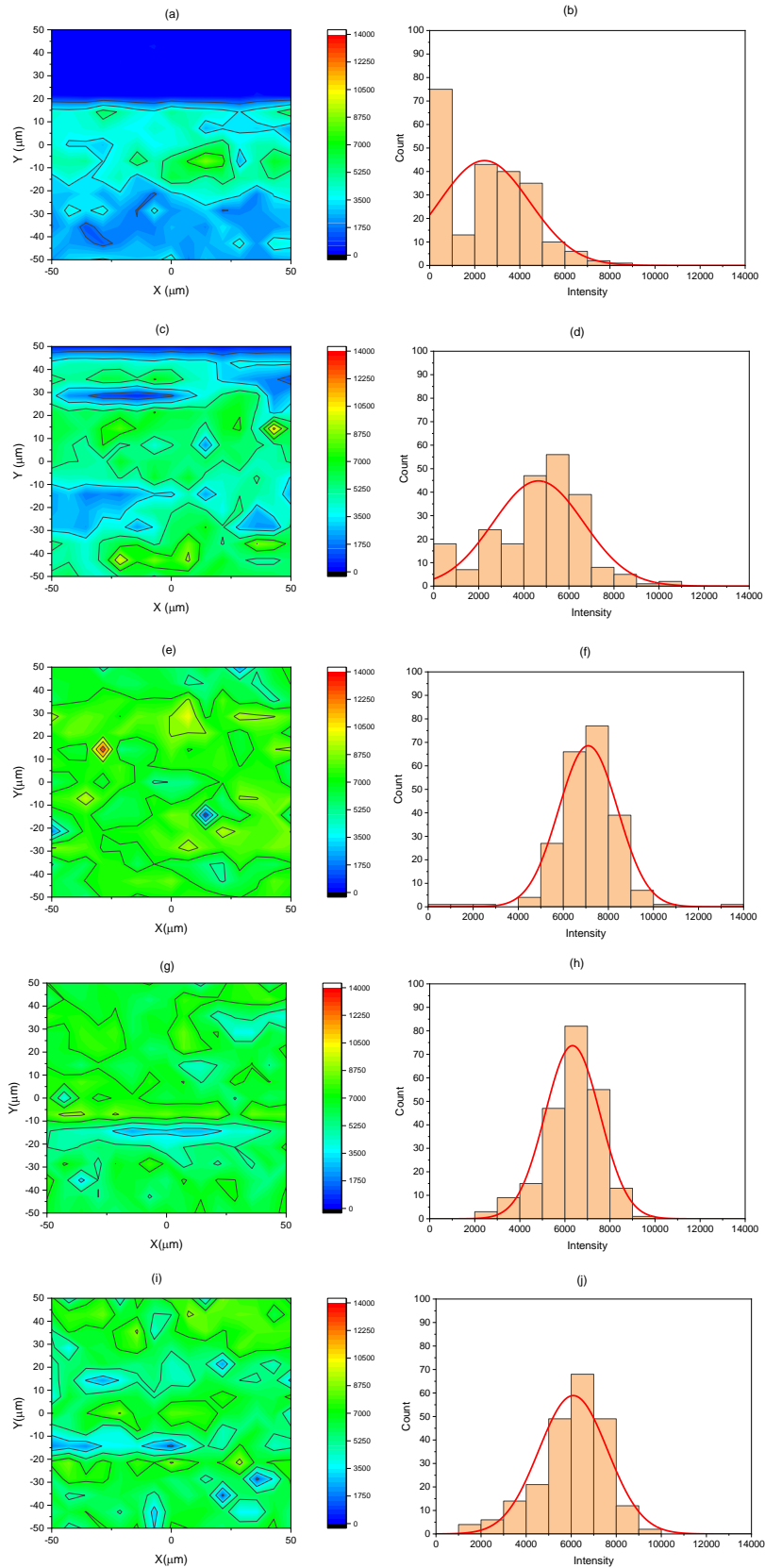


Figure 6-12 Raman spectroscopy; 180ppm – (a) intensity mapping, (b) intensity frequency distribution, 350ppm – (c) intensity mapping, (d) intensity frequency distribution, 500ppm – (e) intensity mapping, (f) intensity frequency distribution, 750ppm – (g) intensity mapping, (h) intensity frequency distribution, and 1000ppm – (i) intensity mapping, (j) intensity frequency

Three main aspects of the Raman mapping data can be analyzed; coverage, distribution, and intensity, to understand Mo's concentrations impact on the MoS₂ formed within the tribofilm.

The only Raman map from Figure 6-12, which does not produce full coverage, is 180 ppm. This map also has the lowest frequency distribution of intensity within the tribofilm by a noticeable amount. The coverage and intensity distribution of MoS₂ increases as the Mo concentration is increased from 180 to 350 ppm. However, the intensity distribution is still lower than the Mo concentrations ≥ 500 ppm. Therefore, 350 ppm total intensity counts are also less than concentrations ≥ 500 ppm. The higher total intensity counts within ≥ 500 ppm could be one factor that leads to the slight decrease in friction observed under a constant lambda ratio coupled with the increase in Mo concentration. Total intensity counts vs friction within the areas used to conduct the Raman analysis are shown in Figure 6-13.

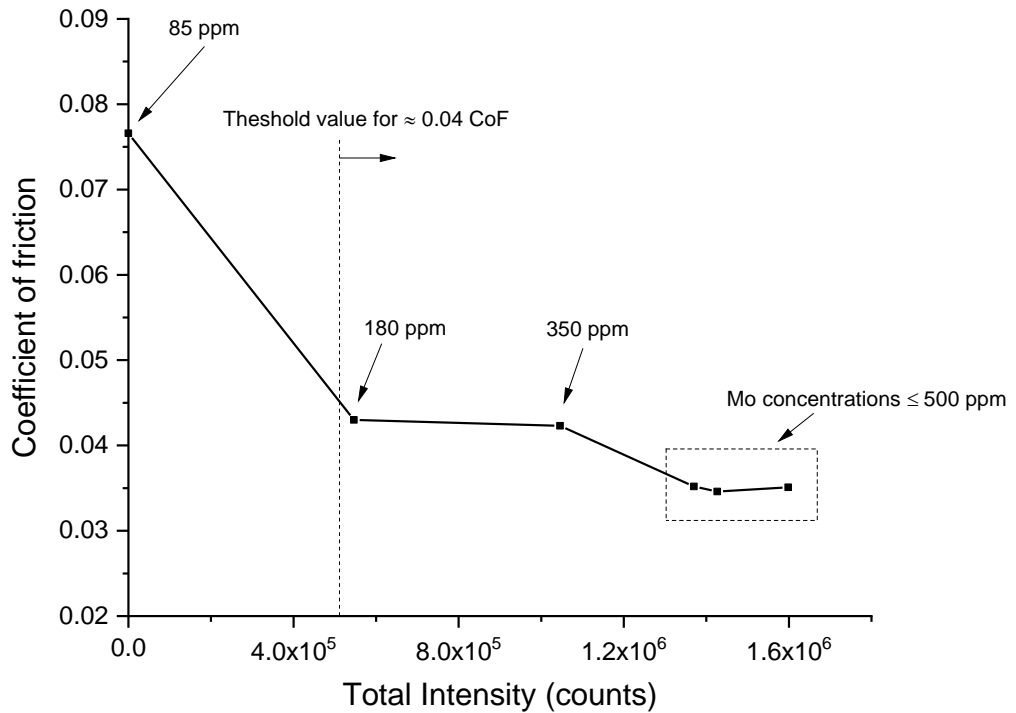


Figure 6-13 Total intensity counts of MoS₂ vs friction for all friction-reducing Mo concentrations.

As the total intensity counts of MoS₂ within the tribofilms increase, the friction decreases to a maximum value. Once a certain intensity count/amount of MoS₂ has formed within the tribofilm, the friction does not decrease further. From Figure 6-13, the distribution frequency of the counts does not significantly change past a specific concentration in this study, 500 ppm. Therefore, increasing Mo concentration above 1000 ppm would not significantly influence the total intensity counts or distribution frequency. The previous research agrees with increasing Mo concentration, increasing the total intensity counts up to a maximum value [132]. A clear threshold value of MoS₂ is required within the tribofilm matrix to produce a ≈ 0.04 friction tribofilm. The XPS, Raman data, and analysis findings coupled with the tribofilm thickness results can explain the increased friction in the Stribeck curves for

180 compared to 350 ppm of Mo. It takes roughly 13 minutes of traction at a constant speed for 180 ppm of Mo to reduce the friction to ≈ 0.04 , which suggests that around this point in the test, MoS₂ layers are relatively thick in the MoDTC/ZDDP/detergent tribofilm matrix. Previous research has shown that reaching a friction value of ≈ 0.04 requires thick MoS₂ layers within the tribofilm matrix [75]. The XPS and Raman data suggest that Mo concentration significantly influences the thickness of MoS₂ layers within the tribofilm matrix and the Stribeck curve friction is highly dependent upon it. However, past a threshold concentration, the thickness of MoS₂ layers is a lot less significantly impacted. The destructive nature of rapidly changing lambda ratios in the Stribeck phase removes part of the tribofilm. As part of the tribofilm is removed, the MoS₂ within the tribofilm reduces significantly for 180 ppm, as shown in Figure 6-11 and Figure 6-12. As Mo concentration increases, this effect on the friction is lowered, Figure 6-7. Therefore, 180 ppm does not produce a MoDTC/ZDDP/detergent tribofilm matrix with thick enough MoS₂ layers to keep a reduced friction value of ≈ 0.04 when the lambda ratio changes from constant to varying. The friction also fluctuates at a constant speed, as shown in Figure 6-2. Once the constant lambda ratio is resumed after the Stribeck curve phase, the MoS₂ layers removed reform in the tribofilm matrix to obtain the ≈ 0.04 friction. This process is constantly repeated should the tribofilm thickness or operating conditions change.

6.6.2 Tribofilm Chemical Composition

6.6.2.1 XPS HR scans

All Mo concentrations tribofilms contained the same chemical states of Ca, P, S and Zn found at 0, and 120 s etch time. The deconvolution of all the Mo concentrations HR signals are not shown, but the spin orbitals, associated binding energies, and bonding from the CasaXPS software are shown in Table 6-4.

Table 6-4 Ca 2p, S 2p, and Zn 2p peak binding energies and associated bonding for all Mo concentrations.

Scan	Spin orbital	Binding energy (eV)	Standard deviation (eV)	Bonding	References
Ca 2p	2p _{3/2}	347.8	0.2	CaCO ₃	[120,123]
	2p _{1/2}	351.5	0.2		
S 2p	2p _{3/2}	161.7 /	0.2	FeS ₂ , ZnS,	
		162.3			
S 2p	2p _{1/2}	162.9 /	0.2	MoS ₂	
		163.6			
Zn 2p	2p _{3/2}	1022	0.5	ZnS and	
	2p _{1/2}	1045	0.5	ZnO	

All tribofilms for the Mo concentrations contained the same peaks in both 0 and 120 s etch time for the HR scans. Regardless of Mo concentration or the addition of MoDTC, the compounds formed from the boundary active additives do not change.

As expected, for all tribofilms, the Zn 2p and Ca 2p peaks increase in counts per second (CPS) as the etching time increases from 0 to 120 s. It suggests that the bonding associated with the peaks such as ZnS and ZnO from the Zn 2p signal becomes larger in the tribofilm layers towards the substrate.

6.6.2.2 Phosphate Chain Lengths

The BO/NBO ratios and Zn3s – P_{23/2} binding energy (eV) for three chosen Mo concentrations are shown in Table 6-5. Previous literature has shown that bridging oxygen, BO (P-O-P) and non-bridging oxygen, NBO (P=O and P-O-M), can determine the glass phosphates' chain length within the tribofilm. Specifically the intensity ratio BO/NBO and peak difference between Zn 3s and P 2p_{3/2} [59,60,135].

Table 6-5 BO/NBO ratios and the peak difference between Zn3s and P2p.

Mo concentration	BO/NBO ratio	Zn3s – P _{23/2} binding energy (eV)
0	0.35	6.13
350	0.15	6.55
1000	0.20	6.44

The phosphate chain length decreases as MoDTC is added to the oil in a friction-reducing quantity. The composition of the tribofilm changes from polyphosphate, 0 ppm, to pyrophosphate, 350 and 1000 ppm. The Zn 3s and P 2p binding energy difference increases as the chain lengths decrease.

The addition of MoDTC reduces ZDDP formation from all the tribofilm chemical composition analyses completed. However, when increasing the Mo concentration from the lowest friction-reducing value to 1000 ppm, there is not a hugely significant change in ZDDP thickness and contents.

6.6.2.3 Raman Spectra

The mean Raman spectrum for the Mo concentrations, which produced friction values of ≈ 0.04 , is shown in Figure 6-14. All spectra contain the same peaks within their tribofilms, and Fe_2O_3 peaks are observed ≈ 220 and 290 cm^{-1} . Additionally, for 500 ppm, an extra Fe_2O_3 peak is found $\approx 1250 \text{ cm}^{-1}$. MoS_2 E_{2g} and A_{1g} peaks at ≈ 381 and 408 cm^{-1} , and finally, an S-S stretching peak at $\approx 459 \text{ cm}^{-1}$ are present in all tribofilms. The difference between the Mo concentrations spectra is the intensity of the peaks. These peaks are typical of tribofilms generated from fully formulated oils with MoDTC and ZDDP [78]. Previous research has shown that some phosphates can be detected [106]. However, none were found in any tribofilms using Raman only with XPS.

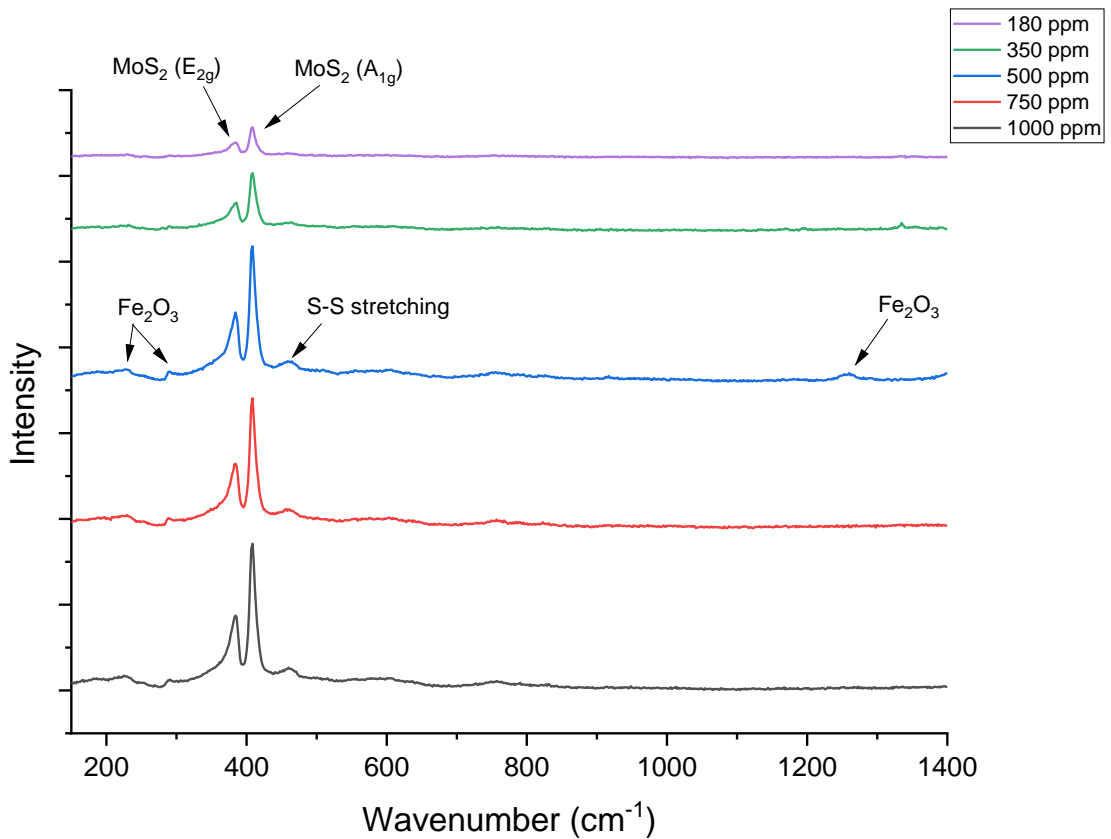


Figure 6-14 Mean Raman spectra for Mo concentrations greater than 180 ppm.

6.7 Mo Concentrations Influence on the MoS₂ Growth

The MTM and Raman spectrometer were used in conjunction with one another to understand how the Mo concentration can affect the MoS₂ tribofilm growth while rubbing the surfaces. The MTM samples were rubbed with Raman scans at 5, 15, 30, 60 and 240 minutes.

From the MTM friction tests, increasing the Mo concentration decreased the induction time to reach a coefficient of friction value of ≈ 0.04 , suggesting higher concentrations form thicker MoS₂ layers within the initial stages of the test.

Figure 6-15 displays the total intensity counts of MoS₂ within the tribofilm matrix at the set intervals during the test. Both Mo concentrations tested produced total intensity count values and spectrums of MoS₂, which increased as test duration increased, similar to previous research monitoring in situ tribofilm growth [106]. Figure 6-15 shows an increase in total intensity counts for the higher Mo concentration at the 5-minute interval during the test. An increase in total intensity counts implies more MoS₂ formed within the tribofilm, most likely due to the higher concentration being able to supply more MoDTC to the rubbing surface. As the test duration increases, the total intensity counts for 1000 ppm sharply increase compared to 350 ppm while increasing as the test duration increases. MoS₂ must be embedded within the layers of the ZDDP dominant tribofilm as it increases in thickness during the test.

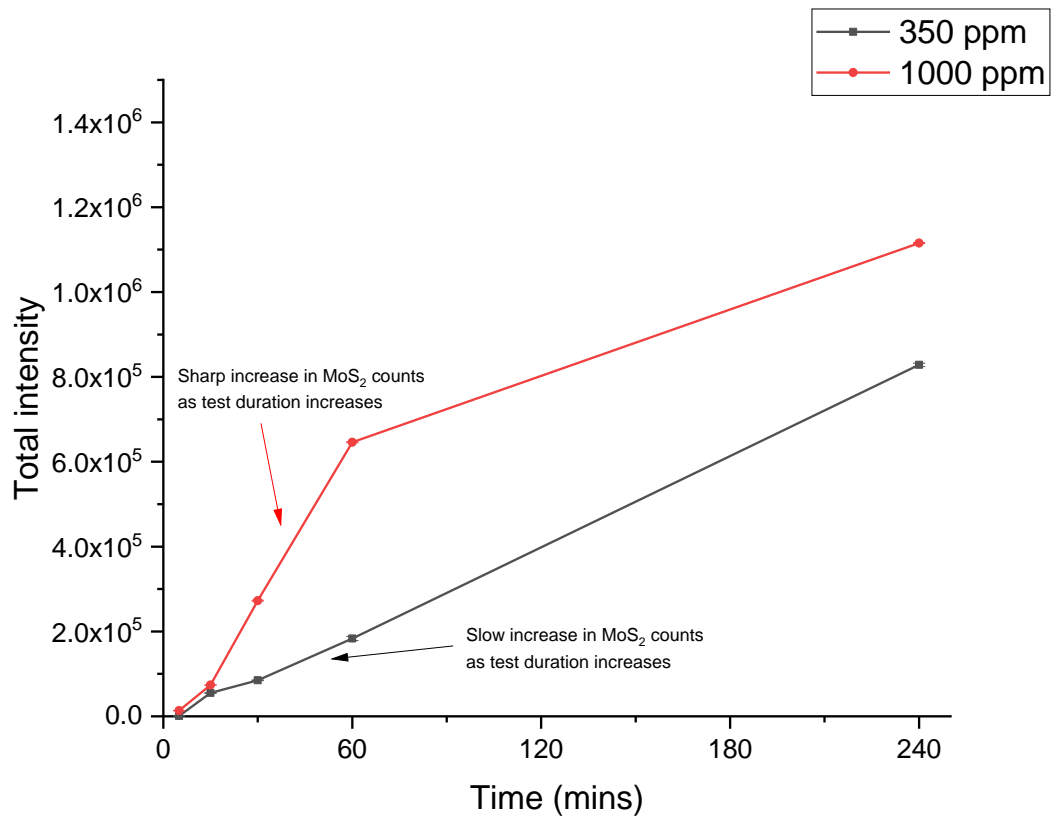


Figure 6-15 Total intensity counts of MoS₂ within the tribofilm matrix at intervals during the friction tests for 350 and 1000 ppm oils.

Figure 6-16 and Figure 6-17 show the comparison of Mo concentration's total intensity counts of MoS₂ and the film thickness measurements from the SLIM unit. For 350 ppm, there is a sharp increase in the ZDDP film thickness between 5 and 60 minutes into the test. At the same time, MoS₂ has a much smaller growth within the time range, suggesting small amounts of MoS₂ is forming within the tribofilm matrix, but sufficient amounts required to reduce the friction, as seen from the friction results. Once the ZDDP tribofilm has reached its steady-state film thickness value, typically after 60 minutes of traction, as most literature reports [112,136], the total intensity counts of MoS₂ within the tribofilm spikes significantly.

Figure 6-17, displaying 1000 ppm's comparison, shows a different graph within the first 60 minutes of traction. A sharp increase in total intensity counts of MoS₂ is observed, indicating more MoS₂ is embedded within the layers of the tribofilm matrix compared to 350 ppm. However, it must be noted that this does not necessarily significantly impact friction. Again, once the steady-state ZDDP film thickness is reached 60 minutes into the test, the total intensity counts spike. Suggesting thick MoS₂ layers are forming on the top layer of the tribofilm matrixes once the ZDDP dominant part of the tribofilm has formed for 350 and 1000 ppm.

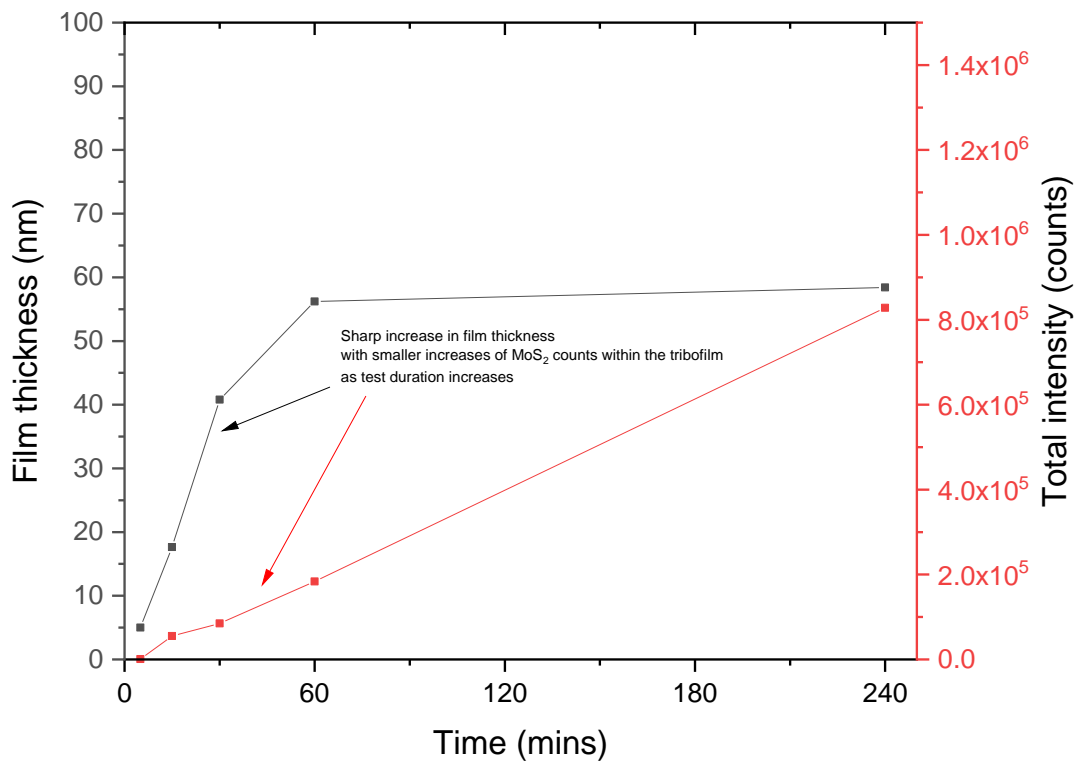


Figure 6-16 Film thickness and total intensity counts of MoS₂ within the tribofilm at intervals during testing for 350 ppm.

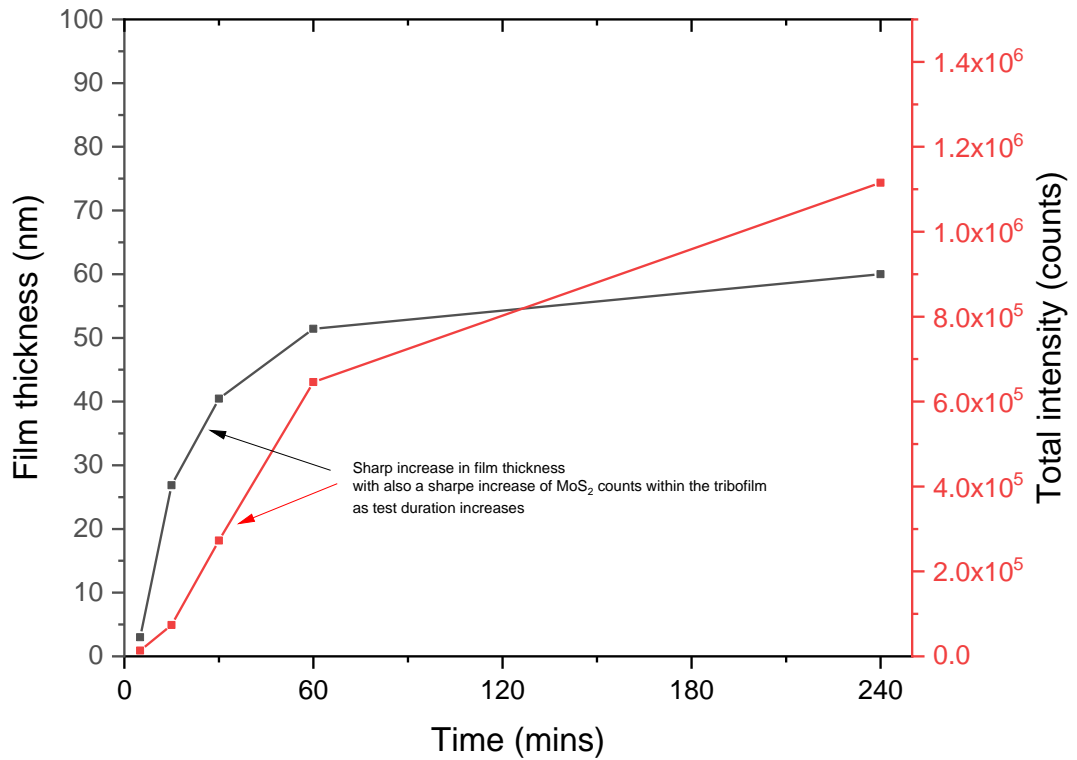


Figure 6-17 Film thickness and total intensity counts of MoS₂ within the tribofilm at intervals during testing for 1000 ppm.

Figure 6-18 shows all the total intensity counts of MoS₂ scans within the tribofilm taken with the friction value during the test. The points include 350 and 1000 ppm tribofilms, with time intervals. High friction is observed when the total intensity is very low within the tribofilm, close to zero. A cluster of data points can be seen when low friction, ≈ 0.04 , is reached. Potentially, there is a threshold value of total intensity counts of MoS₂ within the tribofilm, producing a low friction value regardless of Mo concentration. As the total intensity value increases, the friction is relatively stable. However, the figure observes a slight friction drop when the highest value is reached, suggesting that high total intensity counts further reduce friction.

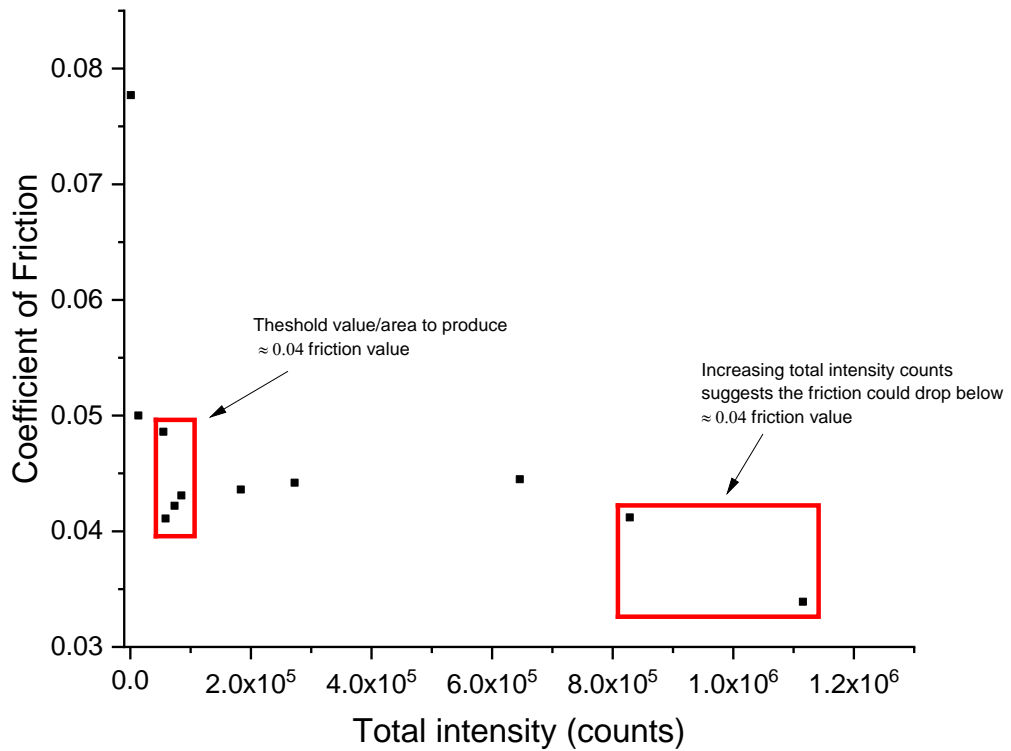


Figure 6-18 Friction values for all intervals total intensity counts of MoS₂ for both 350 and 1000 ppm.

6.8 Wear Analysis

The optimum Mo concentration for new ultra-low viscosity engine oils must not negatively impact the wear of the tribocontacts. Wear and friction are the two most important factors determining where the Mo concentration optimum value is. Therefore, there must be a balance between low friction and low wear. After completing the friction tests and analysis, three Mo concentrations were selected for wear analysis. The sample with no Mo, the sample with the lowest concentration producing the same results as its higher concentration counterparts, and the higher Mo concentration tested.

6.8.1 Wear Coefficient

Figure 6-19 displays the wear coefficients calculated from wear volume loss values, and Table 6-6 shows the average wear scar widths obtained from an optical microscope. Both sets of results are in agreement with each other.

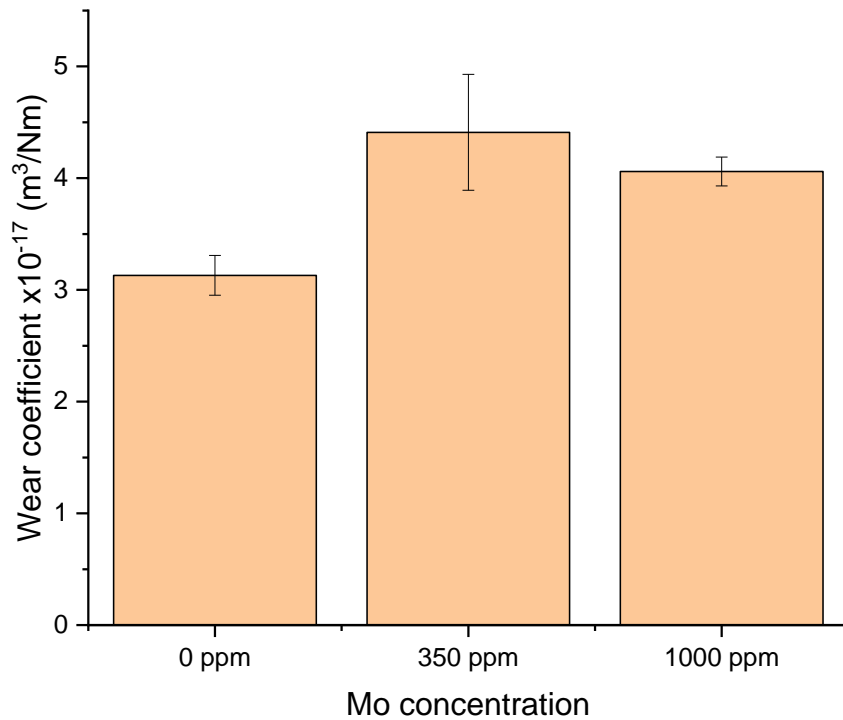


Figure 6-19 Wear coefficients for 0, 350, and 1000 ppm of Mo.

Table 6-6 Average wear scar width for 0, 350, and 1000 ppm of Mo.

The concentration of Mo (ppm)	Average wear scar width (μm) – optical microscope
0	144.48
350	149.83
1000	147.83

From the results, adding MoDTC into a fully formulated oil increases the wear coefficient and average wear scar width. Recent research also agrees with this statement [124]. The authors found that wear generated when using a 0W 20 engine oil with 250ppm of Mo in the form of MoDTC produces a 48% increase compared to the same fully formulated engine oil without MoDTC present. Again, this can be explained by additive competitive adsorption between ZDDP and MoDTC. Other research into the anti-wear performance of organomolybdenum compounds as lubricant additives found that when testing 15W 30 engine oils, the addition of MoDTC did not improve the wear performance [76]. Therefore, regardless of oil viscosity, adding MoDTC into a fully formulated oil increases the wear and decreases the anti-wear properties of the oil.

A slight decrease in wear is observed when increasing the Mo concentration from 350 to 1000 ppm. However, in real-world applications such as the ICE, the difference in wear between the two Mo concentrations is negligible. Therefore, increasing the Mo concentration by $\approx 180\%$ and not negatively impacting the wear is positive. In theory, increasing the Mo concentration

much higher than 1000ppm could negatively impact the wear by preventing ZDDP formation.

6.9 Summary

This chapter has investigated how to optimize the Mo concentration in ultra-low viscosity engine oil. Seven different Mo concentrations with the same additive package are tested. The tribological properties and chemistry of the tribofilm for the different Mo concentrations are investigated using the MTM, Raman, XPS, and, finally, NPFlex. The conclusions drawn from this chapter are.

- The critical Mo concentration for new ultra-low engine oil in this research is between 180 and 350 ppm in fresh engine oil.
- Mo concentrations ≥ 350 ppm up to 1000 ppm do not negatively impact the friction or wear of the tribo-contact. However, concentrations much higher than 1000 ppm could result in negative wear data.
- Increasing the Mo concentration within fully formulated oil decreases the induction time to a steady-state friction value of ≈ 0.04 , which increases the MoS₂ layer thickness in the ZDDP dominant tribofilm in the beginning stages of film formation.
- The formation and removal of MoS₂ within a ZDDP dominant tribofilm is highly dependent on Mo concentration, and the formation rate becomes more significant with increased Mo concentration.
- Increasing the Mo concentration increases the total intensity counts of MoS₂ within the tribofilm. However, once a specific concentration is reached, in this study, 500 ppm, the value does not significantly change, suggesting the MoS₂ layers has a maximum thickness

irrespective of Mo concentration. Therefore, once a threshold value of total intensity counts is reached within the tribofilm, the coefficient of friction decreases to ≈ 0.04 .

- Adding MoDTC or increasing the Mo concentration does not alter the compounds formed within the tribofilm matrix but affects said compounds' concentrations.
- Optical film thickness decreases significantly with the addition of MoDTC. However, increasing the Mo concentration greater than the critical concentration does not change the tribofilm steady-state value.
- Adding MoDTC into a fully formulated oil increases the wear generated due to competitive surface adsorption. However, increasing the Mo concentration greater than the critical concentration does not negatively impact the wear generated, and the differences are negligible.

Chapter 7 Detergents Influence on the Tribological Properties of Ultra-low Viscosity Oil

7.1 Introduction

As explained in Chapter 3, detergents' influence and interactions on the tribological properties are essential to understand, especially in new ultra-low viscosity engine oil where harsher operating conditions occur, making the tribofilm chemistry essential for low friction and wear. The detergent must not negatively impact the ZDDP or MoS₂ formation for low friction and wear. Three different detergents with the same additive package within a 0W-8 oil grade engine oil were used to investigate the influence of different detergents on friction and wear in ultra-low viscosity oil. Detergent A contains only salicylates, with detergent B containing only sulfonates, and finally, detergent C has a mixture of both within its formulation, see Table 7-1 for the oil formulations. Friction was conducted using the MTM with tribofilm thickness measured at intervals during the test using the SLIM attachment. Finally, wear loss was determined using the NPFlex.

7.2 Test Oils

The test oils selected to understand how different detergents affect the friction, wear, and tribochemistry in ultra-low viscosity engine oils are shown in Table 7-1. All the test oils are within the 0W-8 grade bracket, with the only difference being the detergent formulation. Detergent A contains both Ca and Mg salicylates with more Ca salicylates. Detergent B contains both Ca and Mg sulphonates with more Ca sulphonates. Finally, detergent C contains Ca salicylates and Mg sulphonates with more Ca salicylates.

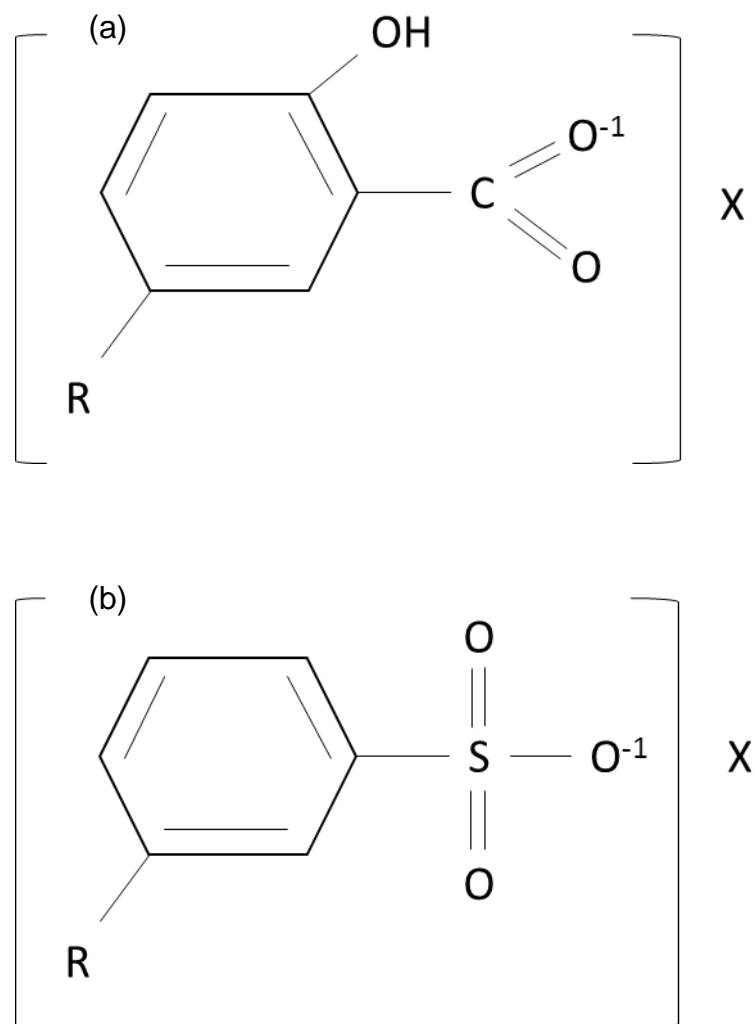
Table 7-1 Test oils used in detergent study.

	Detergent A	Detergent B	Detergent C
Base oil	3+	3+	3+
KV 100/ D445	4.86	4.94	4.94
HTHS 150/D4683	1.76	1.75	1.75
Viscosity Index	149	152	152
Mo (ppm)	810	750	800
Detergent type	Ca + Mg Salicylates	Ca + Mg Sulfonates	Ca Salicylates + Mg Sulfonates

The MTM operating conditions used in this study is shown in Table 4-4. Methodologies for tribochemical and wear analysis are also shown in Chapter 4.

7.3 Detergents Chemical Structures

The detergent chemical structures of salicylates and sulfonates used in the sample oils are shown in Figure 7-1. It must be noted that the sulphonate detergent increases the overall sulfur content within the oil compared to a salicylate. The metals used with both the salicylates and sulphonates are Ca and Mg.



R = alkyl group

X = Divalent metal, usually Ca or Mg

Figure 7-1 Detergent chemical structure for (a) Salicylates and (b) Sulfonates.

7.4 Friction Performance

Figure 7-2 (a) displays the start and steady-state coefficient of friction values taken from the traction phase under a constant speed of 100 mm/s for the three detergents tested. All oils reduce friction to ≈ 0.04 due to the formulations containing MoDTC, with the final friction values in the traction phase not significantly changing with detergent type [71]. However, detergent C with a mixture of both groups does produce an increased steady-state friction value closer to 0.05 rather than 0.04. Tribochemical analysis is required to explain and is found in the later sections.

Figure 7-2 (b) displays the first 600 seconds of friction during the traction phase at a constant speed. A Stribeck curve taken at the 5-minute interval is marked on the graph. Detergent C's induction time to reach a friction value of ≈ 0.04 is the smallest of the three detergent formulations tested, with detergent A the largest. Therefore, each detergent formulation impacts the formation of MoS₂ to produce a significant friction drop. However, with previous research, these detergents do not prevent MoDTC from performing its friction reduction function over the whole test; they influence tribofilm formation and chemistry [123,137]. Figure 7-2 (b) suggests that detergent C's formulation enables a thicker MoS₂ layer formation within the tribofilm matrix, leading to the lowest induction time. Previous research tested the same salicylate and sulfonate detergents groups but with only MoDTC incorporated into the oil [138]. The author also showed that the friction in the beginning stages of the test gradually declined instead of an instant drop usually observed with just MoDTC formulated into a base oil only. Both salicylate and sulfonate detergent formulations produced synergistic effects with MoDTC, with sulfonates slightly reducing the friction more than MoDTC in a base oil.

Overall, the detergent formulations used in this thesis produce synergistic effects with MoDTC.

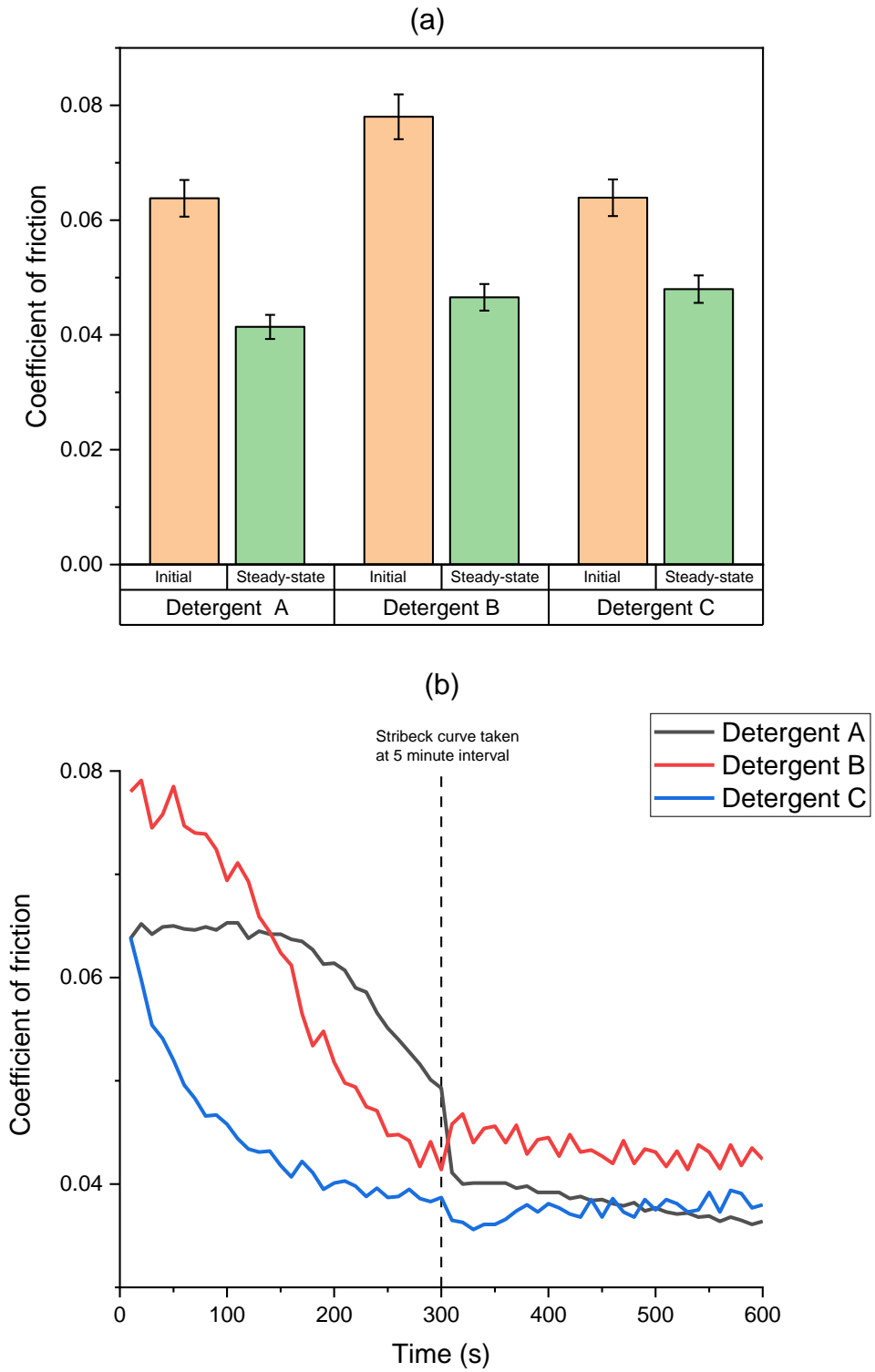


Figure 7-2 (a) Start and steady-state friction values and (b) first 600s of traction.

To further understand how the different detergents can influence the performance of the tribofilm, Stribeck curves under a varying lambda ratio are taken at set intervals for analysis. The initial and final Stribeck curves taken at 0 and 180 minutes, along with the Stribeck curves for each oils test, are shown in Figure 7-3.

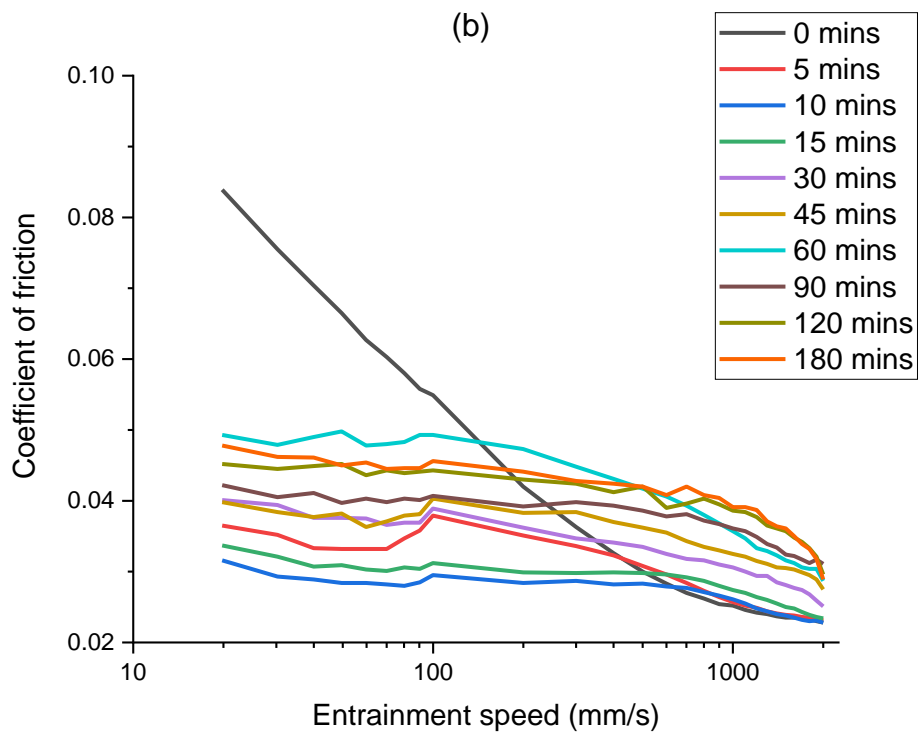
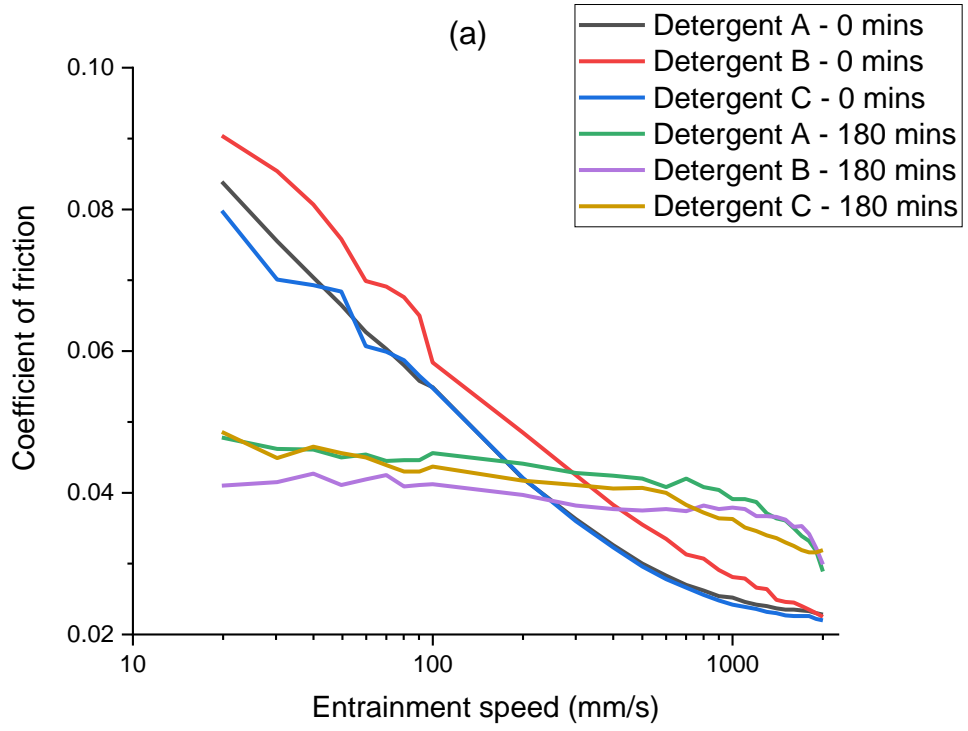
Part (a) displays the initial and final Stribeck curve taken 180 minutes into the test. Both detergents A and C produce similar Stribeck curves at 0 minutes, while C displays an increase in friction over the whole range of entrainment speeds. Since boundary active additives have minimal impact at the start of the test before contact has occurred, the explanation for the friction increase can be given to a reduction in viscosity at the contact.

Asperity contact in the mixed lubrication regime during the Stribeck curve could form a thin tribofilm which would cause an increase in friction as the entrainment speed decreases [51]. However, the latter has a higher probability of causing increased friction. The final Stribeck curves for all three detergents display similar friction over the whole range of entrainment speeds. As shown in Chapter 5 and previous research, the Stribeck curves are very similar to tribofilms which contain MoS₂ embedded within the matrix [133]. The final Stribeck curve shows minimal differences between the effect of the different detergents on friction.

All the Stribeck curves throughout the 4 hrs of traction taken at specific intervals are shown in parts (b), (c), and (d) of Figure 7-3. Two out of the three detergent formulations produce similar Stribeck curves throughout the test, detergent A and C. These oils both contain salicylates, with C containing the additional sulfonate detergent. The Ca salicylate must be decomposing within the tribofilm matrix along with MoDTC and ZDDP decomposition products in

the beginning stages of the test, potentially encouraging the formation of MoS₂. The act of this reduces the friction significantly in the boundary lubrication regime, with entrainment speeds below ≈ 800 mm/s, within the first 15-30 minutes of traction. The Stribeck curves for detergent A are relatively separated until the traction time hits 120 minutes, implying that the tribofilm and friction are unstable. Detergent C's Stribeck curves become stable after 15 minutes of traction, and the addition of sulfonate improves the overall friction. The Stribeck curves for detergent B, part (c) of Figure 7-3, display more friction stability with only sulfonates. The friction is stable after just 5 minutes of traction, with all the Stribeck curves near one another as the test duration increases. Noticeably, at higher entrainment speeds ≥ 1000 mm/s, detergent B's friction significantly drops when entering the mixed lubrication regime, whereas A and C have a less steep friction drop.

From the friction analysis, detergent B has the best synergism with MoDTC to produce stable and reduced friction throughout the traction and Stribeck phases. The combination of salicylates and sulfonates in detergent C produces stable and reduced friction only after 15 minutes of traction. Both improved results compared to only salicylates in detergent A.



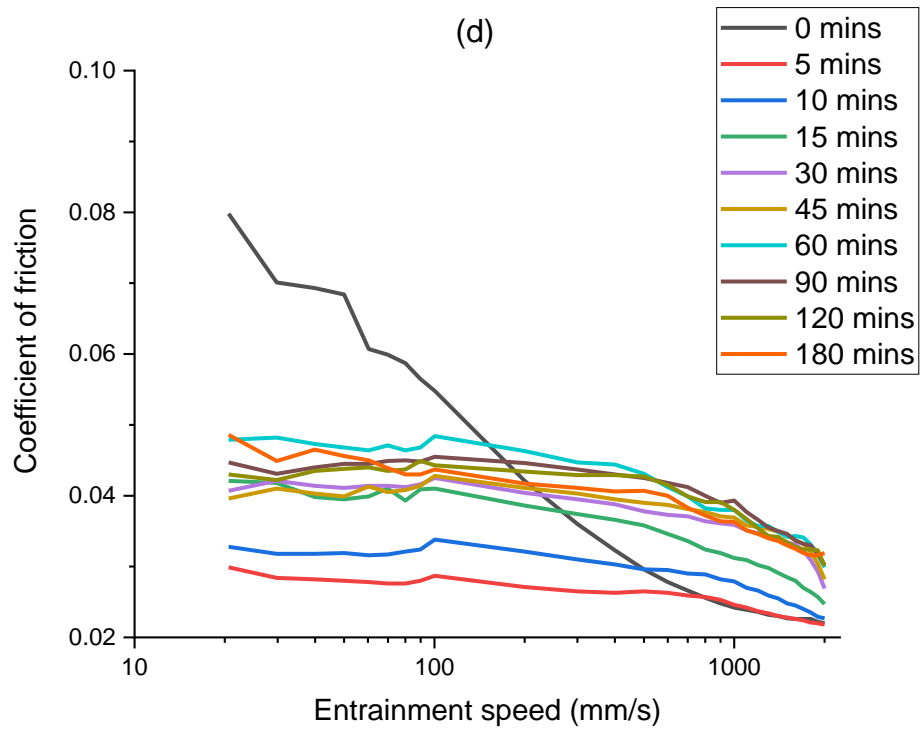
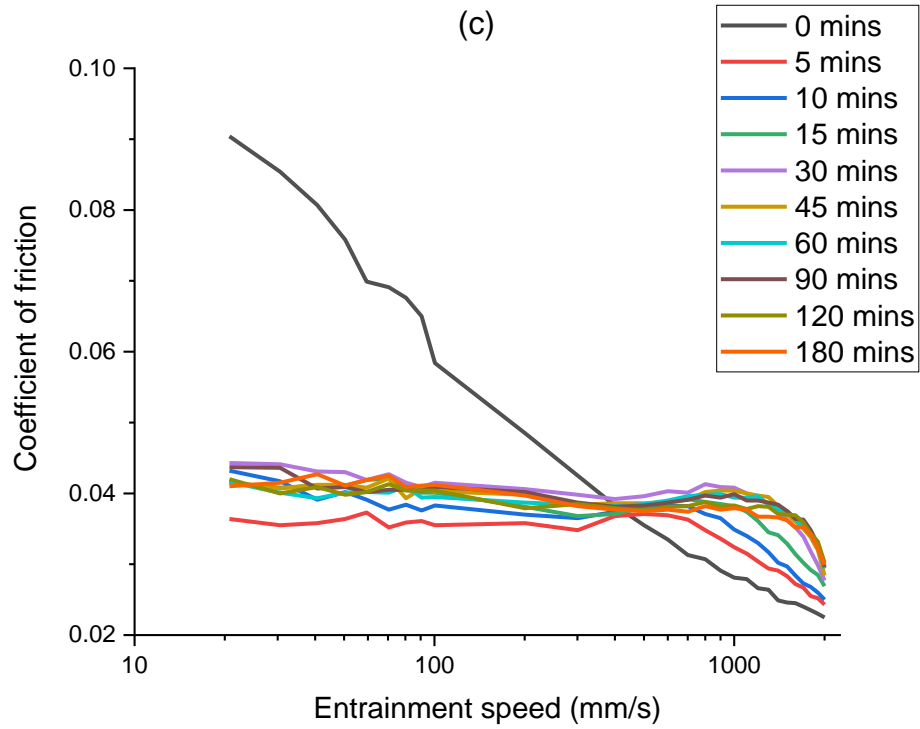


Figure 7-3 Stribeck curves for (a) initial and final for all three oils (b) Detergent A, (c) Detergent B , and (d) Detergent C.

7.5 Tribofilm Growth Rate and Thickness

Figure 7-4 displays the tribofilm film thickness obtained during the MTM tests. All three tribofilms show apparent differences between their steady-state thickness values. The initial tribofilm growths are similar. Within the first 30 minutes of traction, all three detergent formulations have sharp increases in film thickness as testing time increases. The initial tribofilm growth is typical of a ZDDP tribofilm characterized by a significant increase in film thickness [112,136]. However, other additives decomposition products are formed within the tribofilm at this stage as the friction is ≈ 0.04 within the first 5 minutes of traction, mainly MoS_2 . The detergent products will also be present within the tribofilm, as previous research has shown that detergent decomposition products form within the tribofilm matrix [80].

As the test duration increases to 120 minutes of traction, all three tribofilms produce further increases in film thickness values. All three detergent formulations reach their steady-state film thickness from 120 minutes onwards. Typically, a ZDDP tribofilm reaches the steady-state value after ≈ 60 minutes into the test [136]. All three final and steady-state film thicknesses also decrease compared to a fully formed ZDDP tribofilm, usually ≈ 120 nm [112]. Therefore, the boundary active additives, including the detergent formulations and friction modifiers, prevent the ZDDP's full film formation.

Detergent B, comprised of only sulphonates, has the smallest final film thickness value ≈ 55 nm. In comparison, detergent C, comprised of sulphonates and salicylates, produces the highest film thickness value and finally, detergent A, containing only salicylates, produces the medium value. Therefore, the detergent formulation containing only sulphonates has the

largest impact on the ZDDP film thickness, while a combination of sulphonates and salicylates has the smallest impact. An in-depth tribochemical analysis of the tribofilms is required to back the results obtained from the SLIM analysis and is shown in the following sections.

Overall, the ZDDP film thickness measurements from the SLIM technique have shown that the detergent formulation can significantly influence the ZDDP steady-state film thickness value, directly impacting the wear.

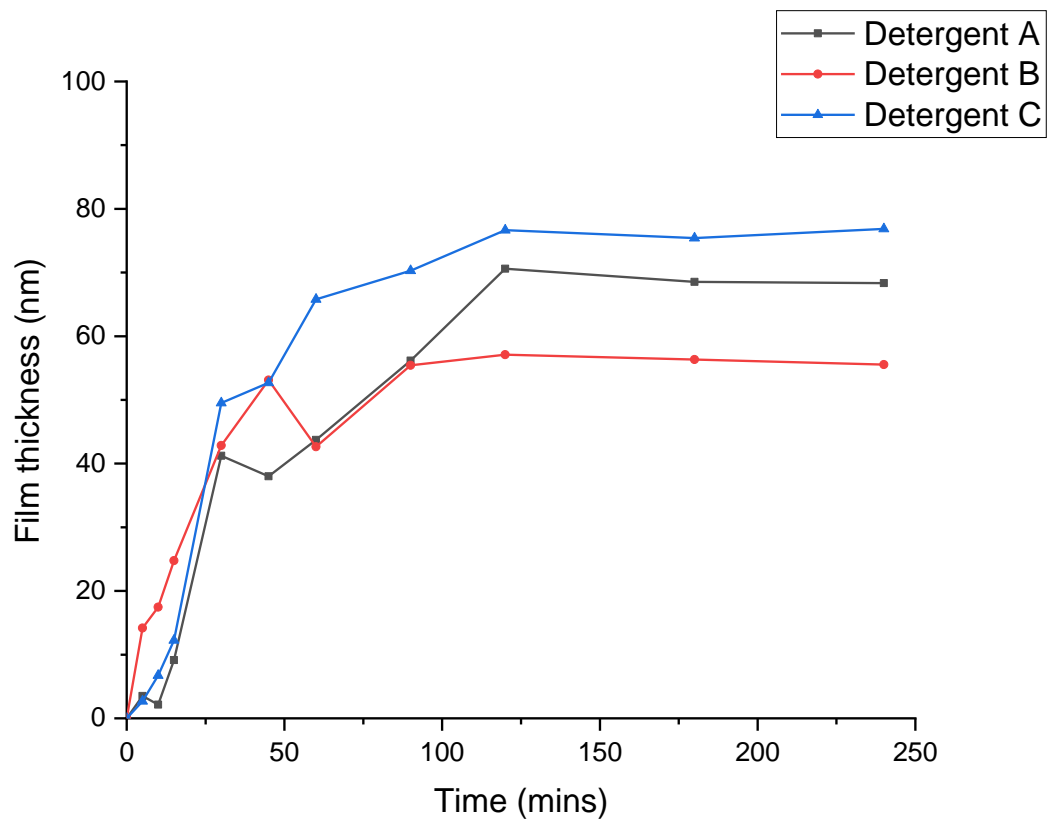


Figure 7-4 Film thickness growth rate vs time for all three detergent formulations.

7.6 Tribochemical changes within the Tribofilms

The friction and film thickness analysis suggest that the tribochemistry of the tribofilms of the three detergent sample oils differ in concentrations and potential compounds. Both Raman and XPS analyses were used to understand how the different detergent formulations can influence tribochemistry and help understand the behaviour of friction, film thickness, and wear results.

7.6.1 Raman Analysis

The average Raman spectrum obtained from the point scans completed within each tribofilm is shown in Figure 7-5. Multiple peaks were detected in each spectrum. The expected E_{2g} and A_{1g} peaks associated with MoS_2 were detected in all three tribofilms, with the additional Fe_2O_3 and S-S stretching peaks typically detected within friction-reducing tribofilms. The same peaks in the spectra were detected in the previous chapter's sample oils.

Detergent A's peaks associated with MoS_2 clearly show a much higher intensity than the other two tribofilms, with detergent C having the lowest intensity. The detergent formulation from sample C, containing salicylates and sulfonates, must suppress the formation of MoS_2 since this is the only difference between all three formulations. It must be noted that the low intensity observed for detergent C compared to A does not prevent friction reduction during rubbing. However, a slightly lower value is observed for detergent A than C in the steady-state friction values.

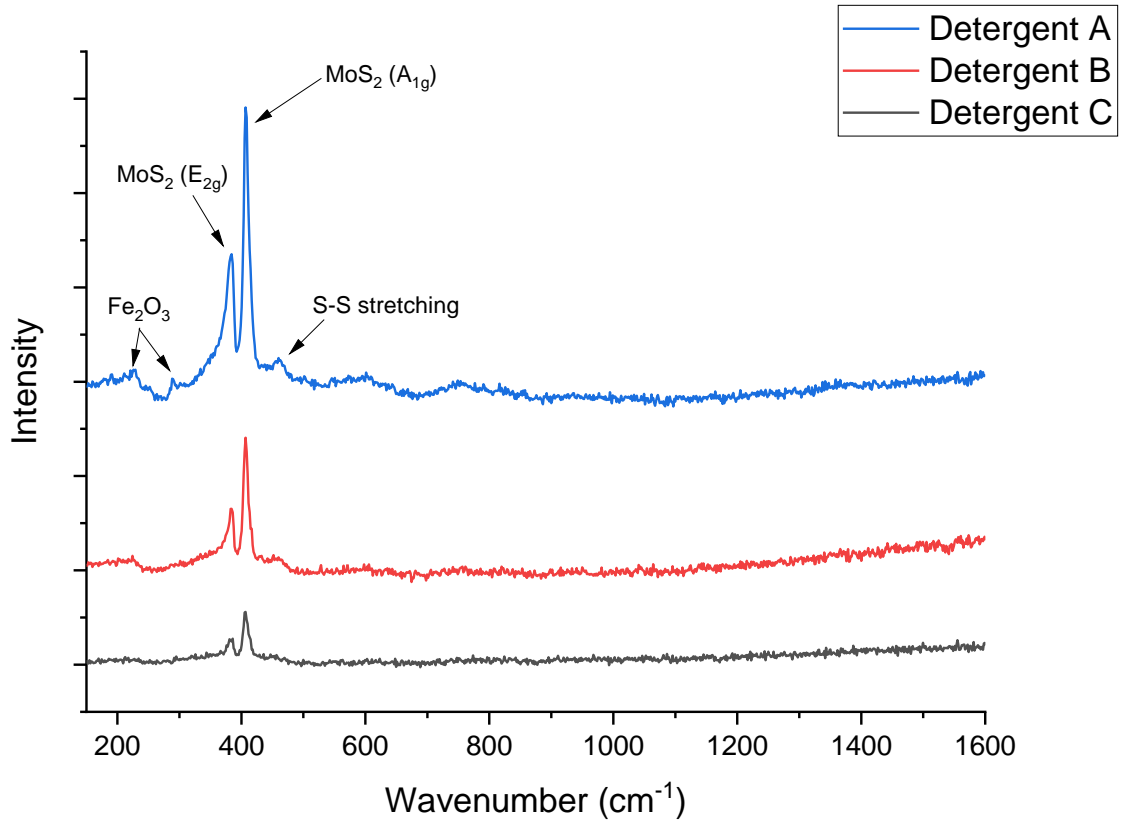


Figure 7-5 Raman spectra example from all three tribofilms.

Figure 7-6 shows each sample oil's total intensity counts of MoS₂ within the tribofilm matrix. There are apparent differences between the total intensities for all three tribofilms, following the same trend of the average spectrums. Detergent A containing salicylates produces a tribofilm with the highest total intensity counts, implying this tribofilm contains the most MoS₂. Detergent B containing only sulfonates has the second-highest total intensity counts, and finally, detergent C containing both, has the least intensity by a significant amount. The results show that detergent C with both detergent types within the formulation suppresses the formation of MoS₂ compared to the other sample oils. However, the friction results for detergent C show that the friction decreases rapidly within the first 5 minutes of traction, suggesting that a thick

and sufficient MoS₂ layer has formed within the ZDDP/detergent tribofilm matrix. Once the threshold value of MoS₂ intensity is reached to reduce the friction to ≈ 0.04 , the ZDDP and detergent parts of the tribofilm matrix can continue to form at a higher rate.

Very recent research investigating the tribological properties of MoDTC and its interactions with metal detergents used three different detergents in a binary system. A low and high-based calcium sulfonate and a middle-based salicylate were used with MoDTC. Mo and S weight percentage reduction within the tribofilm using energy dispersive spectrometry (EDS) was observed for low-based calcium sulfonate and middle-based salicylate. In contrast, an increase in both elemental weight percentages was seen in the high-based calcium sulfonate tribofilm [138]. However, the Mo and S weight % can be associated with other compounds rather than just MoS₂, for example, ZnS or MoO₃. It was determined that all three compound detergent additives produced transfer films containing MoS₂ and CaCO₃. XPS analysis of the tribofilms will determine the concentrations and products formed from ZDDP and the detergents and how they affect the MoS₂ concentration within the tribofilm matrix.

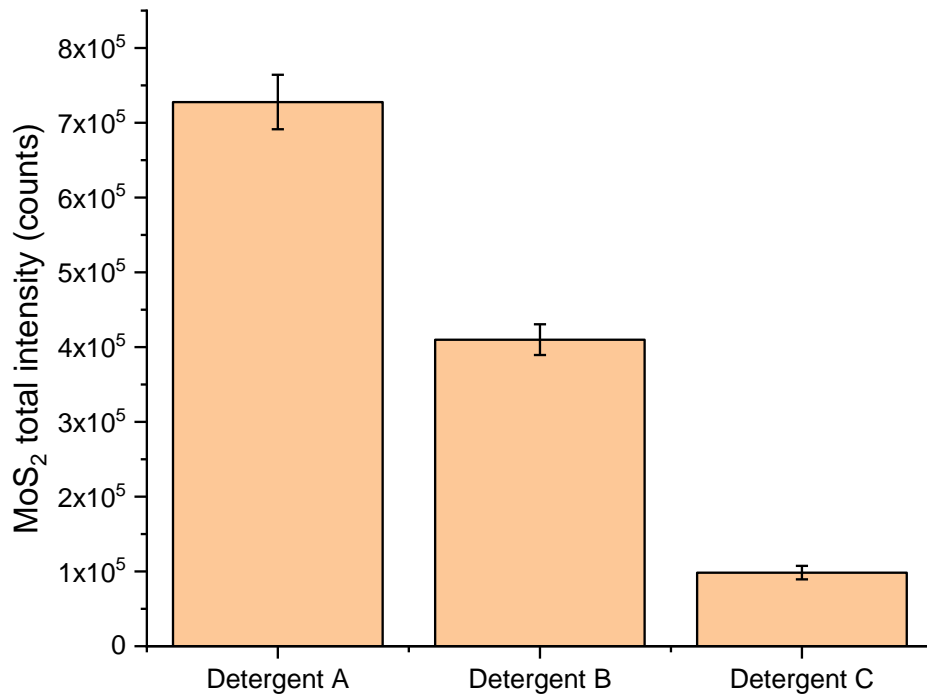


Figure 7-6 Total intensity counts of MoS₂ within each tribofilm.

7.6.2 XPS Analysis

7.6.2.1 MoDTC Decomposition Products

Figure 7-7 shows the deconvolution of the Mo3d signals obtained using XPS for tribofilms and etching times of all three detergents. At 0 s etching time, all three tribofilms produce S 2s, Mo (IV) and Mo (VI) peaks. The previous chapter and literature show that these peaks are typical of friction-reducing tribofilms containing metal sulphide, MoS₂ and Mo oxide compounds. The top layer scans differ in the Mo (IV): Mo (VI) ratios, with A to C, 67.21: 12.14, 64.12: 12.54 and 61.63: 14.48. It can be determined that detergent A's tribofilm has the most MoS₂ within its top layer and detergent C with the least amount. The increased MoS₂ observed in both Raman and XPS analysis

explains the slightly reduced friction produced from detergent A's tribofilm compared to C's.

When all tribofilms are etched into, the additional Mo (V) peak is detected within the signals, producing similar results as in the previous chapter when etching into a friction-reducing tribofilm. The Mo (V) peak is associated with the amorphous structure MoO_xS_y . There are minimal differences between the Mo3d signals, only slight changes in the Mo (IV): Mo (VI) ratios. All three tribofilms still produce similar Mo3d signals after 120 seconds of etching time.

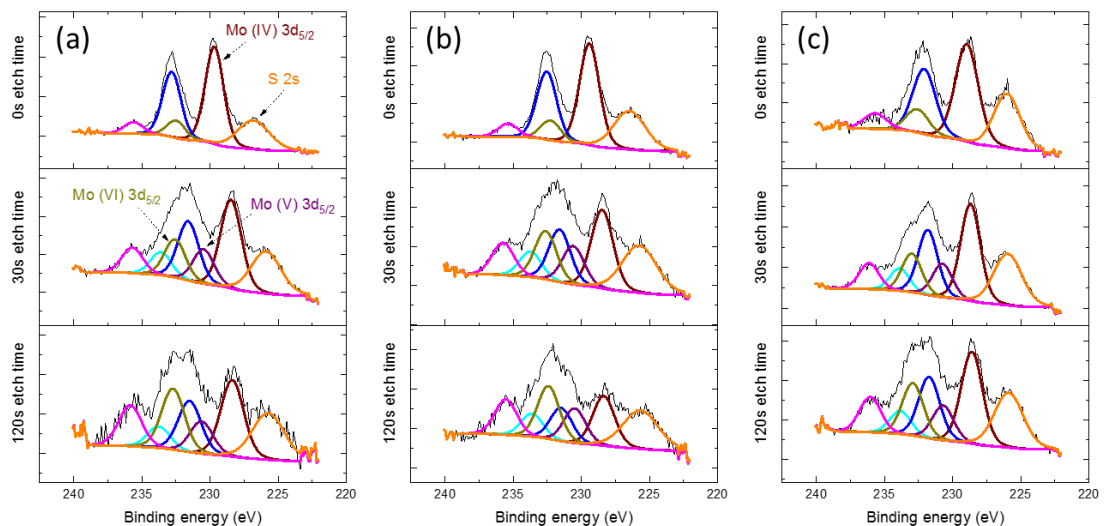


Figure 7-7 Mo 3d signal peaks for all HR scans (a) Detergent A, (b) Detergent B and (c) Detergent C.

7.6.2.2 ZDDP and Detergent Decomposition Products

Figure 7-8 displays the average weight % of elements associated with ZDDP and detergent decomposition products within 120 seconds of etching time, with four survey scans in total.

Elements that are only associated with the ZDDP decomposition products are Zn and P. S has a crossover with MoDTC decomposition products. Detergent

C containing Ca salicylates and Mg sulfonates produce a tribofilm with the most Zn and P weight percentages compared to the other sample oils. From ZDDP tribofilm thickness measurements, detergent C was determined to have the thickest film. XPS analysis agrees with the data, with C having a higher average % weight of ZDDP decomposition elements. The data suggest that the detergent C formulation will produce the smallest wear since the ZDDP part of the tribofilm has grown the most. Detergent A and B's tribofilms contain similar amounts of Zn, with B having higher amounts of P. Both tribofilms also have similar ZDDP film thicknesses from the SLIM analysis data.

Previous research shows that the critical elements associated with all the detergent decomposition products used are Ca, Mg, and O [80,84,139]. Decomposition products which can form on the rubbing surfaces generated from Ca detergents are CaCO_3 and Ca phosphates. Research shows that the products formed within the tribofilm matrix from Mg detergents are hard to determine [140]. However, results have shown that MgSO_4 can be detected within tribofilm matrixes [141]. Detergent A has the least amount of Ca and O but the most Mg within its tribofilm matrix. In comparison, detergent B has the most Ca and O with the least amount of Mg out of the three tribofilms. However, it must be noted that detergent C's tribofilm does have Ca and O percentages closer to the highest values.

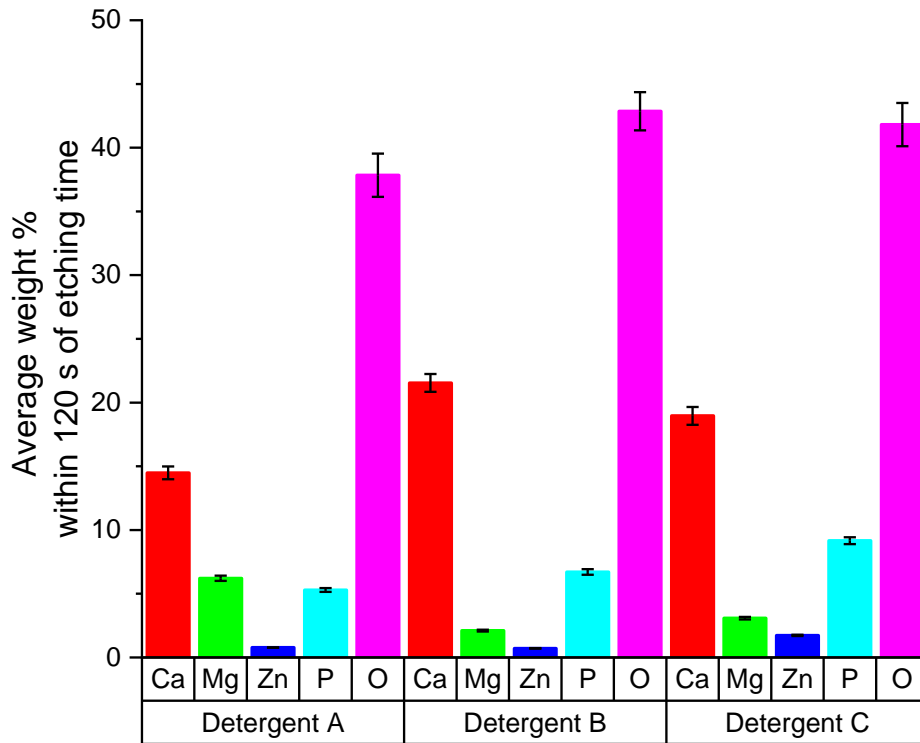


Figure 7-8 Average weight % of elements associated with ZDDP and detergent decomposition products within 120 seconds etching time.

Overall, from the tribofilm chemical analysis, the detergent formulation for sample C suppresses the formation of MoS₂, which allows more formation of ZDDP and detergent decomposition products within the tribofilm matrix. During the test, the tribofilms film thickness resembles tribofilms containing large amounts of ZDDP species. In theory, this should produce the lowest wear out of the three detergent formulations.

Detergent A has the highest amount of MoS₂ and the least amount of ZDDP and detergent decomposition species within its tribofilm. The detergent

formulation of only salicylates suppresses the ZDDP formation allowing for more MoS₂ growth. In the beginning stages of tribofilm growth, little to no ZDDP tribofilm could be measured from the SLIM images, implying the tribofilm is formed from MoDTC decomposition products, providing low unstable friction. Even though detergent A has the highest total intensity counts of MoS₂, the friction performance under a varying lambda ratio is not the best out of the three detergent formulations. However, it does produce the lowest friction under a constant lambda ratio.

Detergent B, containing only sulfonates, produces a tribofilm film matrix with the highest detergent decomposition products and medium amounts of ZDDP and MoS₂. The tribofilm matrix formation from detergent B produces the most stable friction during varying lambda ratios and low steady-state friction under a constant lambda ratio.

7.7 Wear Performance

Figure 7-9 displays the average wear volume loss for a 0.4x0.35 μm area on the wear track of the MTM discs. Detergent A's formulation produces the highest wear, with detergent C producing the least and B medium. The tribochemical analysis of the tribofilms implied that detergent C would have the least amount of wear due to higher amounts of anti-wear additive species. Previous research has also proven this to be true [142]. The salicylate detergents in the detergent A formulation could create Ca phosphates, which prevents long-chain polyphosphates from forming. Large amounts of MoS₂ detected within detergent A's tribofilm also prevents the anti-wear film's complete formation due to competitive surface absorption.

Detergent B produces the medium wear loss from the different samples. Ca sulfonates in previous literature have been found to produce tribofilms with anti-wear properties [82]. However, Ca salicylates and sulfonates produce CaCO_3 and Ca phosphates within the tribofilms. Clearly, the results from this study show that sulfonates have a more synergistic effect with the anti-wear additive than salicylates when formulated separately. Ca salicylates and Mg sulfonates formulated in a fully formulated oil, including ZDDP and MoDTC, produce even better synergistic effects with the anti-wear additive.

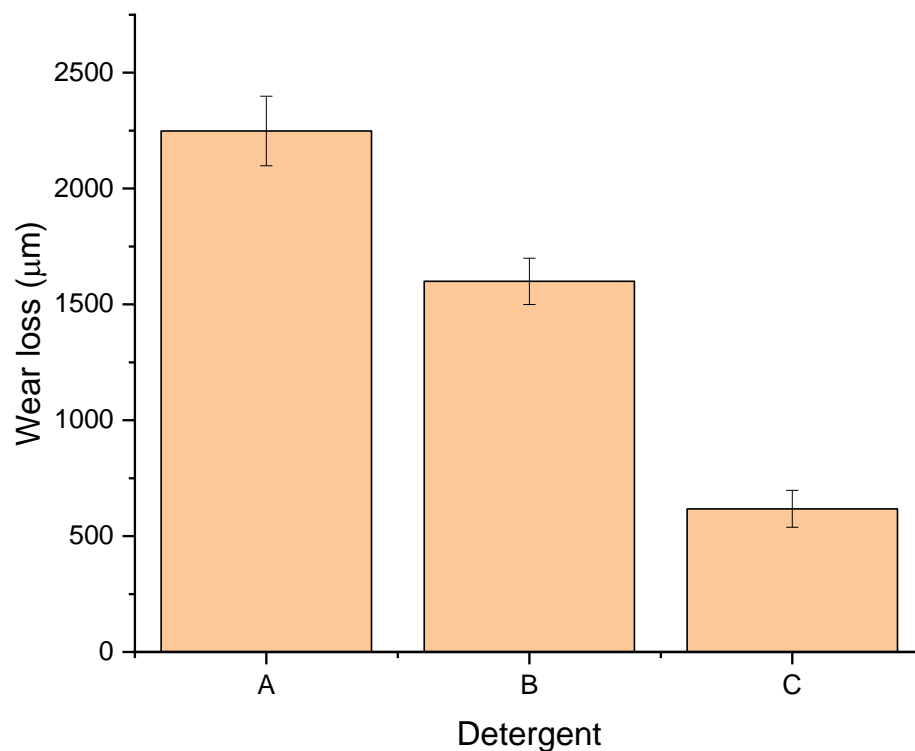


Figure 7-9 Average wear loss for a 0.4x0.35 µm area.

7.8 Summary

This chapter has tested three different detergent formulations in low viscosity fully formulated engine oil. Detergent A contained Ca and Mg salicylates. Detergent B consisted of Ca and Mg sulfonates. Finally, detergent C is comprised of Ca salicylates and Mg sulfonates. All detergent formulations have higher Ca detergent weighed percentages than the Mg detergents. The oils were all tested using the MTM-SLIM to understand the influence of these different detergent formulations on friction. Any physical or chemical changes within the tribofilms for the three sample oils were analysed using the SLIM, Raman and XPS techniques. Finally, wear generated from the friction tests was analysed using the NPFlex. The following conclusions drawn from this chapter are as follows.

- The detergent formulations used in this study impact the steady-state and Stribeck friction values. Detergent selection can significantly impact the friction performance of oils.
- Detergent B containing Ca and Mg sulfonates produce the most stable and best friction performance. Detergent C's formulation produces the worst out of the three tested.
- The combination of Ca salicylates and Mg sulfonates suppresses the formation of MoS₂ within the tribofilm due to more significant amounts of ZDDP and detergent species forming within the tribofilm. A larger

steady-state tribofilm thickness is also observed for detergent C's combination.

- According to Raman and XPS techniques, detergent A's combination of Ca and Mg salicylates allows for the most MoS₂ formation. The detergent combination also has a minor impact within the tribofilm as the detergent decomposition species is the lowest amount.
- Detergent C's formulation produces the least amount of wear; detergent A generates the most, and B with the medium.
- Detergent A's formulation has the most synergistic effect with MoDTC. Detergent C's formulation has the most synergistic effect with ZDDP. Finally, Detergent B's formulation has both synergistic effects with MoDTC and ZDDP compared to the other two formulations.

Chapter 8 The effect on Tribological Properties: a comparison between lab-based simulated oil ageing process and oil ageing in engine conditions.

8.1 Introduction

The main driving factor which depletes MoDTC from the oil is oxidation and degradation from high temperatures. This significantly impacts the longevity of the friction-reducing properties of the oils [63,85,95,99]. Previous research has shown that friction-reduction properties are lost after 80% of additive depletion [93]. Other research into the oxidation of a 0W 20 fully formulated oil containing 700ppm of Mo concluded that after 15 hrs of ageing, equivalent to ≈ 5 km, the friction-reducing properties are lost [143]. An investigation into reducing CO₂ emissions and cost analysis of ultra-low viscosity engine oil showed that extending the ODI is as essential as reducing viscosity [8]. To enable the extension of the ODI, MoDTC must form a friction-reducing tribofilm over a long period $> 15,000$ km. This information highlights the importance of balancing the Mo concentration to obtain positive friction results in fresh and aged engine oils, leading to improved fuel economy. It is crucial to investigate and understand engine oils that have been subjected to oxidation, which gives application to used engine oils in operation.

It is essential to have good lab-based artificial oil ageing processes to avoid unnecessary test times and costs on engine ageing testing. Due to time and extra costs, researchers use artificial ageing to screen sample oils before engine testing. However, little research has been conducted comparing artificial and engine ageing effects on the tribological performance of low viscosity oils. This study compares how the different ageing techniques, artificial and engine ageing, affect the sample oils' tribological performance,

specifically referring to MoDTC and oil oxidation. Analysis of the oil oxidation was conducted using FTIR and changes in viscosity before and after ageing. Friction performance was investigated using MTM with the additional SLIM unit to provide film thickness measurements throughout the test. MoS₂ analysis was performed using RAMAN spectroscopy, and finally, wear generated from rubbing was determined via the NPFlex.

8.2 Test Oils

The Sinopec Lubrication company provided all fresh and engine-aged sample oils for this study. Two oil pairs were provided for testing and analysis to compare the standard used in artificial ageing and engine ageing processes with differences between oil formulations and engine age processes. The CCL-48-00 standard artificial ageing process was used to oxidate the fresh oils in the laboratory. The details of the process can be found in Chapter 4.

The test oils used in this study are shown in Table 8-1. All the sample oils have different engine ageing processes. Oil A's kinematic viscosities at 100 and 40 °C are within the oil grade bracket 0W-20, while oil B is 0W-8 according to ASTM D445. All engine oil ageing processes can be found in Chapter 4.

Table 8-1 Test oils used to compare artificial and engine ageing processes.

Sample label	Oil A	Oil B
Oil grade	0W-20	0W-8
Base oil	Group 3+	
HTHS 150/D4683	2.73	1.75
Mo (ppm)	880	800
S (ppm)	3060	2840
Zn (ppm)	830-840	
P (ppm)	760	
Ca (ppm)	1300-1480	

The MTM operating conditions used in this study is shown in Table 4-4. Methodologies for tribochemical and wear analysis are also shown in Chapter 4.

8.3 Oil Analysis

Oil analysis was conducted before and after artificial and engine ageing to investigate the oxidation effects on the oils. Viscosity and FTIR measurements were taken to check that oxidation and ageing occurred within the oils. Any changes in the viscosity of the oils at different temperatures signals changes in the physical properties. While changes in specific bonding peaks from literature using FTIR imply that additive depletion and oxidation have occurred during ageing.

8.3.1 Viscosity

8.3.1.1 Oil A

The dynamic viscosities of oil A at 40°C and 100°C before and after both ageing processes are shown in Table 8-2. Increasing viscosity values are observed at tested temperatures for both ageing processes. Previous research has documented that the formation of by-products from oxidation causes an increase in viscosity and decreases the VI number [144].

Table 8-2 Oil A's dynamic viscosities.

Temperature (°C)	Fresh (mPa.S)	Artificially aged (mPa.S)	Engine-aged (mPa.S)
40	13.80	14.30	15.85
100	3.54	3.63	3.59

8.3.1.2 Oil B

Oil B's dynamic viscosities at 40°C and 100°C before and after both ageing processes are shown in Table 8-3. The artificially ageing process increases the oil's viscosity at both temperatures tested, indicating oxidation has taken place. However, the engine ageing process does the opposite, decreasing the oil's viscosity at both tested temperatures. The results for the engine-aged oil are not typical in research when oxidation has taken place. Unwanted non-lubricants such as fuel or solvents or breakdown of viscosity modifiers within the oil could explain the oil's viscosity decrease observed, as documented in past research studies [145,146].

Table 8-3 Oil B's dynamic viscosities.

Temperature (°C)	Fresh (mPa.S)	Artificially aged (mPa.S)	Engine-aged (mPa.S)
40	14.42	15.66	14.03
100	3.25	2.45	3.19

8.3.2 Additive Depletion and By-products

8.3.2.1 Oil A

Figure 8-1 to Figure 8-3 show specific bonding peaks from FTIR associated with additive depletion and oxidation by-products formed directly from oxidation for oil A's oils. The first peak, shown in Figure 8-1, is the P-O-C and P=S bonding from the ZDDP molecule. Both ageing processes show signs of reduction in peak transmittance, indicating that oxidation has depleted the ZDDP additive and is a common theme in previous literature to identify oxidation within aged oils [147].

Two bonding peaks, S=O and S-O, associated with sulphation are shown in Figure 8-2. Both ageing processes produce peaks with higher transmittance percentages than fresh oil. Again from the literature, this indicates sulfur by-products have formed within the oil due to the ageing process [148]. Artificial ageing produces a higher peak compared to engine ageing.

Finally, the bonding peak associated with carbon oxidation, C=O, is shown in Figure 8-3. This peak is from by-products of the oxidation of carboxylic. Both ageing processes increase the peak, with artificial ageing having the highest transmittance percentage.

Overall, both ageing processes for oil A have changed the oils physically with increased viscosity and chemical properties according to FTIR measurements. The peak comparison between the engine and artificially ageing processes suggests the latter has a harsher effect on the oil.

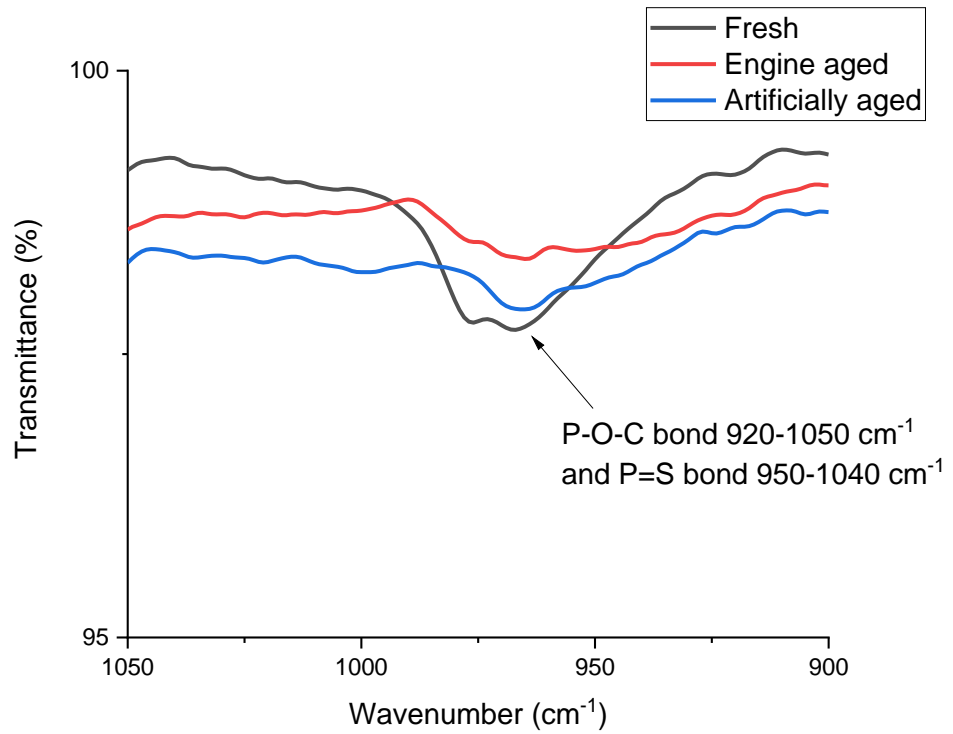


Figure 8-1 Oil A's ZDDP (P-O-C and P=S) bonding peak.

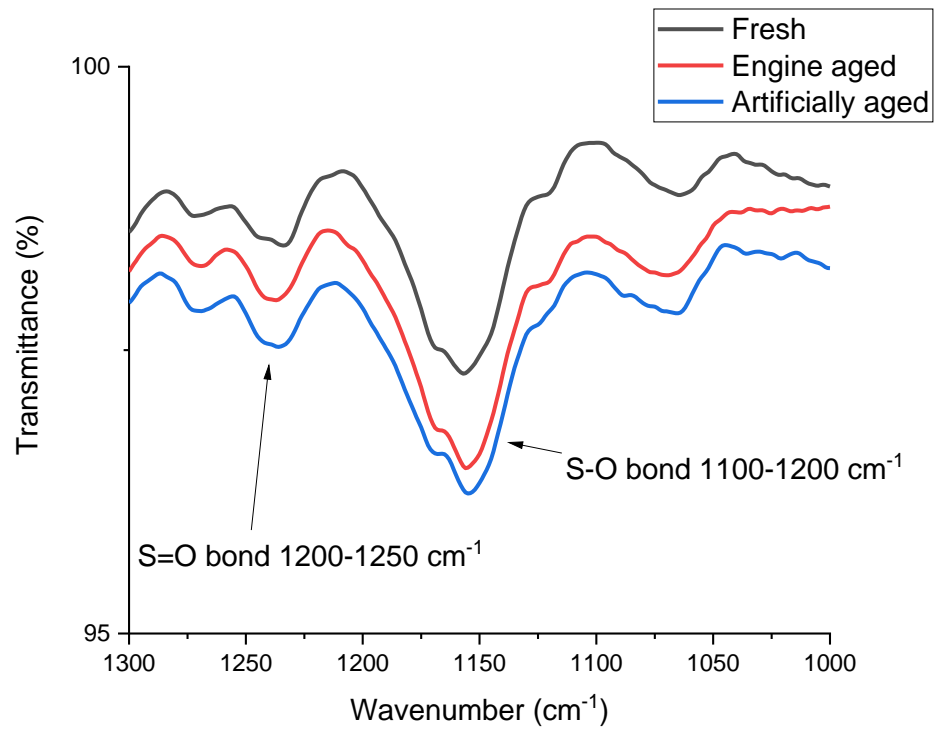


Figure 8-2 Oil A's sulphation (S=O and S-O) bonding peaks.

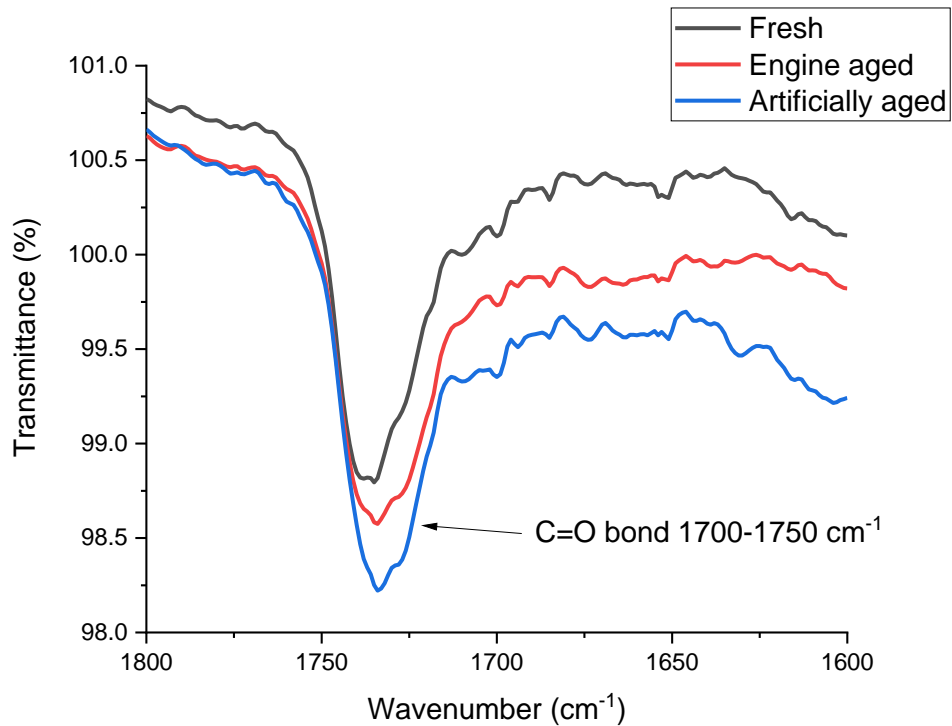


Figure 8-3 Oil A's Carbon oxidation (C=O) bonding peak.

8.3.2.2 Oil B

Figure 8-4 to Figure 8-6 display the specific bonding peaks associated with ageing for oil B's FTIR spectrums. Oil A's spectrums differ from oil B's due to the oil formulations and the engine's ageing process.

The peak associated with bonding from the ZDDP molecule is shown in Figure 8-4. The engine and artificially ageing processes deplete the ZDDP additive molecule due to a smaller peak than the fresh engine oil.

Figure 8-5, showing the S-O bond associated with sulphation within the oils indicates that sulfur by-products have formed after engine and artificially ageing. The engine ageing process produces a peak with a higher transmittance percentage, implying higher amounts of sulfur by-products have formed.

The carbon oxidation peak from the bonding C=O shown in Figure 8-6 displays very different peaks for the ageing processes compared to the fresh engine oil. The carbonyl compound peak from the literature is typically similar to oil A's peak at 1700-1750 cm^{-1} [102,149]. However, even though the peak has shifted position, an increase in transmittance percentage is observed for both ageing processes, implying that the ageing processes have impacted the oil. Again, the engine ageing process produces a higher transmittance percentage peak than the artificial ageing process.

Overall, from the FTIR peak analysis, both ageing processes have changed the physical and chemical properties of the oils. The sulphation and carbon oxidation peaks imply that the engine ageing process has had a harsher effect on the oil than the artificially ageing process.

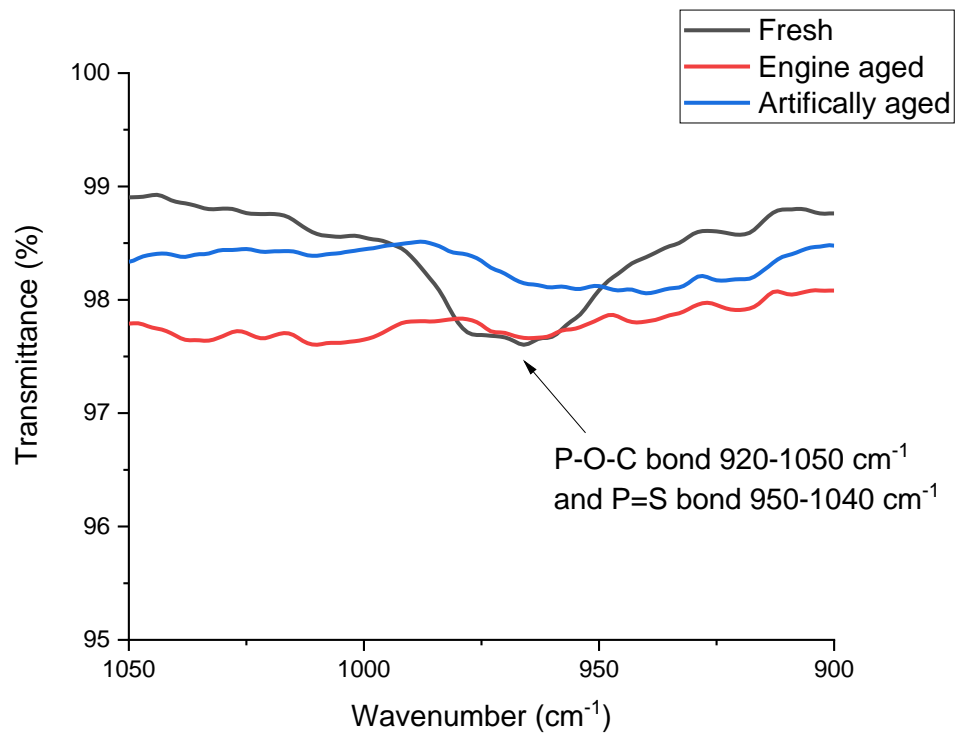


Figure 8-4 Oil B's ZDDP (P-O-C and P=S) bonding peak.

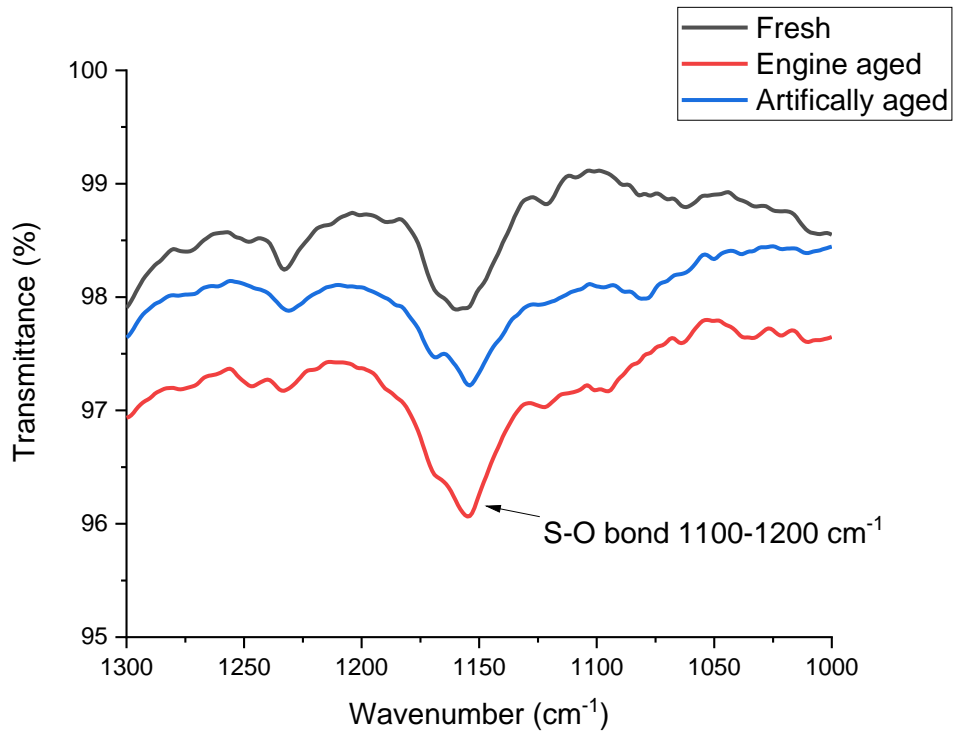


Figure 8-5 Oil B's sulphation S-O bonding peaks.

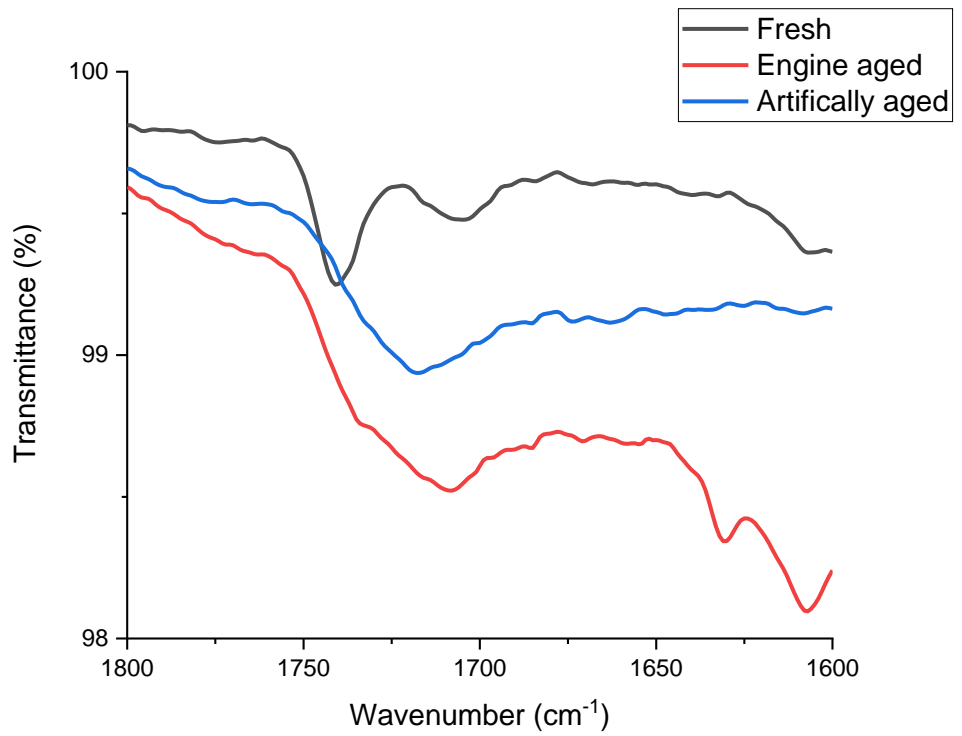


Figure 8-6 Oil B's Carbon oxidation (C=O) bonding peak.

8.4 Friction Analysis

8.4.1 Oil A

Figure 8-7 displays the initial and final Stribeck curves for sample A's fresh, artificially and engine-aged oils. The initial Stribeck curve shows no difference between the fresh and artificially aged oils, producing similar curves. However, engine-aged oil produces increased friction across the whole range of entrainment speeds. Higher friction in the boundary and mixed lubrication regime at the start of the test implies lower viscosity at the contact point. Therefore, the engine ageing process changes the fresh oil's physical properties more than the artificial ageing process.

Similar to the initial Stribeck curves, the final curves for the fresh and artificial aged have similar friction in the boundary lubrication regime. Even after artificially ageing, the oil has still kept its friction-reducing properties. At higher entrainment speeds, the artificially aged oil has higher friction than the fresh due to differences in tribofilm composition. The engine-aged oil's Stribeck curve significantly increases friction across the whole range of entrainment speeds, opposite to the artificially aged oil. The engine ageing process has completely removed the oil's ability to reduce friction. However, the Stribeck curve is similar to tribofilms, mostly comprised of ZDDP and detergent decomposition species, as shown in the previous studies of this thesis and literature [50,52]. Even though the friction ability is lost, the ageing process does not prevent the formation of the anti-wear additive. Previous literature has also reported ZDDP formation after ageing processes [95]. In the later sections, film thickness measurements and tribofilm chemical analysis will be used to confirm this.

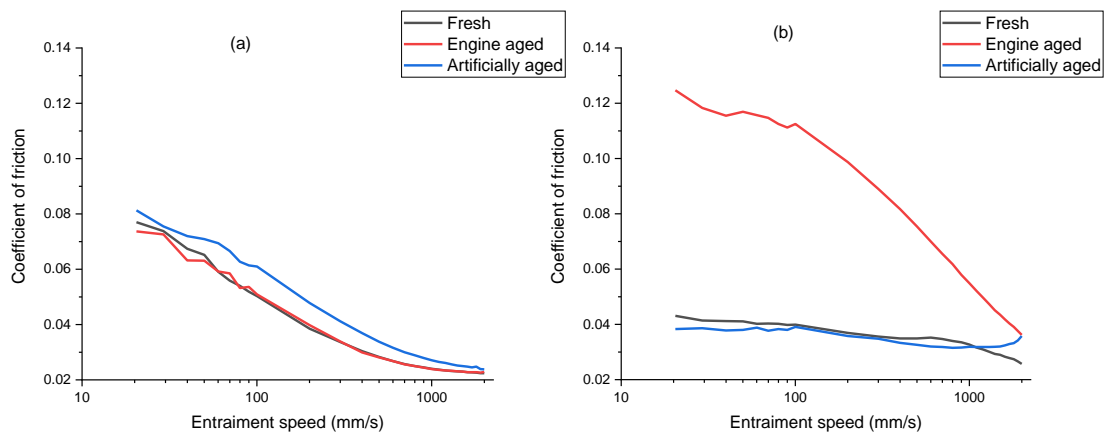


Figure 8-7 (a) initial and (b) final Stribeck curves for oil A before and after ageing.

Figure 8-8 to Figure 8-10 show the Stribeck curves taken at every interval during the tests for all the sample A oils to understand the changing friction under a varying lambda ratio. The first Figure 8-8 displays the Stribeck curves for the fresh engine oil. Significant friction reduction is observed within the first 5 minutes, and stable friction is achieved from the 15-minute interval mark until the end of the test. The Stribeck curves are typical of oils containing high amounts of MoDTC, as shown in Chapter 6.

Figure 8-9 shows the artificially aged oils Stribeck curves. Although similar end friction is achieved compared to fresh oil, reaching it is very different. Friction in the boundary lubrication regime increases in the first 30 minutes of traction, with friction in the mixed regime at higher entrainment speeds not significantly changing. The friction at higher entrainment speeds increases after 60 minutes of rubbing, with a decrease in friction, observed at very low speeds, suggesting some form of MoS₂ is starting to produce friction reduction. After 60 minutes of rubbing, the Stribeck intervals produce significant friction reductions in the boundary lubrication regimes. These

curves are typical of tribofilms that contain MoS₂, as seen in the previous chapters. However, compared to the fresh Stribeck curves, they are less stable and further apart. Therefore, there must be a difference between the tribofilm matrixes. Tribochemical analysis in the later sections will further develop an understanding of this.

Finally, Figure 8-10 shows all the Stribeck curves taken for the engine-aged oil. The friction increases as the test duration increase across the whole range of entrainment speeds. After 120 minutes of traction, the Stribeck curves are closer together after each interval, creating more stable and steady-state friction. Typically with fresh engine oil with no friction modifier present, the friction becomes stable and steady-state around the 60-minute interval [150]. Therefore, engine ageing potentially slows tribofilm formation. SLIM measurement shown in the later section will confirm this.

The engine ageing process has a much harsher effect on the oil than the artificial ageing process from the friction results. The statement is not a surprise since the artificial ageing process does not contain pumping of the oil through components or soot contamination from the actual use of the ICE.

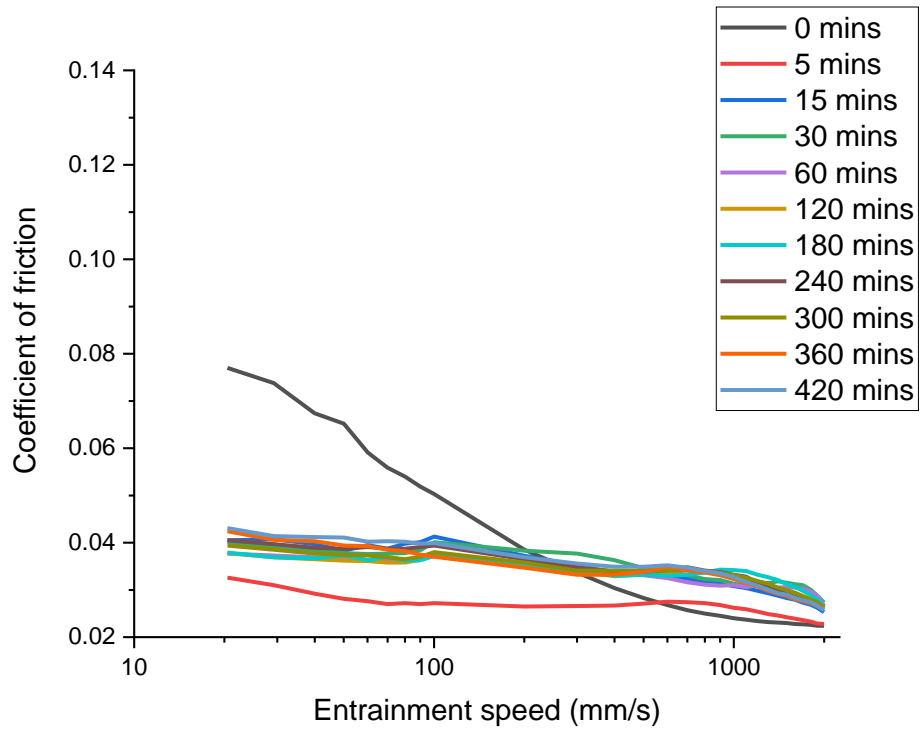


Figure 8-8 All Stribeck curves for the fresh engine oil.

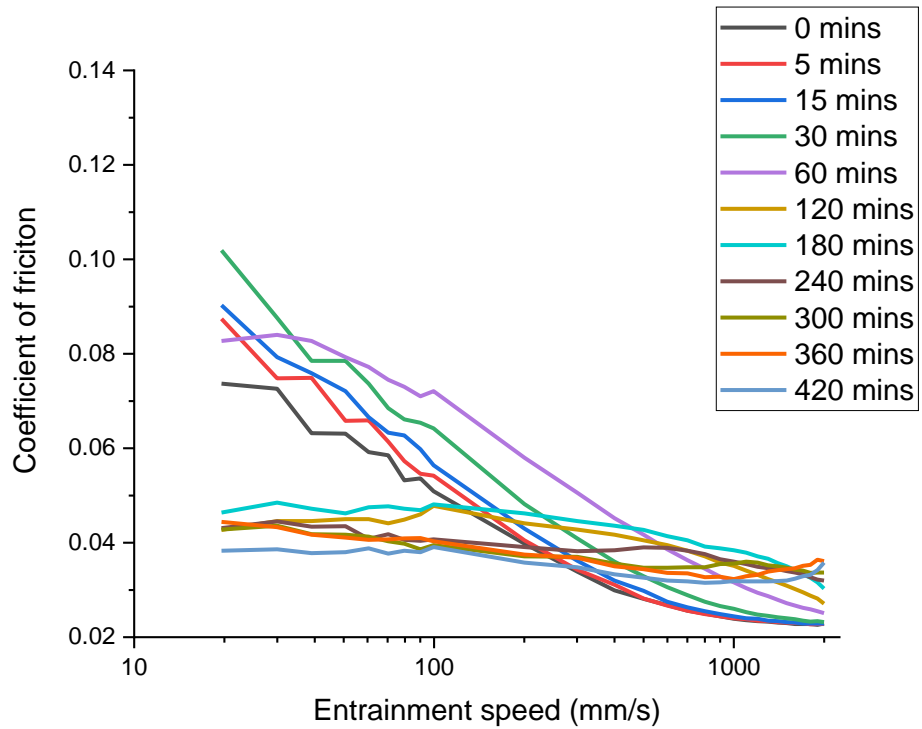


Figure 8-9 All Stribeck curves for the artificially aged engine oil.

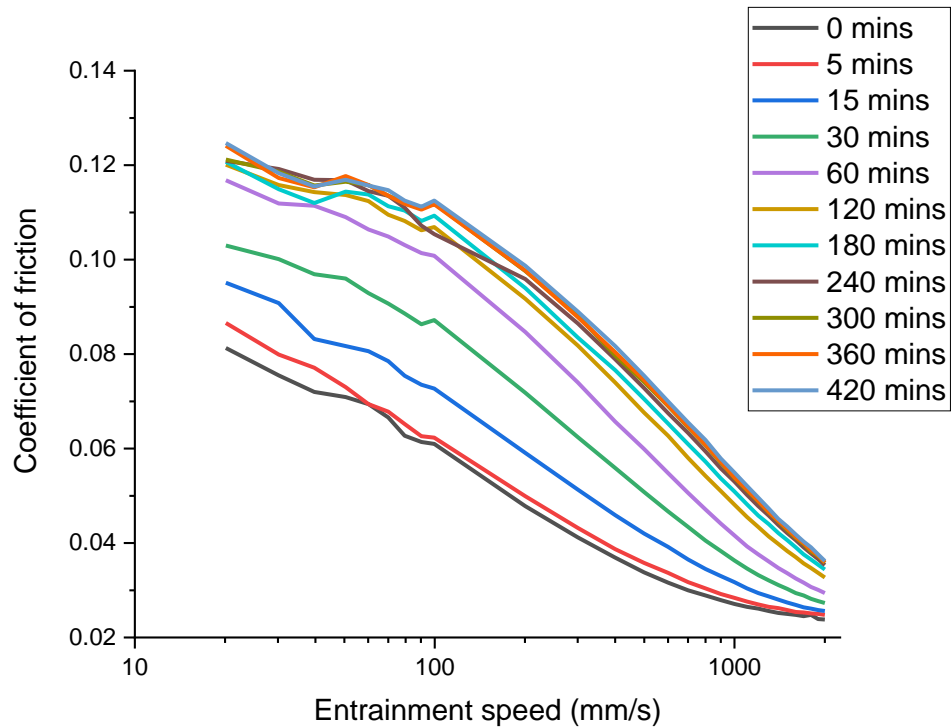


Figure 8-10 All Stribeck curves for the engine aged oil.

8.4.2 Oil B

Figure 8-11 displays the initial and final Stribeck curves for sample B's fresh, artificially aged, and engine-aged oils. From the initial Stribeck curves, both ageing processes produce a slight friction increase in the boundary and mixed regimes, possibly due to the decrease in viscosity caused by both ageing techniques.

The final Stribeck curves for both ageing techniques produce significantly more friction than the fresh oil across the whole range of entrainment speeds. Therefore, both ageing techniques altogether remove the friction-reducing capabilities of the oil. However, there are significant differences between the final Stribeck curves for both ageing processes. The engine-aged oil produces a Stribeck curve similar to tribofilms containing mostly ZDDP species, implying

the anti-wear additive can form even after engine ageing. The Stribeck curve has increased friction for the artificially aged oil but not to the higher levels of the engine-aged oil. It has a similar curve structure to the initial Stribeck curves implying very little tribofilm has formed. The artificially ageing process has a less harsh effect on friction. However, the initial friction analysis suppressed the anti-wear additive formation, implying that the wear will be more significant for the artificially aged oil than the engine-aged oil.

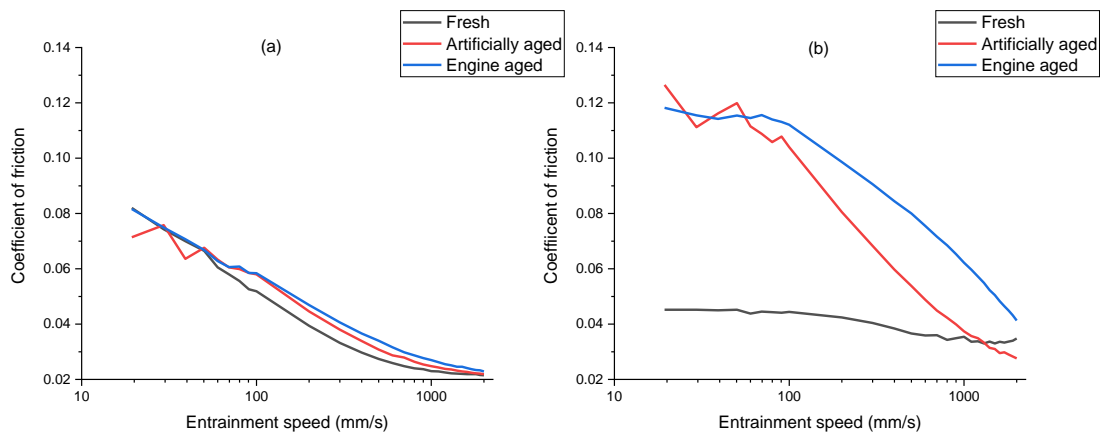


Figure 8-11 (a) initial and (b) final Stribeck curves for oil B before and after ageing.

Figure 8-12 to Figure 8-14 show all the Stribeck curves taken for B's sample oils. The Stribeck curves taken from the fresh oil, displayed in Figure 8-12, show a significant reduction in friction with a steady-state value of ≈ 0.04 - 0.05 . As previous chapters and sections show, the fresh oil Stribeck curves are typical of tribofilms containing friction-reducing MoS₂. The friction becomes steady-state after 30 minutes into the traction, with lower friction before reaching it. Friction data for the fresh oil suggest thick MoS₂ has formed within the tribofilm matrix, typical of engine oils with higher amounts of MoS₂, as shown in Chapter 6.

The artificially aged oil's Stribeck curves are shown in Figure 8-13. The artificially ageing process suppresses the formation of anti-wear and friction-reducing additives. As the test duration increases, the friction over the whole range of entrainments increases to a steady-state Stribeck curve after 120 minutes of traction. After the initial curve, all the Stribeck curves have the same structure, very different from what is typically seen in aged oils. A less sharp increase from high entrainment to low entrainment is observed compared to oils that produce a tribofilm with high amounts of ZDDP species. The Stribeck curve is dissimilar to those found in literature, and this research implies that very little tribofilm has formed [50,52].

Finally, Figure 8-14 shows all the Stribeck curves for the engine-aged oil. The Stribeck curves observed for the engine-aged oil are more typical of Stribeck curves that heavily comprise the anti-wear additive. The Stribeck curve friction increases as the test duration increases and reaches a steady-state friction curve after 180 minutes of traction. Steady-state friction is achieved after 180 minutes of traction, typically longer than fresh engine oil with ZDDP and no friction modifier. The engine ageing process has removed the ability of friction reduction, similar to the artificial ageing process, and delays the complete formation of ZDDP. However, unlike the artificially aged oil, a sharper friction increase is observed when the entrainment speed decreases from high to low speeds, suggesting a thicker ZDDP dominant tribofilm has formed.

Overall, the artificially ageing process has produced the highest friction from the results of the Stribeck curve. The ageing process has removed the ability of the oil to reduce friction and produce a thick ZDDP-dominant tribofilm. Even though the engine ageing process removed the friction-reducing capabilities, a Stribeck curve similar to tribofilms with thick ZDDP dominant species was

observed. The friction Stribeck curves suggest that the engine ageing process wear will be less than the artificial ageing process.

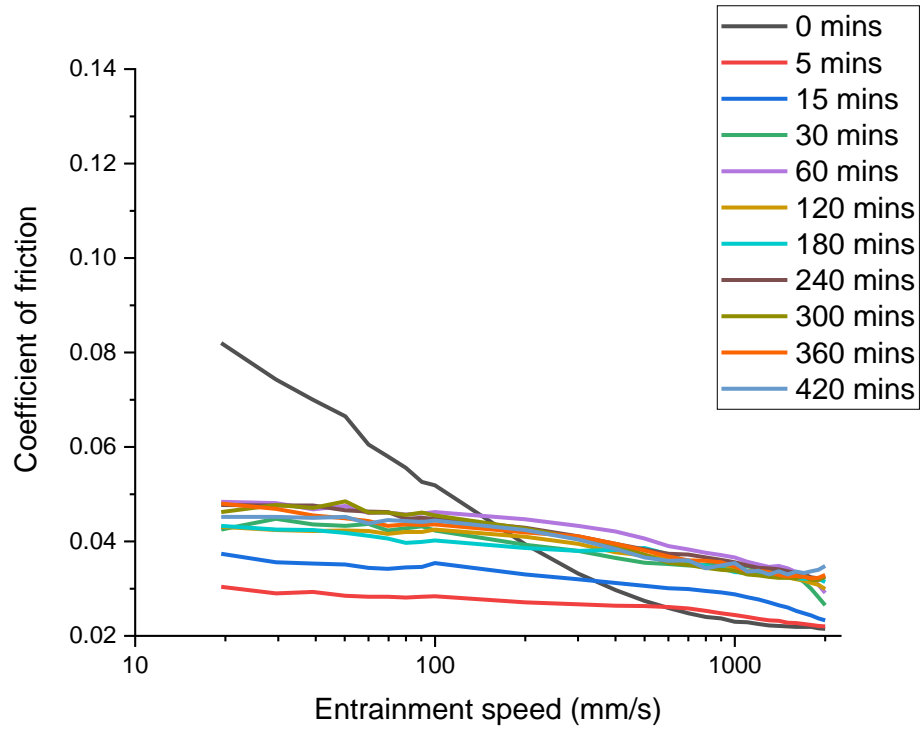


Figure 8-12 All Stribeck curves for the fresh engine oil.

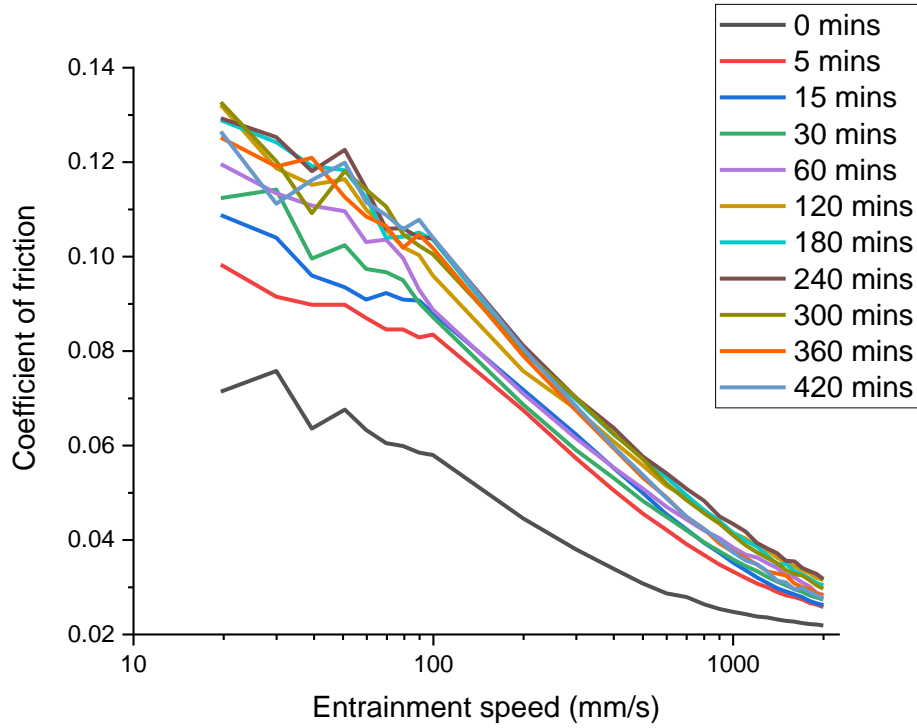


Figure 8-13 All Stribeck curves for the artificially aged engine oil.

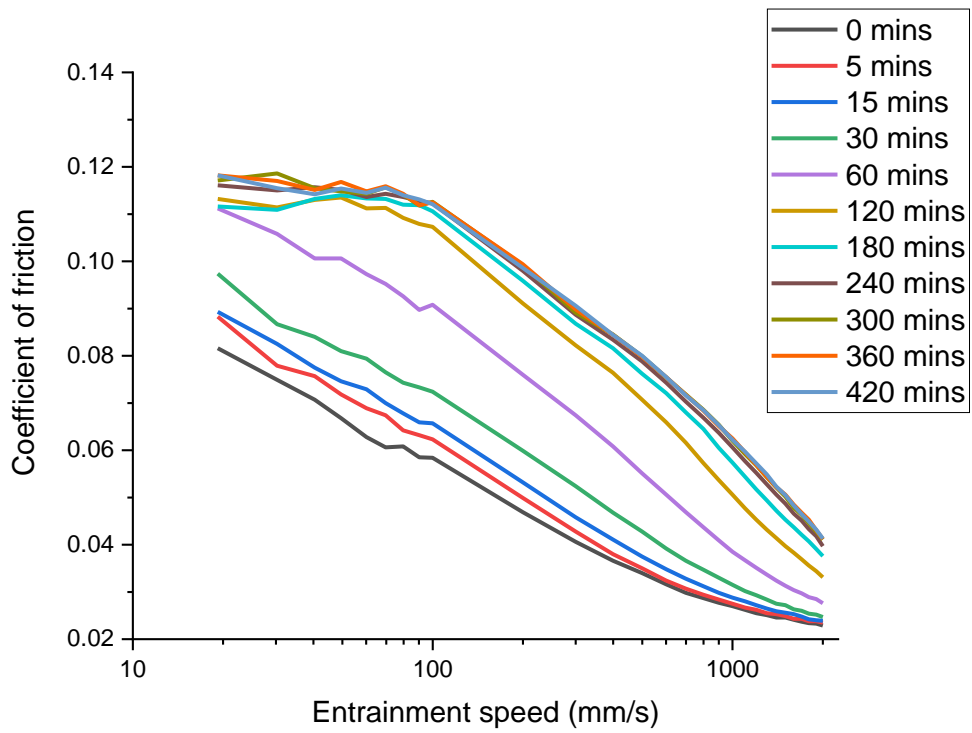


Figure 8-14 All Stribeck curves for the engine aged engine oil.

8.5 Tribofilm Thickness

8.5.1 Oil A

The ZDDP film thickness growth during the test for oil A's samples is shown in Figure 8-15. Fresh oil produces a typical ZDDP tribofilm growth with high amounts of MoDTC [151]. Significant increases are observed up to ≈ 60 minutes of traction, with steady-state film thickness for the remainder of the test duration. Steady-state ZDDP film thickness for the fresh engine oil is $\approx 50-60$ nm.

The artificial ageing process delays the formation of the ZDDP-dominant tribofilm. The artificially aged oil's ZDDP film thickness has a slower growth rate in the beginning stages of the test. However, it steadily increases to a $\approx 60-70$ nm steady-state value, around 10 nm higher than the fresh engine oil's tribofilm. Between 60 and 120 minutes, the friction analysis from Figure 8-9 shows the friction reductions to ≈ 0.04 and a significant spike in ZDDP tribofilm thickness from Figure 8-15.

The film thickness growth for the engine-aged oil is similar to formulated oils with no friction modifier and ZDDP [92,151]. There is a high probability that the tribofilm is created from the anti-wear and detergent additives dominated by ZDDP species. Unlike fresh oils with ZDDP, the tribofilm does not form until 30 minutes of traction. However, a significant spike in film thickness is observed in the initial formation stage, followed by a steady increase, showing characteristics of ZDDP tribofilm formation, as shown in Figure 8-15. The engine ageing process delays the formation of the ZDDP tribofilm, potentially leading to high wear compared to fresh oil. However, the ZDDP tribofilm can fully form after a specific period. The friction, shown in Figure 8-10, for the

engine-aged oil also implied no MoS₂ had formed within the tribofilm matrix due to high friction.

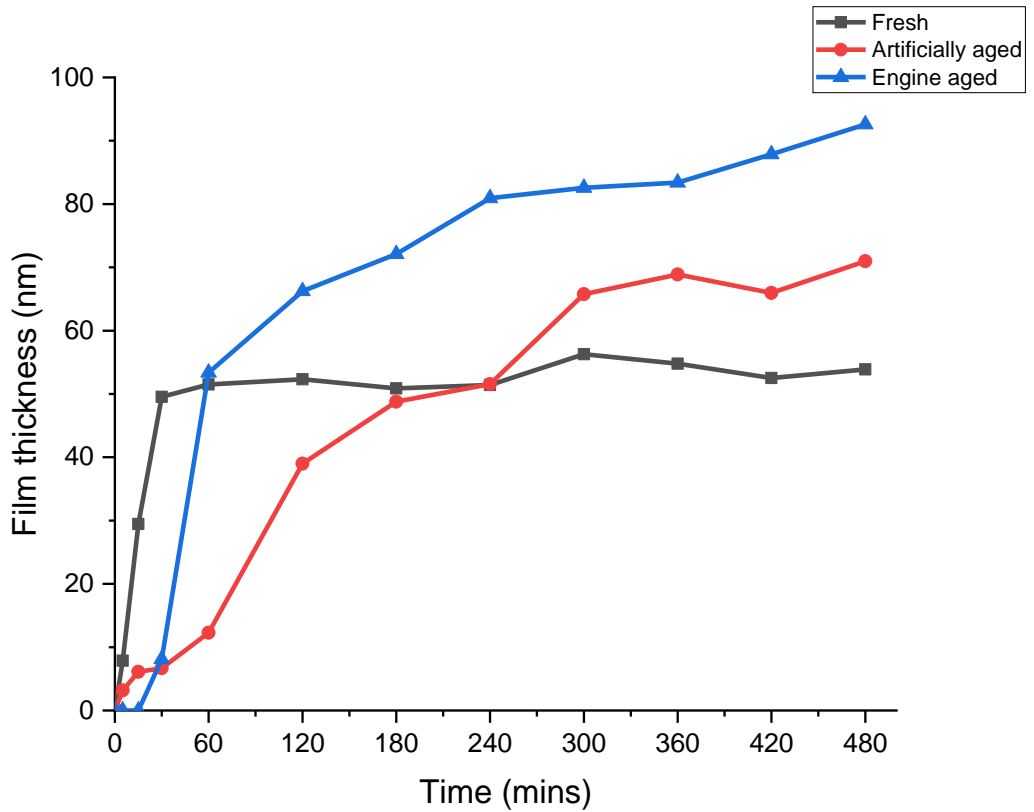


Figure 8-15 Oil A's ZDDP tribofilm thickness.

8.5.2 Oil B

Figure 8-16 shows the ZDDP film thickness measurements for oil B's samples during the friction tests. Again, similar to oil A's fresh engine oils tribofilm, the fresh oil for sample B produces a film thickness curve similar to oils with ZDDP and high amounts of MoDTC [151]. Oil B has a higher steady-state film thickness than oil A due to the lower viscosity creating a harsher contact condition, enabling a thicker ZDDP tribofilm.

The artificial ageing process has removed the oil's ability to form a thick anti-wear and anti-friction tribofilm. During the test, the artificially aged oil's ZDDP

tribofilm thickness differs significantly from the fresh engine oil. Throughout the whole duration, little to no tribofilm is formed. Both oil A and B's artificially aged oils produce significantly different results.

The aged engine oils ZDDP tribofilm has the same curve structure as fully formulated oils with no MoDTC. However, the start of the tribofilm growth is massively delayed. It does not begin until around 60 minutes. Then a massive spike in film thickness is observed, with a steady-state tribofilm thickness of \approx 80-90 nm after \approx 300 minutes of traction. The ZDDP tribofilm formation is delayed, but after the formation, the tribofilms can form relatively high film thicknesses compared to oils with only ZDDP. Once again, the trend observed for oil B's engine-aged oil is similar to oil A's.

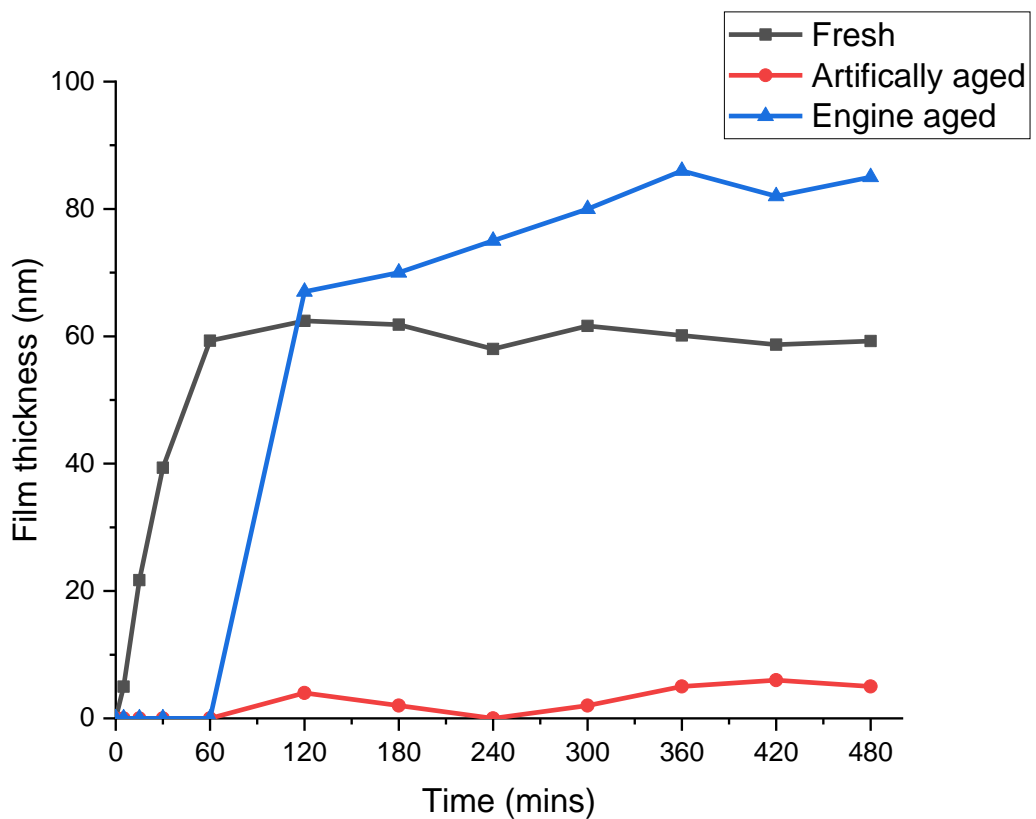


Figure 8-16 Oil B's ZDDP tribofilm thickness.

8.6 MoS₂ Raman Analysis

8.6.1 Oil A

Figure 8-17 shows a typical spectrum from each tribofilm for oil A's fresh, artificially, and engine-aged oils. From the friction results in the previous sections of this chapter, fresh and artificially aged engine oils produced low friction, while the engine-aged oil had high friction [151]. The figure shows that low friction was achieved for the fresh and artificially aged oils due to MoS₂ formation within the tribofilm matrix. No MoS₂ was formed within the engine-aged oils tribofilm, leading to the high friction observed. Again, similar to the previous chapter on optimizing the Mo concentration, Raman detected Fe₂O₃ and S-S stretching peaks for fresh and artificially aged oils.

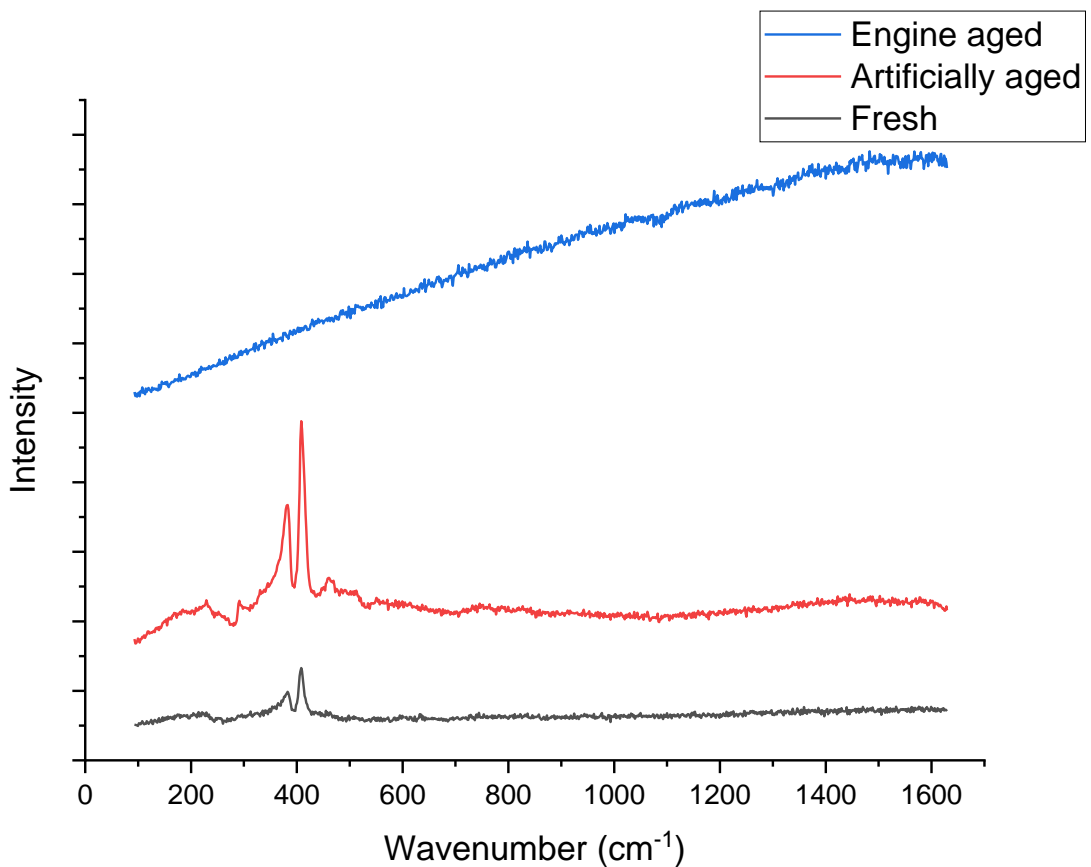


Figure 8-17 Raman spectra comparison for oil A.

Figure 8-18 displays the total intensity counts and steady-state friction within each tribofilms. The counts comprise a 50x50 μm area with a 10 μm step size, and scans are completed after eight hours of traction.

Both fresh and artificially aged tribofilms produce low friction, and different total intensity counts between the end MoS_2 within the tribofilm using Raman spectroscopy from the analysis. However, the tribofilm growth and friction of the fresh and artificially aged have significant differences, as shown in the previous sections. The artificially ageing process has enabled a thicker MoS_2 tribofilm than the fresh and engine ageing processes. As expected, the engine-aged tribofilm had no intensity counts of MoS_2 , explaining the observed high friction.

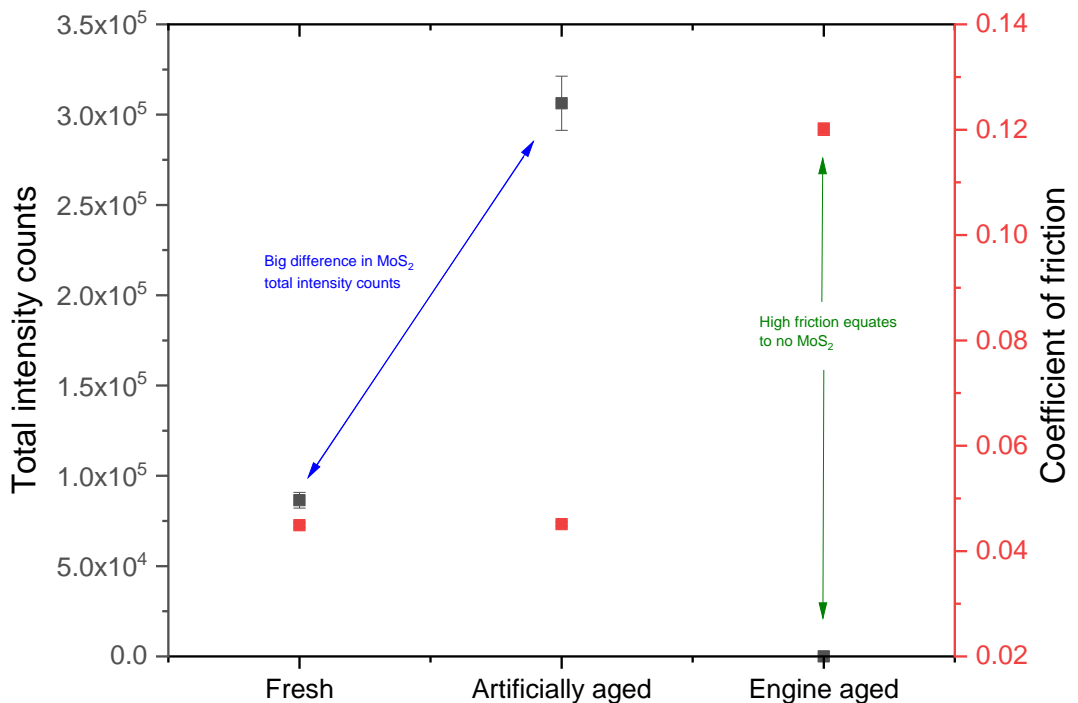


Figure 8-18 Total intensity counts and steady-state friction for oil A

Figure 8-19 displays the ZDDP film thickness and total intensity counts at set intervals during the test to understand how the MoS₂ total intensity counts develop within the artificially aged tribofilm. The previous chapter showed that higher Mo concentrations have a much sharper rise in MoS₂ total intensity counts in the first 60 minutes of traction when the steady-state ZDDP tribofilm thickness is achieved [151]. As the concentration decreases, the total intensity increase in the first 60 minutes is less prominent. In Figure 8-19, the total MoS₂ intensity counts steadily increase throughout the duration of the test. A steady increase in MoS₂ from 60 minutes to 120 minutes is where the decrease in friction begins. After 60 minutes, a sharp increase in ZDDP film thickness suggests rapid growth occurs after the interval. A steady MoS₂ total intensity count within the tribofilm throughout the tests implies that the artificial ageing process has reduced the concentration of MoDTC within the oil. Previous research has shown that ageing processes dramatically decrease the concentration of additives [92]. Moreover, the formation of the ZDDP tribofilm being different from fresh oil is another impacting factor on the formation of MoS₂ within the tribofilm.

Overall, the Raman analysis has shown that both ageing processes significantly impact the formation of MoS₂. The engine ageing process completely removes the ability to form MoS₂, while the artificial ageing process delays the formation of ZDDP but promotes a thicker MoS₂ tribofilm.

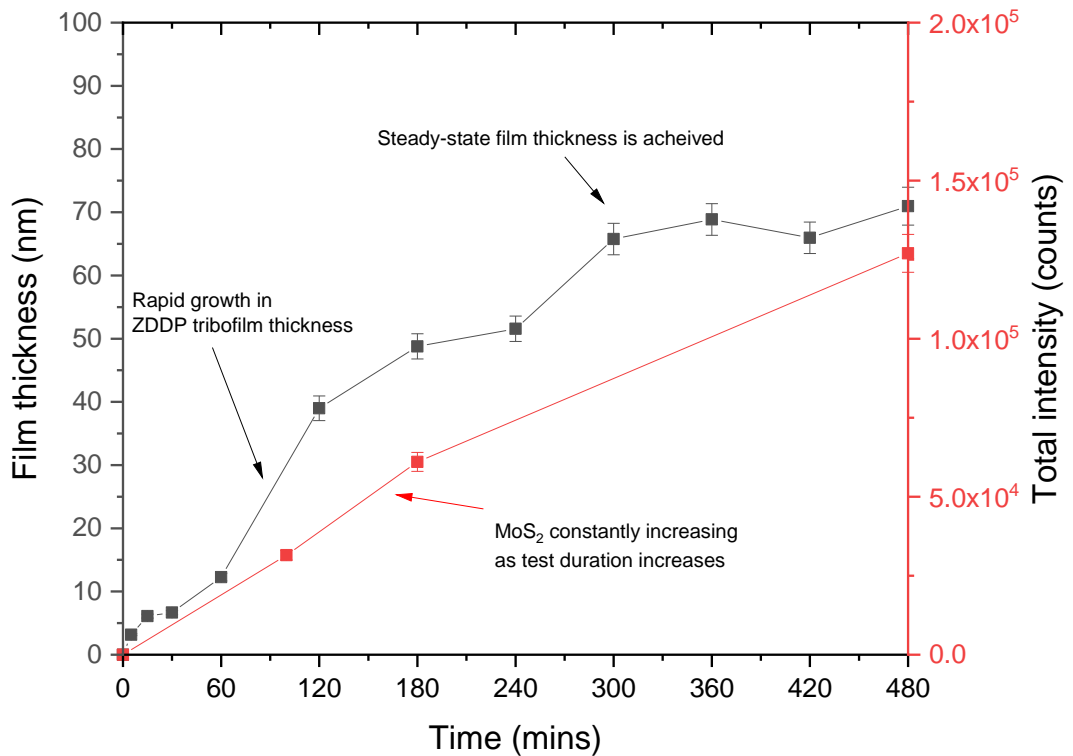


Figure 8-19 Artificially aged oil A's film thickness with MoS₂ intensity counts at set intervals during testing.

8.6.2 Oil B

Figure 8-20 displays the typical spectra of each tribofilm for oil B. Once again, the area scans on the Raman for oil A were kept the same for oil B's tribofilms. The friction analysis for the sample oils in B, from Figure 8-11, implied that only the fresh oils tribofilm would contain MoS₂, with artificial and engine-aged tribofilms having none. Figure 8-11 is in agreement with the friction analysis. Only the fresh oil tribofilm produces a Raman spectrum with peaks associated with MoS₂. Again, the peaks Fe₂O₃ and S-S stretching peaks are also detected. Film thickness analysis showed that the engine-aged tribofilm had a large steady-state thickness at the end of the test, while the artificially aged tribofilm had a minimal value. The increase in intensity observed for the

engine-aged tribofilm compared to the artificially aged tribofilm is due to the different fluorescence of the tribofilm. This suggests that the tribofilm matrices of both ageing processes are different.

The film thickness measurements also showed a high steady-state thickness. The XPS technique, shown in the following sections, was used to analyse both aged tribofilms thoroughly.

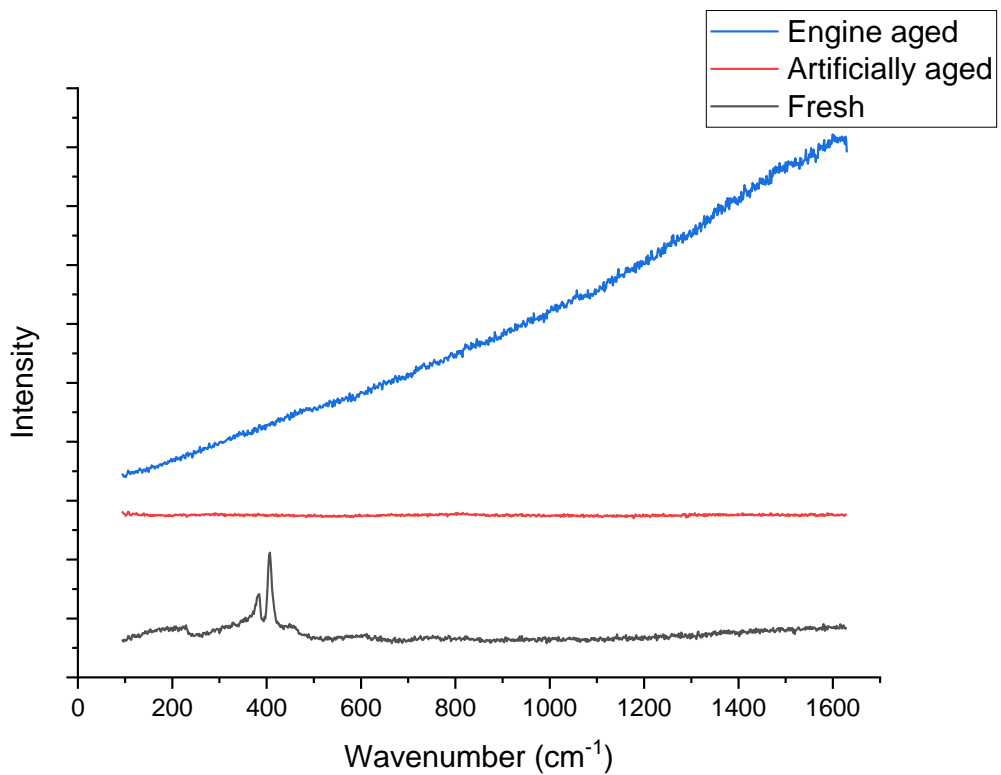


Figure 8-20 Raman spectra comparison for oil B.

Figure 8-21 displays the total intensity counts of MoS₂ within each tribofilm and the steady-state coefficient of friction at the end of the tests. As expected from the friction and single Raman spectra analysis, both ageing processes which produce high friction values have no MoS₂ intensity within the tribofilms. However, the fresh oil tribofilm has a total intensity of around 1×10^5 , similar to oil A's fresh tribofilm but ultimately a higher value. Both oil, A and B, have

similar Mo concentrations but have different viscosities. Oil B has a lower viscosity, leading to harsher contact with the same operating conditions. Again, previous research has shown viscosity to have little impact on MoS₂ formation when that is the only differing factor [132,151].

Overall, from the Raman analysis, it is clear that both ageing processes have removed the oil's ability to produce MoS₂ and increased friction significantly.

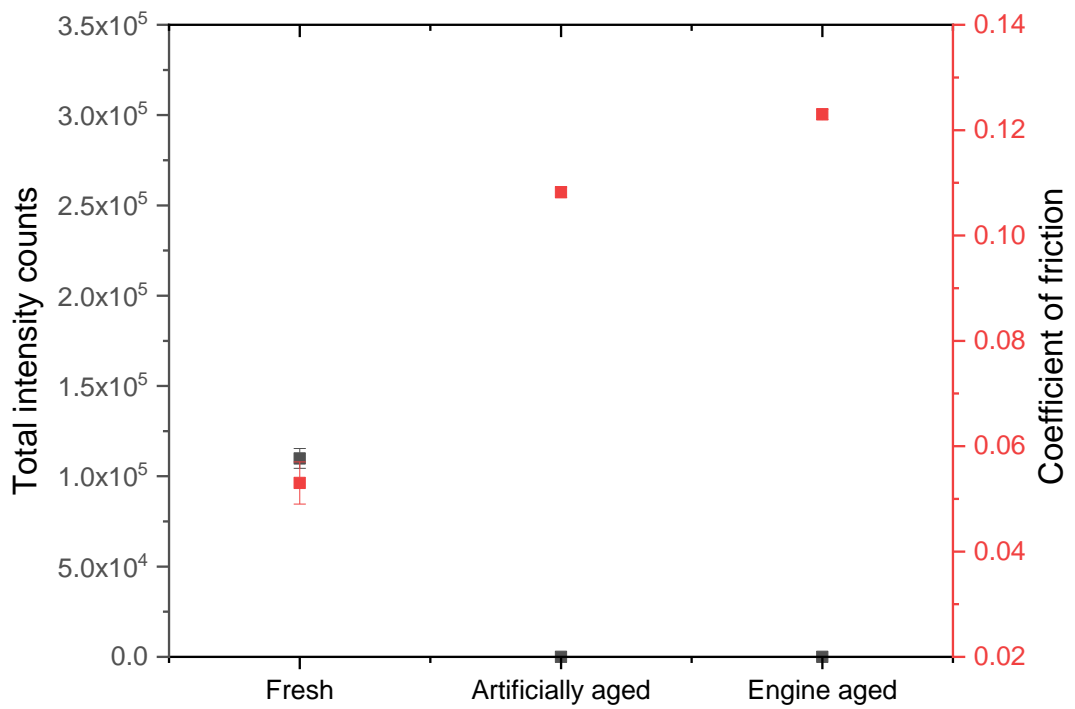


Figure 8-21 Total intensity counts and steady-state friction for oil B.

8.7 XPS Tribofilm Analysis

8.7.1 Oil A

8.7.1.1 Elemental Analysis

The tribofilms for the fresh, artificially aged, and aged engine oils were etched for four times of 30 seconds, with the total etching time equalling 120 seconds. Figure 8-22 shows the weight percentages of the chemical elements at every etching interval associated with the tribofilm generated from the boundary additives.

Both ageing processes affect the element weight percentages within the tribofilm when using the fresh engine oil tribofilm as a reference.

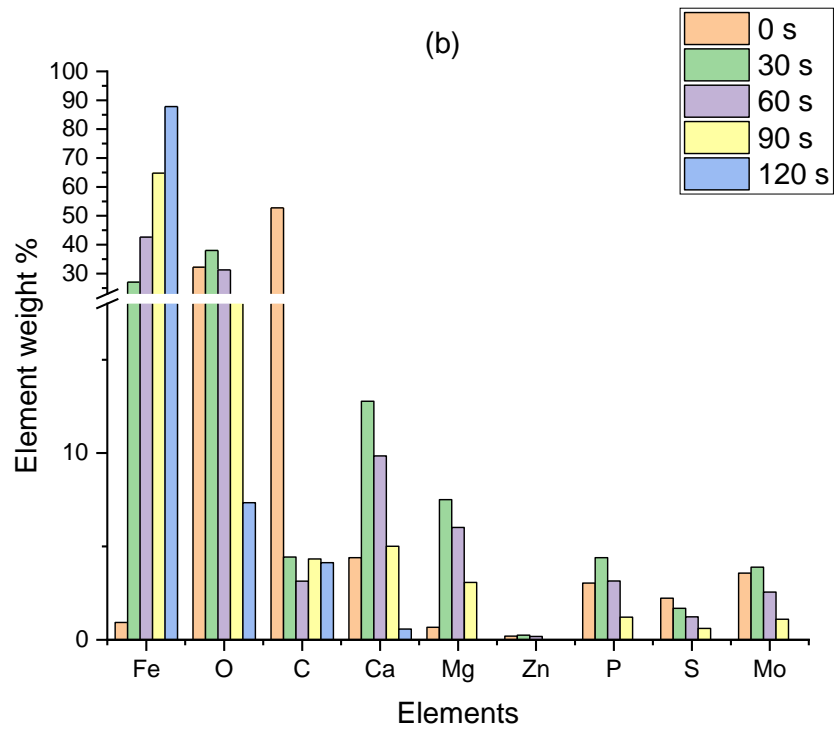
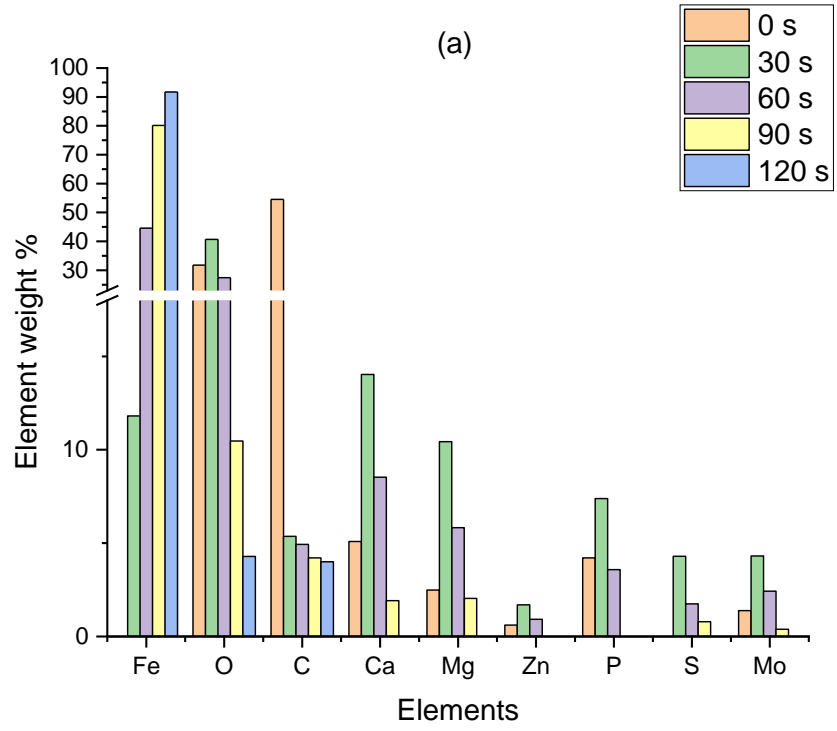
The XPS element analysis shown in Figure 8-22 has multiple noticeable differences between the artificially aged tribofilm and the fresh tribofilm. The engine aged tribofilm is thicker than both other tribofilms as less Fe, and more elements such as Ca are detected at 90 and 120 s etching times. All high-resolution scans become unreadable at 120 seconds of etching time except for Fe and only Ca for the artificially aged tribofilm. A thicker tribofilm from the XPS analysis agrees with the SLIM analysis. Significantly less Zn can be found within the layers of the artificially aged tribofilm with more Mo. Higher amounts of Ca, Mg and O, are also detected for the artificially aged tribofilm at higher etching times than the fresh. The results suggest that the artificially aged tribofilm could have higher wear due to the smaller amounts of anti-wear elements detected towards the surface of the MTM ball.

As shown in Figure 8-22, there are many more noticeable differences between the fresh and engine-aged tribofilm than fresh and artificially-aged tribofilms. The engine-aged tribofilm has significantly less Mo and S in the layers than

the fresh tribofilm due to no MoS₂ detected within the aged engine tribofilm using Raman. Significant increases in Zn and P are detected within the layers of the engine-aged tribofilm, with overall larger amounts of Ca, Mg and O. The increased amount of these elements implies a thicker anti-wear tribofilm has formed, which could lead to decreased wear.

At higher etching times, 90 and 120 seconds, the engine-aged tribofilm has significantly less Fe and more elements detected across the whole range apart from Mo and S. The results imply the engine-aged tribofilm is thicker than the fresh, once again in agreement with the SLIM analysis.

From the XPS elemental analysis within the layers of the tribofilms, the engine ageing process prevents Mo and S formation within the tribofilm. At the same time, depletion of MoDTC from the engine ageing process allows more ZDDP formation within the tribofilm. In comparison, the artificial ageing process prevents Zn and P. The reduction in Zn and P could be due to the formation of MoS₂ observed from friction and Raman analysis producing competitive absorption.



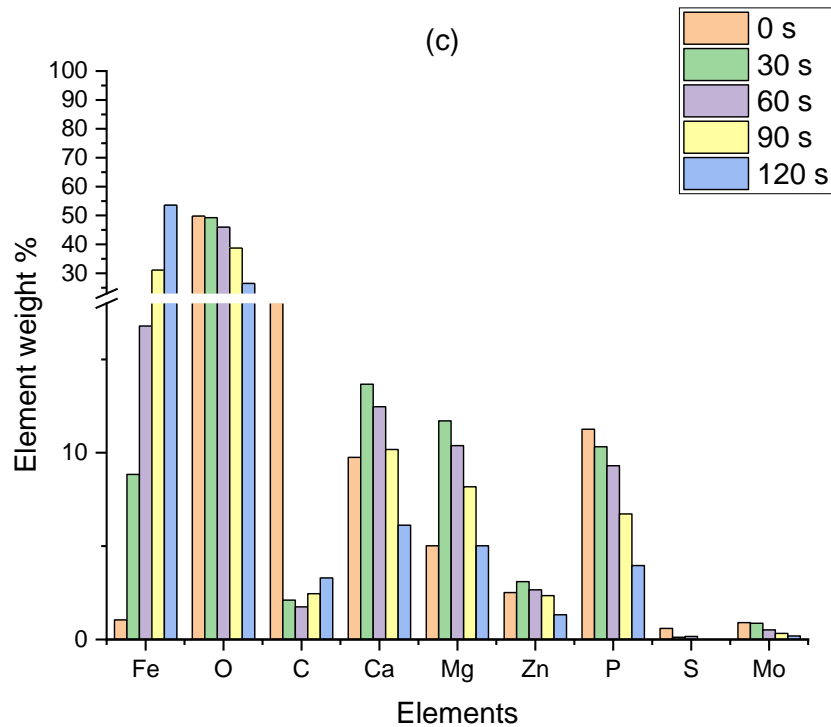


Figure 8-22 XPS element weight %s after each etching time for oil A (a) fresh, (b) artificially aged and (c) engine aged tribofilms.

8.7.1.2 HR scans

Deconvolution of XPS high-resolution scans is required to determine certain compounds formed and further understand how the ageing processes change the tribofilm chemistry. XPS elemental analysis shown in the previous section does not suffice on its own for this study.

8.7.1.2.1 Mo 3d

Figure 8-23 displays the deconvoluted Mo 3d signals for all three tribofilms at 0 and 120 s etching times. It must be noted that the peaks detected above 240 eV are associated with Argon implanted from the sputtering process [152].

At 0 s etching time, the fresh engine oil produces a signal with peaks characteristic of a friction-reducing tribofilm [151]. Additionally, Mo (V) is detected in a minimal area percentage. Indicating that the amorphous structure MoS_xO_y could be present within the top layer of the tribofilm. However, the difference would be minimal if Mo (V) was removed from the deconvolution process. No peaks are detected after 120 s etching time associated with Mo or S.

Part (b) of Figure 8-23 shows the artificially aged Mo 3d deconvoluted signal. Similar to the fresh oil at 0 s etching time, the peaks detected are the same. The same peaks detected at 0s etching time were expected since the tribofilm produced low friction at the end of the test. The difference between the fresh and artificially aged Mo 3d signals is the area percentages of the peaks, with fresh producing a Mo (IV): Mo (VI) ratio of 55.18: 22.28 and the artificially aged producing a 45.66: 38.28 ratio. These ratios imply that the artificially aged tribofilms top layers have less MoS_2 with more Mo oxides. After 120 s etching time, Mo (V) and Mo (VI) peaks are detected within the signal for the artificially aged tribofilm. Therefore, the artificially aged tribofilm is thicker than the fresh oil. SLIM film thickness analysis also shows the artificially aged tribofilm to be thicker than the fresh. After 120 s etching time, the layers are very close to the metal substrate due to the high Fe content from elemental analysis and no peaks detected in the fresh tribofilm. The artificially aged tribofilm shows that the layers very close to the metal substrate contain minimal amounts of MoS_2 and the amorphous structure MoS_xO_y . In the early stages of tribofilm formation, MoDTC or another

compound containing Mo, produced from ageing, can still decompose to form MoS₂.

The engine-aged tribofilm showed no friction reduction during the friction tests. Film thickness measurements also determined that a thick ZDDP dominant tribofilm had formed. Part (c.) of Figure 8-23 displays the Mo 3d signal for the engine-aged tribofilms layers at 0 and 120 s etching time. It must be noted that before engine ageing, the fresh oil had 800 ppm of Mo in the form of MoDTC. After ageing, the MoDTC would have been depleted. However, Mo will still be present within the oil but in the form of a different compound due to oxygen-sulfur substitution [63]. The peaks detected at 0 s etching time for the engine-aged tribofilm are S 2s and Mo (V) and (VI). These peaks imply metal sulfides, Mo oxides, and the amorphous structure MoS_xO_y has formed within tribofilm but with no MoS₂. After 120 s etching time, the same peaks are detected but in tiny quantities compared to 0 s. Even though the friction-reducing capabilities of the oil are lost after engine ageing, the new compounds formed with Mo can decompose into Mo oxides and MoS_xO_y.

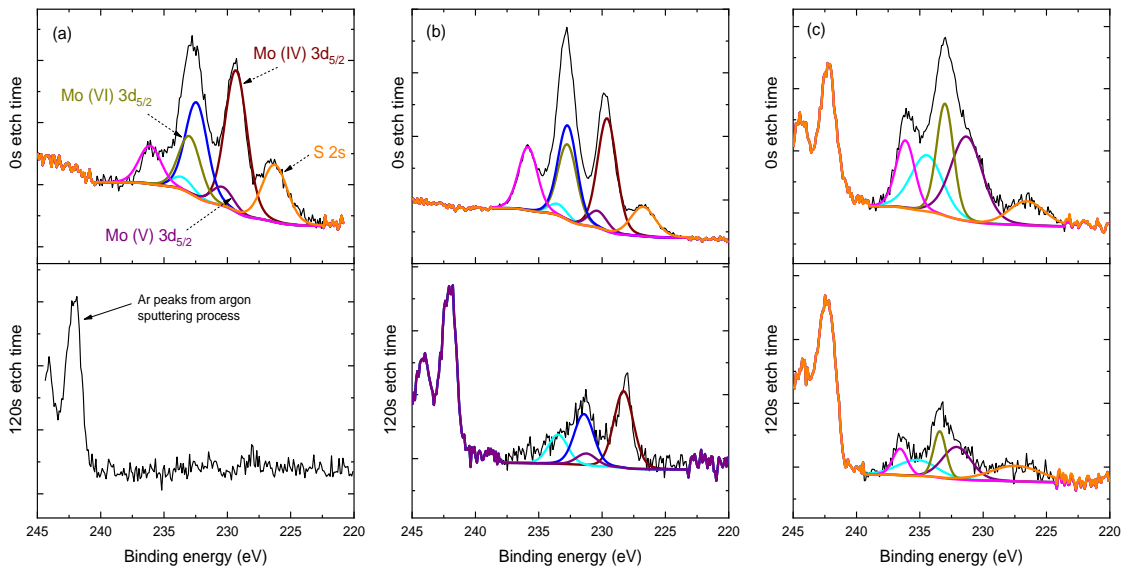


Figure 8-23 Mo 3d signals for oil A's (a) fresh, (b) artificially aged and (c) engine aged tribofilms.

8.7.1.2.2 P 2p, Zn 2p and O 1s

P 2p, Zn 2p, and O 1s signals produce peaks associated with the ZDDP decomposition products within the tribofilm. Specifically, as previous research shows, polyphosphate chain lengths can be determined using O 1s and P 2p peaks [59].

Figure 8-24 displays the P 2p deconvoluted signals for all three tribofilms. Part (a), the fresh tribofilm, produces two peaks associated with the spin orbitals P 2p_{3/2} and 2p_{1/2} and Zn 3s at 0s etching time. The spin-orbital peak(s) at ≈ 133eV is associated with phosphates, while the Zn 3s peak at ≈ 140 eV is linked to ZnS or ZnO [123]. No peaks are detected once the tribofilm is etched for 120 seconds, indicating the tribofilm has been removed.

Part (b) for the artificially aged tribofilm shows very different results than the fresh. At 0 s etching time, only the spin-orbital P 2p_{3/2} and 2p_{1/2} are detected

with no Zn 3s. Usually, the difference in binding energy between P 2p and Zn 3s is used to determine the phosphate chain lengths along with BO/NBO ratio. No Zn 3s being detected implies the phosphate chain lengths are small. The BO/NBO ratios from the O 1s signal will be used to understand the phenomenon further. Again, similar to the fresh tribofilm, no peaks are detected after 120 s etching time.

Part (c) at 0 s etching time, for the engine-aged tribofilm, shows the same peaks as the fresh tribofilm. The difference between the two signals is the difference in binding energy between the P 2p and Zn 3s peaks. The same peaks are detected after 120 s etching time, unlike the fresh and artificially aged tribofilms. The detected peaks at 120 s etching time indicate that the engine-aged tribofilm is thicker than the other tribofilms. The SLIM analysis also agrees that the aged engine tribofilm is thicker than the fresh and artificially aged tribofilms.

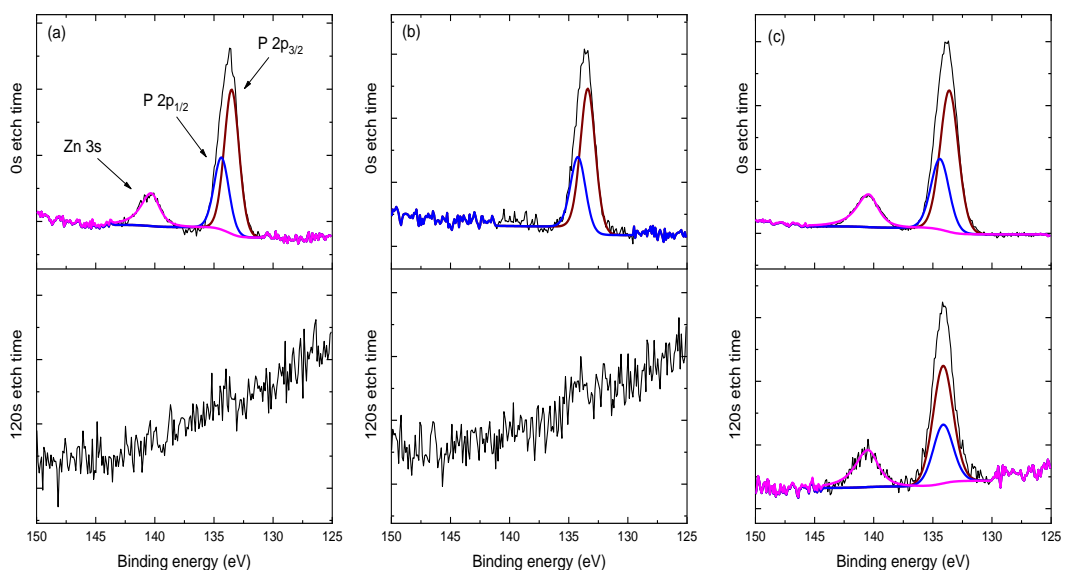


Figure 8-24 P 2p signals for oil A's tribofilms.

Figure 8-25 displays the Zn 2p signals for all three tribofilms from oil A. All three tribofilms at 0 s etching time produce the same spin-orbital peaks, Zn 2p_{3/2} and 2p_{1/2}. These peaks are associated with ZnS and ZnO bonding [121]. The artificially aged tribofilms signal is noticeably weaker than fresh and engine-aged, implying less quantity of the compounds in the top layer. After 120 s etching time, both fresh and artificially aged tribofilm produce no peaks. The engine-aged tribofilm produces the same peaks but with a weaker signal.

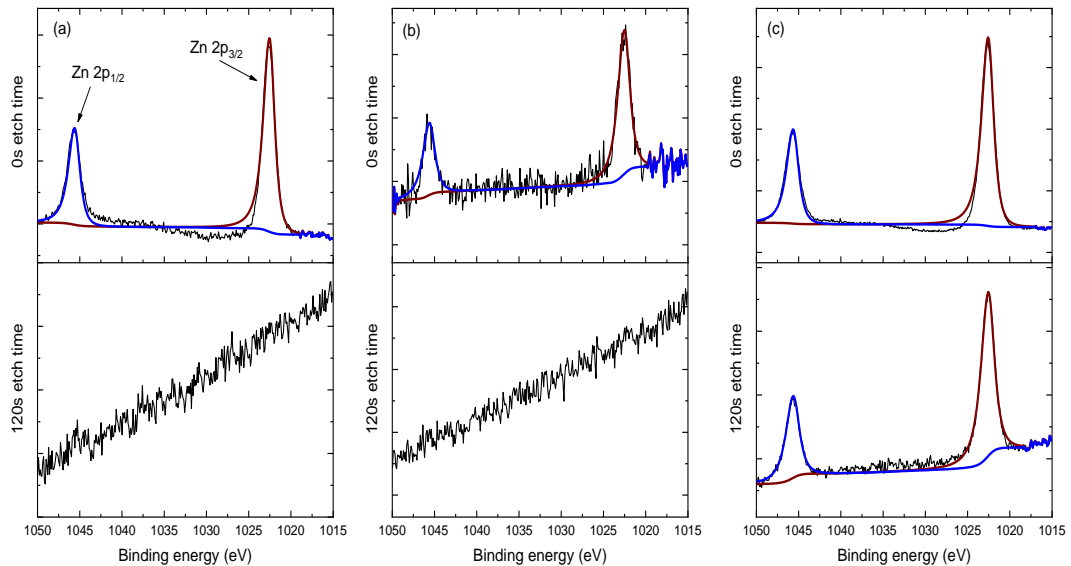


Figure 8-25 Zn 2p signals for oil A's tribofilms.

Table 8-4 shows the BO/NBO ratios from the O 1s signal at 0 s etching time and the binding energy difference between the P 2p and Zn 3s peaks from the P 2p signal. From previous literature, the higher the BO/NBO ratio and Δ binding energy between Zn 3s and P 2p., the longer the zinc polyphosphate chain lengths [59]. It is clear from the data that the engine-aged tribofilm has the longest polyphosphate chain lengths with a value corresponding to pyrophosphates. In comparison, the fresh has shorter chain lengths

corresponding to orthophosphate, and finally, the artificially aged tribofilm has significantly short or no polyphosphates.

Table 8-4 BO/NBO ratio and Δ binding energy between Zn 3s and P 2p for oil A.

	BO/NBO	Δ Zn 3s and P 2p
Fresh	0.113	6.81
Artificially aged	0.022	0
Engine-aged	0.197	6.83

All the data from the high-resolution scans and elemental analysis associated with ZDDP indicate that the artificially aged oil has significantly fewer ZDDP species in polyphosphates, ZnS, and ZnO than the fresh oil and engine-aged. The data implies that the artificially aged oil would produce more wear than the fresh and engine-aged oils.

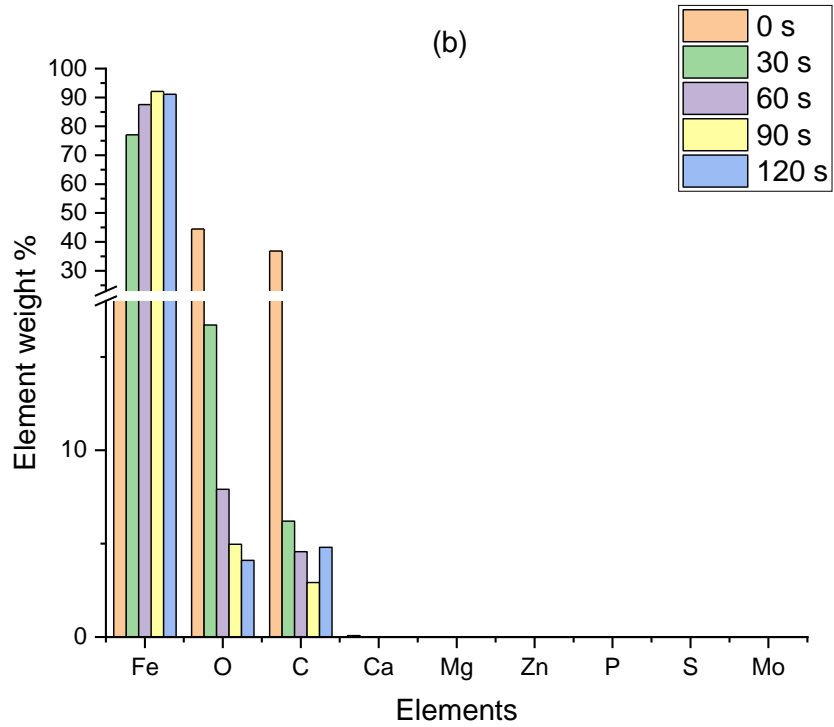
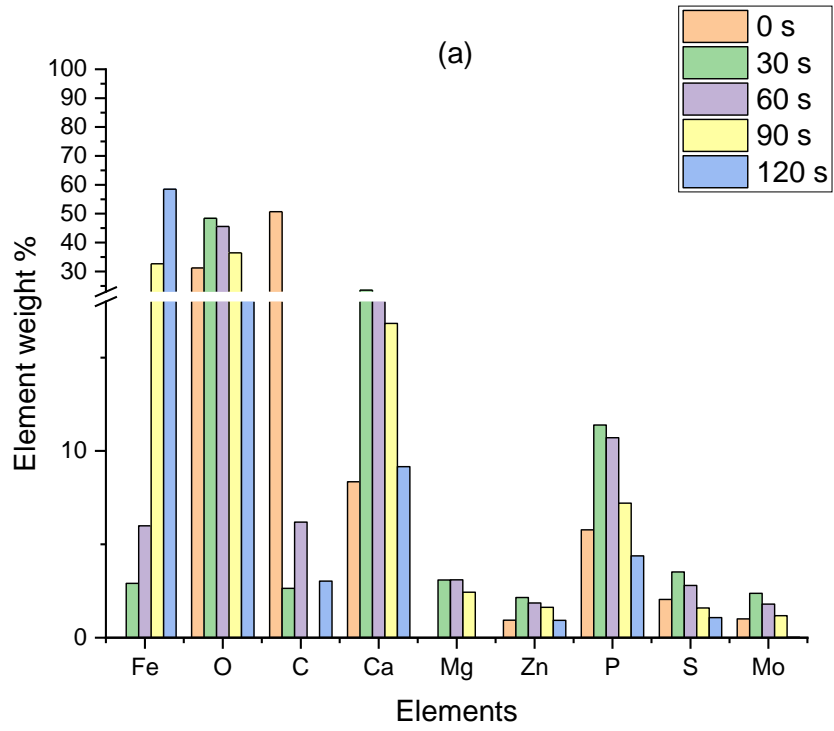
8.7.2 Oil B

Figure 8-26 shows the element weight percentages for each etching time interval for all three tribofilms. The artificial ageing process prevents any tribofilm from forming on the rubbing surfaces, which would lead to large amounts of wear compared to the fresh oil. The friction, tribofilm thickness and Raman analysis determined that the artificially aged oil produces a minimum to zero tribofilm. XPS element analysis shown in Figure 8-26 also produces the same results. No elements associated with boundary active additives are detected throughout all etching intervals. Etching times after 30 seconds also

produce very high amounts of Fe, with the only other two elements detected being C and O.

The engine-aged tribofilm produces significantly higher amounts of Zn, P and Mg within the tribofilm layers. In comparison, the fresh tribofilm contains more Mo, S and Ca. Comparing the element weight percentages within the tribofilm suggests a thicker ZDDP tribofilm has formed from the engine-aged oil. The SLIM analysis agrees with the engine-aged oil producing a thicker ZDDP tribofilm than the fresh oil. Both tribofilms have similar amounts of Fe after 120 seconds of etching, suggesting similar overall tribofilm thicknesses.

The artificial ageing process depends on oil formulation as the impact on oil A and B is different, but the ageing technique is the same. A similar trend is observed for oil B and A concerning the engine-aged oils, even though they are different formulations and are engine-aged using different techniques. The engine ageing process depletes the MoDTC additive, which allows the less depleted ZDDP to form a thick tribofilm. ZDDP's anti-oxidation properties prevent its function from being completed removed [152].



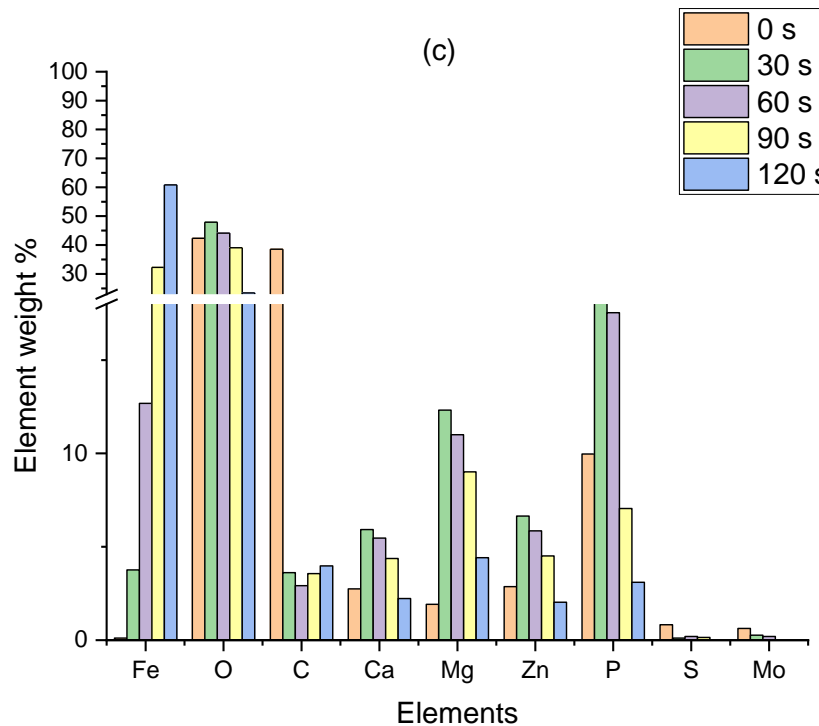


Figure 8-26 XPS element weight %s after each etching time for oil B (a) fresh, (b) artificially aged and (c) engine aged tribofilms.

8.7.2.1 HR Scans

8.7.2.1.1 Mo 3d

Figure 8-27 displays the deconvoluted Mo 3d signals for oil B's tribofilms. The fresh tribofilm, part (a) of the figure, has the same peaks as the fresh tribofilm for oil A. Again, the signal and peaks are typical of a tribofilm, reducing the steady-state friction to ≈ 0.04 [78,151]. Once the tribofilm is etched for 120 seconds, little to no peaks are detected within the signal, indicating the Mo compounds have been removed and are only present in the top layers. The peaks observed at higher binding energy after 120 s etching time are associated with argon from the sputtering process.

All previous results for the artificially aged oil suggest that little to no tribofilm has been formed. The Mo 3d signal, part (b) of the figure, agrees with the previous results. At 0 s etching time, a very weak signal is formed. A peak has been detected potentially associated with Mo (V) or (VI). However, the signal is too weak to analyse.

The engine-aged tribofilm, part (c) of the figure, shows the same peaks as the engine-aged tribofilm for oil A. Mo (V) and (VI). MoS₂ cannot form in both cases, but Mo oxides and the amorphous MoO_xS_y structure can. The different engine ageing processes must be depleting the MoDTC additive so that the new formed compound's decomposition does not allow MoS₂ to form. After 120 s etching time, no peaks are detected associated with Mo bonding, implying they are found within the higher layers of the tribofilm.

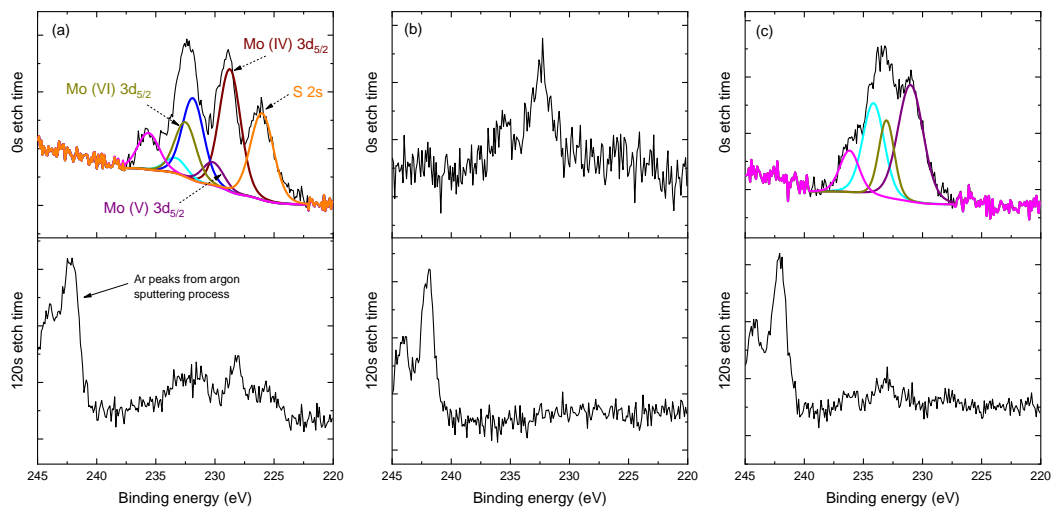


Figure 8-27 Mo 3d signals for oil B's tribofilms.

8.7.2.1.2 P 2p, Zn 2p and O 1s

Figure 8-28 displays the deconvoluted peaks for the P 2p signal for oil B's tribofilms. At 0 s etching time, the fresh tribofilm produces the same peaks as oil A's fresh tribofilm. Bonding is associated with phosphates, ZnS and ZnO. After 120 s etching time, the same peaks are detected. However, the signal is weaker since the layer is close to the metal substrate. The Δ binding energy between Zn 3s and P 2p decreases as etching time increases, implying shorter phosphate chain lengths are closer to the substrate. In line with previous research [59,60].

The artificially aged tribofilm, part (b), again for both 0 and 120 s etch times, has weak signals with no peaks. Adding to the results and data showing little to no tribofilm has formed.

The engine-aged tribofilm, again similar to the fresh tribofilm, has the same peaks detected at 0 and 120 s etching time. The same trend is observed for the engine and fresh tribofilms, where an increase in etching time decreases the Δ binding energy between Zn 3s and P 2p. A higher area percentage and a stronger signal for 120 s etching time engine tribofilm than the fresh indicates a thicker ZDDP tribofilm.

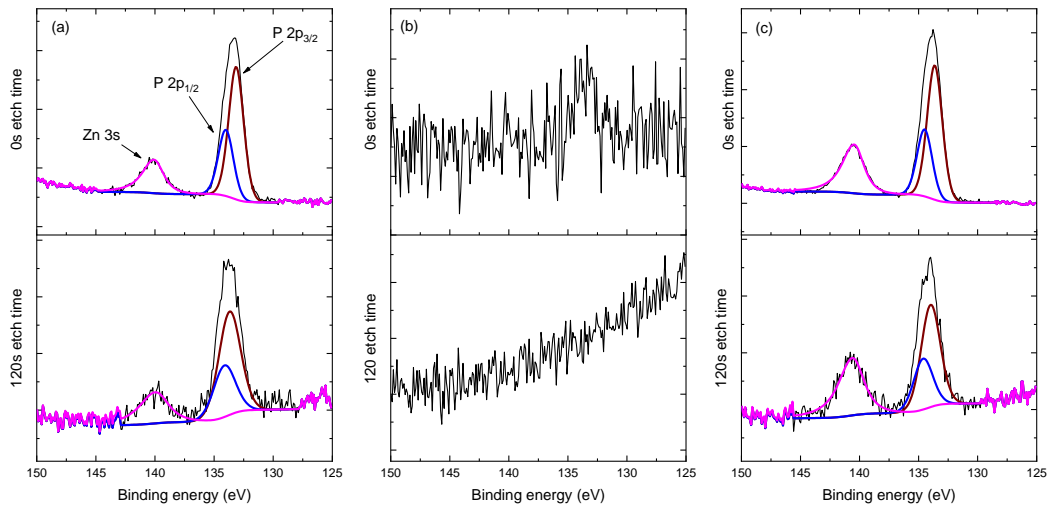


Figure 8-28 P 2p signals for oil B's tribofilms.

Figure 8-29 displays the Zn 2p signals for all oil B tribofilms at 0 and 120 s etching time. The fresh tribofilm produces peaks associated with ZnO and ZnS at 0 and 120 s etching times. After 120 s etching time, a weaker signal implies a lower quantity of Zn bonding, and the layer is close to the substrate.

The artificially aged tribofilm produces weak signals for both etching times.

The engine-aged tribofilm produces the same peaks as the fresh tribofilm at 0 and 120 s etching times. However, after 120 s etching time, a stronger signal is observed for the engine-aged tribofilm than the fresh. In agreement with the SLIM analysis, the XPS data shows a thicker tribofilm for the engine-aged oil than the fresh.

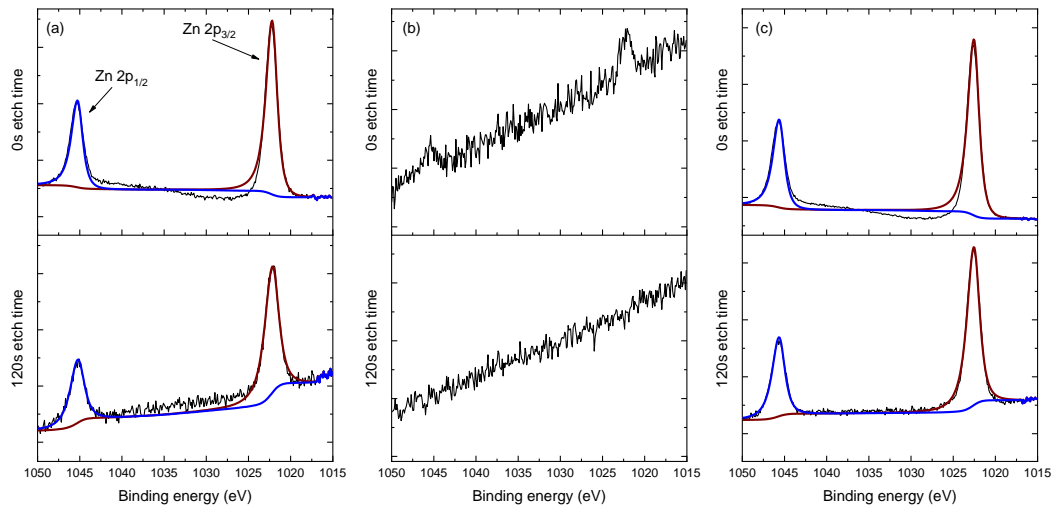


Figure 8-29 Zn 2p signals for oil B's tribofilms.

Table 8-5 shows the BO/NBO ratios from the O 1s signal at 0 s etching time and the binding energy difference between the P 2p and Zn 3s peaks from the P 2p signal. The top layers of both fresh and engine-aged tribofilms contain similar polyphosphate chain lengths called pyrophosphate. The difference between the tribofilms is the overall thickness, determined from SLIM and XPS analysis. The engine-aged ZDDP tribofilm is thicker than the fresh engine oil, which should produce minor wear. As expected, the artificially aged tribofilm does not show any signs of containing polyphosphates.

Table 8-5 BO/NBO ratio and Δ binding energy between Zn 3s and P 2p for oil B.

	BO/NBO	Δ Zn 3s and P 2p
Fresh	0.20	6.95
Artificially aged	0	0
Engine-aged	0.25	6.83

All data and analysis from the high resolutions' scans associated with the ZDDP tribofilms show that the artificial ageing process destroys the ability of the oil to form a thick ZDDP tribofilm. Weak signals for high-resolution scans and polyphosphate chain length analysis are the determining factors.

The engine ageing process has minimal impact on the ZDDP tribofilm formation. The same peaks from the Zn 2p and P 2p high-resolution scans are formed as the fresh tribofilm, including similar polyphosphate chain lengths.

8.8 Wear Analysis

Figure 8-30 displays an example of the wear scar after EDTA solutions are applied to the wear scar when using the NPFlex. It is clear from the NPFlex image that a high percentage of the tribofilm has been removed, leaving the wear scar to be analysed.

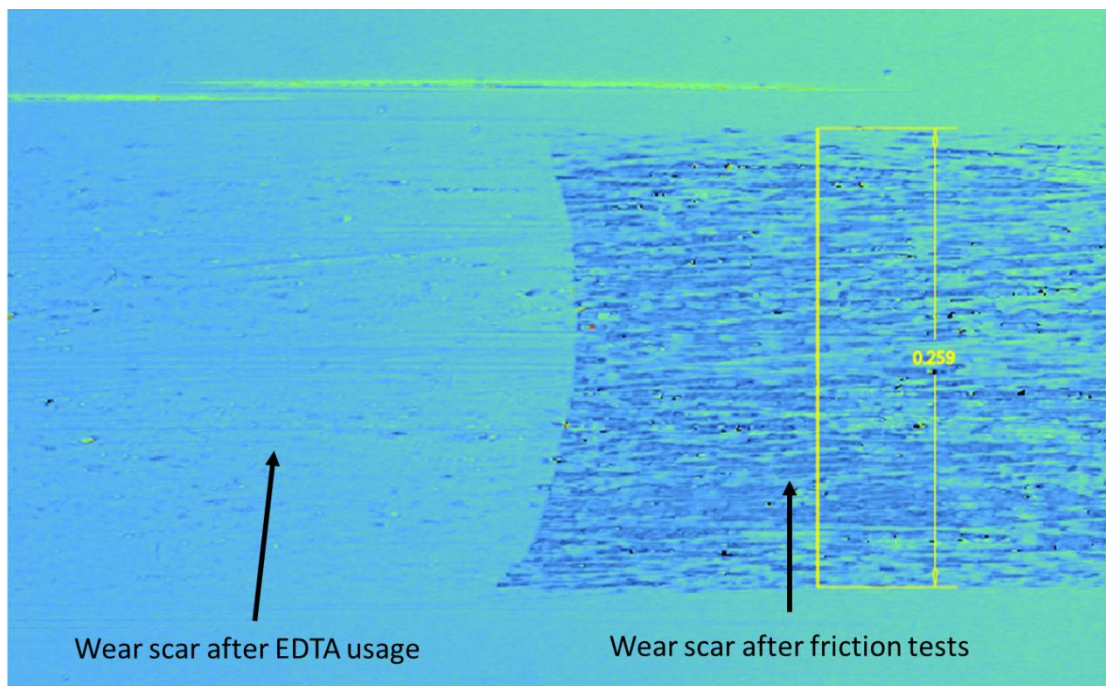


Figure 8-30 Example NPFlex image of EDTA solution removal.

8.8.1 Oil A

Figure 8-31 shows the wear volume loss and wear scar width for oil A's samples. An area of $0.4 \times 0.4 \mu\text{m}$ was taken from each wear scar for analysis. Three areas were taken on each wear scar. The averages of the wear volume losses and the average wear scar widths are shown in the figure. Both fresh and engine-aged oils produce similar wear, with the artificially aged oil displaying higher wear. The higher wear observed for the artificially aged oil can be attributed to a reduction in ZDDP species within the tribofilm

from XPS analysis. The artificially aged oil has a similar wear scar width to the fresh oil, with the engine-aged oil having the largest wear scar width. It must be noted that the wear generated for all three samples is minimal, and the difference between them in an actual world application is negligible. Both ageing processes do not significantly impact the wear generated. The impact on the wear from the ageing process can change when using different formulations, and viscosities are shown in research [95].

Oil A has a high HTHS value of 2.73 with an oil grade of 0W-20. After ageing, the dynamic viscosity at high temperatures does not significantly change. Therefore, the lambda ratio of the contact is similar for all three oils. Under both ageing conditions, the anti-wear additive could still perform its function of keeping wear to a minimum. However, the friction modifier's ability to reduce friction after engine ageing only was removed. The depletion of additives and chemical changes in the oil is the main factor influencing the tribological properties. The harsher operating conditions and additional contaminants inside the engine compared to the artificially ageing process can highly impact the oil's chemical composition. More oil analysis would be required to fully understand the impact engine ageing has on the additive concentration.

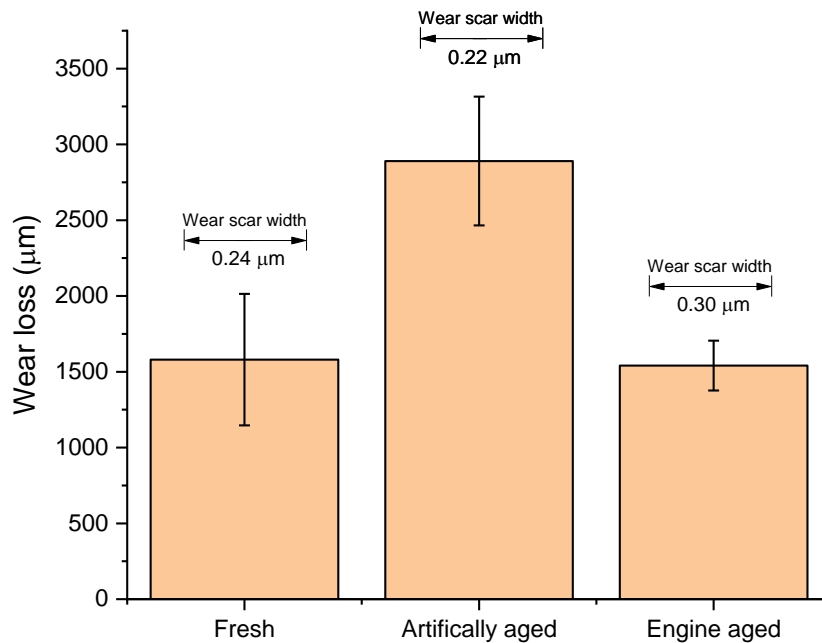


Figure 8-31 Wear loss of 0.4x0.4 µm area with wear scar widths for oil A.

8.8.2 Oil B

Figure 8-32 displays the wear volume loss and wear scar. The process used for oil A was repeated for oil B.

The figure shows that the engine-aged oil produces less wear than the fresh oil, while the artificially aged oil has significantly higher wear. The engine-aged oil produces minor wear due to increased ZDDP species within the tribofilm from XPS analysis compared to the fresh tribofilm.

The artificially aged oil has noticeably much larger wear and over double the wear scar width of the other sample oils. The high wear resulting from the artificially aged oil was expected as friction, and film thickness measurements initially implied that little to no tribofilm had been formed.

XPS analysis also showed that little to no tribofilm had formed.

High wear is expected when no tribofilm has been formed in harsh boundary conditions. Previous research has shown that the wear does not significantly change from the new state after artificially ageing a fully formulated 5W-30 engine oil using the same method [99]. The oil used had a much higher viscosity and different formulations. Additionally, no oxygen was supplied to the oil during the ageing process, which could have sped up the degradation process in the study undertaken in this thesis.

The wear analysis clearly shows that the artificially ageing process has a detrimental effect on the wear generated from friction testing. Oil B's HTHS value is 1.75, with a very low oil viscosity grade of 0W-8. After the ageing processes, the artificially aged oil's viscosity at a high temperature significantly drops while the engine-aged oil's viscosity does not significantly change. Therefore, the artificially aged oils lambda ratio was significantly lower than both fresh and engine-aged due to the considerable reduction in viscosity at high temperatures. Coupled with the depletion of additives due to the ageing process, the impact on the wear is noticeable. Interestingly, the engine ageing process had little to no impact on the wear generated. However, the friction was heavily affected.

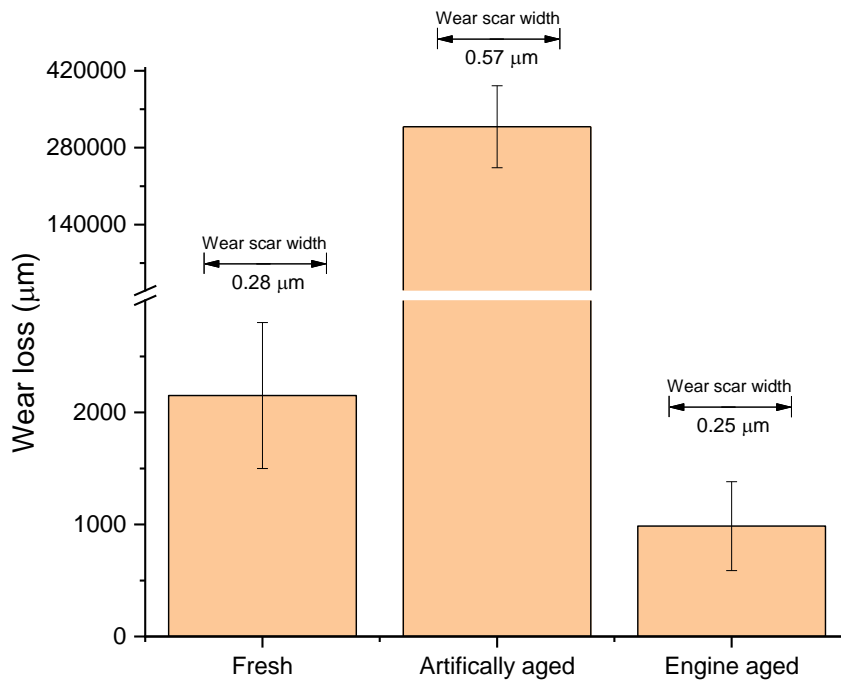


Figure 8-32 Wear loss of 0.4x0.4 µm area with wear scar widths for oil B.

8.9 Summary

The chapter has investigated the different effects of artificially and engine ageing on two different oils with two different engine ageing processes. Oil A is a 0W-20 engine oil with an HTHS value of 2.73, while oil B is a 0W-8 engine oil with an HTHS value of 1.75. Both oils have similar concentrations of the Mo, S, Zn, P and Ca elements associated with the active boundary additives. The findings from this study are as follows.

- At higher temperatures, the artificial ageing process had little impact on the higher viscosity oil, while a significant reduction in viscosity was observed for the low viscosity oil.
- The engine ageing process removed both oils' ability to reduce friction to ≈ 0.04 . The anti-wear additives were still able to form with a slow initial growth rate.
- The artificial ageing process completely removed oil B's ability to reduce friction. However, it only delayed oil A's for roughly 60 minutes before reduction occurred. Both contain similar Mo concentrations.
- Both aged engine oils were able to form a thick ZDDP tribofilm compared to both artificially aged oils.
- Both engine ageing processes produced better wear performance than the artificially ageing process.
- Regardless of the engine ageing process, the effects on the oils were very similar. In contrast, the same artificially ageing process used for both oils had significantly different effects.

Chapter 9 Discussion

The current chapter will present the overall discussion created from the studies in this thesis. It is split into the following key points, shown in Figure 9-1.

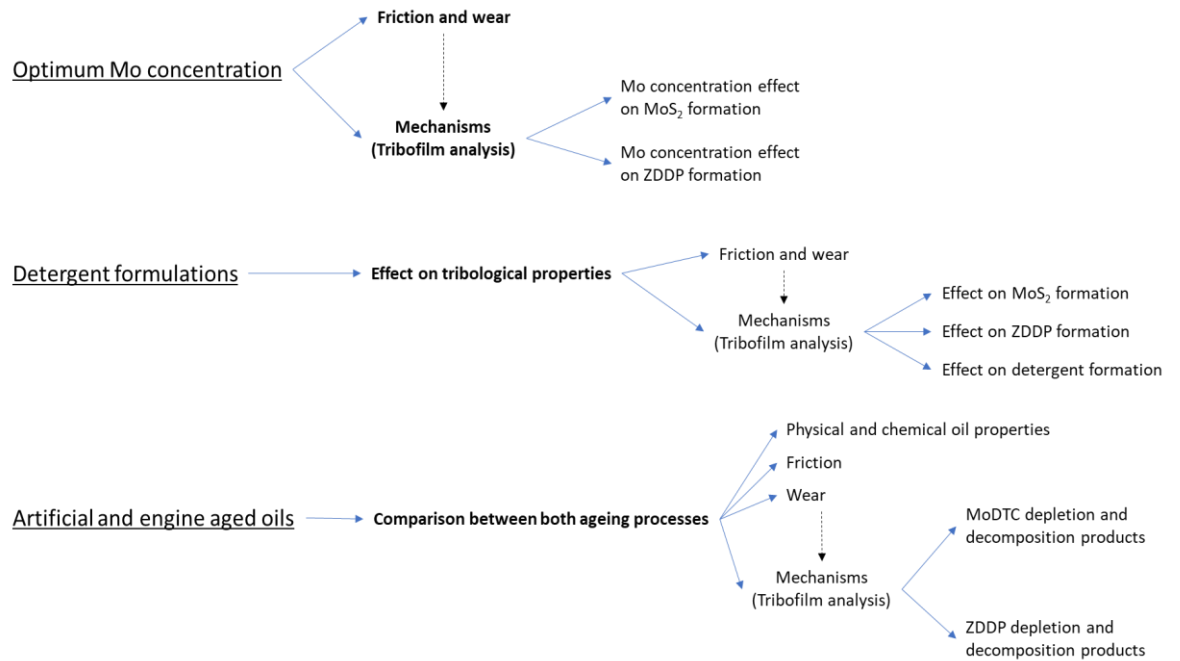


Figure 9-1 Schematic of the key points within the discussion.

9.1 Optimum Mo Concentration

9.1.1 Criteria

The results shown in Chapter 6 determined that the optimised Mo concentration is within the range of 180 to 350 ppm, with a higher probability of it being at the top end of the range. The value is similar to research conducted using a binary system of base oil and MoDTC with a similar kinematic viscosity at 100 °C, where ≈ 180 ppm was determined as the critical concentration [66]. However, only friction under a constant lambda ratio was considered. Additionally, friction under a varying lambda ratio must be

considered to mimic the conditions in the real-world application of the ICE. Adding other additives within the oil increases the critical concentration compared to the binary system due to competitive surface adsorption between the additives as shown in Figure 6-3 and Figure 6-4. However, MoDTCs decomposition nature and friction mechanism will always form the core components of its tribofilm first. Another major factor that must be considered is viscosity's impact on the Mo concentrations' optimum range. Previous research has shown that low Mo concentrations are affected by increased oil viscosity at low lambda ratios and in comparison, increased oil viscosity has minimal impact on higher Mo concentration oils [132].

Therefore, the criteria behind the decision from the study in this thesis were based on the following;

- Steady-state friction values under a constant lambda ratio
- Friction values under a varying lambda ratio
- Wear values

9.1.2 Friction and Wear

Research has determined that different MoDTC concentrations significantly influence friction performance [77]. However, extensive research has not been completed on a significant quantity and range of Mo concentrations to understand the friction results' mechanisms and the critical or optimum concentration.

As shown in Figure 9-2, the 350 ppm Mo concentrations' friction values under a constant and varying lambda ratio do not significantly differ from their higher concentration counterparts. A general trend is observed for both constant and varying lambda ratios. When increasing the Mo concentration, the friction

decreases to a maximum value. Further Mo concentration increases do not significantly change the friction. An explanation for the Mo concentrations \geq 180 ppm producing a \approx 0.04 friction value during rubbing is attributed to the formation and removal rate of MoS₂, which Mo concentration significantly influences. The rate of formation and removal has been covered in previous research when the friction reduction mechanism of MoS₂ was investigated [75]. The mechanism of friction reduction coupled with the Mo concentration research conducted in this thesis will be discussed in detail in the later sections of this chapter.

Figure 9-3 displays the selected Mo concentrations' steady-state friction and wear coefficients. The sample oil with 0 ppm of Mo produces the lowest wear, with the 350 and 1000 ppm sample oils producing similar increased wear values. The research conducted in the study; Chapter 6 determines that adding MoDTC into a fully formulated oil increases the wear generated. A research study that agrees with the statement determined that wear generated using 250 ppm of Mo 0 W-20 engine oil increased the wear generated by 48% compared to the same oil with no MoDTC [124]. The cause of an increase in wear could be related to competitive surface adsorption and prevention of AW ZDDP full formation. Others also report similar findings, where adding MoDTC into a fully formulated 15 W-30 engine oil increases the wear generated under high loads [76].

It must be noted that MoDTC does possess anti-wear properties when in a binary system with a base oil [71,77]. It produces FeS₂, which is a protective layer. However, when added to a fully formulated oil with ZDDP, MoS₂ and other decomposition products of MoDTC compete with the anti-wear additive

to form on the surface of the substrate. Therefore, the effectiveness of the anti-wear additive is reduced.

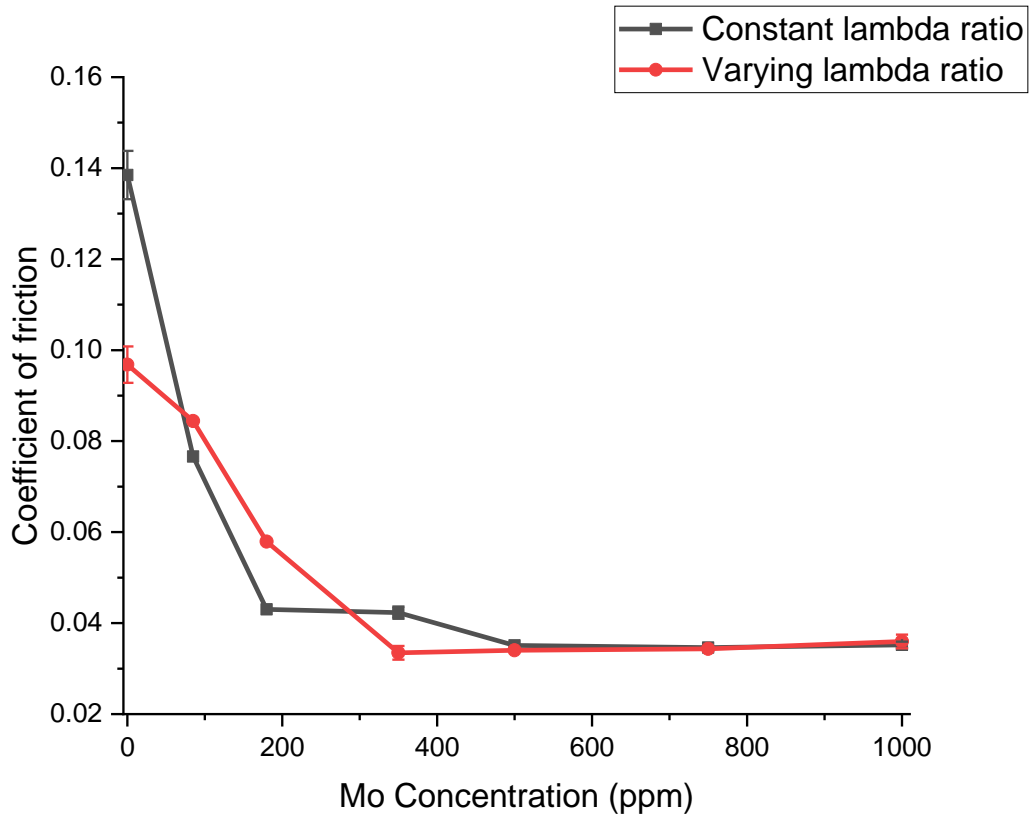


Figure 9-2 Average friction values for a constant and varying lambda ratio at different Mo concentrations.

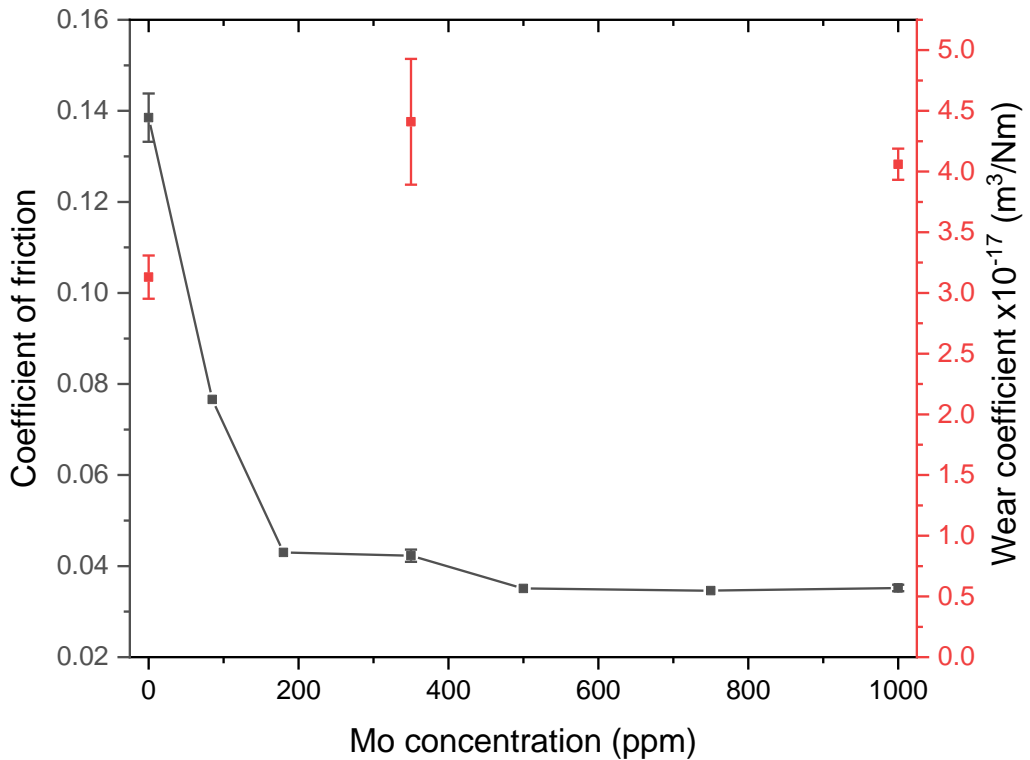


Figure 9-3 Steady-state friction and wear coefficients for selected Mo concentrations.

9.2 Mo Concentration effect on the initial MoS₂ Formation

The effect Mo concentration has on the initial MoS₂ formation is discussed in this section. The initial MoS₂ formation is within the initial stages of rubbing when no tribofilm has been formed. It must be noted that the oil viscosity will affect the initial MoS₂ formation but not the fundamentals behind it [77,132]. However, it is highly dependent on Mo concentration. If the oil viscosity is high, the lower Mo concentrations will have a lesser effect due to the increase in lambda ratio at the contact point. However, higher oil viscosity will not affect higher Mo concentrations. The effect of oil viscosity on Mo concentration on the initial MoS₂ formation is shown in Figure 9-4. A higher oil viscosity could

increase the critical Mo concentration if all operating conditions are kept constant.

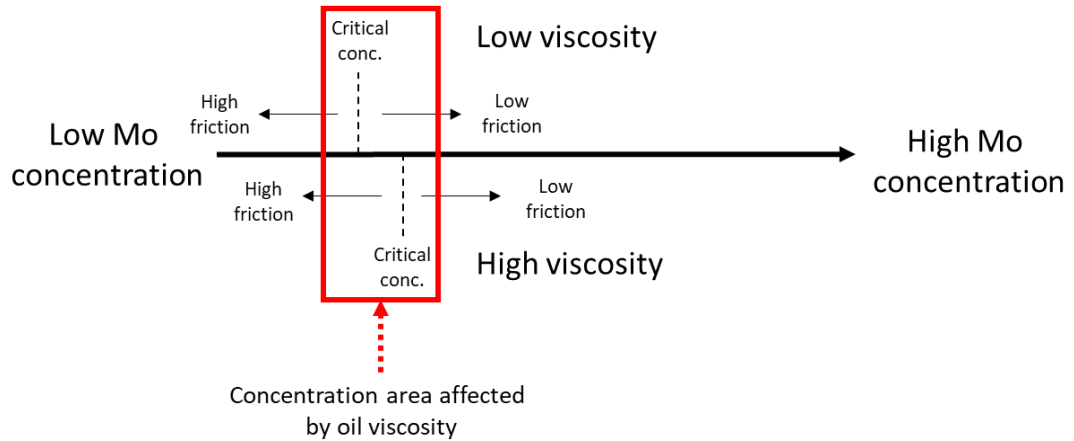


Figure 9-4 Oil viscosity influence on Mo concentration's ability to reduce friction within the tribofilm.

As shown in the figure above, the impacted area of the Mo concentration from differing oil viscosity is small. The mechanisms and theories for how Mo concentration affects the tribological performance can be created under a general overview. Different oil viscosity does not change the mechanisms' fundamental principles. For example, if the oil viscosity was increased by a large amount, the lubrication regime would move to a less metal-on-metal contact, directly reducing the additives' ability to form a tribofilm, since MoS_2 and friction reduction require asperity contact. For decreasing oil viscosity, it is more complicated. From Chapter 6, it was determined that past a threshold concentration, the friction does not significantly decrease. If all conditions and concentrations were kept the same with the oil viscosity decreased, the critical concentration required to reduce the friction to ≈ 0.04 decreases in value.

9.2.1 Induction Time

Chapter 6 determined that increasing the Mo concentration decreased the induction time to reach ≈ 0.04 . Previous research is in agreement with the statement [77,132]. Figure 9-5 shows schematically the dependence of low friction induction time as a function of MoDTC concentration in the oil using previous research and the research in this study.

Increasing the Mo concentration decreases the friction induction time. When Mo concentrations are equal to the critical concentration ($= 180 - 350$ ppm), increases in the Mo concentration will significantly impact the friction induction time. Once the Mo concentration is significantly higher than the critical concentration (≥ 500 ppm), further increases in Mo concentration will only produce small decreases in the friction induction time. Increasing the Mo concentration at extremely high (≥ 1000 ppm) will produce minimal decreases in induction time or no change.

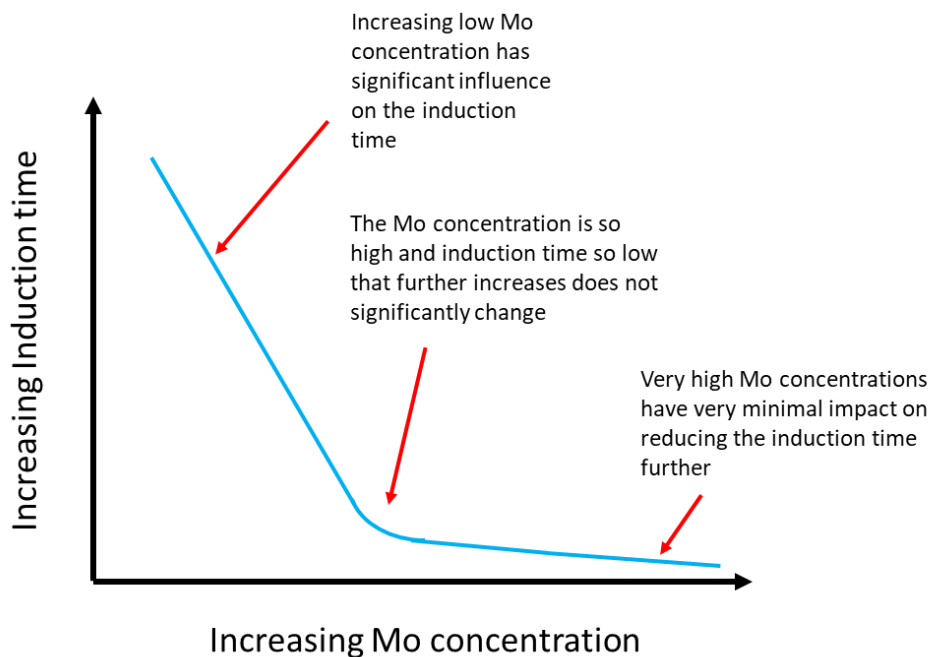


Figure 9-5 Dependence of low friction induction time as a function of MoDTC concentration in the oil.

9.2.2 Early-stage MoS₂ Formation

To understand the effect Mo concentration has on the initial MoS₂ formation, which leads to a reduction in induction time, the tribochemistry of early tribofilm formation needs to be investigated.

Previous research investigating the friction reduction mechanism of MoDTC when incorporated into a PAO and ZDDP oil determined that the MoS₂ coverage must reach a “saturated value” to reduce the friction to ≈ 0.04 [75]. To reach the “saturated value”, a balance between MoS₂ formation and removal must be achieved in the “saturated region.” *In-situ* Raman was used to understand the MoS₂ formation as rubbing time increased. In the initial stages of tribofilm formation, the MoS₂ formation is at its largest vs the removal rate. The MoS₂ layers become thicker in the MoDTC/ZDDP tribofilm matrix as the rubbing continues due to the rate of formation being greater than removal. Once the friction reaches the typical value of ≈ 0.04 or the steady-state value, the MoS₂ formation becomes equal to the removal rate. At that point in the test, the MoS₂ should have extensive coverage and thick layers within the tribofilm matrix.

In Chapter 6, to understand how the Mo concentration can affect early-stage MoS₂ formation, oil samples containing 350 and 1000 ppm of Mo were subjected to MTM testing and Raman analysis at set intervals. Figure 9-6 shows both concentrations' total intensity counts of MoS₂ within the tribofilms. At 5 minutes into the friction test, the higher Mo concentration oil forms a film with a higher total intensity count of MoS₂ compared to the 350 ppm Mo oil, implying thicker layers and/or more crystalline MoS₂ has formed. As test duration increases, the total counts for the 1000 ppm Mo oil significantly increase compared to the 350 ppm Mo oils tribofilm. As the ZDDP tribofilm

forms, the MoS₂ layers become embedded within the tribofilm matrix. When the concentration of Mo is higher in the oil, the MoS₂ layers are thicker, and thus a higher intensity count is detected as the ZDDP thickness becomes much more significant.

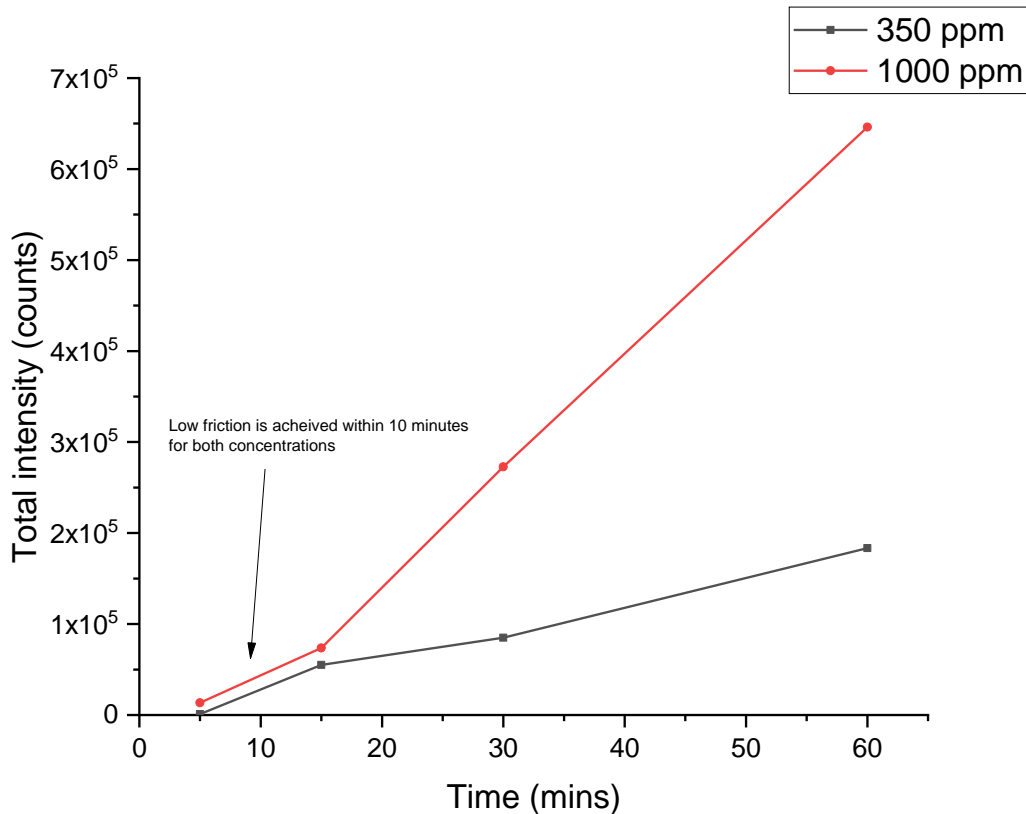


Figure 9-6 Total intensity counts of MoS₂ at set intervals for 350 and 1000 ppm of Mo oils.

9.2.2.1 Other Surface-Active Additives

Along with Mo concentrations effect on MoS₂ formation, the impact of other surface-active additives and their concentrations on the formation is also significant to understand.

Previous research investigating ZDDP concentrations' effect on MoDTC performance showed that the concentration could be optimised to enhance

the formation of MoS₂ [153]. A lower ZDDP ppm value using the same MoDTC ppm generally produced lower steady-state friction and wear. However, a higher ZDDP ppm value decreased the friction induction time.

The research conducted in Chapter 7 and past research papers have shown that detergent formulation impacts MoS₂ formation [138]. MoDTC coupled with higher-based detergents generally leads to lower steady-state friction.

9.2.3 Mo concentration and friction reduction time mechanism

Understanding how increasing the Mo concentration forms a thicker MoS₂ in the initial stages of tribofilm formation and how MoDTC reduces friction in general needs to be explained. From extensive previous research, MoDTC decomposes via shear stress by rupturing the bonds during rubbing. It first adsorbs onto the rubbing surfaces and then decomposes due to shear stress, causing the C-S bond to rupture, leaving the amorphous MoS_x structure. The MoS_x structure is converted to MoS₂ due to increased temperature and shear stress at the tribo-contact [65].

The mechanism for increasing Mo concentration and forming a thicker MoS₂ in the initial stages of tribofilm formation is shown in Figure 9-7. More MoDTC molecules can adsorb on the rubbing surfaces at higher Mo concentrations, creating a higher supply zone. Once rubbing of the surfaces occurs, more MoDTC is broken down into MoS_x, which leads to a higher probability of MoS₂ forming from increased shear stress and temperature at the tribo-contact. The increased amount of MoS₂ forming on the rubbing surfaces from a higher Mo concentration leads to faster MoS₂ formation and thicker MoS₂ in the initial stages of rubbing. The induction time to reach a low friction value depends on temperature and contact pressure [66,72]. Lower temperature and contact pressure would increase the induction time due to the partial decomposition

of MoDTC. However, it can be determined that a higher Mo concentration supplies the rubbing surfaces with more MoDTC enabling thicker MoS₂ layers in the initial stages, leading to a decrease in induction time. However, adsorption of MoDTC onto the surfaces is not enough, the decomposition is needed for low friction, which occurs from contact conditions.

Other lubricant additives influence the formation of MoS₂, as determined in the thesis with different detergent formulations, in Chapter 7. Specifically, Figure 7-2, determined that with the same Mo concentration, changing the detergent formulation can influence the induction time and final steady-state friction. However, compared to the Mo concentration results from Figure 6-6, the impact is minimal. The chemical components formed in the tribofilms from the differing detergents formulations in the oils are the same with different concentrations, Figure 7-7 and Figure 7-8. Regardless of the detergent formulation, the same decomposition products from MoDTC are found.

Previous research has not extensively tested a wide range of Mo concentrations compared to this study. The wide range of Mo concentration tested can be used to strengthen the proposed mechanism of increased Mo concentration, forming a thicker MoS₂ tribofilm in the initial stages of rubbing, leading to faster friction reduction. Research has shown that general additive adsorption increases with increased concentration [154]. Additionally, the decomposition reaction rate is determined by the concentration [65]. These findings support the mechanism produced by the study.

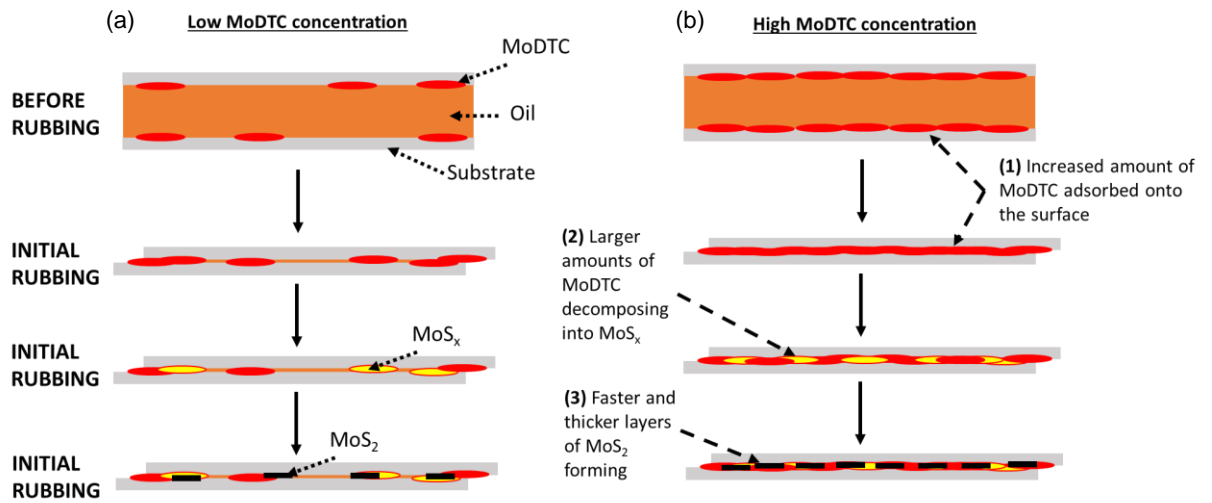


Figure 9-7 Mechanism for increasing Mo concentration which leads to a decrease in friction reduction induction time, (a) low MoDTC concentration and (b) high MoDTC concentration.

9.3 Mo Concentrations effect on the ZDDP Thickness

Chapter 6 determined the effect that MoDTC and its concentration has on the ZDDP tribofilm thickness. The results suggest that adding MoDTC, equal to or greater than the critical concentration, significantly reduces the ZDDP thickness. Once the Mo concentration is increased in the oil, the ZDDP tribofilm thickness does not significantly differ from a much lower MoDTC concentration which produces low friction results.

When ZDDP is the only surface active additive in oil, the tribofilm formed consists of three layers: sulphide/oxide, polyphosphate chains and alkylphosphate precipitates [56,58,59]. The polyphosphate chain lengths are shorter toward the metal substrate. Typically, a fully formed ZDDP tribofilm can be in the range of 80-120 nm. However, once MoDTC is added to oil with ZDDP, the chemistry of the tribofilm changes to incorporate the MoDTC

decomposition products, as previous research and research conducted in this thesis have shown [71,73,151,155].

Figure 9-8 displays the SLIM measurements of the ZDDP film thicknesses from the oils tested in this project. The steady-state ZDDP film thickness is reached after 60 minutes for all oils, but the thicknesses are significantly less compared to the oil with no MoDTC. The addition of MoDTC in a concentration which reduces the friction to low values clearly reduces the overall ZDDP tribofilm thickness. The act of reducing the ZDDP tribofilm thicknesses increases the wear generated as shown in Figure 6-19, however, it can be taken as a very small difference and negligible in the real-world application.

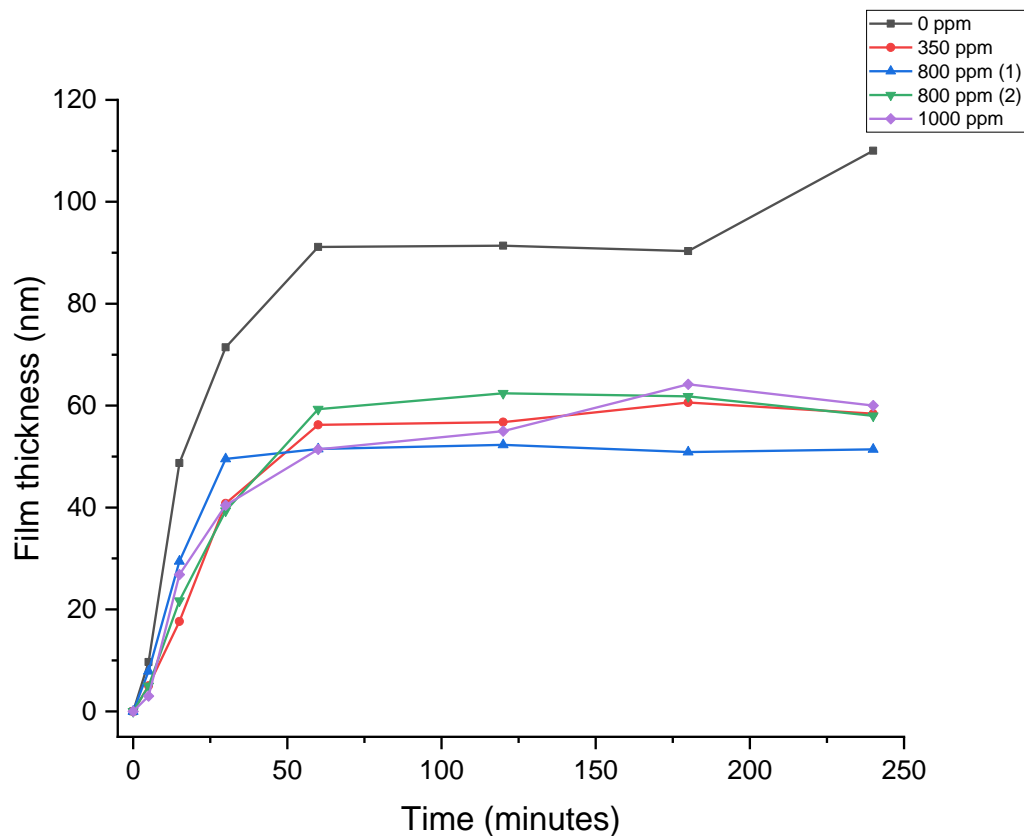


Figure 9-8 ZDDP film thickness vs time for multiple different Mo concentrations using SLIM.

9.3.1 Tribofilm chemistry

The chemical changes which occur to a ZDDP tribofilm once MoDTC is added in adequate quantities to oil must be understood to determine the mechanism of tribofilm formation. Figure 9-9 presents the Fe, P and Zn weight percentages from 0 to 720 seconds of etching time for different Mo concentrations. The addition of MoDTC increases the amount of Fe within the tribofilm at high etching times, indicating a thinner overall tribofilm thickness. Moreover, a general reduction in P and Zn, heavily associated with the decomposition products of ZDDP, is observed as the tribofilms are etched. Table 9-1 displays the polyphosphate chain lengths derived from the BO/NBO ratios obtained from the analysis of XPS O 1s peak. It can be observed that the addition of MoDTC reduces the phosphate chain length, a sign of a reduction in ZDDP film thickness [59]. In ZDDP tribofilms, longer phosphate chain lengths are found within the top layers of the tribofilm, while shorter chains are found within the bottom layers. As the BO/NBO number decreases so does the ZDDP tribofilm thickness. It must be noted that the polyphosphate chain lengths with ZDDP as the only additive in the oil are usually greater than the oil when Mo is added to the oil, as shown in Table 9-1. The reduction in chain length is due to the fully formulated oil containing detergents and dispersants [123,156].

Previous work investigating the interactions between ZDDP and MoDTC also determined a reduction in P and Zn from XPS and EDX analysis once MoDTC was added to a ZDDP oil [72]. MoDTC in a small amount does not significantly change the phosphate chain lengths or ZDDP species. Other research into the chemistry of anti-wear films also agrees with the research [155].

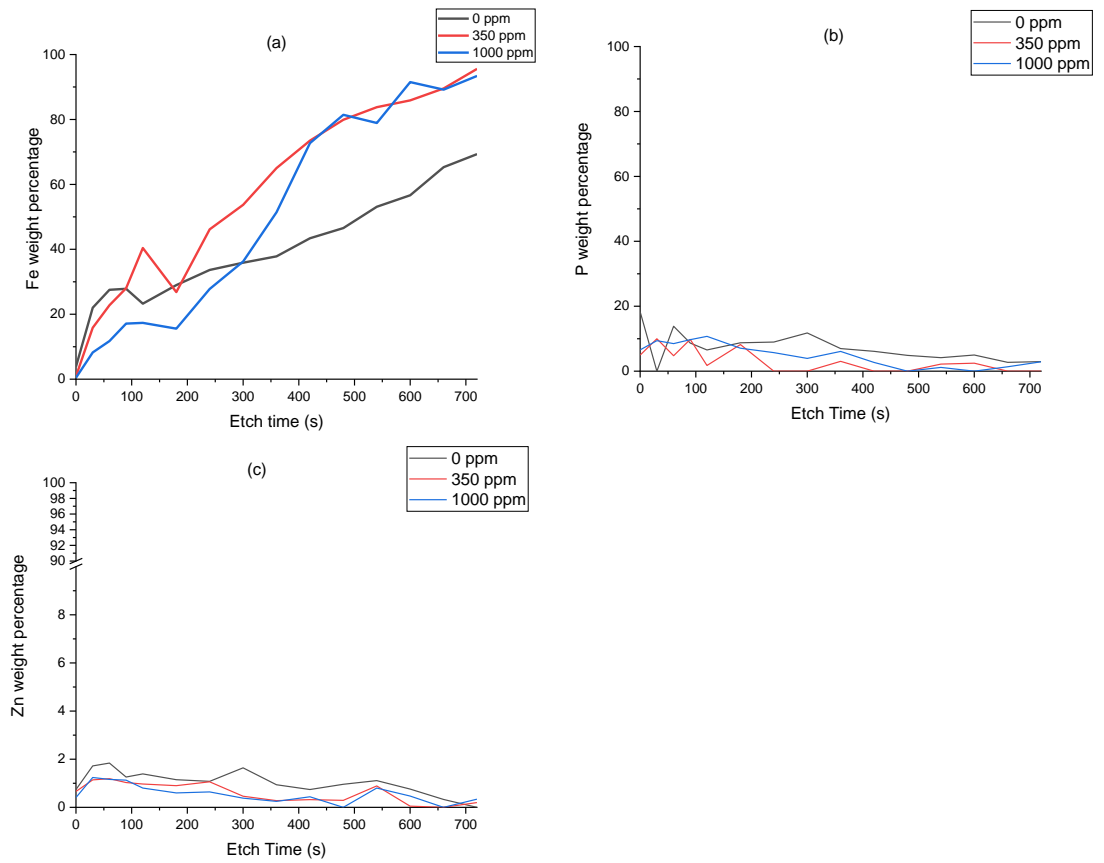


Figure 9-9 ZDDP XPS element weight percentages at different Mo concentrations (a) Fe, (b) P and (c) Zn.

Table 9-1 Phosphate chain length as Mo concentration changes.

Mo concentration	BO/NBO ratio
0	0.35
350	0.15
1000	0.20

9.3.2 Mechanism of MoDTC and ZDDP tribofilm formation

Figure 9-10 displays the tribofilm formations of a fully formulated oil containing the active boundary additives ZDDP and detergents and the additional MoDTC in a friction-reducing concentration to highlight the impact MoDTC has on the ZDDP formation. The mechanism was generated using the research conducted in this thesis and previous research [56,72,151].

It was determined that a friction-reducing MoDTC concentration forms thick MoS_2 layers in the initial stages of rubbing. MoS_2 and other decomposition products such as MoO_xS_y create competitive surface adsorption between ZDDP + detergents and MoDTC. As the layers of the tribofilm build, MoDTC decomposition products such as Mo oxides, MoO_xS_y and MoS_2 become embedded within the matrix. The polyphosphate chains can form, but not what they typically can, due to multiple other compounds added to the tribofilm matrix. The friction also significantly changes due to MoS_2 which would reduce stress and flash temperatures at the contact directly slowing the ZDDP formation [49]. As shown in Figure 6-8, the addition of MoDTC significantly reduces the overall ZDDP tribofilm thickness.

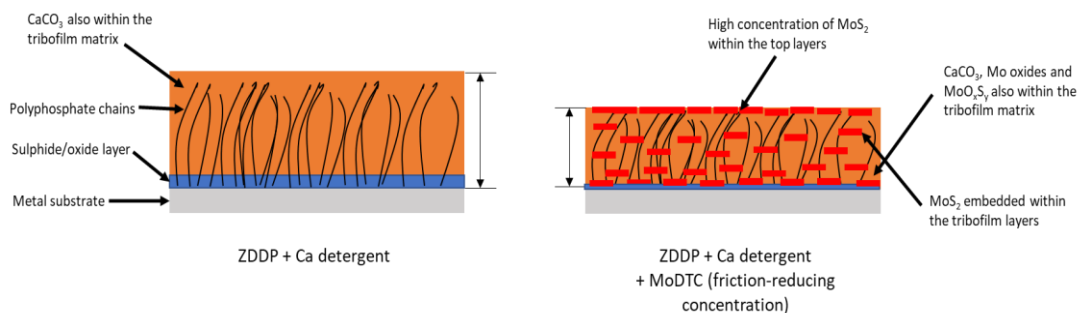


Figure 9-10 Tribofilm formations of a fully formulated oil containing ZDDP and detergent and the additional MoDTC in a friction-reducing concentration.

It has been determined that MoDTC reduces the formation of the ZDDP tribofilm. However, it is crucial to note that the wear generated before and after MoDTC is added in a friction-reducing concentration is not negatively impacted in the real-world application of the ICE. However, a trend is observed that MoDTC increases the wear when added to an oil containing ZDDP. Again, this could be down to the competitive adsorption mechanism, where MoDTC decomposition products form thick layers in the initial stages of the tribofilm formation, reducing the anti-wear additives formation or the tribofilm formed have difference compositions affecting wear differently. A very high percentage of the wear is generated in the initial rubbing of the surfaces as the very first tribofilm layers are formed, hence the increase in wear observed. However, it must also be noted that the decomposition products of MoDTC do have anti-wear properties, which prevent the wear from a harsher increase [71,77].

9.4 Detergents' effect on Tribofilms Tribological Properties

Chapter 7 used three different detergent formulations to understand the influence and essential role detergents have on the tribological properties of fully formulated engine oil.

Different detergent formulations' effects on the tribofilm chemistry must be understood to understand how friction and wear change with each one. This section will use the research conducted in this study and from previous research to understand the impact different detergent formulations have on the tribofilms tribological properties and interactions which occur between detergents and other surface-active additives.

9.4.1 Friction and Wear

Figure 9-11 displays the friction and wear values for the oils containing detergents tested in this study. All three detergents produce friction-reducing tribofilms. It can be determined that these detergents do not hinder the function of the MoDTC additive. Detergents tested in previous literature produce a tribofilm with the decomposition products of the detergent but do not prevent MoDTCs' ability to reduce friction regardless of the formulation. A study investigating the tribological properties of MoDTC and detergents determined that low and high-based calcium sulfonate and middle-based calcium alkyl salicylate all produce non-damaging effects on the function of MoDTC [138]. Another study of the surface films of ZDDP, MoDTC and overbased calcium sulfonates also showed similar findings [123]. Finally, another study showed non-damaging effects on the function of MoDTC with calcium phenate and salicylate detergents [157]. All the detergents do not prevent MoS₂ from forming from MoDTC. However, they could reduce the MoS₂ thickness within the tribofilm matrix since the research conducted in the thesis determined that a threshold value of MoS₂ intensity is required within the tribofilm matrix to reduce friction independent of the formulation, as shown in Figure 6-13. The detergent formulations from Figure 7-1 used in this study also agree with previous research which shows that the MoDTC molecule decomposes to form the friction reducing compound MoS₂ to enable friction reduction as shown in Figure 7-3. However, the detergent formulation does influence the intensity of the MoS₂ even though the friction is still low, as shown in Figure 7-6.

The detergent formulation affects the ZDDP tribofilm formation much more than MoDTC tribofilm in agreement with previous research [80,81]. The wear

volume, shown in Figure 9-11, displays noticeable differences between the detergent formulations. However, it must be noted that the wear is still very low. Wear is affected more than friction.

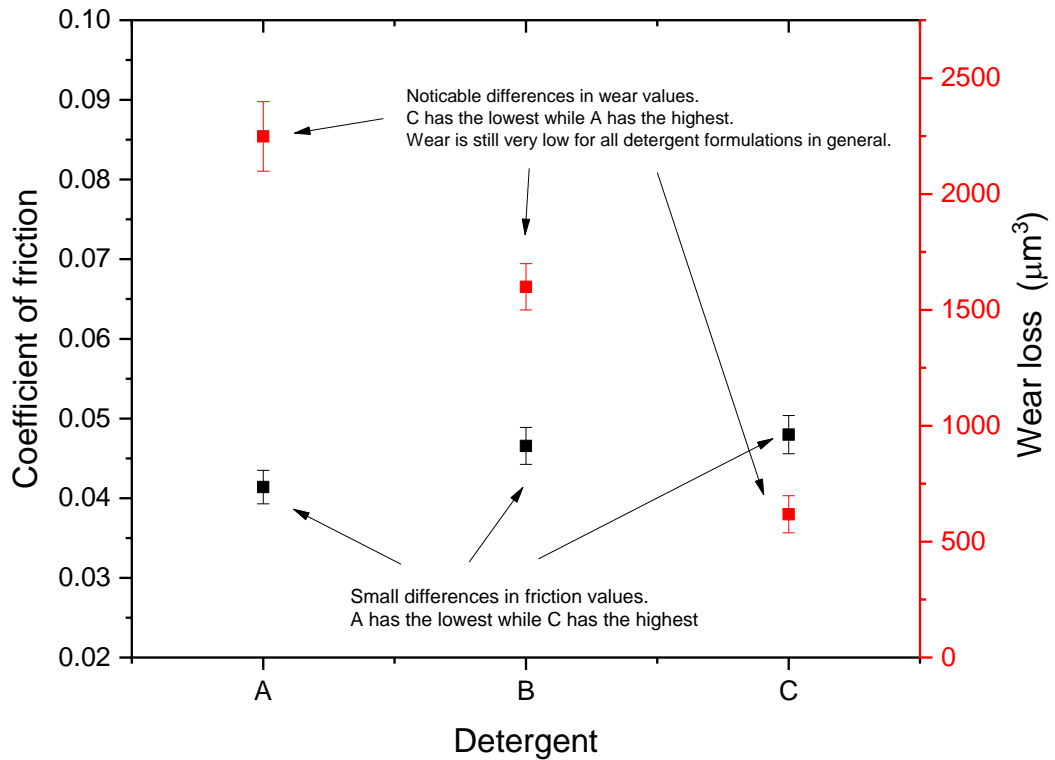
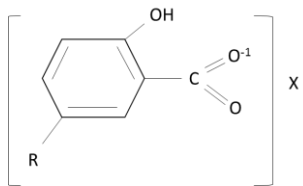
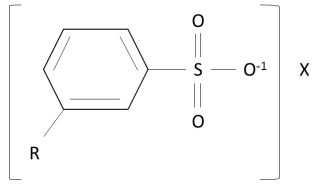


Figure 9-11 Friction and wear values for each detergent formulation

9.4.2 Tribofilm Chemistry

Table 9-2 displays the detergent molecular structure used in fully formulated oils tested in this research. It must be noted that all three detergent formulations have more Ca-weighted detergents than Mg. Meaning each oil has a higher Ca detergent concentration compared to the Mg detergent.

Table 9-2 Detergent formulations

Detergent A	Detergent B	Detergent C
Ca + Mg Salicylates	Ca + Mg Sulfonates	Ca Salicylates + Mg sulfonates
		

Previous research has shown that detergents can form a tribofilm [82]. More specifically, Ca detergents can form thick CaCO_3 films and Ca phosphates with ZDDP on the rubbing surfaces. Due to the competitive surface adsorption mechanism, the other boundary additives, ZDDP and MoDTC, are affected by the detergents used in this study. Moreover, the decomposition products of Mg detergents are hard to determine within the tribofilm matrix [81]. However, a study did detect MgSO_4 within a tribofilm [82].

9.4.2.1 Effect of detergent used in a fully formulated oil on MoS_2

Formation

Figure 9-12 displays the steady-state friction values and total intensity of MoS_2 within the tribofilms from Raman analysis. The friction scale range is small to enable visual differences. Detergent C has less MoS_2 within its tribofilm matrix than B and A from the total intensity counts. However, it still produces friction value of around ≈ 0.05 . The friction for detergent A is the lowest due to the high MoS_2 intensity within the tribofilm, implying thicker MoS_2 layers have formed. The different detergent formulations affect the MoS_2 formation in

different ways. The salicylates allow thicker MoS₂ layers than sulfonates and a mixture of both. However, it must be noted that if the detergents were not present in oils, there would be a high probability that the MoS₂ layers would be even thicker. Previous research showed a reduction in Mo and S weight percentages when a Ca salicylate detergent was added to a single MoDTC oil and determined that both MoS₂ and CaCO₃ formed after the detergent was added. Friction reduction was also observed by adding a detergent [138]. Other research also determined that Ca sulfonates reduce the MoS₂ film thickness [123].

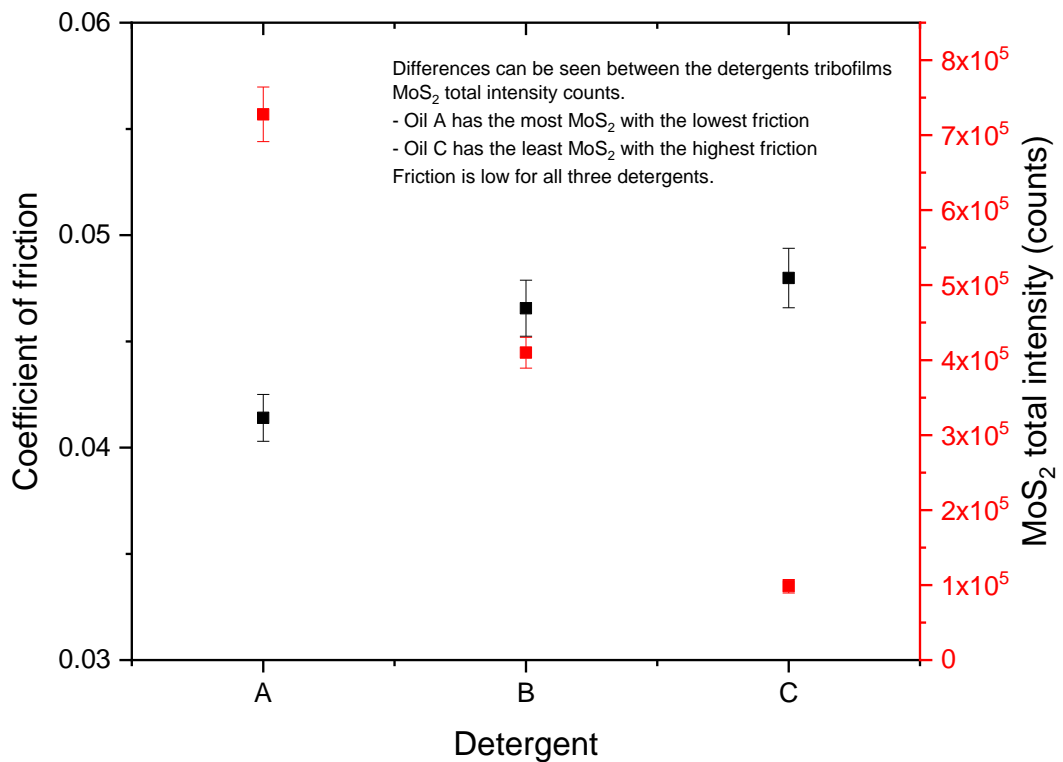


Figure 9-12 Detergents friction and MoS₂ total intensity counts within the tribofilm.

Overall, detergents reduce the formation of MoS₂ within the tribofilm; however, the friction is not negatively impacted, with low friction still achieved. Therefore, it can be determined that detergents do not prevent the MoDTC additive from performing its function. The detergent formulation does effect MoS₂ intensity within the tribofilm matrix.

9.4.2.2 Effect of detergents used in a fully formulated oil on ZDDP

Formation

Figure 9-13 displays the average weight percentages of elements associated with detergent and ZDDP decomposition species within the tribofilm and the wear volume for all three oil formulations. Detergent C, containing Ca salicylates and Mg sulfonates, produces the lowest wear. Its tribofilm contains the highest amount of Zn and P, relating to decomposition compounds formed from ZDDP such as phosphate chains, ZnS and ZnO, implying it is the detergent formulation with the least effect on the ZDDP formation leading to the least wear generated. In comparison, detergent A, containing only salicylates, has the highest wear with the least amount of Zn and P within its tribofilm, preventing ZDDP formation compared to the other oil formulations.

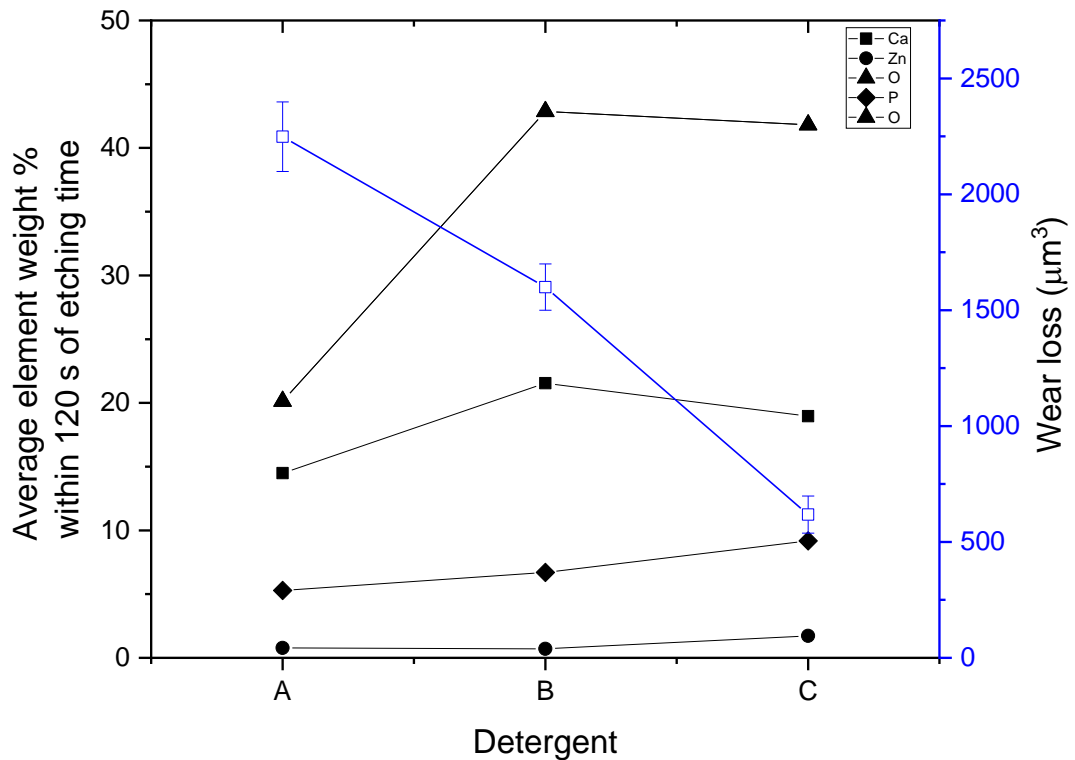


Figure 9-13 Average weight % for anti-wear and detergent species with wear volume loss for all three formulations.

Previous research has shown that Ca salicylates reduces the phosphate chain lengths and ZDDP species within the tribofilm via forming CaCO_3 and replacing zinc phosphates with calcium phosphates [157]. XANES analysis of the P K and L-edges provided evidence for the calcium phosphates. Wear data determined that adding CaCO_3 shortened and substituted phosphate chains within the tribofilm matrix, leading to increased wear. However, the detergent in a binary system reduced wear compared to the base oil. It was also determined that a higher degree of over-basing produced CaCO_3 within the tribofilms.

A research study into the surface films of ZDDP, MoDTC and calcium sulfonates via XPS determined that CaCO_3 is present within the tribofilm

matrix [123]. Again, similar to salicylates, the sulfonates reduced the phosphate film thickness. Another research paper investigating the sulfonates and ZDDP mechanism determined that three types of interactions occur [158];

1. Chemical interaction between both additives in the oil phase.
2. The calcium surfactant molecule preventing basal materials from forming during rubbing.
3. Overbasing agents' role in colloidal dispersion.

It was determined that interactions 2 and 3 are more predominant when an overbased detergent is used.

All previous research, coupled with Chapter 7, concludes that calcium sulfonates and salicylates have similar interaction mechanisms with ZDDP during rubbing. The research from this study shows that the three different detergent oil formulations produced the same decomposition products expected from the ZDDP molecule for low wear. All oil formulations also produced CaCO_3 in the tribofilm. Additionally, previous research has shown Ca replaces Zn within the phosphate chains when using either calcium salicylates or sulfonates due to the hard and soft acids bases (HSAB) principle [84,159].

9.4.3 Mechanism for the interaction of detergent and ZDDP/MoDTC

The mechanism for reducing the ZDDP tribofilm and MoS_2 is due to the addition of CaCO_3 and substitution of Zn phosphates within the tribofilm. The research conducted in this study and from previous literature showed the same decomposition products are formed from the calcium detergents regardless of their formulation [82,138,157]. The main difference is the

quantity of these products formed and their impact on the formation of the friction and anti-wear films, to which the study undertaken in this research showed minor differences in friction and wear.

Adding CaCO_3 naturally increases the competitive surface adsorption between the decomposition products. Ca also replaces the Zn in the phosphate chains due to the HSAB principle, reducing the ZDDP film thickness [84].

From tribochemical analysis in this research, detergents do not chemically interact with MoDTC to the level they do with ZDDP. This is due to Ca replacing Zn in the phosphate chains. Again, MoDTC decomposition products quantities within the tribofilm are reduced due to the addition of detergent decomposition products.

It is essential to note that overall, even though the anti-wear and friction-reducing species are reduced within the tribofilm matrix due to the detergents, the friction and anti-wear additives can still perform their respective functions.

9.5 Artificial Oil Ageing vs Engine oil Ageing

This section will focus on the tribological differences produced from artificial oil and engine ageing processes when comparing them to their fresh oil performance.

9.5.1 Differences in Oil Ageing Processes

An artificial ageing process is essential for engine oil friction and wear performance screening before more expensive engine tests are completed. The artificial ageing process must simulate and affect the engine oil similarly to the engine ageing processes. A commonly used artificial ageing process is

CEC L-48-00, shown in Figure 3-23, while engine ageing processes vary [96–99]. The field engine ageing processes are shown in Table 4-1.

Table 9-3 displays the effects of both artificial and engine ageing processes on two different oils, taken from Chapter 8. Each ageing process is compared to its fresh engine oil counterpart. The artificial ageing process is kept the same for both oil pairs, Figure 3-23, with the engine ageing processes being different, Table 4-1.

Table 9-3 Engine oil artificial vs engine ageing impact on tribological properties compared to their fresh oils.

Oil	Ageing process	High-temperature viscosity	Friction	Wear
0W-20 (A)	Artificial	increase	Low friction – significant delay in reduction	Slightly higher wear
	Engine	increase	Very high friction	Similar wear
0W-8 (B)	Artificial	decrease	High friction	Significantly high wear
	Engine	decrease	Very high friction	Reduced wear

Regardless of the engine running conditions, both engine aged oils produce very high friction and similar or reduced wear compared to the fresh engine oil performance. Previous research investigating engine oils in the field determined that all friction-reducing properties of the oil were lost after ageing [160]. A fully formulated 5W 30 engine oil was tested in the field for 20,000

km, which is considered to be a longer distance than usually tested. Wear also increased by 420%. An explanation for the consistency of the engine ageing process affecting the fresh oils is the harsh conditions within the engine. The oil is subjected to high temperatures, shearing, contamination and pumping around multiple moving components during the ageing process [144].

Alternatively, both artificially aged oils produce different friction and wear results. Therefore, it can be determined that the oil formulation in artificial ageing has significantly more influence on the tribological properties.

9.5.2 Effect of Ageing Oil on Wear

As shown in Figure 8-31 and Figure 8-32, artificial and engine ageing processes produce different wear results than fresh oils. Both sets of results have been combined to highlight the differences, shown in Figure 9-14. The artificially aged oils increase the wear compared to the fresh oil, while the engine aged oils decrease the wear.

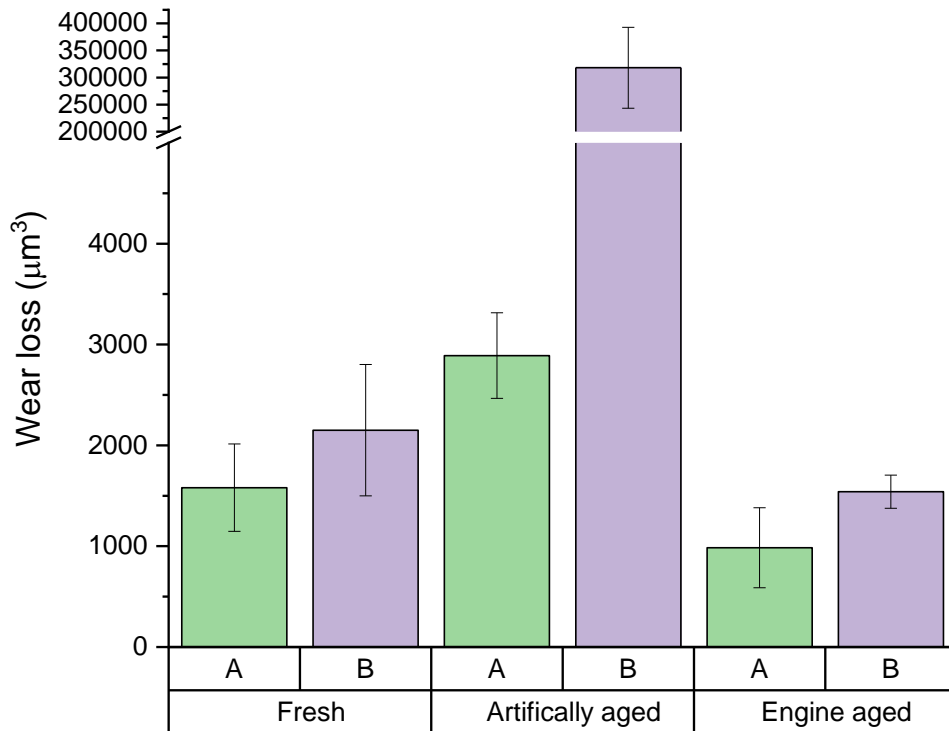


Figure 9-14 Wear loss for both oil A and B.

Oil B's artificially aged oil does not produce a tribofilm, shown in Figure 8-16, explaining the extremely high wear observed. Oil A also produces higher wear when artificially aged, but not the degree of oil B, due to the formation of a tribofilm containing wear-reducing species.

Previous research using the same artificial ageing process showed minimal wear discrepancy between fresh and aged oil [161]. A 5W-30 fully formulated oil containing no MoDTC was artificially aged and tested. It determined that the low wear results indicated that even though the additive intensity can decrease after oxidation, an anti-wear tribofilm can still form. Both FTIR analysis from Chapter 8 and from the previous research showed the main elements of the anti-wear additive to be still present but in lower intensity [161].

These results produced are similar to oil As. However, oil Bs results do not agree, with no tribofilm formed producing very high wear.

Less academic research has been conducted on field engine aged oils than on artificially aged engine oil. In the tests undertaken in this study, both engine aged oils from A and B produce reduced wear and similar friction. The oils are subjected to very harsh conditions during the engine ageing process compared to artificial ageing. A GED test was used to age the engine oil for oil A. Previous research has shown the GED test to use extreme operating conditions [162–164]. The principle behind the test is to test the engine components to withstand high mechanical stresses, wear, fatigue etc, which results in high engine revolutions and maximum loads. It contains a series of steady-states with speed ramp ups and downs. A continuous high-speed durability test was used to age engine oil B. Again, the principle behind the test is similar to oil A; however, the speed is kept relatively constant throughout instead of step cycles.

Previous research into the tribological properties of engine oils in the field determined that the wear increased after 8,000 km of distance travelled [160]. When the oil was aged in the field for 5,000 km, the wear observed was reduced compared to the fresh oil. Similar to the research conducted in this study, the author determined that the 5,000 km aged oil contained large amounts of Zn and P within the tribofilm matrix, the species associated with ZDDP. It was also determined that increasing the ageing time after an initial period increases the wear [160]. The engine oils aged via the field in this study must be within the initial period of ageing where the wear and tribofilm are not negatively impacted. The initial oxidation of ZDDP is not detrimental to the function of the additive. However, a more extended period of oxidation

depletes the additives causing the core oxidized molecule of ZDDP to have no anti-wear properties.

9.5.3 Effect of Ageing on Oil Chemistry

The oil chemistry analysis conducted on oil A and B indicated that oxidation, sulphation, and additive depletion had occurred during the ageing processes. Different techniques were used to identify the effects ageing has on oil chemistry. FTIR determines if oxidation, sulphation, and additive depletion have occurred within the oil. XPS and Raman are used to understand the MoDTC depletion and decomposition products formed in the tribofilm after oil ageing. The FTIR, XPS and Raman are all used for studying ZDDP depletion and its decomposition products formed in the tribofilm from ageing.

Previous literature investigating ageing on oils focuses on three main areas within the FTIR spectrum analysis [165]. These peaks are associated with additive depletion, oxidation, and sulphation, which all show that ageing has changed the chemistry within the oils. The peaks at $\approx 1100\text{-}1200\text{ cm}^{-1}$ and $\approx 1200\text{-}11250\text{ cm}^{-1}$ are associated with S=O and S-O bonding [165]. As ageing occurs, these bonds increase within the oil chemistry as sulphate by-products are formed. Previous literature and the results shown in Figure 8-2 and Figure 8-5 depict an increase in these peaks during and after the ageing process [95,165,166]. Additionally, the peak at $\approx 1700\text{-}1750\text{ cm}^{-1}$ associated with C=O bonding and increases due to carboxylic by-products forming during the ageing process also increases in the results shown in Figure 8-3 and Figure 8-6 and previous literature [95,165,166].

9.5.3.1 MoDTC Depletion and Decomposition Products

It can be presumed that MoDTC depletion occurs similarly between artificial and field ageing processes. The speed of depletion and oxidation is the differing factor.

As shown in the previous section, the friction-reducing properties of MoDTC are entirely lost after engine ageing. Other research has also produced similar results. In comparison, the artificial ageing process has shown friction reduction to be still achievable. However, the oxidation process impacts the mechanism by which MoDTC performs its function, as previous research has shown [92,93,99].

Chapter 8 determined that the ageing processes, artificial or via the engine, delayed or completely removed the formation of MoS₂ within the tribofilm. Previous research has shown that the MoDTC molecule is broken down during additive depletion due to a sulfur-oxygen atom substitution [85]. If the MoDTC molecule is only partially oxidized, MoS₂ can form to reduce friction.

Table 9-4 displays the Mo compounds detected within the tribofilms using XPS and Raman from Chapter 8 for fresh, artificial and engine aged oils. The artificially aged oil formed MoS₂ within the tribofilm after a significant delay of around 60 minutes. Therefore, sulfur-oxygen atom substitution must have taken place within the MoDTC molecule to cause the delay in friction reduction. MoS₂ and MoO_xS_y were detected in minimal quantities in the bottom layers of the artificially aged tribofilm from XPS. However, a threshold amount of MoS₂ within the tribofilm is required for friction reduction, as previous research has shown [75,132].

Previous research into the ageing impact on MoDTC tribological properties showed that the MoO_xS_y compound could have two forms [92,99]. The first has low oxygen content, enabling friction reduction within the tribofilm. The second contains high oxygen content, which produces no friction reduction. It was determined that oxygen replaces the sulfur and $x > y$ when a chemical shift to a higher binding energy occurs.

The engine aged tribofilm in this research contains MoO_xS_y but has no friction reduction, Figure 8-23 and Figure 8-27. Therefore, high oxygen content must be present within the compound. Table 9-5 shows the binding energy comparison of Mo (V) from the Mo 3d signals for all three tribofilms. The results show higher binding energy for the engine aged tribofilm, which produces no friction reduction, implying the MoO_xS_y has a high oxygen content.

The artificially aged tribofilm has a similar binding energy to the fresh, with both tribofilms reducing friction. Overall the results are in agreement with previous literature [99]. It must be noted that other previous research did not detect an increase in binding energy after ageing [92]. It is difficult to distinguish between the low and high oxygen content in MoO_xS_y using XPS as mixed results are recorded. However, previous research does agree with the hypothesis of two Mo oxysulphide species containing low and high oxygen, with the high oxygen species forming after ageing [99].

Table 9-4 Mo compounds detected within fresh, artificial and engine aged tribofilms.

Mo compound	Fresh	Artificially aged	Engine aged
MoS ₂	✓	✓	x
MoO _x S _y	✓	✓	✓
Mo oxide(s)	✓	✓	✓

Table 9-5 Mo (V) binding energy for fresh and aged oils.

	Fresh	Artificially aged	Engine aged
Mo (V) binding energy (eV)	230.42	230.35	232

A decomposition pathway for MoDTC after ageing can be determined using the results obtained in this study and previous literature [75,92,99,132].

1. Oxygen replaces sulfur within the MoDTC molecule during ageing.
2. The new molecules adsorb onto the surfaces.
3. Decomposition occurs through C-S rupturing from shear stress, creating the amorphous MoO_xS_y structure.
4. The Y and X ratios change compared to fresh oil, with X becoming larger. Therefore, more Mo oxides are formed than MoS₂, producing worse friction performance than fresh oil.

9.5.3.2 ZDDP Depletion and Decomposition Products

Compared to MoDTC, ZDDP is significantly less affected by oil oxidation since ZDDP additives are known for their anti-oxidant properties, as previous

research has shown [95]. The current study determined that the main elements of ZDDP survived the ageing process, which can be proved via FTIR analysis, Figure 8-1 and Figure 8-4. ZDDP depletes via replacing its sulfur atoms with oxygen atoms with the release of alkyl side chains [90]. FTIR can still detect the side chains produced from ZDDP depletion since the ZDDP bonding peak is around 970 cm^{-1} , corresponding to the P-O-C bond. Multiple research papers have shown that many alkyl side chains contain the P-O-C bond [90,148].

Chapter 8 determined that the decomposition products of ZDDP within the tribofilm matrix do not significantly differ after the ageing process. The differing factor between the tribofilm matrixes was the quantity of the ZDDP decomposition compounds. The compounds detected from XPS were ZnS, ZnO and different polyphosphate chain lengths.

Figure 9-15 shows the average weight percentage of the elements associated with the ZDDP decomposition products. Both ageing processes produce very different tribofilm chemistry results. Regardless of the oil formulation, grade, or engine ageing process, both tribofilms contain more Zn and P than their fresh counterpart. In comparison, both artificially aged tribofilms contain less than their fresh counterpart. Artificially aged oil Bs tribofilm has little to no Zn and P, while oil A has minimal Zn. Both field engine aged oils contained polyphosphate chains where analysis of the artificially aged oils detected no signs of the chains. The thicker ZDDP tribofilm generated from the engine ageing process reduces wear, while the opposite occurs for the artificially ageing process. Other research agrees that engine ageing processes improve wear when ZDDP is not depleted after excessive ageing [90,148,167,168].

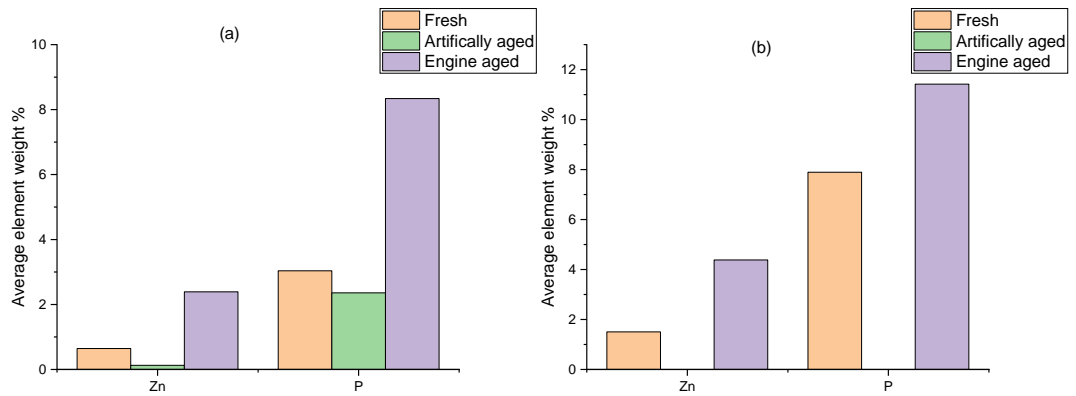


Figure 9-15 Average element weight percentage of Zn and P for (a) oil A and (b) oil B.

The engine ageing processes promote ZDDP formation, while the artificial ageing process inhibits it. An explanation for a thicker ZDDP tribofilm after engine ageing than fresh oil could be due to MoS₂'s inability to form. The prevention of MoS₂ formation keeps friction high, encouraging ZDDP to form. Additionally, the changing of the ZDDP decomposition in the oil from ageing could make the tribofilm formation easier leading to a thicker ZDDP tribofilm.

From the tribofilm chemical analysis completed in the study, it is clear that the artificially aged oils produce tribofilms with minimal amounts of ZDDP species compared to their fresh and field engine aged oil counterparts. The depletion and decomposition pathways of the artificially aged oils are different to produce the results observed. Previous literature has shown similar results; however, it occurs when the ZDDP molecule is completely depleted [90].

Chapter 10 Conclusions and Future Work

This study aimed to understand the interactions between surface-active additives when used in ultra-low viscosity engine oils. The conclusions derived from the different studies conducted in this thesis are presented in this chapter. Additionally, recommendations on future work related to the thesis are also provided.

10.1 Conclusions

10.1.1 Optimization of Mo concentration

1. From the range of concentrations tested in Chapter 6 and previous research from literature, the critical concentration of Mo for new ultra-low viscosity engine in a fresh state is between 180 and 350 ppm. As the viscosity is increased the critical concentration value increases when all conditions are kept the same.
2. Increasing the Mo concentration greater than the critical concentration does not negatively impact the overall friction and wear.

10.1.2 Mo concentrations effect on tribological performance

1. Increasing the Mo concentration decreases induction time to reach a steady-state friction value of ≈ 0.04 . Further increases at extremely high Mo concentrations would not significantly change the induction time. See Figure 9-5.
2. Adding MoDTC into a fully formulated oil containing ZDDP increases the wear generated compared to the same oil containing no MoDTC.

3. Increasing the Mo concentration above the critical concentration slightly decreases the wear generated compared to the critical concentration.

10.1.3 Mo concentrations influence on MoS₂ formation

1. Increasing the Mo concentration past the critical concentration creates thicker MoS₂ layers within the first few layers of the tribofilm matrix. The supply of MoDTC to the contact is increased, and thus more MoDTC can be broken down into MoO_xS_y. See Figure 9-7.
2. The MoS₂ formation and removal rate is highly dependent on Mo concentration.

10.1.4 Mo concentrations influence on ZDDP formation

1. Adding MoDTC into a fully formulated oil containing ZDDP reduces the overall ZDDP film thickness compared to the same oil containing no MoDTC. Increasing the Mo concentration past the critical concentration does not significantly change the ZDDP tribofilm growth rate or final steady-state film thickness.
2. Adding MoDTC into a fully formulated oil containing ZDDP reduces the zinc polyphosphate chain lengths within the tribofilm matrix compared to the same oil containing no MoDTC.
3. A reduction in species associated with ZDDP is observed when MoDTC is added to the oil formulation compared to the same oil containing no MoDTC.

10.1.5 Detergent formulations effect on tribological performance

1. Detergent formulations used in this thesis and from previous literature do not negatively impact the overall friction and wear.
2. Detergent formulations can cause a change in the steady-state friction. However, the difference is insignificant.
3. Detergent formulations impact the Stribeck friction until Steady-state Stribeck friction is achieved due to the formation of the detergent decomposition products within the tribofilm matrix disrupting MoS₂ formation.

10.1.6 Detergents influence on tribofilm chemistry

1. All the detergents tribofilms tested had different quantities of the typical compounds found within an engine oil tribofilm.
 - a. The combination of Ca salicylates and Mg sulfonates suppressed the formation of MoS₂ the most compared with the other detergents. The combination also had the most ZDDP and very high amounts of detergent species within its tribofilm.
 - b. The combination of Ca and Mg salicylates allowed for the most MoS₂ formation. Out of the detergents tested, the combination had the lowest amount of detergent species, suggesting it had the least impact on the tribofilm chemistry.
 - c. The combination of Ca and Mg sulfonates contained the highest amount of detergent species within its tribofilm and medium amounts of MoDTC and ZDDP decomposition products compared to the other two formulations.

2. Sulfonates form thicker detergent specie layers within the tribofilm matrix compared to salicylates.
3. Quantities of MoS₂ and ZDDP decomposition products within all three tribofilms exceed the threshold amounts required for low friction and wear.

10.1.7 Artificial vs field engine ageing processes

10.1.7.1 Oil viscosity

1. Artificial and field ageing processes produced slight increases in viscosity on the higher viscosity grade engine oil at high temperatures.
2. The artificial ageing process significantly reduces viscosity at high temperatures with lower oil viscosity grades. While the field ageing process only produces a slight decrease.

10.1.7.2 Tribological properties

1. Friction reduction is removed regardless of the engine ageing process. Both engine ageing processes increased the friction compared to the fresh engine oil.
2. The artificial ageing process produces inconsistent friction results.
 - a. One oil produced high friction with Stribeck curves indicating no tribofilm has formed. The other had friction reduction but after a significant delay of ≈ 60 minutes.
 - b. The oil's physical and chemical properties significantly influence the impact artificial ageing has on oil performance.
3. The engine ageing process produced better wear performance than the artificial ageing process.

10.1.7.3 Tribofilm chemistry

1. The engine ageing processes produced tribofilms containing thick ZDDP species compared to the artificial oils. MoDTC decomposition products, MoO_xS_y and Mo oxides were also detected. No MoS_2 could be detected in both cases.
2. Both artificial ageing processes produced very different tribofilms for the two oils tested.
 - a. One contained minimal traces of tribofilm species. The other contained a thin ZDDP tribofilm with MoS_2 and other MoDTC decomposition products.

10.1.7.4 MoDTC decomposition during and after ageing

1. The MoDTC molecule changes during ageing via sulfur-oxygen atom substitution.
2. The oxidized MoDTC molecule decomposes onto the rubbing surfaces to form MoO_xS_y . The oxygen and sulfur atoms within the MoO_xS_y structure determine the formation and quantity of MoS_2 and Mo oxides. Before ageing, when no oxidation occurs, $y > x$ —leads to more MoS_2 formation than Mo oxides. However, after oxidation, $x > y$ develops in MoO_xS_y , and $x > y$ or the difference between y and x becomes much smaller. In this case, Mo oxide formation would be greater than MoS_2 leading to higher friction.

10.1.7.5 ZDDP decomposition during and after ageing

1. The ZDDP molecule decomposition during and after ageing does not significantly change compared to the MoDTC molecule.

- a. The main chain of ZDDP remains after oxidation. However, oxygen atoms still replace sulfur atoms with the release of alkyl side chains.
2. Due to its well-known anti-oxidation properties, ZDDP still performs its function as an anti-wear additive to a similar standard as in its pre-oxidized state.

10.2 Future Work

The research undertaken within this thesis discussed specific aspects of the interactions between surface-active additives when using new ultra-low viscosity engine oil. Optimizing the MoDTC concentration, detergent formulation influence and comparing lab and field engine-aged oils were the main aspects of the thesis research. Some additional areas are still required to enhance our understanding of the studies undertaken in this thesis. However, these could not be completed due to time constraints and global events. The future work suggestions to further develop our understanding of this subject are as follows:

- Further, develop our understanding of Mo concentrations' role in tribological performance via optimization of Mo after ageing has occurred by oxidation. This will also develop our understanding of the relationship between MoDTC and oxidation.
- Investigate further optimization of the Mo concentration in new ultra-low viscosity engine oils by adding other additives, such as organic friction modifiers and alternatively combine the new oil combinations with DLC coatings to further optimize the friction performance.

- Conduct further tests to strengthen the initial stages of MoS₂ with MoDTC concentration mechanism shown in Figure 9-7. Additionally, perform TEM/FIB studies of the tribofilms to understand the MoS₂ sheet size and crystallinity to further improve the understanding of Mo concentrations influence on friction performance.
- Investigate additive molecule depletion after ageing using techniques such as HPLC. This will enhance our understanding of MoDTC and ZDDP depletion via ageing and correlate it to tribological performance and field/artificial ageing processes.
- Investigate potential development and changes to existing ageing oil standards to represent better the physical and chemical changes which occur in oils via field engine ageing.

List of References

1. Wang Z, Liu H, Reitz RD. Knocking combustion in spark-ignition engines. *Prog Energy Combust Sci.* 2017;61:78–112.
2. Liu H, Ma J, Tong L, Ma G, Zheng Z, Yao M. Investigation on the potential of high efficiency for internal combustion engines. *Energies.* 2018;11(3):513.
3. Naber JD, Johnson JE. Internal combustion engine cycles and concepts. *Altern Fuels Adv Veh Technol Improv Environ Perform Towar Zero Carbon Transp.* 2014;197–224.
4. Mihara Y. Research Trend of Friction Loss Reduction in Internal Combustion Engines. *Tribol Online.* 2017;12(3):82–8.
5. Korcek S, Nakada M. Engine oil performance requirements and reformulation for future engines and systems. In: *Proceedings of the International Tribology Conference.* 1995. p. 783–8.
6. Inoue K, Tominaga E, Akiyama K, Ashida T. Effects of lubricant composition on fuel efficiency in modern engines. *SAE Trans.* 1995;728–36.
7. Tanaka H, Nagashima T, Sato T, Kawauchi S. The Effect of 0W-20 Low Viscosity Engine Oil on Fuel Economy. *SAE Tech Pap Ser.* 2010;1(724).
8. Ishizaki K, Nakano M. Reduction of CO₂ emissions and cost analysis of ultra-low viscosity engine oil. *Lubricants.* 2018;6(4):1–13.
9. Devlin M. Common Properties of Lubricants that Affect Vehicle Fuel Efficiency: A North American Historical Perspective. *Lubricants.* 2018;6(3):68.
10. Yan L, Yue W, Wang C, Wei D, Xu B. Comparing tribological behaviors of sulfur- and phosphorus-free organomolybdenum additive with ZDDP and MoDTC. *Tribol Int.* 2012;53:150–8.
11. Morina A, Green JH, Neville A, Priest M. Surface and tribological characteristics of tribofilms formed in the boundary lubrication regime with application to internal combustion engines. *Tribol Lett.* 2003;15(4):443–52.
12. Dowson D. *History of tribology.* Addison-Wesley Longman Limited; 1979.
13. Bhushan B. *Introduction to Tribology.* Wiley; 2013. (Tribology in Practice Series).
14. Goryacheva IG. *Contact Mechanics in Tribology.* Springer Netherlands; 2013. (Solid Mechanics and Its Applications).
15. Liskiewicz T. *MECH 5570M Introduction to Tribology Work Unit 1 Introduction to Tribology and Real Surfaces.*
16. Hutchings I, Shipway P. *Tribology: Friction and Wear of Engineering Materials.* Elsevier Science; 2017.
17. Suh NP, Sin HC. The genesis of friction. *Wear.* 1981;69(1):91–114.

18. Williams J. Engineering Tribology. Cambridge University Press; 2005.
19. Yoshizawa H, Israelachvili J. Fundamental mechanisms of interfacial friction. 2. Stick-slip friction of spherical and chain molecules. *J Phys Chem.* 1993;97(43):11300–13.
20. Tian X, Kennedy FE. Maximum and Average Flash Temperatures in Sliding Contacts. *J Tribol.* 1994;116(1):167.
21. Lansdown AR, Price AL. Materials to Resist Wear: A Guide to Their Selection and Use. Elsevier Science & Technology Books; 1986. (Pergamon materials engineering practice series).
22. Bayer RG. Mechanical Wear Fundamentals and Testing, Revised and Expanded. CRC Press; 2004. (Mechanical Engineering).
23. Czichos H. Tribology: a systems approach to the science and technology of friction, lubrication, and wear. Elsevier Science; 2009. (Tribology series).
24. Arnell RD, Davies P, Halling J, Whomes T. Tribology: Principles and Design Applications: Principles and Design Applications. Palgrave Macmillan; 1991.
25. Bhushan B. Modern tribology handbook. 2. Materials, coatings, and industrial applications. CRC Press; 2001.
26. Jiménez A-E, Bermúdez M-D. 2 - Friction and wear. In: Davim JPBT-T for E, editor. Woodhead Publishing; 2011. p. 33–63.
27. Troyer D. Practicing Oil Analysis. 2002;
28. Mayer A. Practicing Oil Analysis. 2007;
29. Minami I. Molecular Science of Lubricant Additives. *Appl Sci.* 2017;7(5):445.
30. Hamrock BJ, Schmid SR, Jacobson BO. Fundamentals of Fluid Film Lubrication. Taylor & Francis; 2004.
31. Corporation N. Machinery Lubrication. Lubrication Regimes Explained.
32. Ghanbarzadeh A, Wilson M, Morina A, Dowson D, Neville A. Development of a new mechano-chemical model in boundary lubrication. *Tribol Int.* 2016;93:573–82.
33. Gohar R, Rahnejat H. Fundamentals of Tribology: Second Edition. 2012.
34. Holmberg K, Andersson P, Erdemir A. Global energy consumption due to friction in passenger cars. *Tribol Int.* 2012;47:221–34.
35. Taylor RI, Coy RC. Improved fuel efficiency by lubricant design: A review. *Proc Inst Mech Eng Part J J Eng Tribol.* 2000;214(1):1–15.
36. Lubrita. How The Lubrication System Works In An Engine? [Internet]. Available from: <http://www.lubrita.com/news/78/671/How-The-Lubrication-System-Works-In-An-Engine/>
37. Citation S. Assessment of Fuel Economy Technologies for Light-Duty Vehicles. Assessment of Fuel Economy Technologies for Light-Duty Vehicles. 2015.

38. Davison ED, Haviland ML. Lubricant viscosity effects on passenger car fuel economy. SAE Tech Pap. 1975;
39. Wong VW, Tung SC. Overview of automotive engine friction and reduction trends—Effects of surface, material, and lubricant-additive technologies. *Friction*. 2016;4(1):1–28.
40. Taylor RI, Mainwaring R, Mortier RM. Engine lubricant trends since 1990. *Proc Inst Mech Eng Part J J Eng Tribol*. 2005;219(5):331–46.
41. Tanaka H, Nagashima T, Sato T, Kawauchi S. The Effect of 0W-20 Low Viscosity Engine Oil on Fuel Economy. SAE International ; 1999.
42. Okuyama Y, Shimokoji D, Sakurai T, Maruyama M. Study of low-viscosity engine oil on fuel economy and engine reliability. SAE Technical Paper; 2011.
43. Spikes H. The history and mechanisms of ZDDP. *Tribol Lett*. 2004;17(3):469–89.
44. Bares JA, Konicek AR, Mangolini F, Gosvami NN, Carpick RW, Yablou DG. Mechanisms of antiwear tribofilm growth revealed in situ by single-asperity sliding contacts. *Science* (80-). 2015;348(6230):102–6.
45. Aldara Naveira Suárez. The Behaviour of Antiwear Additives in Lubricated Rolling-Sliding Contacts. 2011. 278 p.
46. Fujita H, Glovnea RP, Spikes HA. Study of zinc dialkyldithiophosphate antiwear film formation and removal processes, part I: Experimental. *Tribol Trans*. 2005;48(4):558–66.
47. Mosey NJ, Müser MH, Woo TK. Molecular mechanisms for the functionality of lubricant additives. *Science* (80-). 2005;307(5715):1612–5.
48. Shimizu Y, Spikes HA. The Influence of Slide–Roll Ratio on ZDDP Tribofilm Formation. *Tribol Lett*. 2016;64(2):1–11.
49. Zhang J, Spikes H. On the Mechanism of ZDDP Antiwear Film Formation. *Tribol Lett*. 2016;63(2):1–15.
50. Taylor L, Dratva A, Spikes HA. Friction and wear behavior of zinc dialkyldithiophosphate additive. *Tribol Trans*. 2000;43(3):469–79.
51. Tripaldi G, Vettor A, Spikes H. Friction behaviour of ZDDP films in the mixed, boundary/EHD regime. *SAE Trans*. 1996;1819–30.
52. Taylor LJ, Spikes HA. Friction-enhancing properties of zddp antiwear additive: Part i—friction and morphology of zddp reaction films. *Tribol Trans*. 2003;46(3):303–9.
53. Taylor LJ, Spikes HA. Friction-enhancing properties of zddp antiwear additive: Part ii—influence of zddp reaction films on ehd lubrication. *Tribol Trans*. 2003;46(3):310–4.
54. Smith GC. Surface analytical science and. *Structure*. 2000;187.
55. Nicholls MA, Do T, Norton PR, Bancroft GM, Kasrai M, Capehart TW, et al. Chemical and mechanical properties of ZDDP antiwear films on steel and thermal spray coatings studied by XANES spectroscopy and

- nanoindentation techniques. *Tribol Lett.* 2003;15(3):241–8.
56. Society TR. Relationship between mechanical properties and structures of zinc dithiophosphate anti-wear films. 2014;455(1992):4181–203.
 57. Martin JM, Onodera T, Minfray C, Dassenoy F, Miyamoto A. The origin of anti-wear chemistry of ZDDP. *Faraday Discuss.* 2012;156:311–23.
 58. Minfray C, Martin JM, De Barros MI, Le Mogne T, Kersting R, Hagenhoff B. Chemistry of ZDDP tribofilm by ToF-SIMS. *Tribol Lett.* 2004;17(3):351–7.
 59. Parsaeian P, Ghanbarzadeh A, Van Eijk MCP, Nedelcu I, Neville A, Morina A. A new insight into the interfacial mechanisms of the tribofilm formed by zinc dialkyl dithiophosphate. *Appl Surf Sci.* 2017;403:472–86.
 60. Crobu M, Rossi A, Mangolini F, Spencer ND. Chain-length-identification strategy in zinc polyphosphate glasses by means of XPS and ToF-SIMS. *Anal Bioanal Chem.* 2012;403(5):1415–32.
 61. Parsaeian P. Effect of Water on the Interfacial Mechanisms of the Tribofilms Formed by Zinc Dialkyl Dithiophosphate: Experimental and Analytical Study. University of Leeds; 2017.
 62. Grossiord C, Varlot K, Martin J, Mogne T Le, Esnouf C. MoS₂ single sheet lubrication by molybdenum. *Tribol Int.* 1999;31(12):737–43.
 63. De Feo M, Minfray C, De Barros Bouchet MI, Thiebaut B, Martin JM. MoDTC friction modifier additive degradation: Correlation between tribological performance and chemical changes. *RSC Adv.* 2015;5(114):93786–96.
 64. Onodera T, Miura R, Suzuki A, Tsuboi H, Hatakeyama N, Endou A, et al. Development of a quantum chemical molecular dynamics tribochemical simulator and its application to tribochemical reaction dynamics of lubricant additives. *Model Simul Mater Sci Eng.* 2010;18(3).
 65. Khaemba DN. Raman spectroscopic studies of friction modifier Molybdenum Dialkyldithiocarbamate (MoDTC). 2016;
 66. Graham J, Spikes H, Korcek S. The friction reducing properties of molybdenum dialkyldithiocarbamate additives: part i — factors influencing friction reduction. *Tribol Trans.* 2001;44(4):626–36.
 67. Komaba M, Kondo S, Suzuki A, Kurihara K, Mori S. Effect of Temperature on Tribological Performance of Modtc. 2017;2017.
 68. Khaemba DN, Neville A, Morina A. A methodology for Raman characterisation of MoDTC tribofilms and its application in investigating the influence of surface chemistry on friction performance of MoDTC lubricants. *Tribol Lett.* 2015;59(3):1–17.
 69. Yamamoto Y, Gondo S. Friction and wear characteristics of Molybdenum Dithiocarbamate and Molybdenum Dithiophosphate. *Tribol Trans.* 1989;32(2):251–7.
 70. Trindade ED, Zuleta Durango A, Sinatora A. Friction and wear

performance of MoDTC-containing and ester-containing lubricants over steel surfaces under reciprocating conditions. *Lubr Sci.* 2015;27(4):217–29.

71. Morina A, Neville A, Priest M, Green JH. ZDDP and MoDTC interactions and their effect on tribological performance - Tribofilm characteristics and its evolution. *Tribol Lett.* 2006;24(3):243–56.
72. Morina A, Neville A, Priest M, Green JH. ZDDP and MoDTC interactions in boundary lubrication-The effect of temperature and ZDDP/MoDTC ratio. *Tribol Int.* 2006;39(12):1545–57.
73. Unnikrishnan R, Jain MC, Harinarayan AK, Mehta AK. Additive-additive interaction: An XPS study of the effect of ZDDP on the AW/EP characteristic of molybdenum based additives. *Wear.* 2002;252(3–4):240–9.
74. Bec S, Tonck A, Georges JM, Roper GW. Synergistic effects of MoDTC and ZDTP on frictional behaviour of tribofilms at the nanometer scale. *Tribol Lett.* 2004;17(4):797–809.
75. Xu D, Wang C, Espejo C, Wang J, Neville A, Morina A. Understanding the Friction Reduction Mechanism Based on Molybdenum Disulfide Tribofilm Formation and Removal. *Langmuir.* 2018;34(45):13523–33.
76. Feng X, Jianqiang H, Fazheng Z, Feng J, Junbing Y. Anti-wear performance of organomolybdenum compounds as lubricant additives. *Lubr Sci.* 2007;19(2):81–5.
77. Khaemba DN, Neville A, Morina A. New insights on the decomposition mechanism of Molybdenum DialkylDiThioCarbamate (MoDTC): A Raman spectroscopic study. *RSC Adv.* 2016;6(45):38637–46.
78. Barnes AL, Morina A, Andrew RE, Neville A. The Effect of Additive Chemical Structure on the Tribofilms Derived from Varying Molybdenum-Sulfur Chemistries. *Tribol Lett.* 2021;69(4).
79. Burrington JD, Corporation TL. *Practical Advances in Petroleum Processing.* 2006;(September).
80. Wan Y, Suominen Fuller ML, Kasrai M, Bancroft GM, Fyfe K, Torkelson JR, et al. Effects of detergent on the chemistry of tribofilms from ZDDP: studied by X-ray absorption spectroscopy and XPS. 2008;155–66.
81. Zhang Z, Yamaguchi ES, Kasrai M, Bancroft GM. Interaction of ZDDP with borated dispersant using XANES and XPS. *Tribol Trans.* 2004;47(4):527–36.
82. Greenall A, Neville A, Morina A, Sutton M. Investigation of the interactions between an ovel, organic anti-wear additive, ZDDP and overbased calcium sulphonate. *Tribol Int.* 2012;46(1):52–61.
83. Komvopoulos K, Pennecot G, Yamaguchi ES, Yeh SW. Antiwear properties of blends containing mixtures of zinc dialkyl dithiophosphate and different detergents. *Tribol Trans.* 2009;52(1):73–85.
84. Wan Y, Kasrai M, Bancroft GM. X-ray absorption study of tribofilms from ZDDP and overbased salicylate detergents. *Chinese Chem Lett.*

- 2009;20(1):119–22.
85. de Feo M. Impact of thermo-oxidative degradation of MoDTC additive on its tribological performances for steel-steel and DLC-steel contacts. 2015.
 86. Tuszyński W, Michalczewski R, Piekoszewski W, Szczerek M. Effect of ageing automotive gear oils on scuffing and pitting. *Tribol Int.* 2008;41(9–10):875–88.
 87. Korček S, Jensen RK. Relation between base oil composition and oxidation stability at increased temperatures. *ASLE Trans.* 1976;19(2):83–94.
 88. Abou El Naga HH, Ghany MAA. Chemical structure bases for oxidation stability of neutral base oils. *ASLE Trans.* 1987;30(2):261–8.
 89. Wu MM, Ho SC, Forbus TR. Synthetic lubricant base stock processes and products. In: *Practical advances in petroleum processing.* Springer; 2006. p. 553–77.
 90. Dörr N, Brenner J, Ristić A, Ronai B, Besser C, Pejaković V, et al. Correlation Between Engine Oil Degradation, Tribochemistry, and Tribological Behavior with Focus on ZDDP Deterioration. *Tribol Lett.* 2019;67(2):62.
 91. Jensen RK, Korček S, Johnson MD. Friction-reducing and antioxidant capabilities of engine oil additive systems under oxidative conditions. II. Understanding ligand exchange in a molybdenum dialkyldithiocarbamate/zinc dialkyldithiophosphate additive system in various base oils. *Lubr Sci.* 2001;14(1):25–42.
 92. De Barros Bouchet MI, Martin JM, Le Mogne T, Bilas P, Vacher B, Yamada Y. Mechanisms of MoS₂ formation by MoDTC in presence of ZnDTP: Effect of oxidative degradation. *Wear.* 2005;258(11–12):1643–50.
 93. Martin JM, Le Mogne T, Bilas P, Vacher B, Yamada Y. Effect of oxidative degradation on mechanisms of friction reduction by MoDTC. *Tribol Ser.* 2002;40:207–13.
 94. CEC L. 48-A00: Oxidation stability of lubricating oils used in automotive transmissions by artificial ageing. *Coord Eur Counc Dev Perform Tests Fuels, Lubr Other Fluids.* 2007;
 95. Cen H, Morina A, Neville A. Effect of lubricant ageing on lubricants' physical and chemical properties and tribological performance; Part I: effect of lubricant chemistry. *Ind Lubr Tribol.* 2018;70(2):385–92.
 96. Besser C, Schneidhofer C, Dörr N, Novotny-Farkas F, Allmaier G. Investigation of long-term engine oil performance using lab-based artificial ageing illustrated by the impact of ethanol as fuel component. *Tribol Int.* 2012;46(1):174–82.
 97. Kassler A, Pittenauer E, Doerr N, Allmaier G. Development of an accelerated artificial ageing method for the characterization of degradation products of antioxidants in lubricants by mass spectrometry. *Eur J Mass Spectrom.* 2019;25(3):300–23.

98. Károly J, Betti B. Vehicle and Automotive Engineering 2. Vol. 9, Lecture Notes in Mechanical Engineering. 2018. 3–532 p.
99. De Feo M, Minfray C, De Barros Bouchet MI, Thiebaut B, Le Mogne T, Vacher B, et al. Ageing impact on tribological properties of MoDTC-containing base oil. *Tribol Int.* 2015;92:126–35.
100. Raja PM V, Barron AR. ICP-AES Analysis of Nanoparticles. Rice University; 2021.
101. Patty DJ, Lokollo RR. FTIR Spectrum Interpretation of Lubricants with Treatment of Variation Mileage. *Adv Phys Theor Apl.* 2016;52:2225–638.
102. Abdul-Munaim AM, Holland T, Sivakumar P, Watson DG. Absorption wavebands for discriminating oxidation time of engine oil as detected by FT-IR spectroscopy. *Lubricants.* 2019;7(3):22–5.
103. Lubrecht AA, Venner CH, Colin F. Film thickness calculation in elasto-hydrodynamic lubricated line and elliptical contacts: The Dowson, Higginson, Hamrock contribution. *Proc Inst Mech Eng Part J J Eng Tribol.* 2009;223(3):511–5.
104. Liu H, Jin J, Li H, Yamamori K, Kaneko T, Yamashita M, et al. 0W-16 Fuel Economy Gasoline Engine Oil Compatible with Low Speed Pre-Ignition Performance. Vol. 10, SAE International Journal of Fuels and Lubricants. 2017.
105. Luiz JF, Spikes H. Tribofilm Formation, Friction and Wear-Reducing Properties of Some Phosphorus-Containing Antiwear Additives. *Tribol Lett.* 2020;68(3):1–24.
106. Okubo H, Tadokoro C, Sasaki S. In situ raman-SLIM monitoring for the formation processes of MoDTC and ZDDP tribofilms at Steel/Steel contacts under boundary lubrication. *Tribol Online.* 2020;15(3):105–16.
107. Carlson TA. X-ray photoelectron spectroscopy. Vol. 2. Dowden, Hutchinson & Ross; 1978.
108. Thornley B, Beadling R, Bryant M, Neville A. Investigation into the Repassivation Process of CoCrMo in a Simulated Biological Environment. *CORROSION.* 2020;
109. Komaba M, Kondo S, Suzuki A, Kurihara K, Mori S. The effect of temperature on lubrication property with MoDTC-containing lubricant —temperature dependence of friction coefficient and tribofilm structure—. *Tribol Online.* 2018;13(5):275–81.
110. Soltanahmadi S, Morina A, Van Eijk MCP, Nedelcu I, Neville A. Investigation of the effect of a diamine-based friction modifier on micropitting and the properties of tribofilms in rolling-sliding contacts. *J Phys D Appl Phys.* 2016;49(50).
111. Zhang S-L. Raman spectroscopy and its application in nanostructures. John Wiley & Sons; 2012.
112. Topolovec-Miklozic K, Forbus TR, Spikes HA. Film thickness and roughness of ZDDP antiwear films. *Tribol Lett.* 2007;26(2):161–71.

113. Benedet J, Green JH, Lamb GD, Spikes HA. Spurious mild wear measurement using white light interference microscopy in the presence of antiwear films. *Tribol Trans.* 2009;52(6):841–6.
114. GFEI. How vehicle fuel economy improvements can save \$ 2 trillion and help fund a long-term transition to plug-in vehicles. 2014;
115. Bovington C, Korcek S, Sorab J. The importance of the Stribeck curve in the minimisation of engine friction. *Tribol Ser.* 1999;36:205–14.
116. Yamamori K, Uematsu Y, Manabe K, Miyata I, Motor T, Kusuvara S. Development of Ultra Low Viscosity 0W-8 Engine Oil. 2020;1–7.
117. Nagashima T, Saka T, Tanaka H, Satoh T, Akira Y, Tamoto Y. Research on low-friction properties of high viscosity index petroleum base stock and development of upgraded engine oil. *SAE Tech Pap.* 1995;104(1995).
118. Sorab J, Korcek S, Bovington C. Friction reduction in lubricated components through engine oil formulation. *SAE Tech Pap.* 1998;(724).
119. Deshpande P, Minfray C, Dassenoy F, Le Mogne T, Jose D, Cobian M, et al. Tribocatalytic behaviour of a TiO₂ atmospheric plasma spray (APS) coating in the presence of the friction modifier MoDTC: A parametric study. *RSC Adv.* 2018;8(27):15056–68.
120. Gorbachev O, De Barros Bouchet MI, Martin JM, Léonard D, Le-Mogne T, Iovine R, et al. Friction reduction efficiency of organic Mo-containing FM additives associated to ZDDP for steel and carbon-based contacts. *Tribol Int.* 2016;99:278–88.
121. Heuberger R, Rossi A, Spencer ND. XPS study of the influence of temperature on ZnDTP tribofilm composition. *Tribol Lett.* 2007;25(3):185–96.
122. Sgroi M, Gili F, Mangherini D, Lahouij I, Dassenoy F, Garcia I, et al. Friction Reduction Benefits in Valve-Train System Using IF-MoS₂ Added Engine Oil. *Tribol Trans.* 2015;58(2):207–14.
123. Costello MT, Urrego RA. Study of surface films of the ZDDP and the MoDTC with crystalline and amorphous overbased calcium sulfonates by XPS. *Tribol Trans.* 2007;50(2):217–26.
124. Moody G, Eastwood J. The performance and mechanisms of organic polymeric friction modifiers in low viscosity engine oils. 2020;
125. McQueen JS, Gao H, Black ED, Gangopadhyay AK, Jensen RK. Friction and wear of tribofilms formed by zinc dialkyl dithiophosphate antiwear additive in low viscosity engine oils. *Tribol Int.* 2005;38(3):289–97.
126. Erdemir A. Review of engineered tribological interfaces for improved boundary lubrication. *Tribol Int.* 2005;38(3):249–56.
127. Gandhi HS, Shelef M. Effects of sulphur on noble metal automotive catalysts. *Appl Catal.* 1991;77(2):175–86.
128. Spikes H. Low-and zero-sulphated ash, phosphorus and sulphur anti-wear additives for engine oils. *Lubr Sci.* 2008;20(2):103–36.

129. Espejo C, Thiébaud B, Jarnias F, Wang C, Neville A, Morina A. MoDTC tribochemistry in steel/steel and steel/diamond-like-carbon systems lubricated with model lubricants and fully formulated engine oils. *J Tribol.* 2019;141(1):1–12.
130. Komaba M, Kondo S, Suzuki A, Kurihara K, Mori S. Kinetic study on lubricity of MoDTC as a friction modifier. *Tribol Online.* 2019;14(4):220–5.
131. Rai Y, Neville A, Morina A. Transient processes of MoS₂ tribofilm formation under boundary lubrication. *Lubr Sci.* 2016;28(7):449–71.
132. Vaitkunaite G, Espejo C, Wang C, Thiébaud B, Charrin C, Neville A, et al. MoS₂ tribofilm distribution from low viscosity lubricants and its effect on friction. *Tribol Int.* 2020;151(July).
133. Kaneko T, Yamamori K, Suzuki H, Onodera K, Ogano S. Friction Reduction Technology for Low Viscosity Engine Oil Compatible with LSPI Prevention Performance. *SAE Tech Pap.* 2016;2016-Octob.
134. Tabibi M. Dispersant Effects on Zinc Dialkyldithiophosphate (ZDDP) Tribofilm Structure and Composition. 2015;
135. Crobu M, Rossi A, Mangolini F, Spencer ND. Tribochemistry of bulk zinc metaphosphate glasses. *Tribol Lett.* 2010;39(2):121–34.
136. Fujita H, Glovnea RP, Spikes HA. Study of zinc dialkyldithiophosphate antiwear film formation and removal processes, part I: Experimental. *Tribol Trans.* 2005;48(4):558–66.
137. Grossiord C, Martin JM, Varlot K, Vacher B, Le Mogne T, Yamada Y. Tribochemical interactions between Znntp, Modtc and calcium borate. *Tribol Lett.* 2000;8(4):203–12.
138. Zhang D, Li Z, Wei X, Wang L, Xu J, Liu Y. Study Tribological Properties of MoDTC and Its Interactions with Metal Detergents. *J Tribol.* 2020;142(12):1–10.
139. Wan Y, Kasrai M, Bancroft GM, Zhang J. Characterization of tribofilms derived from zinc dialkyldithiophosphate and salicylate detergents by X-ray absorbance near edge structure spectroscopy. *Tribol Int.* 2010;43(1–2):283–8.
140. Rounds FG. Additive interactions and their effect on the performance of a zinc dialkyl dithiophosphate. *Asle Trans.* 1978;21(2):91–101.
141. Costello MT, Kasrai M. Study of surface films of overbased sulfonates and sulfurized olefins by X-Ray Absorption Near Edge Structure (XANES) spectroscopy. *Tribol Lett.* 2006;24(2):163–9.
142. Yin Z, Kasrai M, Bancroft GM, Tan KH, Feng X. X-ray-absorption spectroscopic studies of sodium polyphosphate glasses. *Phys Rev B.* 1995;51(2):742.
143. Johnson MD, Jensen RK, Clausing EM, Schriewer K, Korcek S. Effects of Aging on Frictional Properties of Fuel Efficient Engine Oils. *SAE International;* 1995.
144. Sikora G, Mischczak A. The Influence of Oil Ageing on the Change of Viscosity and Lubricity of Engine Oil. *Solid State Phenom.* 2013 Mar

- 1;199:182–7.
145. Krpan H, Matanović I, Ljubas D. Influence of engine oils dilution by fuels on their viscosity, flash point and fire point. *Naft Explor Prod Process petrochemistry*. 2010;61(2):73–9.
 146. Costa HL, Spikes H. Effects of Ethanol Contamination on Friction and Elastohydrodynamic Film Thickness of Engine Oils. *Tribol Trans*. 2015;58(1):158–68.
 147. Al Sheikh Omar A, Motamen Salehi F, Farooq U, Morina A, Neville A. Chemical and physical assessment of engine oils degradation and additive depletion by soot. *Tribol Int*. 2021;160(April):107054.
 148. Dörr N, Agocs A, Besser C, Ristić A, Frauscher M. Engine Oils in the Field: A Comprehensive Chemical Assessment of Engine Oil Degradation in a Passenger Car. *Tribol Lett*. 2019;67(3):1–21.
 149. Heredia-Cancino JA, Ramezani M, Álvarez-Ramos ME. Effect of degradation on tribological performance of engine lubricants at elevated temperatures. *Tribol Int*. 2018;124(April):230–7.
 150. Zhang J, Ueda M, Campen S, Spikes H. Boundary Friction of ZDDP Tribofilms. *Tribol Lett*. 2021;69(1):1–17.
 151. Thornley A, Wang Y, Wang C, Chen J, Huang H, Liu H, et al. Tribology International Optimizing the Mo concentration in low viscosity fully formulated oils. *Tribol Int*. 2022;168(January):107437.
 152. Taylor JA, Lancaster GM, Rabalais JW. Surface alteration of graphite, graphite monofluoride and teflon by interaction with Ar⁺ and Xe⁺ beams. *Appl Surf Sci*. 1978;1(4):503–14.
 153. Okubo H, Yonehara M, Sasaki S. In Situ Raman Observations of the Formation of MoDTC-Derived Tribofilms at Steel/Steel Contact Under Boundary Lubrication. *Tribol Trans*. 2018;61(6):1040–7.
 154. Dacre B, Bovington CH. The adsorption and desorption of zinc diisopropylidithiophosphate on steel. *Asle Trans*. 1982;25(4):546–54.
 155. Kasrai M, Cutler JN, Gore K, Canning G, Bancroft GM, Tan KH. The Chemistry of Antiwear Films Generated by the Combination of ZDDP and MoDTC Examined by X-ray Absorption Spectroscopy. *Tribol Trans*. 1998;41(1):69–77.
 156. Yin Z, Kasrai M, Bancroft GM, Fyfe K, Colaianni ML, Tan KH. Application of soft X-ray absorption spectroscopy in chemical characterization of antiwear films generated by ZDDP Part II: The effect of detergents and dispersants. *Wear*. 1997;202(2):192–201.
 157. Wan Y, Fuller MLS, Kasrai M, Bancroft GM, Fyfe K, Torkelson JR, et al. Effects of detergent on the chemistry of tribofilms from ZDDP: studied by X-ray absorption spectroscopy and XPS. In: *Tribology series*. Elsevier; 2002. p. 155–66.
 158. Kapsa P, Martin JM, Blanc C, Georges JM. Antiwear mechanism of ZDDP in the presence of calcium sulfonate detergent. 1981;
 159. Kasrai M, Fuller MS, Bancroft GM, Ryason PR. X-ray absorption study of the effect of calcium sulfonate on antiwear film formation generated

- from neutral and basic ZDDPs: Part 1—phosphorus species. *Tribol Trans.* 2003;46(4):534–42.
160. Agocs A, Besser C, Brenner J, Budnyk S, Frauscher M, Dörr N. Engine oils in the field: a comprehensive tribological assessment of engine oil degradation in a passenger car. *Tribol Lett.* 2022;70(1):1–18.
 161. Salehi FM, Morina A, Neville A. The effect of soot and diesel contamination on wear and friction of engine oil pump. *Tribol Int.* 2017;115:285–96.
 162. dos Santos Filho D, Tschiptschin AP, Goldenstein H. Effects of ethanol content on cast iron cylinder wear in a flex-fuel internal combustion engine—A case study. *Wear.* 2018;406:105–17.
 163. Barber GC, Ludema KC. The break-in stage of cylinder-ring wear: a correlation between fired engines and a laboratory simulator. *Wear.* 1987;118(1):57–75.
 164. Slattery BE, Perry T, Edrisky A. Microstructural evolution of a eutectic Al–Si engine subjected to severe running conditions. *Mater Sci Eng A.* 2009;512(1–2):76–81.
 165. Omar AAS, Salehi FM, Farooq U, Morina A, Neville A. Chemical and physical assessment of engine oils degradation and additive depletion by soot. *Tribol Int.* 2021;160:107054.
 166. Salehi FM. The Effect of Oil Properties on Engine Oil Pump Failure Mechanisms. 2016;235.
 167. Besser C, Agocs A, Ronai B, Ristic A, Repka M, Jankes E, et al. Generation of engine oils with defined degree of degradation by means of a large scale artificial alteration method. *Tribol Int.* 2019;132:39–49.
 168. Uy D, Simko SJ, Carter Iii RO, Jensen RK, Gangopadhyay AK. Characterization of anti-wear films formed from fresh and aged engine oils. *Wear.* 2007;263(7–12):1165–74.